

Optimal Allocation of Measurement Devices for Distribution System State Estimation Using New Hybrid Multi-Objective Evolutionary Algorithms

Thesis

Submitted in partial fulfillment of the requirements
for the award of the degree of

**Doctor of Philosophy
in
Electrical Engineering**

by

**Sachidananda Prasad
(Roll No. 714007)**

Supervisor

**Dr. D.M. Vinod Kumar
Professor**



**Department of Electrical Engineering
National Institute of Technology Warangal
(An Institute of National Importance)
Warangal – 506004, Telangana State, India
July – 2018**

APPROVAL SHEET

This Thesis entitled "**Optimal Allocation of Measurement Devices for Distribution System State Estimation Using New Hybrid Multi-Objective Evolutionary Algorithms**" by **Sachidananda Prasad** is approved for the degree of Doctor of Philosophy in Electrical Engineering

Examiners

Supervisor

Dr. D.M. Vinod Kumar
Professor
EED, NIT Warangal

Chairman

Dr. Somasekhar V. T
Professor & Head,
EED, NIT Warangal

Date: _____

**DEPARTMENT OF ELECTRICAL ENGINEERING
NATIONAL INSTITUTE OF TECHNOLOGY WARANGAL
WARANGAL – 506 004**

**DEPARTMENT OF ELECTRICAL ENGINEERING
NATIONAL INSTITUTE OF TECHNOLOGY WARANGAL**



CERTIFICATE

This is to certify that the thesis entitled "**Optimal Allocation of Measurement Devices for Distribution System State Estimation Using New Hybrid Multi-Objective Evolutionary Algorithms**", which is being submitted by **Mr. Sachidananda Prasad** (Roll No. 714007), is a bonafide work submitted to National Institute of Technology Warangal in partial fulfilment of the requirements for the award of the degree of **Doctor of Philosophy** in Electrical Engineering. To the best of my knowledge, the work incorporated in this thesis has not been submitted elsewhere for the award of any degree.

Date:

Place: Warangal

Dr. D.M. VINOD KUMAR

(Thesis Supervisor)

Professor

Department of Electrical Engineering
National Institute of Technology Warangal
Warangal – 506004

DECLARATION

This is to certify that the work presented in the thesis entitled "**Optimal Allocation of Measurement Devices for Distribution System State Estimation using New Hybrid Multi-Objective Evolutionary Algorithms**" is a bonafide work done by me under the supervision of **Dr. D.M. Vinod Kumar**, Professor, Department of Electrical Engineering, National Institute of Technology Warangal, India and was not submitted elsewhere for the award of any degree.

I declare that this written submission represents my ideas in my own words and where others ideas or words have been included; I have adequately cited and referenced the original sources. I also declare that I have adhered to all principles of academic honesty and integrity and have not misrepresented or fabricated or falsified any idea/date/fact/source in my submission. I understand that any violation of the above will be a cause for disciplinary action by the institute and can also evoke penal action from the sources which have thus not been properly cited or from whom proper permission has not been taken when needed.

Date:

Place: Warangal

Sachidananda Prasad
(Roll No: 714007)

ACKNOWLEDGEMENTS

It gives me immense pleasure to express my deep sense of gratitude and thanks to my supervisor **Dr. D.M. Vinod Kumar**, Professor, Department of Electrical Engineering, National Institute of Technology Warangal, for his valuable guidance, support, and suggestions. His knowledge, suggestions, and discussions helped me to become a capable researcher. He has shown me the interesting side of this wonderful and potential research area. His encouragement helped me to overcome the difficulties encountered in my research as well in my life.

I am very much thankful to **Prof. Somasekhar V. T**, Head, Department of Electrical Engineering for his constant encouragement, support and cooperation.

I take this privilege to thank all my Doctoral Scrutiny Committee members, **Dr. Ch. Venkaiah**, Associate Professor, Department of Electrical Engineering, **Dr. B.L.Narasimharaju**, Assistant Professor, Department of Electrical Engineering and **Dr. G. Rajesh Kumar**, Professor & Head, Department of Civil Engineering for their detailed review, constructive suggestions and excellent advice during the progress of this research work. I would also like to thank **Sri. R. Mohan**, Associate Professor, Department of School of Management and **Dr. M. Raja Vishwanathan**, Assistant Professor, Department of Humanities & Social Science for their valuable suggestions, support and cooperation.

I also appreciate the encouragement from teaching, non-teaching members, and fraternity of Department of Electrical Engineering of NIT Warangal. They have always been encouraging and supportive.

I wish to express my sincere thanks to **Prof. N. V. Ramana Rao**, Director, NIT Warangal for his official support and encouragement.

I convey my special thanks to contemporary Research Scholars Mr. Kiran Teeparthi, Mr. Ramesh Rahul Jammy, Mr. Hareesh Meeneni and Mr. Mahanandeswar Goud of our batch mate.

I would also like to thank my friends, Mr. Kalyan Chakravarthi and Mr. Kiran Babu for extending their technical and personal support.

I acknowledge my gratitude to all my teachers and colleagues and seniors at various places for supporting and co-operating me to complete the work.

I express my deep sense of gratitude and reverence to my beloved Father and Mother Mr. **Rajendra Prasad** and **Smt. Sebati Dei**, brother **Anil Prasad**, **Sunil Prasad**, **Ramanuja Prasad**, sister **Sanjukta Prasad**, **Sasmita Prasad** and **Rasmita Prasad**, my wife **Gayatree**, for their sincere prayers, blessings, constant encouragement, shouldering the responsibilities and moral support rendered to me throughout my life, without which my research work would not have been possible. I would like to express my greatest admiration to **all my family members** for their positive encouragement that they showered on me throughout this research work. Without my

family's sacrifice and support, this research work would not have been possible. It is a great pleasure for me to acknowledge and express my appreciation to all **my well wishers** for their understanding, relentless supports, and encouragement during my research work. Last but not the least, I wish to express my sincere thanks to all those who helped me directly or indirectly at various stages of this work.

Above all, I express my deepest regards and gratitude to "**ALMIGHTY**" whose divine light and warmth showered upon me the perseverance, inspiration, faith and enough strength to keep the momentum of work high even at tough moments of research work.

Sachidananda Prasad

＊

ABSTRACT

The power distribution networks are becoming more dynamic and complex structures than before, because of the huge integration of renewable sources, distributed energy storage, intelligent electronic devices (IED) and Smart meters (SMs). Furthermore, distribution network configuration is also changing dynamically to achieve minimum power loss and voltage deviations. Due to lack of metering infrastructure in distribution networks, real time reliable monitoring of the system becomes more challenging for power engineers. Therefore, the currently existing metering infrastructure of the distribution network needs to be modeled for reliable and secure operation of the system. Thus, the overall objective of the thesis is to design an efficient optimization model and algorithm for optimal allocation of measurement devices to improve the state estimation accuracy for real time monitoring and control of the smart distribution networks.

The contributions of this thesis are as follows:

- A new multi-objective hybrid PSO-Krill Herd (KH) algorithm is proposed to optimize number and location of the measurement devices for accurate state estimation in smart distribution networks. Three objectives that need to be minimized are: (i) the total configuration cost (ii) the average relative percentage error (APE) of bus voltage magnitude and (iii) APE of bus voltage angle. As the objective functions conflict with respect to each other, a multi-objective Pareto-based non-dominated sorting hybrid PSO-KH optimization algorithm is proposed. In this approach, the random variation in loads and the metrological error of the measurement devices are also taken into account. Furthermore, the impacts of DG on state estimation performance have also been investigated.
- A new multi-objective hybrid Estimation of distribution algorithm (EDA)-interior point method (IPM) algorithm is proposed to obtain the optimal location of measuring devices for state estimation in active distribution networks. The objective functions to be minimized are, the total network configuration cost, the average relative percentage error (APE) of bus voltage magnitude and angle estimates. As the objectives are conflicting in nature, a multi-objective Pareto-based non-dominated sorting EDA has been proposed. Moreover, due to poor exploitation capability of the EDA, it is hybridized with IPM to improve its local searching ability in the search space. The hybridization of EDA and IPM brings a higher degree of balance between the exploration and exploitation capability of the algorithm during

the search process. Furthermore, the loads and generators are treated as stochastic variable and the impact of different types of DGs on state estimation performance has also been investigated.

- In distribution grids, due to the presence of different kinds of actors such as distributed generation (DG), energy storage devices systems become more complex, dynamics and uncertain in nature. Because of this changing behavior of actors, real-time monitoring and control becomes more challenging task for the power system engineers. Thus, PMUs are of great interest because they provide synchronized measurements of voltage and current. The application of PMU for state estimation in transmission system has been widely used to improve the performance of the state estimator. Therefore it would be more advantageous to use PMU in DSSE. Therefore, in this thesis, a novel multi-objective optimization problem is proposed to find trade-offs in deployment of phasor measurement units (PMUs) and intelligent electronic devices (IEDs) for state estimation in active distribution networks. A new hybrid estimation of distribution algorithm (EDA) has been used to find the optimal number and location of measurement devices such as PMUs and IEDs for accurate state estimation. The objective functions to be minimized in this optimization problem are the total cost of PMUs and IEDs, as well as RMS value of state estimation error. Since, the objectives are conflicting in nature, a multi-objective Pareto-based non-dominated sorting EDA algorithm is proposed. Moreover, to improve the local searching capability of the traditional EDA algorithm, the Interior point method (IPM) is hybridized with EDA to get near global optimal solution. Furthermore, the random variation in loads and generators is also considered to check the reliability of the proposed meter placement technique.
- The robustness of the proposed multi-objective optimization model in presence of wind generators is also carried out in this thesis. All the DGs are considered as wind generators and the output of each DG is modeled using Weibull distribution function. Furthermore, trade-offs in deployment of phasor measurement units (PMUs) and intelligent electronic devices (IEDs) for state estimation in active distribution networks is obtained. The objective functions considered to be minimized are the total cost of PMUs and IEDs as well as the RMS value of state estimation error. To get best optimal solution, multi-objective hybrid PSO-Krill Herd algorithm has been used. Moreover, the random variation in loads and generators is also considered to check the reliability of the proposed meter placement technique.

Contents

Acknowledgements	v
Abstract	vi
List of Figures	xiii
List of Tables	xx
Abbreviations	xxii
List of Symbols	xxiv
Chapter 1 Introduction	1
1.1 State Estimation Overview	2
1.2 Distribution System State Estimation (DSSE)	5
1.2.1 Evolution of distribution systems	5
1.2.2 Characteristics of Distribution Systems	7
1.3 Weighted Least Square (WLS) based State Estimation	8
1.3.1 Measurement Model	9
1.3.2 Mathematical Model of the WLS Method	9
1.4 Branch Current Based Distribution System State Estimation(BC-DSSE)	10
1.4.1 Measurement functions $h(x)$ and Jacobian Matrix Formulation $H(x)$	11
1.4.2. BC-DSSE Algorithm	13
1.5 Meta-heuristic Optimization Algorithm.....	14
1.6 Phasor Measurement Units (PMUs).....	15
1.7 Intelligent Electronics Devices (IEDs).....	15
Chapter 2 Literature Review	16
2.1 General Overview.....	17
2.1.1 DSSE based on conventional WLS method	17
2.1.2 DSSE based on load modeling.....	18
2.1.3 DSSE based on computational intelligence and heuristic techniques	19
2.1.4 DSSE based on meter placement technique	20
2.2 Motivation	22
2.3 Contribution	23
2.4 Thesis Organization	24
2.5 Summary	27

Chapter 3 Optimal Allocation of Measurement Devices for Distribution System State Estimation Using Multi-objective hybrid PSO-Krill Herd Algorithm28

3.1 Introduction	29
3.2 Problem Formulation	30
3.3 Krill Herd Algorithm (KHA)	32
3.3.1 Lagrangian Model of the KHA	32
3.3.1.1 Induced movement of Krill individuals.....	32
3.3.1.2 Foraging motion.....	32
3.3.1.3 Physical diffusion.....	33
3.3.2 Movement process in KHA.....	33
3.3.3 Genetic operator.....	33
3.3.3.1 Cross over.....	33
3.3.3.2 Mutation	34
3.4 Proposed Hybrid PSO-KH algorithm	34
3.5 Proposed Multi-objective Hybrid PSO-KH algorithm	35
3.5.1 Non-dominated sorting approach	35
3.5.2 Crowding distance	36
3.6 Robust Optimal Meter Placement in Distribution Networks	39
3.7 Test and Simulation Conditions	40
3.7.1 Fuzzy set theory.....	42
3.7.1 IEEE 69 bus system	43
3.7.2 Practical Indian 85 bus system	51
3.8 Summary.....	58

Chapter 4 A Multi-objective Hybrid Estimation of Distribution Algorithm-Interior Point Method based Meter Placement for Active Distribution State Estimation59

4.1 Introduction	60
4.2 Problem Formulation	60
4.3 Solution Methodology	62
4.3.1 Estimation of Distribution Algorithm (EDA)	62
4.3.2 Interior Point Method (IPM)	62
4.3.3 Proposed Multi-objective Hybrid EDA-IPM algorithm	63

4.4 Test and Simulation Conditions.....	67
4.4.1. IEEE 69 bus system	69
4.4.2 Practical Indian 85-bus System	77
4.5 Comparison results analysis	85
4.5.1 Comparison results analysis of IEEE 69-bus system.....	86
4.5.2 Comparison result analysis of practical Indian 85-bus system.....	92
4.6 Summary.....	98
Chapter 5 Trade-offs in PMU and IED Deployment for Active Distribution State Estimation Using Multi-objective Hybrid EDA-IPM Algorithm	99
5.1 Introduction	100
5.2 Distribution system state estimation in presence of PMUs and IEDs	101
5.3 Mathematical Model of the Proposed Multi-objective Optimization Problem (MOOP)	103
5.4 Solution Methodology	104
5.4.1 Estimation of Distribution Algorithm (EDA)	104
5.4.2 Interior Point Method (IPM)	105
5.4.3 Proposed Multi-objective Hybrid EDA-IPM algorithm	106
5.5 Test and Simulation Conditions	109
5.5.1 IEEE 69-bus system	112
5.5.2 Practical Indian 85-bus System	118
5.5 Summary.....	124
Chapter 6 Robust Meter Placement for Distribution System State Estimation in Presence of Wind Generators using Multi-objective Hybrid PSO-KH Algorithm.....	126
6.1 Introduction	127
6.2 Distribution system state estimation in presence of PMUs and IEDs	110
6.3 Mathematical model of the proposed meter placement technique	129
6.4 Solution Methodology	130
6.4.1 Krill Herd Algorithm (KHA)	130
6.4.2 Particle Swarm Optimization (PSO)	131
6.4.3 Optimal placement of PMU and IED using Multi-objective Hybrid PSO-KH Algorithm.....	132

6.5 Test and Simulation Conditions	134
6.5.1 Modelling of wind generator output using Weibull distribution.....	136
6.5.3 Simulation result and discussions.....	137
6.5.3.1 IEEE 69 bus system	137
6.5.3.2 Practical Indian 85 bus System	144
6.6 Comparison results analysis.....	150
6.6.1 Comparison results of IEEE 69-bus system.....	151
6.6.2 Comparison results of Practical Indian 85-bus system.....	157
6.7 Summary.....	157
Chapter 7 Conclusions.....	159
7.1 General.....	160
7.2 Summary of important findings.....	160
7.2 Scope for Future Work.....	162
References	164
Appendix.....	174
Publications	184
Curriculum Vitae	185

List of Figures

Figure 1.1:	Flow chart of the typical power system state estimator.....	4
Figure 1.2:	Schematic representation of Energy Management System (EMS).....	5
Figure 3.1:	Flow chart of the proposed hybrid PSO-KH algorithm.....	38
Figure 3.2(a):	Optimal Pareto-front between no. of flow meters and F_3 for 1% error in real measurements and 50% in pseudo-measurements.....	44
Figure 3.2(b):	Optimal Pareto-front between no. of flow meters and F_2 for 1% error in real measurements and 50% in pseudo-measurements.....	45
Figure 3.2(c):	Optimal Pareto-front between objectives F_2 and F_3 for 1% error in real measurements and 50% in pseudo-measurements.....	45
Figure 3.3(a):	Optimal Pareto-front between no. of flow meters and F_2 for 3% error in real measurements and 50% in pseudo-measurements.....	46
Figure 3.3(b):	Optimal Pareto-front between no. of flow meters and F_3 for 3% error in real measurements and 50% in pseudo-measurements.....	46
Figure 3.3(c):	Optimal Pareto-front between objectives F_2 and F_3 for 3% error in real measurements and 50% in pseudo-measurements.....	47
Figure 3.4(a):	Optimal Pareto-front between no. of flow meters and F_2 for 5% error in real measurements and 50% in pseudo-measurements.....	47
Figure 3.4(b):	Optimal Pareto-front between no. of flow meters and F_3 for 5% error in real measurements and 50% in pseudo-measurements.....	48
Figure 3.4(c):	Optimal Pareto-front between objectives F_2 and F_3 for 5% error in real measurements and 50% in pseudo-measurements.....	48
Figure 3.5(a):	Optimal Pareto-front between no. of flow meters and F_2 for 1% error in real measurements and 50% in pseudo-measurements.....	54
Figure 3.5(b):	Optimal Pareto-front between no. of flow meters and F_3 for 1% error in real measurements and 50% in pseudo-measurements.....	54
Figure 3.5(c):	Optimal Pareto-front between objectives F_2 and F_3 for 1% error in real measurements and 50% in pseudo-measurements.....	55

Figure 3.6(a):	Optimal Pareto-front between no. of flow meters and F_2 for 3% error in real measurements and 50% in pseudo-measurements.....	55
Figure 3.6(b):	Optimal Pareto-front between no. of flow meters and F_3 for 3% error in real measurements and 50% in pseudo-measurements.....	56
Figure 3.6(c):	Optimal Pareto-front between objectives F_2 and F_3 for 3% error in real measurements and 50% in pseudo-measurements.....	56
Figure 3.7(a):	Optimal Pareto-front between no. of flow meters and F_2 for 5% error in real measurements and 50% in pseudo-measurements.....	57
Figure 3.7(b):	Optimal Pareto-front between no. of flow meters and F_3 for 5% error in real measurements and 50% in pseudo-measurements.....	57
Figure 3.7(c):	Optimal Pareto-front between objectives F_2 and F_3 for 5% error in real measurements and 50% in pseudo-measurements.....	58
Figure 4.1:	Flowchart of the proposed multi-objective hybrid EDA-IPM algorithm.....	65
Figure 4.2(a):	Optimal Pareto front between objectives F_3 and F_2 (1% error in real and 50% in pseudo-measurements).....	71
Figure 4.2(b):	Optimal Pareto front between number of flow meters and F_2 (1% error in real and 50% in pseudo-measurements).....	72
Figure 4.2(c):	Optimal Pareto front between number of flow meters and F_3 (1% error in real and 50% in pseudo-measurements).....	72
Figure 4.3(a):	Optimal Pareto front between objectives F_3 and F_2 (3% error in real and 50% in pseudo-measurements).....	73
Figure 4.3(b):	Optimal Pareto front between number of flow meters and F_2 (3% error in real and 50% in pseudo-measurements).....	73
Figure 4.3(c):	Optimal Pareto front between number of flow meters and F_3 (3% error in real and 50% in pseudo-measurements).....	74
Figure 4.4(a):	Optimal Pareto front between number of flow meters and F_2 (5% error in real and 50% in pseudo-measurements).....	74
Figure 4.4(b):	Optimal Pareto front between number of flow meters and F_3 (5% error in real and 50% in pseudo-measurements).....	75

Figure 4.5(a):	Optimal Pareto front between number of flow meters and F_2 (1% error in real and 50% in pseudo-measurements).....	79
Figure 4.5(b):	Optimal Pareto front between number of flow meters and F_3 (1% error in real and 50% in pseudo-measurements).....	79
Figure 4.5(c)	Optimal Pareto front between objective F_2 and F_3 (1% error in real and 50% in pseudo-measurements).....	80
Figure 4.6(a):	Optimal Pareto front between number of flow meters and F_2 (3% error in real and 50% in pseudo-measurements).....	80
Figure 4.6(b):	Optimal Pareto front between number of flow meters and F_3 (3% error in real and 50% in pseudo-measurements).....	81
Figure 4.6(c)	Optimal Pareto front between objective F_2 and F_3 (3% error in real and 50% in pseudo-measurements).....	81
Figure 4.7(a):	Optimal Pareto front between number of flow meters and F_2 (5% error in real and 50% in pseudo-measurements).....	82
Figure 4.7(b):	Optimal Pareto front between number of flow meters and F_3 (5% error in real and 50% in pseudo-measurements).....	82
Figure 4.7(c)	Optimal Pareto front between objective F_2 and F_3 (5% error in real and 50% in pseudo-measurements).....	83
Figure 4.8(a):	Optimal Pareto fronts between the objectives F_2 and F_3 for 1% error in real meters and 50% in pseudo-measurements.....	86
Figure 4.8(b):	Optimal Pareto fronts between no. of power flow meters and the objective F_2 for 1% error in real meters and 50% in pseudo-measurements.....	87
Figure 4.8(c):	Optimal Pareto fronts between no. of power flow meters and the objective F_3 for 1% error in real meters and 50% in pseudo-measurements.....	87
Figure 4.9(a):	Optimal Pareto fronts between the objectives F_2 and F_3 for 3% error in real meters and 50% in pseudo-measurements.....	88
Figure 4.9(b):	Optimal Pareto fronts between no. of power flow meters and the objective F_2 for 3% error in real meters and 50% in pseudo-measurements.....	88
Figure 4.9(c):	Optimal Pareto fronts between no. of power flow meters and the objective F_3 for 3% error in real meters and 50% in pseudo-measurements.....	89

Figure 4.10(a):	Optimal Pareto fronts between the objectives F_2 and F_3 for 5% error in real meters and 50% in pseudo-measurements.....	89
Figure 4.10(b):	Optimal Pareto fronts between no. of power flow meters and the objective F_2 for 5% error in real meters and 50% in pseudo-measurements.....	90
Figure 4.10(c):	Optimal Pareto fronts between no. of power flow meters and the objective F_3 for 5% error in real meters and 50% in pseudo-measurements.....	90
Figure 4.11(a):	Optimal Pareto fronts between the objectives F_2 and F_3 for 1% error in real meters and 50% in pseudo-measurements.....	92
Figure 4.11(b):	Optimal Pareto fronts between no. of power flow meters and the objective F_2 for 1% error in real meters and 50% in pseudo-measurements.....	92
Figure 4.11(c):	Optimal Pareto fronts between no. of power flow meters and the objective F_3 for 1% error in real meters and 50% in pseudo-measurements.....	93
Figure 4.12(a):	Optimal Pareto fronts between the objectives F_2 and F_3 for 3% error in real meters and 50% in pseudo-measurements.....	93
Figure 4.12(b):	Optimal Pareto fronts between no. of power flow meters and the objective F_2 for 3% error in real meters and 50% in pseudo-measurements.....	94
Figure 4.12(c):	Optimal Pareto fronts between no. of power flow meters and the objective F_3 for 3% error in real meters and 50% in pseudo-measurements.....	94
Figure 4.13(a):	Optimal Pareto fronts between the objectives F_2 and F_3 for 5% error in real meters and 50% in pseudo-measurements.....	95
Figure 4.13(b):	Optimal Pareto fronts between no. of power flow meters and the objective F_2 for 5% error in real meters and 50% in pseudo-measurements.....	95
Figure 4.13(c):	Optimal Pareto fronts between no. of power flow meters and the objective F_3 for 5% error in real meters and 50% in pseudo-measurements.....	96
Figure 5.1(a):	Optimal Pareto front between objective J_1 and J_2 (1% error in IEDs and 50% for Pseudo-measurements).....	113
Figure 5.1(b):	Optimal Pareto front between objective J_1 and J_3 (1% error in IEDs and 50% for Pseudo-measurements).....	114
Figure 5.1(c):	Optimal Pareto front between objective J_2 and J_3 (1% error in IEDs and 50% for Pseudo-measurements).....	114

Figure 5.2(a):	Optimal Pareto front between objective J1 and J2 (3% error in IEDs and 50% for Pseudo-measurements).....	115
Figure 5.2(b):	Optimal Pareto front between objective J1 and J3 (3% error in IEDs and 50% for Pseudo-measurements).....	115
Figure 5.2(c):	Optimal Pareto front between objective J2 and J3 (3% error in IEDs and 50% for Pseudo-measurements).....	116
Figure 5.3(a):	Optimal Pareto front between objective J1 and J2 (5% error in IEDs and 50% for Pseudo-measurements).....	116
Figure 5.3(b):	Optimal Pareto front between objective J1 and J3 (5% error in IEDs and 50% for Pseudo-measurements).....	117
Figure 5.3(c):	Optimal Pareto front between objective J2 and J3 (5% error in IEDs and 50% for Pseudo-measurements).....	117
Figure 5.4(a):	Optimal Pareto front between objective J1 and J2 (1% error in IEDs and 50% for Pseudo-measurements).....	119
Figure 5.4(b):	Optimal Pareto front between objective J1 and J3 (1% error in IEDs and 50% for Pseudo-measurements).....	120
Figure 5.4(c):	Optimal Pareto front between objective J2 and J3 (1% error in IEDs and 50% for Pseudo-measurements).....	120
Figure 5.5(a):	Optimal Pareto front between objective J1 and J2 (3% error in IEDs and 50% for Pseudo-measurements).....	121
Figure 5.5(b):	Optimal Pareto front between objective J1 and J3 (3% error in IEDs and 50% for Pseudo-measurements).....	121
Figure 5.5(c):	Optimal Pareto front between objective J2 and J3 (3% error in IEDs and 50% for Pseudo-measurements).....	122
Figure 5.6(a):	Optimal Pareto front between objective J1 and J2 (5% error in IEDs and 50% for Pseudo-measurements).....	122
Figure 5.6(b):	Optimal Pareto front between objective J1 and J3 (5% error in IEDs and 50% for Pseudo-measurements).....	123
Figure 5.6(c):	Optimal Pareto front between objective J2 and J3 (5% error in IEDs and 50% for Pseudo-measurements).....	123
Figure 6.1:	Variations of wind speed for (a) k=1 and (b) k=3.....	136

Figure 6.2(a):	Optimal Pareto fronts between the objectives J_1 and J_2 for 1% error IED and 50% in pseudo-measurements.....	138
Figure 6.2(b):	Optimal Pareto fronts between the objectives J_1 and J_3 for 1% error IED and 50% in pseudo-measurements.....	138
Figure 6.2(c):	Optimal Pareto fronts between the objectives J_2 and J_3 for 1% error IED and 50% in pseudo-measurements.....	139
Figure 6.3(a):	Optimal Pareto fronts between the objectives J_1 and J_2 for 3% error IED and 50% in pseudo-measurements.....	139
Figure 6.3(b):	Optimal Pareto fronts between the objectives J_1 and J_3 for 3% error IED and 50% in pseudo-measurements.....	140
Figure 6.3(c):	Optimal Pareto fronts between the objectives J_2 and J_3 for 3% error IED and 50% in pseudo-measurements.....	140
Figure 6.4(a):	Optimal Pareto fronts between the objectives J_1 and J_2 for 5% error IED and 50% in pseudo-measurements.....	141
Figure 6.4(b):	Optimal Pareto fronts between the objectives J_1 and J_3 for 5% error IED and 50% in pseudo-measurements.....	141
Figure 6.4(c):	Optimal Pareto fronts between the objectives J_2 and J_3 for 5% error IED and 50% in pseudo-measurements.....	142
Figure 6.5(a):	Optimal Pareto fronts between the objectives J_1 and J_2 for 1% error IED and 50% in pseudo-measurements.....	144
Figure 6.5(b):	Optimal Pareto fronts between the objectives J_1 and J_3 and for 1% error IED and 50% in pseudo-measurements.....	145
Figure 6.5(c):	Optimal Pareto fronts between the objectives J_2 and J_3 for 1% error IED and 50% in pseudo-measurements.....	145
Figure 6.6(a):	Optimal Pareto fronts between the objectives J_1 and J_2 for 3% error IED and 50% in pseudo-measurements.....	146
Figure 6.6(b):	Optimal Pareto fronts between the objectives J_1 and J_3 and for 3% error IED and 50% in pseudo-measurements.....	146
Figure 6.6(c):	Optimal Pareto fronts between the objectives J_2 and J_3 for 3% error IED and 50% in pseudo-measurements.....	147

Figure 6.7(a):	Optimal Pareto fronts between the objectives J_1 and J_2 for 5% error IED and 50% in pseudo-measurements.....	147
Figure 6.7(b):	Optimal Pareto fronts between the objectives J_1 and J_3 for 5% error IED and 50% in pseudo-measurements.....	148
Figure 6.7(c):	Optimal Pareto fronts between the objectives J_2 and J_3 for 5% error IED and 50% in pseudo-measurements.....	148
Figure 6.8(a):	Optimal Pareto fronts between the objectives J_1 and J_2 for 1% error IED and 50% in pseudo-measurements.....	151
Figure 6.8(b):	Optimal Pareto fronts between the objectives J_1 and J_3 and for 1% error IED and 50% in pseudo-measurements.....	151
Figure 6.8(c):	Optimal Pareto fronts between the objectives J_2 and J_3 for 1% error IED and 50% in pseudo-measurements.....	152
Figure 6.9(a):	Optimal Pareto fronts between the objectives J_1 and J_2 for 3% error IED and 50% in pseudo-measurements.....	152
Figure 6.9(b):	Optimal Pareto fronts between the objectives J_1 and J_3 and for 3% error IED and 50% in pseudo-measurements.....	153
Figure 6.9(c):	Optimal Pareto fronts between the objectives J_2 and J_3 for 3% error IED and 50% in pseudo-measurements.....	153
Figure 6.10(a):	Optimal Pareto fronts between the objectives J_1 and J_2 for 5% error IED and 50% in pseudo-measurements.....	154
Figure 6.10(b):	Optimal Pareto fronts between the objectives J_1 and J_3 for 5% error IED and 50% in pseudo-measurements.....	154
Figure 6.10(c):	Optimal Pareto fronts between the objectives J_2 and J_3 for 5% error IED and 50% in pseudo-measurements.....	155

List of Tables

Table 3.1	Parameter values of KH, PSO and NSGA-II Algorithm.....	42
Table 3.2	DG installation bus and capacity.....	42
Table 3.3	IEEE-69-bus system: optimal location of the power flow meters under different loadings including metrological errors of the flow meters.....	50
Table 3.4	IEEE 69-bus system: optimal location of the power flow meters under different loadings including metrological errors of the flow meters (with two DGs at bus no. 50 and 61).....	51
Table 3.5	Indian 85-bus system: Optimal location of the power flow meters under different loadings including metrological errors of the flow meters.....	53
Table 3.6	Indian 85-bus system: Optimal location of the power flow meters under different loadings including metrological errors of the flow meters (with DGs at bus no. 45 and 61).....	53
Table 4.1	Parameter values of PSO, NSGA-II and EDA algorithm.....	69
Table 4.2	Distribution generation (DG) installation bus and capacity.....	69
Table 4.3	IEEE 69-bus system: The number and location of the power flow meters of different meter accuracy (with no DG).....	75
Table 4.4	IEEE 69-bus system: The number and location of the power flow meters of different meter accuracy (Type 1 DG at bus 50 and 61).....	76
Table 4.5	IEEE 69-bus system: The number and location of the power flow meters in presence of type 2 and 3 DGs at bus 50 and 61.....	77
Table 4.6	Indian 85-bus system: The number and location of the power flow meters of different meter accuracy (with no DG).....	83
Table 4.7	Indian 85-bus system: The number and location of the power flow meters of different meter accuracy (Type 1 DG at bus 45 and 61).....	84
Table 4.8	Indian 85-bus system: The number and location of the power flow meters in presence of type 2 and 3 DGs at bus 45 and 61.....	85
Table 4.9	IEEE 69-bus system: The number and location of the power flow meters of different meter accuracy (without DG).....	91
Table 4.10	Indian 85-bus system: The number and location of the power flow meters of different meter accuracy (without DG).....	97

Table 5.1	Parameters used in EDA, NSGA-II and SA algorithm	111
Table 5.2	Distribution generation (DG) installation bus and capacity.....	111
Table 5.3	Optimal location of PMU and IED in IEEE 69-bus active distribution system....	118
Table 5.4	Optimal location of PMU and IED in Indian 85-bus active distribution system...	124
Table 6.1	Parameter values of KH, PSO and NSGA-II algorithm.....	135
Table 6.2	Wind generators base case value and their locations.....	136
Table 6.3	Parameters value for wind generators.....	136
Table 6.4	Optimal location of PMU and IED in IEEE 69-bus active distribution system....	142
Table 6.5	Optimal location of PMUs and IEDs in Indian 85-bus active distribution system.	150
Table 6.6	Optimal location of PMUs and IEDs in IEEE 69- bus active distribution system.....	156
Table 6.6	Optimal location of PMUs and IEDs in Indian 85- bus active distribution system.....	157

Abbreviations

APE	Average relative percentage Error
BC-DSSE	Branch Current Based Distribution System State Estimation
DER	Distributed Energy Resources
DG	Distributed Generation
DP	Dynamic Programming
DSE	Distribution State Estimation
DSSE	Distribution System State Estimation
EDA	Estimation of Distribution Algorithm
EMS	Energy Management Systems
EV	Electric Vehicle
GA	Genetic Algorithm
IED	Intelligent Electronic Devices
IPM	Interior-Point Method
KH	Krill Herd
KKT	Karush-Kuhn Tucker
MASE	Multi-area State Estimation
MC	Monte-Carlo
MOO	Multi-objective Optimization
MOOP	Multi-objective Optimization Problem
NC	Number of operating Condition
NSGA-II	Non-Dominated Sorting Genetic Algorithm
OOA	Ordinal Optimization Algorithm
PMU	Phasor Measurement Unit
PSO	Particle Swarm Optimization
PSO-KH	Particle Swarm Optimization- Krill Herd
RMS	Root Mean Square
RTU	Remote Terminal Unit
SCADA	Supervisory Control and Data Acquisition
SE	State Estimation

UTC	Coordinated Universal Time
VMM	Voltage Magnitude Measurement
WLS	Weighted Least Square

List of Symbols

n	Number of buses
z	Measurement vector
$h(x)$	Non-linear measurement function
e	Small Gaussian noise
$J(x)$	Objective function of the weighted least square method
w_i	Weight associated with i^{th} measurement
M	Number of objective functions
W	Covariance matrix of the measurements
Δx^k	Corrections at k^{th} iteration
$G(x_k)$	Gain Matrix at k^{th} iteration
$H(x_k)$	Jacobian Matrix at k^{th} iteration
x^k	Value of the state variable x at k^{th} iteration
x^{k+1}	Value of the state variable x at $(k+1)^{th}$ iteration
$ \Delta x $	Absolute value of the change in x
ϵ	Tolerance limit
P_{km}	Magnitude of real power flow in a line km
Q_{km}	Magnitude of reactive power flow in a line km
V_k	Voltage Magnitude at k^{th} bus
I_{km}	Current Magnitude in line km
δ_k	Voltage angle at k^{th} bus
α_{km}	Impedance angle of the line km
θ_{km}	Branch current angle of the line km
\vec{V}_k	Voltage phasor at k^{th} bus
P_k	Injected real power at k^{th} bus
Q_k	Injected reactive power at k^{th} bus

\vec{V}_{n+1}	Voltage phasor at $(n+1)^{th}$ bus
\vec{V}_0	Voltage phasor at reference bus
\vec{Z}	Impedance of a line in phasor form
F_1	Total cost of Power flow meters and voltage magnitude meters
F_2	Average relative percentage error in bus voltage magnitude
F_3	Average relative percentage error in bus voltage angle
F_i	Foraging motion of the i^{th} particle
$C_{pf,i}$	Cost of a power flow meter in pu
$P_{pf,i}$	A binary decision variable represents present or absence of a power flow meter
$C_{VMM,i}$	Cost of a voltage magnitude meter in pu
$P_{VMM,i}$	A binary decision variable represents present or absence of a power flow meter
V_i^a	Actual value of the voltage magnitude at i^{th} bus
V_i^{est}	Estimated value of the voltage magnitude at i^{th} bus
δ_i^a	Actual value of the bus voltage angle at i^{th} bus
δ_i^{est}	Estimated value of the bus voltage angle at i^{th} bus
L_i	Position of the i^{th} particle
M_i	Induced motion of the i^{th} particle
D_i	Random diffusion of the i^{th} Krill individuals
M^{\max}	Maximum induced speed
w_n	Inertia weight of the induced motion
α_i	Direction of the motion induced by i^{th} krill individual
α_i^{local}	Local effect produced by the neighbors
α_i^{target}	Target direction produced by the best krill individual
v_f	Foraging speed
w_f	Inertia weight of the foraging motion
ϕ_i^{food}	Food attractiveness

ϕ_i^{best}	Effect of the best fitness of the i^{th} Krills
D^{max}	Maximum diffusion speed
d	Random directional vector
Δt	Time interval
C_t	Constant number between [0, 2]
u_i	Upper limits of i^{th} Krill individuals
l_i	Lower limits of i^{th} Krill individuals
$L_{i,j}$	Position of the i^{th} Component of the j^{th} Krill individual
C_p	Crossover probability
$K_{i,\text{best}}$	Best previously visited position of the i^{th} Krill individual
M_p	Crossover probability
popsize	Population size
$p_s(x)$	Probability that an individual being among the selected population
$f(x)$	Objective function
y^T	Dual variables
μ	Barrier parameter
$g(x)$	Inequality constraint
$C1$	Learning factors
$C2$	Learning factors
W_{max}	Maximum value of weight used in PSO
W_{min}	Minimum value of weight used in PSO
M_c	Mutation rate in NSGA-II algorithm
P_c	Crossover rate in NSGA-II algorithm
W_{IED}	Covariance matrix of the uncertainty of the IED measurement
W_s	Covariance matrix of the measurements obtained from substation
W_{PMU}	Covariance matrix of the uncertainty of measurements obtained from PMU
W_p	Covariance matrix of the pseudo-measurements

W_V	Covariance matrix of the virtual-measurements
z_S	Substation measurements
$h_S(x)$	Non-linear measurement function of the substation measurements
z_{IED}	Measurement vector of IED measurements
$h_{IED}(x)$	Non-linear measurement function of the IED measurements
$h_{PMU.}$	Non-linear measurement function of the PMU measurements
z_{PMU}	Measurement vector of PMU measurements
z_P	Measurement vector of pseudo-measurements
$h_P(x)$	Non-linear measurement function of the pseudo-measurements
z_V	Measurement vector of virtual-measurements
$h_V(x)$	Non-linear measurement function of the virtual-measurements
E_{xx}	Error covariance matrix
E_x	Operator of statistical expectation
J_1	Total cost of IED
J_2	Total cost of PMU
J_3	Average value of the RMS value of state estimation error
$C_{IED.}$	Cost of a IED in pu
P_{IED}	Binary representation of the presence or absence of a IED
$C_{PMU.}$	Cost of a PMU in pu
P_{PMU}	Binary representation of the presence or absence of a PMU
$pbest_i$	Personal best of i^{th} particle in PSO
$gbest$	Global best solution
v_i^k	Velocity of i^{th} particle at k^{th} iteration

Chapter 1

Introduction

Chapter 1

Introduction

1.1 State Estimation Overview

The development of the State Estimation (SE) methods for electrical power systems evolved in 1970s. The use of SE techniques was first introduced by Fred Schweppe to estimate the states of the transmission networks more accurately from available information. Schweppe proposed that SE is a combination of load flow and estimation theory based on statistics [1-3]. Fundamentally, SE is a data processing algorithm which processes raw data obtained from the field and network data such as line impedance and connectivity of the network etc., to produce accurate estimation of the operating state of a system. According to Schweppe, the operating state of an electrical power system can be determined after knowing the voltage magnitudes and angles at all the buses of the network. As, the rest of the quantities such as power flow in a line, losses and voltage drops can be computed. It provides an overall situational awareness of an electrical power system.

Basically, SE provides a mathematical link between the system states such as bus voltage magnitudes and phase angles, and available measurements obtained from the meters deployed at the field. These measurement data are collected through Supervisory Control and Data Acquisition (SCADA) system installed at Energy Management System (EMS). In fact, these measurements are prone to errors due to the limited accuracy level of the measurement devices. Furthermore, while transferring the measurement data from the field to the control center, there may be a chance of communication errors, loss of telemetry data, presence of bad data and instrument failures. Therefore, the obtained measurement data should not be processed directly for taking controlling actions in a system. As a result, a suitable data processing technique is needed to filter out the errors intrinsically associated with measurements, to handle the possibility of communication failure and to remove any bad data if these are present in the measurement set. Hence, SE plays a very crucial role in EMS for real time monitoring, control and protection of electrical power systems. It acts as the heart of the energy management systems.

Many researchers have proposed numerous state estimation techniques to enhance the estimation accuracy at the control centers. A comprehensive study on transmission system state estimation can be found in [4-6].

In general, the main function of the state estimator in power system is shown in figure

1.1. The functions of an estimator are as follows:

1. **Topology Processor:** The function of the topology processor is to build the connectivity of the network by using the information about the status of the switches and circuit breakers in a network. It represents current topology of the system.
2. **Observability analysis:** The measurements obtained from the grid are to be analyzed to see if the system is observable with the available measurements. If sufficient measurements are not available to make the system observable, then pseudo-measurements are used to maintain the redundancy level to make the system observable. SE can then be run to determine the status of the network.
3. **State estimation algorithm:** It is a digital filtering algorithm which processes the raw data obtained from the field and produces reliable data. After estimating the states of the system various control actions are initiated at the control centre.
4. **Bad data detection and identification:** After SE, this step is to be carried out to detect, identify and remove any bad data present in the measurement set. Basically, bad data are present due to the malfunctioning of the measuring instrument or communication errors. A bad data checking can also be performed before running the state estimation algorithm to immediately present the occurrence of bad measurements in the measurement set.

The flow chart of the typical power system state estimator is shown in Figure 1.1. Each of the steps discussed above is an important function of the state estimator and the sequence of operation is shown in the flow chart. During the sequence of operation, if bad data or network topological error is detected, then SE algorithm has to be run repeatedly because these errors drastically reduces the accuracy of the state estimation results. There is plenty of research going on at each stages of the state estimator to achieve quality SE results as well as for better functionality such as monitoring, control and protection of the power system.

Figure 1.2 represents the schematic diagram of the Energy Management Systems (EMS). There are two functional blocks in every EMS center such as state estimator and control scheduling blocks. The SE block is the heart of the EMS which processes the input data such as network parameter, measurements and status of the switches, circuit breaker to produce reliable data for various controlling actions in power system. The controlling actions such as automatic

generation control, switching of capacitor, loads and circuit breakers, security and contingency analysis are carried out after the output obtained from the state estimator.

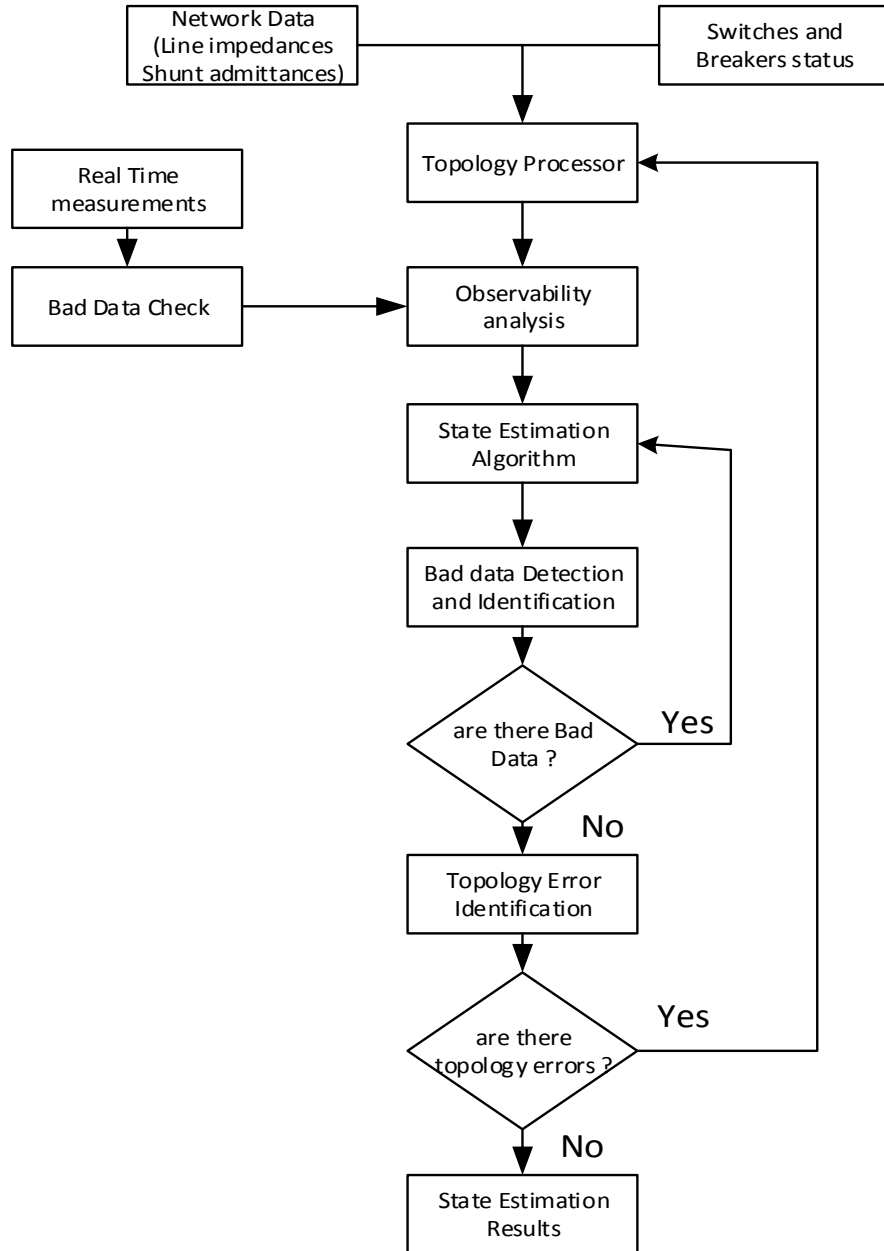


Figure 1.1: Flow chart of the typical power system state estimator

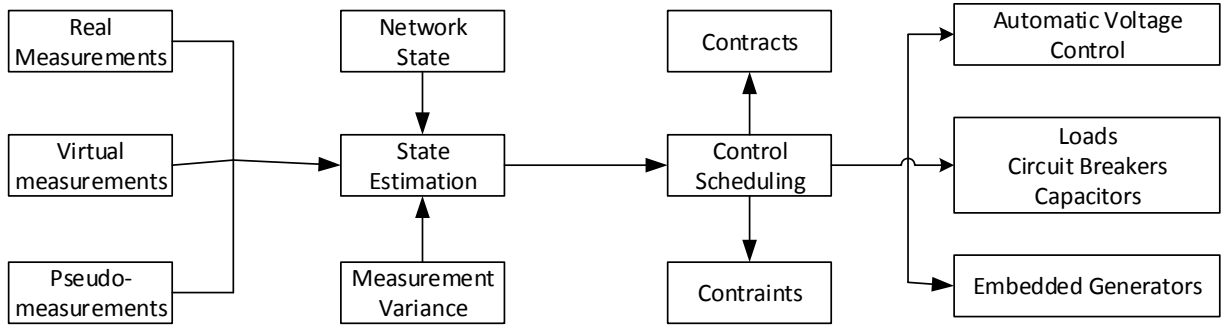


Figure 1.2: Schematic representation of Energy Management Systems (EMS)

1.2 Distribution System State Estimation (DSSE)

1.2.1 Evolution of distribution systems

In recent years there has been a growing interest towards distribution automation to operate the distribution systems more efficiently and economically. The main function of the distribution automation is real time monitoring, control and protection of distribution systems. The future growth of the distribution grids is leading towards the use of sustainable and environmental friendly energy sources. Therefore, many countries are providing the facility in terms of incentives for the installation of renewable energy sources such as photovoltaic cell and wind generator etc. As a result, a large number of renewable energy sources have been installed at the distribution level to the so called distributed generators (DGs) to fulfill the customer load demand. Furthermore, it is expected that in upcoming future, there will be a massive deployment of Electric Vehicles (EVs) and energy storage devices throughout the distribution networks for electricity usage [7]. All these elements such as DGs, EVs and energy storage devices are called distributed energy sources (DERs). The availability of DERs provides more flexible and efficient use of electrical energy in a distribution network.

In recent times the distribution grids are more dynamic and complex in structures because of the integration of renewable sources, distributed energy storage as well as intelligent electronic devices (IED) and Smart meters. The increasing integration of distributed generation (DG) in a distribution network will affect the planning operation and control of a distribution network significantly. The active integration of DG results in bi-directional power flows from distribution level to sub-transmission level as well as exacerbating voltage unbalance in distribution networks [8]. Furthermore, the reconfiguration of the distribution system is used to minimize the power

loss, voltage deviations and restoration time. In most of the cases the distribution networks are weakly meshed structures. Thus, the states of distribution systems such as bus voltage magnitude and angles have to be estimated more accurately for real-time monitoring and control of the networks. To achieve this, real meters have been appended in distribution systems to estimate the states more accurately for other control actions such as network reconfiguration, Volt/Var control, generation control, restoration, voltage regulation, etc [9]. Actually, meters can be placed at each and every point of the distribution network. However, it would affect the total configuration cost of the distribution system.

Basically, in distribution networks, pseudo-measurements are being used more significantly than real measurements. Therefore, state estimation (SE) algorithm is employed to estimate the state of a system more accurately from the noisy data available at the distribution control centers [10]. However, in distribution system sufficient real time measurements are not available. Therefore, accurate SE is a more challenging task for power engineers. So, a large number of pseudo-measurements have been incorporated in SE algorithms to make the system fully observable and also to avoid non-convergence of the state estimation algorithm. In fact, the pseudo-measurements are comparatively less accurate in nature because these are extracted from the historical customer load data. As a consequence, more accurate state estimation cannot be expected in this scenario. Therefore, adequate number of additional real meters has to be located at suitable locations in a distribution network to produce quality of state estimation solution.

In distribution grids, due to the presence of different kinds of actors such as distributed generation (DG), energy storage devices, the system becomes more complex, dynamics and uncertain in nature [11]. Because of this changing behavior of actors, real-time monitoring and control becomes a more challenging task for the power system engineers. Thus, PMUs are of great interest because they provide synchronized measurements of voltage, current and power. The application of PMU for state estimation in transmission system has been widely used to improve the performance of the state estimator. Therefore it would be more advantageous to use PMU in DSSE. In transmission systems, PMUs have been used widely to improve the state estimator performance using different approaches. Therefore, utilization of the phasor measurements in distribution network for state estimation is of great interest. The PMU provides synchronized measurements e.g. voltage and current phasors, power and frequency along with some indirect measurements. The measurements obtained from the PMUs are synchronized with

the coordinated Universal Time (UTC). In transmission systems, the synchronized measurements obtained from PMUs along with the non-synchronized measurements from SCADA system have been used by many researchers for improvising the performance of state estimator [12-17].

However, due to lack of sufficient direct measurements in distribution networks, locating PMUs is economically unreasonable. Therefore, the techniques used for locating PMUs in transmission grids cannot be directly transformed at the distribution level. In order to compensate this, a large number of pseudo-measurements derived from historical customer load data are being used for the state estimation in distribution systems. But, as a result, the accuracy of state estimation deteriorates to a very large extent. Many researchers have proposed different techniques to deploy PMUs in distribution grids.

1.2.2 Characteristics of Distribution Systems

Due to the peculiar characteristics of the distribution systems, state estimation algorithm used in transmission system cannot be simply transferred to distribution system. There are several aspects under which distribution networks are different from transmission system. Typical characteristics of distribution networks affecting DSSE are as follows [18]:

- 1) **Unbalanced Nature:** Basically transmission and distribution grids are three-phase networks. Transmission networks are treated as balanced system due to transposition and can be modeled as single phase equivalent representing the positive sequence of the network. However, distribution grids are unbalanced in nature due to the presence of unbalance loads as well as some two-phase and single-phase feeders in the network. Therefore, distribution grids rely on a three phase model. Moreover, large integration of small sized distribution generation at distribution level again results once again in imbalance in the grids [19-20].
- 2) **Network Topology:** Generally, transmission networks are designed as meshed structure to make the system more reliable whereas distribution grids are radial and weakly meshed structures. Therefore, the state estimation algorithms are differently designed for distribution networks. For this reason branch current based state estimation algorithm has been used instead of node voltage based state estimation formulation. It is faster and more efficient to exploit a radial as well as weakly meshed network than a node voltage formulation.
- 3) **Line Parameters:** The transmission and distribution lines are designed differently due to different voltage levels and physical properties. In transmission lines, series resistance is significantly smaller than reactance in the equivalent π model of the network. Therefore, the

R/X ratio of the transmission line is very low. Hence, series line resistance can be neglected for all practical purposes. However, in distribution grids the R/X ratio is too high and cannot be neglected. Due to high R/X ratio, the decoupling version of the DSSE algorithm is not that much easy to obtain.

- 4) Network Size: This plays a very critical role for distribution systems. Generally, in medium voltage distribution grids, the number of nodes is larger than the number of nodes in transmission grids. As a consequence, the computational cost of the DSSE algorithm for state estimation is increased to a great extent and it also demands data acquisition and storage at the control centers. Therefore, an efficient DSSE algorithm is needed for this. To reduce computational burden, a Multi-area distribution system state estimation offers an alternative solution. In multi-area state estimation (MASE), the total network is divided into sub areas and DSSE is run for each sub area to estimate the states of the whole network. Though MASE technique reduces the execution time but careful attention needs to be paid during the formulation of MASE algorithms. However, MASE techniques may lead to significant loss of accuracy in the estimation process and also it may also give rise to some additional communication problem between the sub-areas.
- 5) Limited Measurement Devices: Basically, in distribution grids, a very limited number of measurement devices is placed due to the large size of the network. As a consequence, the redundancy of measurements is not sufficient for state estimation process and hence the network becomes unobservable. To make the network observable, sufficient pseudo-measurements have been used. These measurements are derived from the historical customer load data. To create pseudo-measurements, power injections at all the buses are used. The use of pseudo-measurement helps to observe the network as well as to run DSSE algorithm [21-23]. However, the main drawbacks in including pseudo-measurements in DSSE study is, these measurements are associated with a large error. Therefore, to improve the accuracy of the state estimator, many researchers are using meter placement technique for state estimation. The optimal location of the meters is determined to reduce configuration cost and to produce quality of state estimation.

1.3 Weighted Least Square (WLS) based State Estimation

State estimation can be performed by using different statistical approaches such as weighted least square (WLS), maximum likelihood criteria or minimum variance approach. All

the above methods use the same measurement model discussed below. The measurement model used for state estimation algorithm is shown as follows:

1.3.1 Measurement Model

For state estimation the commonly used measurement model is:

$$z = h(x) + e \quad (1.1)$$

where:

- z is the vector of available measurements at the control center which is used as input to the state estimation algorithm. Different kinds of measurements are obtained from the grid at the control center such as voltage magnitude at the nodes, current, real and reactive power flows in lines or injections at all the buses.
- x represents vector of state variables. Traditionally, voltage magnitude and angle are chosen as state variables in a transmission system. However, the state of a system represents a variable through which all other quantities of a system can be determined. Therefore, variables other than voltage magnitude and angle can be chosen for a system.
- $h(x)$ indicates the vector of measurement functions which establish a relationship between state variable and measurements. It is a function of state variable x .
- e represents the vector of the measurement errors. They are assumed to be normal distribution with zero mean.

1.3.2 Mathematical Model of the WLS Method

Many alternative methods have been proposed for state estimation in the literature, but in most of the cases WLS method has been used both in transmission and distribution systems. Because of its best performance in terms of consistency and quality of estimation, it can be the best choice for DSSE [24-29].

The main objective of WLS method is to minimize the weighted sum of the square of the difference between the measured and estimated value of the quantity. Mathematically, it can be defined as follows:

$$J(x) = \sum_{i=1}^m w_i [z_i - h_i(x)]^2 \quad (1.2)$$

where m represents the total number of measurements available, w_i is the weight associated

with the i^{th} measurement. The term $[z_i - h(x)]$ is called measurement residual which is the difference between the measured value and the estimated value of the quantity.

The above equation can be written in matrix form as follows

$$J(x) = [z - h(x)]W[z - h(x)]^T \quad (1.3)$$

where W represents weighting matrix and consists of weights w on the diagonal elements of the $m \times m$ matrix. The weighting matrix plays a vital role in WLS method. It consists of different reliability of measurements.

The solution of the above objective function is obtained using an iterative method such as Newton method to find a correction at each step k as follows:

$$\Delta x^k = G(x_k)^{-1} [H(x_k)^T W^{-1}] [z - h(x_k)] \quad (1.4)$$

$$x^{k+1} = x^k + \Delta x^k \quad (1.5)$$

$$x_{k+1} = x_k + G(x_k)^{-1} [H(x_k)^T W^{-1}] [z - h(x_k)] \quad (1.6)$$

$$G(x_k) = H(x_k)^T W^{-1} H(x_k) \quad (1.7)$$

where H is the Jacobian matrix of the measurement function $h(x)$, $G(x)$ represents Gain matrix and Δx is the correction at k^{th} iteration used to compute the new value of the state variable for the $(k+1)^{th}$ iteration shown in equation (1.5). The Jacobian matrix is calculated by taking the differentiation of each measurement function with respect to each state variable. Mathematically it can be expressed as follows:

$$H(x) = \frac{\partial h(x)}{\partial x} \quad (1.8)$$

In WLS method the iterative process is continued until a specified convergence criterion is met. Basically, the largest value of the correction vector obtained in each iteration is compared with a pre-defined tolerance limit ϵ and the iteration count stops when the maximum value of the absolute value of the correction Δx is within the specified threshold limit ϵ . Mathematically this can be defined as follows:

$$\max(|\Delta x|) \leq \epsilon \quad (1.9)$$

1.4 Branch Current Based Distribution System State Estimation (BC-DSSE)

The distribution system has different features than transmission system, therefore, the state estimation algorithm used for transmission case cannot be used at distribution level. In

transmission system, traditionally, bus voltage magnitude and angle is considered as state variable. But, in distribution system the branch current magnitude and angle is taken as state variable to estimate the states efficiently. Many alternative methods have been discussed in literature for state estimation techniques in distribution system. A general form of DSSE algorithm is discussed as follows:

1.4.1 Measurement functions $h(x)$ and Jacobian Matrix Formulation $H(x)$

In BC-DSSE algorithm, the measurements used for state estimation are, real and reactive power flow in a line, voltage magnitude measurements, current magnitude measurements, real and reactive power injections at the buses etc. The elements of the Jacobian matrix are calculated by taking the differentiation of each measurement function with respect to each state variable described in equation (1.8). In this work it is assumed that the distribution system is a balanced system, therefore the single-phase model of the distribution network is presented. The measurement functions and Jacobian entries are described as follows:

- 1) Branch Power Measurements: The power flow in a line km at the end k is stated as follows:

$$P_{km} + jQ_{km} = V_k I_{km} [\cos(\delta_k - \alpha_{km}) + j \sin(\delta_k - \alpha_{km})] \quad (1.10)$$

The corresponding Jacobian entries can be determined as

- When the state variable and the power flow measurements are in the same line the corresponding Jacobian elements are:

$$\frac{\partial P_{km}}{\partial I_{km}} = V_k \cos(\delta_k - \theta_{km}) \quad (1.11)$$

$$\frac{\partial P_{km}}{\partial \theta_{km}} = V_k I_{km} \sin(\delta_k - \theta_{km}) \quad (1.12)$$

$$\frac{\partial Q_{km}}{\partial I_{km}} = V_k \sin(\delta_k - \theta_{km}) \quad (1.13)$$

$$\frac{\partial P_{km}}{\partial \theta_{km}} = -V_k I_{km} \cos(\delta_k - \theta_{km}) \quad (1.14)$$

- When the branch power measurements and the state variables are not in the same line segment then the Jacobian entries will be zero.

2) Power injection measurements:

Suppose in a network power is injected at bus k and there are n buses connected to bus k. It is assumed that current is flowing from bus k to bus 1..... m and it also flows from bus m+1....n to bus k. Therefore, buses 1....m are considered as upstream buses of k bus and buses m+1 to n are treated as downstream buses of k bus. The total power injected at bus k can be expressed as follows:

$$P_k + jQ_k = \vec{V}_k \left(\sum_{i=1}^m I_{ik} - \sum_{m+1}^n I_{ki} \right)^* \quad (1.15)$$

Hence, three different cases are formed to find the entries of the Jacobian matrix given below:

Case 1: When bus k is connected to its upstream buses and the state variable are in the same line segment then the Jacobian entries are determined as follows:

$$\frac{\partial P_k}{\partial I_{ik}} = V_k \cos(\delta_k - \theta_{ik}) \quad (1.16)$$

$$\frac{\partial P_k}{\partial \theta_{ik}} = V_k I_{ik} \sin(\delta_k - \theta_{ik}) \quad (1.17)$$

$$\frac{\partial Q_k}{\partial I_{ik}} = V_k \sin(\delta_k - \theta_{ik}) \quad (1.18)$$

$$\frac{\partial Q_k}{\partial \theta_{ik}} = -V_k I_{ik} \cos(\delta_k - \theta_{ik}) \quad (1.19)$$

Case 2: When bus k is connected to its downstream buses and the state variable are in the same line segment then the Jacobian entries are determined as follows:

$$\frac{\partial P_k}{\partial I_{ik}} = -V_k \cos(\delta_k - \theta_{ik}) \quad (1.20)$$

$$\frac{\partial P_k}{\partial \theta_{ik}} = -V_k I_{ik} \sin(\delta_k - \theta_{ik}) \quad (1.21)$$

$$\frac{\partial Q_k}{\partial I_{ik}} = -V_k \sin(\delta_k - \theta_{ik}) \quad (1.22)$$

$$\frac{\partial Q_k}{\partial \theta_{ik}} = V_k I_{ik} \cos(\delta_k - \theta_{ik}) \quad (1.23)$$

Case 3: If the line is not connected to the bus at which the power is injected, then the corresponding Jacobian entries are taken as zero.

3) Voltage magnitude measurements:

Suppose the magnitude of voltage is measured at bus k and there are n lines connecting bus k to reference bus 0 and also it is assumed that all lines current are flowing away from the reference node. Then, the voltage at bus k can be determined as follows:

$$\vec{V}_{n+1} = \vec{V}_0 - \sum_{i=1}^{n+1} \vec{I}_{(i-1,i)} \vec{Z}_{i-1,i}$$

The corresponding Jacobian elements are determined as:

Case 1: If the line is lying between the reference node and the bus where the voltage is measured then the Jacobian elements are:

$$\frac{\partial V_{n+1}}{\partial I_{i-1,i}} = -\cos \delta_{n+1} \cdot Z_{i-1,i} \cos(\theta_{i-1,i} + \alpha_{i-1,i}) - \sin \delta_{n+1} \cdot Z_{i-1,i} \sin(\theta_{i-1,i} + \alpha_{i-1,i}) \quad (1.24)$$

$$\frac{\partial V_{n+1}}{\partial \theta_{i-1,i}} = \cos \delta_{n+1} \cdot I_{i-1,i} \cdot Z_{i-1,i} \sin(\theta_{i-1,i} + \alpha_{i-1,i}) - \sin \delta_{n+1} \cdot I_{i-1,i} \cdot Z_{i-1,i} \cos(\theta_{i-1,i} + \alpha_{i-1,i}) \quad (1.25)$$

Case 2: If the line is not lying between the reference node and the bus where the voltage is measured then the corresponding all Jacobian elements are set to zero.

1.4.2 BC-DSSE Algorithm Steps

The BC-DSSE method is based on iterative approach consists of three main steps are discussed as follows:

1. Updated input measurements
2. Solution of the equation (1.4) of the WLS algorithm
3. Forward sweep method to calculate bus voltages at each node of the network.

The BC-DSSE algorithm is based on the following steps:

1) Initialization:

The initialization of the branch current phasor has a great impact on the convergence of the state estimation algorithm. Therefore, a two step approach has been used to initialize the state variables. In the first step, the voltage at every node is set at 1 pu and then by using backward approach, the current at all the lines is determined through injected power at every node. In the second step, the forward sweep method is used to calculate the initial value of voltage.

2) Updates the system states using equation (1.5).

$$x^{k+1} = x^k + \Delta x^k$$

$$x_{k+1} = x_k + G(x_k)^{-1} \left[H(x_k)^T W^{-1} \right] [z - h(x_k)]$$

- 3) Use forward approach to calculate voltages at every node.
- 4) If the convergence criterion is met i.e. $\max(|\Delta x|) \leq \epsilon$ then stop. If it is not satisfied then go to step 2 and repeat till the convergence is achieved. If it is not satisfied the criterions till the maximum number of generation then it does not converge.

1.5 Meta-heuristic Optimization Algorithm

The meta-heuristic optimization algorithms have been used often in various engineering discipline to solve optimization problems. It guides a subordinate heuristic by intelligently combining different concepts to explore and exploit the search space more efficiently. Different learning strategies are being used to find an effective optimal solution. These optimization algorithms are classified into two categories:

- i) Population-based methods (multiple solution based methods) and
- ii) Trajectory –based methods (single-solution based methods)

Basically, the population based algorithms are inspired from nature whereas trajectory based method are inspired from physics. The population based algorithms such as Genetic algorithm (GA), Particle Swarm Optimization (PSO), Ant Colony Optimization (ACO) etc., use multiple solutions to search for an optimal solution. On the other hand, trajectory based methods such as Simulated Annealing (SA), Tabu search, tree search algorithms etc., use a single solution move in a piece-wise manner in the search space to find an optimal solution. The steps of the trajectory based methods trace a trajectory in the search space during the search process to find an optimal solution. The general properties of the meta-heuristic optimization techniques are as follows:

- These are straight forward and guide the search process.
- The goal is to efficiently explore the search space in order to find near global optimal solutions.
- Techniques which constitute meta-heuristic algorithm range from simple local search procedures to complex learning processes.

- They can incorporate mechanism to avoid getting trapped in confined areas of the search space.
- Meta-heuristic algorithms are non-problem specific.
- Meta-heuristic algorithms are non-deterministic in nature.
- These algorithms can make use of domain specific knowledge in the form of heuristics that are controlled by upper level strategy.

1.6 Phasor Measurement Units (PMUs)

PMU is a device which measures the electrical waves on an electricity grid using a common time source for synchronization. Time synchronization allows synchronized real time measurements of multiple remote measurement points on the grid. The resulting measurement is called as a synchrophasor. It is used to measure voltage and current phasors, frequency and other indirect measurements in an electrical network. The measurements obtained from the PMUs are synchronized with the coordinated Universal Time. In transmission systems, the synchronized measurements obtained from PMUs along with the non-synchronized measurements from Supervisory Control and Data Acquisition (SCADA) system have been used by many researchers for improvising the performance of state estimator

1.7 Intelligent Electronics Devices (IEDs)

An Intelligent Electronic Device (IED) is a microprocessor-based controller of power system equipment such as circuit breakers, transformers and capacitor banks. It has the ability to monitor processes and can communicate directly to a SCADA system. It can be used as a measuring device which can measure real and reactive power flow in a feeder. Mainly, it is used as a protecting device in power system. In this work, it is considered that it measures real and reactive power flow in a line. It provides non-synchronized measurements.

Chapter 2

Literature Review

Chapter 2

Literature Review

2.1 Introduction

State estimation (SE) technique is generally used to find the system state variables under different operating condition of the power system. It brings a mathematical relation between measurements and system variables to make secure operations in power system. Most of the field measurements are subjected to some errors. So, SE is used to process the unreliable or noisy data to produce reliable data which can be used for system analysis. There are various functions of state estimator such as network topology processor, observability analysis, state estimation and bad data detection and identification. The function of the topology processor is to ensure that the network parameters given to the estimator are correct and also ensure that the network model is accurate. The observability analysis ensures that sufficient measurements are available for SE or else sufficient Pseudo-measurements like real power flow and injections are used to make the system observable. The function of SE is to estimate the system states accurately using available measurement data. Finally, bad data processor is used to identify and remove any bad data present in system measurements. There are numerous techniques developed for power system state estimation. Because of the peculiar characteristics of distribution networks such as high r/x ratio, unbalanced nature, radial structure and limited available measurements, SE techniques used in transmission system cannot be applied to distribution systems directly. The techniques developed for distribution system state estimation are discussed as follows.

2.1.1 DSSE based on conventional WLS method

In [31], Baran and Kelly proposed a three-phase SE algorithm based on node voltage formulation using weighted least square (WLS) approach. The authors considered bus voltage magnitudes and phase angles as state variables. A three-phase model of the distribution feeder has been developed and the coupling effect between the feeders taken into consideration. In [32], the authors have proposed branch current based SE in distribution network which is more efficient and reliable than node voltage formulation method because it is computationally more efficient. Furthermore, this approach considers a few loops in a network. In [33], a three-phase DSSE algorithm is proposed. A current based formulation is proposed which considers a rectangular form of branch current as state variable. In [34]-[35], DSSE based on WLS approach

and three-phase modeling of distribution network is proposed. In [36], a probabilistic approach for state estimation in distribution network is proposed. It takes into account the real-time measurements as solution constraints and also includes load diversity concept in order to account for the non-normally distributed load in state estimation.

A robust three-phase state estimation algorithm is proposed for unbalanced distribution network [37]. In [38], a highly efficient algorithm for using current measurements for state estimation in distribution network is proposed. The authors have developed a new algorithm which makes the gain matrix constant and also decouples it on phase basis. Therefore, the computational time is reduced. In [39], a branch estimation based SE for distribution network is proposed. It decomposes the whole WLS problem into a series of sub problems and each sub problem deals with a single branch state estimation only. An efficient branch current based state estimation technique is proposed using WLS approach [40]. The authors have used magnitude and phase angles of branch currents as state variables for SE. An efficient branch current based DSSE is introduced using synchronized measurements data [41]. The authors have considered both radial and weakly meshed topology for state estimation. The state variables are expressed both in polar and rectangular coordinates including slack bus voltage as state variables. In [42], a state estimation method based on power summation method is proposed for three-phase balanced and unbalanced distribution system.

All the methods discussed above are based on network topology modeling to develop new efficient algorithm for SE. The next section will discuss state estimation techniques based on load modeling approach.

2.1.2 DSSE based on load modeling

Load modeling and estimation plays a very important role in improvement of the accuracy of the distribution state estimator. In the absence of loads which are highly diverse and distributed in nature, pseudo measurements with appropriate mean and standard deviations are used for state estimation. The pseudo-measurements are naturally modeled through Gaussian distribution because it is more compatible with WLS based maximum likelihood estimation. Many researchers have used the concept of load modeling to improve the performance of the state estimator in a distribution network. In [43], a real-time load modeling technique is introduced in distribution state estimation. It incorporates customer class load curves for

estimation purpose. In this paper the load modeling technique is combined with state estimation based on probabilistic approach to estimate the states of a distribution circuit.

A load allocation model is proposed which generates a fuzzy load allocation and then corrected by a fuzzy state estimator procedure in order to generate a crisp power flow compatible with a set of load allocations and correlated with available real measurements available from the SCADA [44]. In [45]-[46], because of limited real-time measurements, a load modeling technique is used which estimates the real-time customer load profile. This can be used as pseudo-measurements for SE in distribution networks. In [47]-[48], WLS method and sensitivity method based load estimation in unbalanced distribution network is discussed. [49], introduces a method which can estimate the unavailable measurements due to metering problems in a distribution network. A regression based model has been used along with correlated loads which are geographically very close to each other to improve SE performance. From the results it is found that this method gives acceptable performance for measurement loss of up to a week.

2.1.3 DSSE based on computational intelligence and heuristic techniques

Many alternative methods have been developed for advance control and monitoring of the distribution networks. Some of the SE methods are based on the statistical and load modeling formulation. The former methods of SE are usually based on Newton method i.e. iterative convergence methods and load estimation methods are based on sensitivity analysis. The objective functions of the conventional DSE methods are assumed as continuous and differentiable. However, when non-linear practical equipments are present in distribution systems, the objective functions cannot be differentiable and continuous. In that case it is more difficult to apply conventional DSE methods to estimate the state of the systems. Therefore, Meta-heuristic methods are widely used to solve non-linear optimization problem. It does not require the objective functions to be contiguous and differentiable. Some of the DSSE methods based on heuristic techniques are discussed as follows.

In [50], a hybrid particle swarm optimization (PSO) algorithm is used for state estimation in practical distribution network. This method can estimate distributed generation (DG) output and load by minimizing the difference between the measured and calculated values of bus voltage magnitudes and branch currents. In [51], a three phase state estimation in practical distribution network using hybrid particle swarm optimization algorithm is proposed. In SE, bus voltage magnitude, angle and transformer taps are considered as state variables to control the voltage i.e.

the state vector includes both continuous and discrete variables. In [52], ordinal optimization algorithm based state estimation in unbalanced distribution network is proposed. The authors have considered the combination of continuous and discrete variable in state vector. The discrete variables are on-load transformer taps. The performance of the OOA is found to be better than conventional WLS method in estimating the state and losses in a distribution network.

2.1.4 DSSE based on meter placement technique

SE is a digital filtering algorithm which can accurately determine the states of the system from noisy data. However, due to the limited number of real time measurements, accurate SE in distribution systems is more challenging. So, a large number of pseudo-measurements (historical data) retrieved from a priori knowledge are necessary to maintain observability of the network and convergence of SE algorithm. Additionally, the accuracy of pseudo-measurements is comparatively low. As a consequence, estimation accuracy is not as much accurate as is expected. Therefore, some additional meters need to be appended at appropriate locations in the distribution systems to achieve better estimation accuracy. In recent years, many alternative methods have been proposed by various researchers for enhancement of state estimation accuracy using meter placement techniques in distribution networks. In [53], Baran et al. introduced a rule based meter placement strategy and proposed three empirical rules based on observations i.e. meters have to be placed at all the main switches and fuse locations that have to be monitored, meters have to be placed at feeder line sections and on normally open tie switches used for feeder reconfiguration. This method of meter placement gives a good compromise between the accuracy and computational complexity but it does not guarantee optimal number of meters with minimum cost.

In [54], a heuristic technique based meter placement method is introduced. The optimization problem is designed as a nonlinear combinatorial constraint optimization problem and the objective function minimizes the mean of the weighted sum of the variance of the estimated quantities. The constraints imposed on this optimization problem is that the system would be observable with established accuracy with minimum number of meters. The authors have proposed dynamic programming (DP) following a step by step approach to find the optimal number of meters with required accuracy level.

In [55], J. Liu et al. proposed a meter placement technique in SE using Genetic algorithm (GA). The objective function considered for this optimization problem is the minimization of the

total cost combined with the specified accuracy index of the state estimation. The authors have used relative voltage and phase angle deviation as performance index for the optimization problem. Furthermore, an optimal trade-off solution is obtained between phasor measurement units and smart metering devices using GA. Pegoraro and Sulis [56], proposed a dynamic programming (DP) based meter placement technique to find the optimal placement of the measuring devices. The authors have considered both the network parameter uncertainty and decay of metrological characteristic of the measurement devices in distribution system state estimation. Sing et al. [57], addressed an ordinal optimization algorithm based meter placement scheme in distribution network. In this approach, the meters are placed progressively until the errors are below the pre-specified thresholds in 95% of the simulated cases. However, the solution obtained using ordinal optimization algorithm (OOA) may not be a global optimal solution, but it results in at least one of the suboptimal solutions. Shafiu et al. [58], have used a heuristic technique to deploy certain number of voltage measurements to reduce the standard deviations in estimated voltage at unmonitored buses. This method only reduces error in voltage magnitude not in phase angle. In [60], a circuit representation model was proposed for the optimal deployment of current and voltage measurements to represent estimation errors. The authors have transformed the optimization problem to a mixed integer linear programming problem. M.G. Damavandi et al. [62], proposed a robust meter placement in active distribution network for state estimation. A robust sub-modular saturation algorithm has been used to find the optimal location of PMUs and voltage magnitude meters in active distribution systems. The authors considered a fixed number of meters to find their optimal location. The major disadvantage of these optimization algorithms is that the solution obtained may not guarantee a global optimal solution because these are based on sequential placement of measurement devices to achieve the required state estimation accuracy. The sequential meter placement techniques may not achieve minimum number of meters with required accuracy level.

In distribution grids, due to the presence of different kinds of actors such as distributed generation (DG) and energy storage devices, the system becomes more complex, dynamics and uncertain in nature. Because of this changing behavior of actors, real-time monitoring and control becomes a more challenging task for the power system engineers. Thus, PMUs are of great interest because they provide synchronized measurements of voltage, current and power. The application of PMU for state estimation in transmission system has been widely used to improve

the performance of the state estimator. Therefore it would be more advantageous to use PMU in DSSE. In transmission systems, PMUs have been used widely to improve the state estimator performance using different approaches [62]-[70]. Therefore, utilization of the phasor measurements in distribution network for state estimation is of great interest. The PMU provides synchronized measurements e.g. voltage and current phasors, power and frequency along with some indirect measurements. The measurements obtained from the PMUs are synchronized with the coordinated Universal Time (UTC). In transmission systems, the synchronized measurements obtained from PMUs along with the non-synchronized measurements from Supervisory Control and Data Acquisition (SCADA) system have been used by many researchers for improvising the performance of state estimator [72]-[83].

2.2 Motivation

This thesis presents an extensive review of the research topic and optimal location of measurement devices for distribution system state estimation using meta-heuristic techniques. State estimation is the heart of energy management systems, which is used for real time monitoring, alarming and control of distribution networks. Therefore, accurate estimation of system states is more challenging for power system engineers.

- The quality of SE suffers because of a large number of pseudo-measurements which have very high variances. This can be improved by placing additional real measurements which have very low variances. Therefore, the design of an efficient algorithm for solving meter placement problem in distribution networks is needed.
- A multi-objective problem formulation is required instead of single-objective to establish a trade-off solution between objectives such as configuration cost of the network and state estimation accuracy.
- Due to high penetration of renewable energy sources, electric power system operation and control has become a complex and challenging issue for Energy Management Centers. Amongst all renewable energy sources, wind energy is the most proven around the world. Therefore, there is scope to develop a robust meter placement technique to enhance the estimation accuracy in presence of wind generators.

The thesis in general addressed the optimal allocation of measurement devices for distribution system state estimation using multi-objective hybrid evolutionary algorithms.

2.3 Contributions

The overall objective of the thesis is to design an efficient optimization model and algorithm for optimal allocation of measurement devices to improve the state estimation accuracy for online monitoring and control of the distribution networks.

The contributions made in the thesis are as follows:

- A new multi-objective hybrid PSO-Krill Herd Pareto based optimization algorithm to optimize number and location of the measurement devices for accurate state estimation in smart distribution networks is proposed. The idea is to minimize the following: (i) total network configuration cost (ii) average relative percentage error (APE) of bus voltage magnitude and (iii) APE of bus voltage angle. As the objective functions conflict with respect to each other, a multi-objective Pareto-based non-dominated sorting hybrid PSO-KH optimization algorithm is proposed. In this approach, the random variation in loads and the metrological error of the measurement devices are also taken into account. Furthermore, the impacts of DG on state estimation performance is also investigated.
- A new multi-objective hybrid Estimation of distribution algorithm (EDA)-interior point method (IPM) algorithm is proposed to obtain the optimal location of measuring devices for state estimation in active distribution networks. The objective functions to be minimized are, the total network configuration cost, the average relative percentage error (APE) of bus voltage magnitude and angle estimates. As the objectives seem to in conflict with each other, a multi-objective Pareto-based non-dominated sorting EDA has been proposed. Moreover, due to the poor exploitation capability of EDA, it is hybridized with IPM to improve its local searching ability in the search space. The hybridization of EDA and IPM brings a higher degree of balance between the exploration and exploitation capability of the algorithm during the search process. Furthermore, the loads and generators are treated as stochastic variables and the impact of different types of DGs on state estimation performance has also been investigated.
- A novel multi-objective optimization problem to find trade-offs in deployment of phasor measurement units (PMUs) and intelligent electronic devices (IEDs) for state estimation in active distribution networks is proposed. A new hybrid estimation of distribution algorithm (EDA) has been used to find the optimal number and location of measurement devices such

as PMUs and IEDs for accurate state estimation. The objective functions to be minimized in this optimization problem are the total cost of PMUs and IEDs, as well as the RMS value of state estimation error. Since the objectives are conflicting in nature, a multi-objective Pareto-based non-dominated sorting EDA algorithm is proposed. Moreover, to improve the local searching capability of the traditional EDA algorithm, Interior point method (IPM) is hybridized with EDA to get near global optimal solution. Furthermore, the random variation in loads and generators is also considered to check the reliability of the proposed meter placement technique.

- A novel multi-objective optimization model is developed to find trade-offs in deployment of phasor measurement units (PMUs) and intelligent electronic devices (IEDs) for state estimation in active distribution networks. All DGs are taken to be wind generator and the output of each DG is modeled using Weibull distribution function. The objective functions that require to be minimized are the total cost of PMUs and IEDs as well as the RMS value of state estimation error. To get best optimal solution, multi-objective hybrid PSO-Krill Herd algorithm has been used. Furthermore, the random variations in loads and generators are also considered to check the reliability of the proposed meter placement technique in presence of wind generators.

2.4 Thesis Organization

The thesis is organized as follows:

Chapter 1 introduces the basic to power system state estimation with relevant terms and various challenges posed for distribution system state estimation. It also explains in brief the need of state estimation techniques and the peculiar characteristics of distribution network. It also discusses the method used for estimation of system states in a distribution network.

Chapter 2 presents a detailed literature review on the research topic with past and present research. The literature reviewes various methods/ techniques used for distribution system state estimation such as load modeling, heuristic techniques based state estimation in distribution network and conventional WLS method based state estimation in distribution system. Later, the literature on meter placement techniques based distribution system state estimation is also reviewed with relevant analysis.

Following an extensive literature survey on the topic, motivation for the proposed research work is presented and then the contributions and organization of the thesis.

Chapter 3 begins with an introduction to distribution system state estimation. The multi-objective optimization model is designed. New multi-objective hybrid PSO-Krill Herd Pareto based optimization algorithm is presented to optimize the number and location of the measurement devices for accurate state estimation in smart distribution networks. Three objectives require to be minimized: (i) the total network configuration cost (ii) the average relative percentage error (APE) of bus voltage magnitude and (iii) APE of bus voltage angle. As the objective functions are conflicting with respect to each other, a multi-objective Pareto-based non-dominated sorting hybrid PSO-KH optimization algorithm is proposed. Furthermore, the impacts of DG on state estimation performance are also investigated. The feasibility of the proposed algorithm is demonstrated on IEEE 69-bus system and practical Indian 85-bus radial distribution network. The results obtained are compared with conventional Krill Herd (KH) algorithm, Particle swarm Optimization (PSO), with well known multi-objective non-dominated sorting genetic algorithm (NSGA-II) for validation.

Chapter 4 proposes a new multi-objective hybrid Estimation of distribution algorithm (EDA)-interior point method (IPM) algorithm to obtain the optimal location of measuring devices for state estimation in active distribution networks. The objective functions to be minimized are, the total network configuration cost, the average relative percentage error (APE) of bus voltage magnitude and angle estimates. As the objectives are conflicting in nature, a multi-objective Pareto-based non-dominated sorting EDA has been proposed in this chapter. Moreover, due to poor exploitation capability of the EDA, it is hybridized with IPM to improve its local searching ability in the search space. The hybridization of EDA and IPM brings a higher degree of balance between the exploration and exploitation capability of the algorithm during the search process. Furthermore, the loads and generators are treated as stochastic variables and the impact of different type of DGs on state estimation performance has also been investigated. The efficiency of the proposed algorithm is tested on IEEE 69-bus system and Indian 85-bus radial distribution network. The results thus obtained are compared with conventional EDA, PSO and non-dominated sorting genetic algorithm (NSGA-II).

Chapter 5 addresses a new multi-objective optimization problem to find trade-offs in deployment of phasor measurement units (PMUs) and intelligent electronic devices (IEDs) for

state estimation in active distribution networks. A new hybrid estimation of distribution algorithm (EDA-IPM) has been used to find the optimal number and location of measurement devices such as PMUs and IEDs for accurate state estimation. The objective functions to be minimized in this optimization problem are the total cost of PMUs and IEDs, and the root mean square (RMS) value of state estimation error. Since, the objectives are conflicting in nature, a multi-objective Pareto-based non-dominated sorting EDA algorithm is proposed. Moreover, to improve the local searching capability of the traditional EDA algorithm, the Interior point method (IPM) is hybridized with EDA to get near global optimal solution. The viability of the proposed algorithm has been tested on IEEE 69-bus system and Indian 85-bus system to validate the results. The obtained results have been compared with conventional EDA algorithm, non-dominated sorting genetic algorithm (NSGA-II) and also with hybrid EDA-simulated annealing algorithm existing in the literature.

Chapter 6 presents the inclusion of wind generation in a distribution network for state estimation. A new multi-objective optimization model is developed to find trade-offs in deployment of phasor measurement units (PMUs) and intelligent electronic devices (IEDs) for state estimation in active distribution networks. The objective functions considered to be minimized are the total cost of PMUs and IEDs as well as the RMS value of state estimation error. Since the objectives are conflicting, a multi-objective Pareto-based non-dominated sorting algorithm has been employed to get a compromised solution. To get the best optimal solution, multi-objective hybrid PSO-Krill Herd algorithm has been used. Furthermore, the random variation in loads and generators is also considered to check the reliability of the proposed meter placement technique. All DGs are considered as wind generator and output of each DG is modeled using Weibull distribution function. The viability of the proposed algorithm has been tested on IEEE 69-bus system and Indian 85-bus system to validate the results. The obtained results have been compared with Particle Swarm Optimization (PSO), Krill herd (KH) algorithm and also with well known Non-dominated sorting genetic algorithm (NSGA-II).

Chapter 7 summarizes the research contribution, findings and observations on the present research. It then presents the scope for future work based on what has gone before.

2.5 Summary

In this chapter a general discussion on existing work relevant to the distribution system state estimation is presented. Power system state estimation is an extensive research area of interest; however distribution system state estimation is comparatively a new area of research. Due to the peculiar characteristics of distribution systems, the development of distribution system state estimation (DSSE) is more challenging. Existing research proposes various classical optimization methods as well as some novel estimation techniques for DSSE solutions. This chapter has included discussion on various DSSE techniques proposed for state estimation in distribution networks.

Current distribution networks do not have sufficient real time measurements. To achieve quality state estimation, enhanced real time meter placement is essential in distribution networks. Similar to state estimation in distribution network, the existing meter placement techniques used for transmission network cannot be directly used for distribution systems. The typical challenges and the relevant literature on the development of meter placement algorithms for distribution networks have been presented in this chapter. Furthermore, the motivation, contribution and organization of the thesis are presented in this chapter.

Chapter 3

Optimal Allocation of Measurement Devices for Distribution System State Estimation Using Multi-Objective Hybrid PSO-Krill Herd Algorithm

Chapter 3

Optimal Allocation of Measurement Devices for Distribution System State Estimation Using Multi-Objective Hybrid PSO-Krill Herd Algorithm

3.1 Introduction

Recently, distribution systems have been increasingly subjected to integration of distributed generation (DG) and frequent changes in network configuration which are creating new problems of monitoring, control and reliability issues in smart grid environment. The active injections of renewable sources and loading conditions result in bi-directional power flow and exacerbation of voltage unbalance in a distribution network. The bi-directional power flow occurs when the DG generation exceeds local load and it has stronger impact on voltage profile of the distribution network. Furthermore, the network configuration of the smart distribution network will be changing dynamically to achieve minimum power loss and voltage deviations. The real time monitoring of distribution network is becoming increasingly challenging due to the increasing dynamics and changing behavior of actors in distribution systems. Therefore, knowledge about the system states are required more accurately and reliably for online monitoring and control of the distribution networks. To resolve these issues, meter placement techniques have been used widely in distribution systems for state estimation.

This chapter proposes a new multi-objective hybrid PSO-Krill Herd Pareto based optimization algorithm to optimize number and location of the measurement devices for accurate state estimation in smart distribution networks. Three objectives are considered to be minimized: (i) the total configuration cost (ii) the average relative percentage error (APE) of bus voltage magnitude and (iii) APE of bus voltage angle. As the objective functions are in conflict with respect to each other, a multi-objective Pareto-based non-dominated sorting hybrid PSO-KH optimization algorithm is proposed. Furthermore, the random variation in loads and the metrological error of the measurement devices are also taken into account. The proposed algorithm minimizes the cost and enhances the accuracy of the distribution state estimator for better monitoring and control of the system. Moreover, the impact of DG on state estimation performance is also investigated. The feasibility of the proposed algorithm is demonstrated on

IEEE 69-bus system and Practical Indian 85-bus radial distribution network. The results obtained are compared with conventional Krill Herd (KH) algorithm, Particle swarm Optimization (PSO), with well known multi-objective non-dominated sorting genetic algorithm (NSGA-II) for validation.

3.2 Problem Formulation

The main objectives of this chapter are to determine the optimal number and position of measurement devices to be placed in a given distribution network to achieve an observable system with minimum cost and ensure the state variables to be in compliance with predefined accuracy. Three objective functions have been considered for minimizing: (i) the total cost (ii) the average relative percentage error (APE) of bus voltage magnitude and (iii) APE of bus voltage angle. By trial and error basis it is found that, if the number of power flow measurements is higher, then the relative deviation in bus voltage magnitude and angle is lower and vice-versa i.e., the objective functions described above conflict with respect to each other. Hence, the meter placement problem can be formulated as a multi-objective Pareto based optimization problem which can be solved by using fast non-dominated sorting approach. This chapter proposed a hybridized algorithm for placing minimum number of meters for ensuring the relative deviations of voltage magnitudes and angles within the pre-specified thresholds for 95% of the simulated cases. Hence, the meter placement problem is based on the minimization of the following objective functions:

$$F_1 = \sum_{i=1}^{nl} C_{pf,i} P_{pf,i} + \sum_{i=1}^n C_{VMM,r} P_{VMM,i} \quad (3.1)$$

$$F_2 = \frac{1}{m} \sum_m \frac{1}{n} \left(\sum_{i=1}^n \left| \frac{V_i^a - V_i^{est}}{V_i^a} \right| \right) \times 100 \quad (3.2)$$

$$F_3 = \frac{1}{m} \sum_m \frac{1}{n} \left(\sum_{i=1}^n \left| \frac{\delta_i^a - \delta_i^{est}}{\delta_i^a} \right| \right) \times 100 \quad (3.3)$$

Subjected to constraints: In 95% of the simulated cases, the maximum relative percentage deviation in voltage magnitude and phase angle are 1% and 5% respectively and this can be expressed as:

$$\left| \frac{V_i^a - V_i^{est}}{V_i^a} \right| \times 100 \leq 1 \quad (3.4)$$

$$\left| \frac{\delta_i^a - \delta_i^{est}}{\delta_i^a} \right| \times 100 \leq 5 \quad (3.5)$$

where F_1 , F_2 and F_3 are three objective functions to be minimized, n and nl are the number of buses and lines in a network, C_{pf} and C_{VMM} are respectively, the relative costs of a power flow (PF) measurement device and voltage magnitude measurement (VMM) device normalized with respect to a conventional unitary cost. Since voltage measurement devices are treated as default measurements, the cost of a power flow meter and VMM meter are assumed to be same in the optimization process. Throughout the iterative process the location and the number of default measurements are same for all algorithms used in this work. Therefore, it would not affect the cost function. However, different costs can also be assigned to power flow meters or to voltage meters. In practice, the cost of a measuring device depends on specific investment and application scenarios. P_{pf} and P_{VMM} represents the binary decision vectors, if a meter is present in a line or at node then it becomes one or else its value is zero, V_i^a and δ_i^a are the actual bus voltage magnitude and phase angle of i^{th} bus respectively, V_i^{est} and δ_i^{est} are the estimated bus voltage magnitude and phase angle of i^{th} bus respectively.

The quality of state estimation solution deteriorates due to most of the measurements are pseudo-measurements with high variances. But, it can be improved by placing some additional real meters with low variances. In this work, only power flow meters and voltage magnitude meters have been used for SE in distribution networks. Furthermore, branch current based state

estimation (BC-DSSE) is used for estimation of system states where branch current magnitudes and their phase angles are considered as state variables [40].

3.3 Krill Herd Algorithm (KHA)

KHA is a new bio-inspired swarm intelligence algorithm, which takes its inspiration from the herding behavior of the krill swarms in searching for food in nature [84]. The fitness of each krill individual depends on its distances from the food position and the density of krill particles. The movement of each krill within the search space is based on three actions:

- a) Induced movement of krill individuals,
- b) Foraging motion, and
- c) Random diffusion.

3.3.1 Lagrangian Model of the KHA

The Lagrangian model of the Krill herd algorithm in a n dimensional decision space can be expressed as:

$$\frac{dL_i}{dt} = M_i + F_i + D_i \quad (3.6)$$

where M_i is the induced motion of each krill individual, F_i is the foraging motion and D_i is the random diffusion of the krill individuals.

3.3.1.1 Induced movement of Krill individuals

The direction of motion induced is expressed by three effects: local effect, target effect and repulsive effect. For each krill individual the movement can be expressed as:

$$M_i^{\text{new}} = M^{\text{max}} \alpha_i + w_n M_i^{\text{old}} \quad (3.7)$$

where

$$\alpha_i = \alpha_i^{\text{local}} + \alpha_i^{\text{target}} \quad (3.8)$$

M^{max} is the maximum induced speed, w_n is the inertia weight and its value lies between [0, 1], α_i direction of motion induced by i^{th} Krill individual, α^{local} is the local effect produced by the neighbors and α^{target} is the target direction produced by the best Krill individual.

3.3.1.2 Foraging motion

The foraging motion of krill individual depends on two parameters, one is food location and the second one is previous food location. The foraging motion for i^{th} krill individual can be

expressed as:

$$F_i = v_f \varphi_i + w_f F_i^{\text{old}} \quad (3.9)$$

Where

$$\varphi_i = \varphi_i^{\text{food}} + \varphi_i^{\text{best}} \quad (3.10)$$

where v_f is the foraging speed, w_f is the inertia weight of the foraging motion lies between $[0, 1]$, φ_i^{food} is the food attractiveness and φ_i^{best} is the effect of the best fitness of the i^{th} Krills.

3.3.1.3 Physical diffusion

It is a random process of the krill individuals to improve the population diversity within the search space. This motion can be expressed as,

$$D_i = D^{\text{max}} d \quad (3.11)$$

where D^{max} is the maximum diffusion speed and d is the random directional vector, lies between $[-1, 1]$.

3.3.2 Movement process in KHA

Based on the above mentioned movements, the positions of the i^{th} Krill individual in the time interval t to $t + \Delta t$ can be expressed as:

$$L_i(t + \Delta t) = L_i(t) + \Delta t \frac{dL_i}{dt} \quad (3.12)$$

Δt represents the time interval can be defined as:

$$\Delta t = C_t \sum_{i=1}^{n_v} (u_i - l_i) \quad (3.13)$$

where n_v is the number of variables and C_t is a constant number between $[0, 2]$ and u_i, l_i are the upper and lower limits of i^{th} Krill individuals.

3.3.3 Genetic operator

To improve the performance of KH algorithm genetic operators are incorporated into the algorithm. The genetic operators are crossover and mutation process which are derived from DE algorithm.

3.3.3.1 Crossover

The crossover process is controlled by using a parameter called crossover probability (C_p). The position of a krill can be modified, by interacting each krill individuals with other. In

in this process, the position of the j^{th} component of the i^{th} Krill can be expressed as:

$$L_{i,j} = \begin{cases} L_{m,j} & \text{if } rand \leq C_p \\ L_{i,j} & \text{if } rand > C_p \end{cases} \quad (3.14)$$

$$C_p = 0.2K_{i,best} \quad (3.15)$$

where $m \in \{1, 2, 3, \dots, i-1, i+1, \dots, N\}$, $L_{m,j}$ represents the j^{th} component of the i^{th} Krill individual, C_p is the crossover probability and $K_{i,best}$ is the best previously visited position of the i^{th} Krill individual.

3.3.3.2 Mutation

The mutation operation is controlled by a parameter called mutation probability (M_p).

The mutation process can be formulated as:

$$L_{i,m} = \begin{cases} L_{best,m} + \mu(L_{p,m} - L_{q,m}) & rand_{i,m} \prec M_p \\ L_{i,m} & \text{else} \end{cases} \quad (3.16)$$

$$M_p = 0.05/K_{i,best} \quad (3.17)$$

where $K_{i,best}$ is the best previously visited position of the i^{th} Krill individual and μ is a number lies between 0 and 1.

3.4 Proposed Hybrid PSO-KH algorithm

In all modern meta-heuristic algorithms, the balance between the intensification and diversification plays a crucial role for better performance of the algorithms. Intensification refers to a local search around the neighborhood of an optimal or near optimal solution and diversification refers to the complete exploration of the search space efficiently and effectively. Exhaustive search or excessive diversification increases the convergence time of the searching as well as causing the solution to move around the near optimal solution. On the other hand excessive exploitation causes the algorithm to trap into a local optima point and it may not reach global optimal solution. Therefore, a proper balance between the exploration and exploitation is required to ensure faster convergence characteristics and good quality of solution.

The Krill herd (KH) algorithm has proven its capability to find the global regions in a reasonable amount of time. However, it is seen that the conventional KH algorithm is not

efficient in performing the local searches effectively. Therefore, hybrid KH algorithm is proposed to improve the local search capability of the KH algorithm and also to achieve better balance between the intensification and diversification during the searching process. In order to achieve improvisation in local searching process, the KH algorithm is hybridized with the PSO algorithm to get near global optimal solution.

Basically, PSO is a population based multi-point evolutionary algorithm. The searching process in PSO starts with a population of particles that move in a search space by following the current optimum particles and changing their positions and velocity to find the best particle position. During its movement particles distribute information among them to search for a good area in search space. The local search capability and the neighborhood search ability provides hybrid KH algorithm to search for good area of the search space. These two features are added to the hybrid KH algorithm to get near global optimal solution.

3.5 Proposed Multi-Objective Hybrid PSO-KH algorithm

The simultaneous optimization of the multiple objectives needs a compromised solution because no solution can improve itself in one objective without worsening the other objectives. In order to get a better compromised solution, non-dominated sorting approach i.e., Pareto-optimality principle has been adopted [88], [89]. This principle states that, in a non-dominated Pareto front all solutions are equally important i.e. no solution is inferior to other. In multi-objective optimization problem, the solution relies on a set of solutions rather than a single solution like single objective optimization problem. In this work, non-dominated sorting approach has been incorporated with hybrid PSO-KH in order to achieve the best trade-offs solution between the objective functions.

In this chapter, hybrid multi-objective PSO-KH algorithm is proposed. In PSO-KH algorithm, the Krills individuals are ranked based on the non-dominated sorting approach and to get good spread in the Pareto optimal solution, crowding distance operator has been used [88]. Both the strategies are described below:

3.5.1 Non-dominated sorting approach

For the meter placement problem three objectives function have been considered to be optimized, they are: (i) the total configuration cost (ii) average percentage error (APE) of bus voltage magnitude and (iii) APE of voltage phase angle. Since the objective functions (i), (ii)

and (i), (iii) are conflicting with one another, so a compromised solution has to be established to find the best optimal solution. Therefore, non-dominated sorting technique has been incorporated in this optimization problem [88]. In multi-objective case, each solution is compared with others to check its dominating nature. For a solution $s^{(1)}$ to be dominating other solution $s^{(2)}$ if :

- 1) The solution $s^{(1)}$ is better than $s^{(2)}$ in all objectives.
- 2) The solution $s^{(1)}$ is strictly better than $s^{(2)}$ in at least one objective.

If any of the above condition is satisfied then, the solution $s^{(2)}$ is said to be dominated by $s^{(1)}$.

3.5.2 Crowding distance

The crowding distance operator is used to find the density of solutions that are surrounding a particular solution [89].

From the above two definitions, it can be stated that, a solution $s^{(1)}$ is said to be better than another solution $s^{(2)}$ (krill individuals), if it has satisfied any one of the following criteria: (a) the rank of solution $s^{(1)}$ has to be smaller than the solution $s^{(2)}$, or (b) if both the solutions belong to same front (same rank), then the crowding distance of solution $s^{(1)}$ has to be larger than that of solution $s^{(2)}$.

The steps of the proposed algorithm are described as follows:

Step1. Initialization: initialize the parameters of the algorithms

$$D^{\max}, M^{\max}, W_f, w_{\max}, w_{\min}, C1 \text{ and } C2$$

Step 2. Fitness evaluation:

- 1) Randomly generate number of power flow meters and their locations for each krill individuals in the population.
- 2) Evaluate the fitness functions using weighting approach for each krill individual.
- 3) Rank the evaluated population based on the non-dominated sorting scheme.
- 4) Sort the population according to their fitness values and calculate the best and worst fitness value i.e. best and worst Krills among the population.

Step 3. Generate new Krills using PSO.

Step 4. For each Krill individual calculate the following motions:

- 1) Induced motions
- 2) Foraging motions
- 3) Physical diffusions

- Step 5. Update the position of the Krill individuals in the search space.
- Step 6. Genetic operator: Apply crossover and mutation operator to the updated positions.
- Step 7. Evaluate the objective functions based on the new positions of the krill individuals and sort them based on the non-dominated sorting scheme.
- Step 8. Calculate the current best and worst krill.
- Step 9. Repeat steps 3-8 for maximum generation times.
- Step10. Use fuzzy theory to find the best compromised solution [24].

The initial value of the parameters used in the proposed algorithm is decided based on the nature of the optimization problem. For unimodal cost functions smaller value for maximum induced speed (M^{\max}) and inertia weight (w_f) is recommended and for multimodal case higher values is recommended for better performance of the algorithm. The value of M^{\max} and w_f is considered as 0.025 and 0.9 respectively. The other parameters are decided based upon the repeated trial of tests. In PSO, the appropriate value of w_{\max} and w_{\min} is 0.9 and 0.4 and the values are independent to problems as recommended by many papers. The most appropriate value of C1 and C2 (i.e. C1=C2) is 2 [86]-[87]. For population size of different values like $popsize = 10, 20$ and 50 have been tried. For the IEEE 69-bus system and Indian 85-bus system there is no much variation in results for taking different population sizes ($popsize$) is observed. Finally, it is found that, $popsize=20$ is sufficient for getting near optimal value. The parameter values are provided in Table 3.1.

After the initialization of the parameters and positions of the Krill particles, the fitness value of the Krill is evaluated using weighting sum approach. The weighting sum method has been used extensively for multi-objective optimization (MOO) to provide multiple solution points by varying the weights consistently. The value of weights is significant relative to other weights and also relative to its corresponding objective function value. It is also stated that if the weights are representing the trade-off between the objective function (paired comparison method), then it is better to retain the original units of the objectives without transferring them between 0 and 1. This approach only provides a basic approximation of one's preference function. Even if the weights are acceptable a priori but the final solution may not reflect accurately the initial preferences. Therefore, the decision maker has to choose an appropriate combination of weights

to reproduce a representative part of the optimal Pareto front. The flow chart of the proposed hybrid PSO-KH algorithm is shown in Figure 3.1.

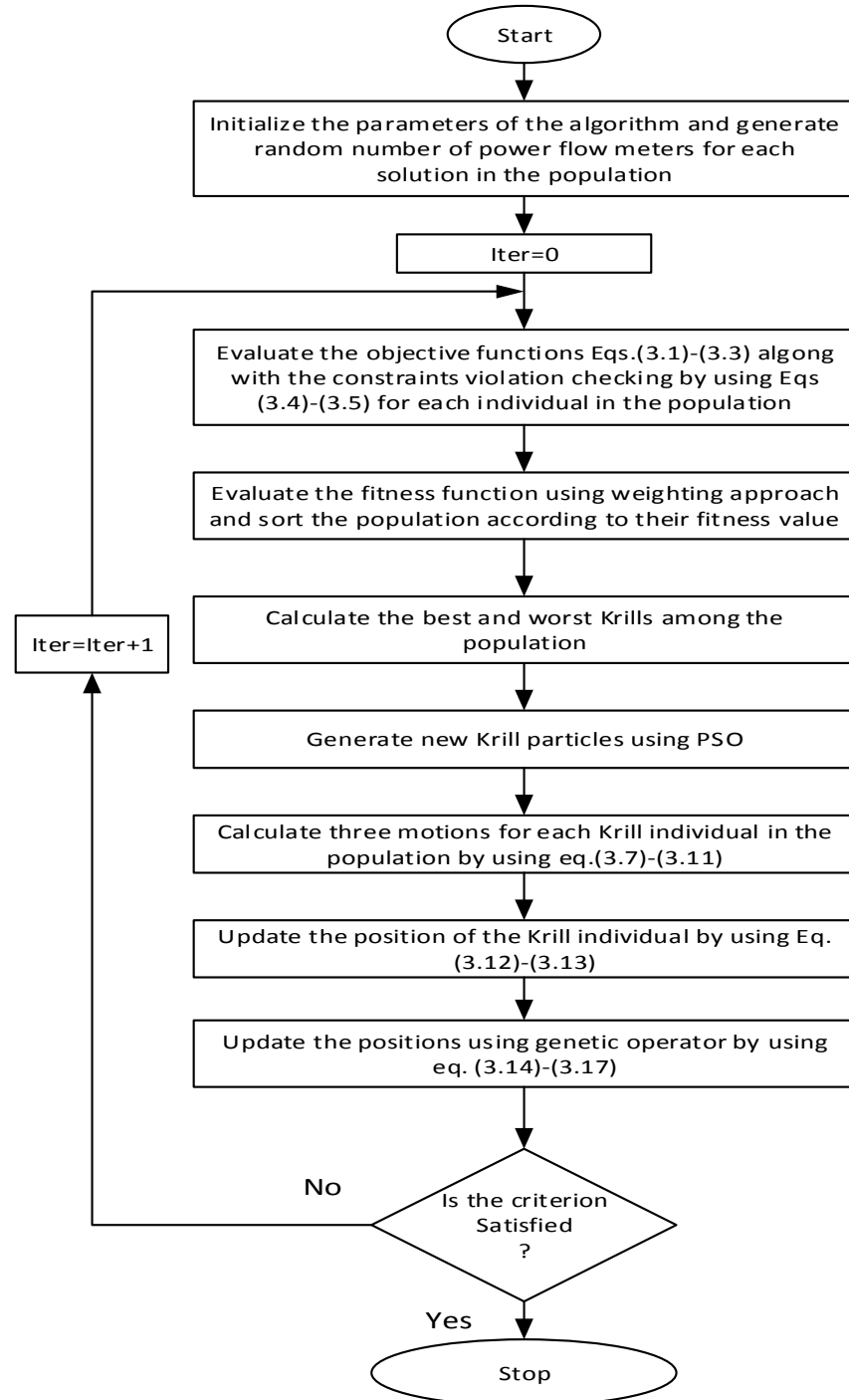


Figure 3.1: Flow chart of the proposed multi-objective hybrid PSO-KH algorithm

Each objective function represented in eq. (3.1), (3.2) and (3.3) are evaluated based upon the initial position of the power flow meters for all the Krill individuals using DSE algorithm. The obtained fitness values are ranked using non-dominated sorting technique. Then the best and worst Krills are determined based upon the overall fitness value of each Krill. In order to achieve better performance, the position of the Krills is first updated using PSO discussed in Section 3. After the first updation, KH algorithm is implemented to find the new updated position of the Krill particles. During the evaluation of the fitness the constraints violation checking is also carried out. For each Monte Carlo step, the relative percentage error in bus voltage magnitude and angle is determined at each bus. For a particular number of meters and their locations, if in 95% of the simulated cases, the relative errors in voltage and phase angle estimates are brought down below the pre-specified thresholds, then the value of the objective functions are determined and stored. On the contrary, if in 95% of the cases, the estimation errors are not below the specified thresholds, then for that particular meter location a higher value of the objective functions is assigned. So that in the next immediate generation of the algorithm this particular solution will be removed from the list because of non-dominated sorting and crowding distance approach. Then the above procedure is repeated until the convergence is achieved.

3.6 Robust Optimal Meter Placement in Distribution Networks

The multi-objective hybrid PSO-KH algorithm is based on the fact that the selected optimal solution of different alternatives in a decision space is robust with respect to estimation noise. In view of this, the meter placement problem is formulated as multi-objective Pareto based optimization problem. The most interesting application of the proposed approach is that a trade-off solution between the relative errors in voltage magnitude and phase angle is established with respect to the total cost of meters to achieve best compromised solution between the cost and state estimation accuracy. The hybrid PSO-KH algorithm is applied to address the whole problem of robustness of the DSE technique to obtain an optimal meter placement that takes into account different metrological characteristics of the measurement devices, random load variations and measurement uncertainties. This algorithm does not enumerate all feasible solutions due to the computational complexity and is possible because of its efficient exploration and exploitation capability. Therefore, this algorithm is able to find the near global optimal solution. Furthermore, an overall optimization is performed in which each combination of default meters and power

flow meters under random load variations as well as for different metrological characteristic of the real meters is reported. Additionally, it is observed that the maximum deviations in voltage and phase angle estimates are significantly lower than the other algorithms used in this work for comparison purpose.

The robustness of the proposed approach of meter placement is also tested in presence of DGs in distribution network. In the simulation study, it is assumed that the DGs output is a random variable following Gaussian distribution. The optimal location and number of meters in presence of DGs under various operating scenarios has been tested to find a robust meter placement that can guarantee a desired level of accuracy for state estimation.

3.7 Test and Simulation Conditions

To analyze the effectiveness of the proposed algorithm, the following test and simulation conditions have been considered in MATLAB 2014b environment.

Branch current based state estimation (BC-DSSE) algorithm is used for the estimation of system states [40]. For testing, the base case load flow is run to obtain the reference or true values of the quantities to be measured. The uncertainty of the measurements is obtained by adding errors following the normal distribution to the reference values obtained from base case load flow solution. In SE, four types of measurements with different accuracies are considered such as: substation measurements, real measurements, pseudo-measurements (historical data) and virtual measurements [75]. The measurement uncertainties are considered based on maximum percentage of error associated with the measurements. The following conditions are considered for the measurement uncertainties:

- 1) Substation Measurements: These measurements are called default measurements because these are already present in the substation. In this, one voltage magnitude measurement meter and one power flow meter are assumed to be present at the substation. The maximum error of 1% is considered for substation measurements.
- 2) Real measurements: For real measurements power flow meters are used which measures both real and reactive power in a line. Different metrological errors in real measurement devices are considered such as 1%, 3% and 5% to observe the impact of metrological error on state estimation accuracy and number of devices required.

- 3) Pseudo-measurements: The accuracy of the pseudo measurements is relatively low because it is derived from the historical load data. Therefore, the maximum percentage error considered for this is 50% [75].
- 4) Virtual-measurements: The zero injection buses are modeled as virtual measurements with low variance of 10^{-7} [94].

In this work, the stochastic nature of loads and generators are taken into consideration for better visualization of the proposed technique. Different network conditions are simulated by considering the load demands and generator output as stochastic variables following the Gaussian distribution around the mean values with prefixed standard deviation. Additionally, Monte Carlo algorithm is used to study the impacts of measurement uncertainties on state estimation performance. In order to consider the measurement uncertainties, Monte Carlo algorithm has been used to generate 1000 number of different network state from each network condition by applying the instrument uncertainty to the measured data. Thus, total number of cases considered in this simulation is 100×1000 .

Furthermore, the results obtained using various methods considered in this work is not optimized with respect to the position of the voltage meters. Because voltage meters is treated as a default measurements available at the substation and DG locations. Therefore, it is not optimized but the power flow meters are considered in the optimization process for better estimation of system states. The power flow measurements are better as compared to only current magnitude, voltage magnitude and pseudo-measurements in estimating the system states. Moreover, in order to improve the accuracy of the voltage phase angle, power flow meters are appended in distribution network at appropriate locations.

The test conditions assumed in this work are summarized as follows:

- 1) The number of operating conditions, $NC = 100$.
- 2) The standard deviation assumed for the NC operating conditions is $\pm 10\%$ of the base value.
- 3) Number of Monte Carlo trials $MC = 1000$
- 4) Metrological errors of measurement device: 1%, 3% and 5% and
- 5) The total test cases of 100×1000 have been studied.

The number of power flow meters required and their positions in presence of DGs are also investigated in this work. In the simulation study, the location of DGs is kept fixed [97],[98] and

it is assumed that the DGs output is a stochastic variable following the Gaussian distribution with prefixed standard deviation and moreover, all DGs are generating real power to the network. The impacts of DG on state estimation accuracy are presented in the next section. Moreover, the results reported considering DG refer only to a particular case and the impact of possible power flow inversion has not been considered in this work.

To validate the performance of the proposed hybrid PSO-KH algorithm, the results are compared with some well known existing algorithm such as conventional KH, PSO and NSGA-II.

Table 3.1 Parameter values of KH, PSO and NSGA-II Algorithm

KHA	PSO	NSGA-II
Population size=20	Population size=20	Population size=20
D^{\max} (maximum diffusion speed) $\in [0.002 \ 0.01]$	$C1=2, C2=2$	Crossover rate (P_c)=0.8
$C_t \in [0, 2]$	$w_{\max} = 0.9, w_{\min} = 0.4$	Mutation rate (M_c)=0.02
V_f (foraging speed)= 0.02ms^{-1}	Maximum generations=50	Maximum generations=50
W_f (inertia of the foraging motion)=0.9	-	-
$M^{\max} = 0.025\text{ms}^{-1}$ Maximum generations=50	-	-

Table 3.2 DG installation bus and capacity

Test System	Bus Number	DG capacity in MW (Base value)
IEEE 69-bus System	50	0.180
	61	0.270
Practical Indian 85-bus System	45	0.277
	61	0.290

3.7.1 Fuzzy Set theory

Fuzzy set theory has been used to find best optimal solution among all solution obtained in an optimal Pareto-front [95]. The procedure is discussed as follows:

- At first the maximum and minimum value of each objective function is obtained.
- μ is calculated for each objective function as

$$\mu(i, j) = \begin{cases} 1 & F_{i,j} = F_j^{\min} \\ \frac{F_j^{\max} - F_{i,j}}{F_j^{\max} - F_j^{\min}} & F_j^{\min} < F_{i,j} < F_j^{\max} \\ 0 & F_{i,j} = F_j^{\max} \end{cases} \quad (3.18)$$

The membership function for each solution is calculated using the equation given below:

$$\mu_i = \frac{\sum_{j=1}^{N_o} \mu_{(i, j)}}{\sum_{i=1}^M \sum_{j=1}^{N_o} \mu_{(i, j)}} \quad (3.19)$$

where M is the number of Pareto solutions (population size), N_o is the number of objectives. The best compromise solution is the one achieving the maximum membership function. F^{\max} and F^{\min} are the maximum and minimum values of the objective function F .

3.7.2 IEEE 69 bus system

In order to highlight the performance of the proposed algorithm, IEEE 69-bus, 12.66kV radial distribution network has been taken into account. This system comprises of 69 buses and 68 lines, 48 loads and two DGs. The system load information and line parameters are given in [99]. The total load of this system is 3.802MW and 2.692Mvar respectively. Furthermore, this system includes 21 number of zero injection buses. The real and reactive power injections at these buses are considered as virtual measurements with higher accuracy level. In addition, there are two real meters kept at the substation which are called as default measurements (one voltage and one power flow meter), provided in Table 3.3. Distribution system can be of 1, 2 or 3 phase. But in this thesis only single phase balanced system model has been considered. Therefore, feeder modeling and unbalanced load has not taken into consideration.

The obtained results using the proposed algorithm have been reported in Table 3.3 and the optimal Pareto-front plots are shown in Figure 3.2, 3.3 and 3.4 under different operating scenarios such as load variations, generator output variations and different metrological characteristics of measurement devices. It is worth noticing that, the total number of power flow meters required is 5 using the proposed PSO-KH algorithm when the meter accuracy is considered as 1%. But in case of KH, PSO and NSGA-II, the total number of flow measurements

required is 9, 8 and 5 respectively. The average relative percentage error in bus voltage magnitude and phase angle is obtained as 0.0028% and 0.4947% using PSO-KH whereas in case of KH and PSO these are 0.0052%, 0.7837% and 0.0112%, 1.8731% respectively. Though same number of meters is obtained for NSGA-II and PSO-KH but the average relative percentage of error obtained using NSGA-II is 0.0037% and 0.6273% which is more as compared to PSO-KH. The results shown in Table 3.3, are obtained at the final iteration of the iterative process i.e., at the optimal Pareto-front. From the optimal Pareto front, the best compromised solution is obtained using fuzzy theory [95]. The competitive results are shown in Table 3.3, which shows the superiority of the proposed algorithm over other existing algorithm and techniques considered in this work. Furthermore, the minimum and maximum relative percentage errors in voltage magnitude and angle estimates are also reported in Table 3.3 for different methods. The maximum deviations in voltage and angle estimates are found to be significantly lower than the PSO, KH and NSGA-II algorithms.

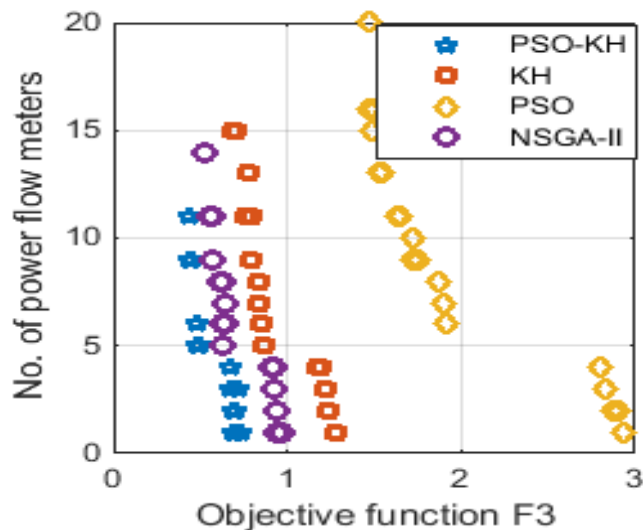


Figure 3.2(a): Optimal Pareto-front between no. of flow meters and F_3 for 1% error in real measurements and 50% in pseudo-measurements.

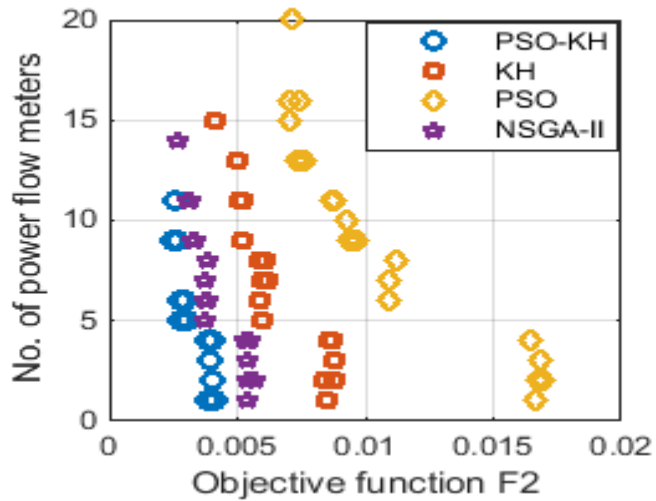


Figure 3.2(b): Optimal Pareto-front between no. of flow meters and F_2 for 1% error in real measurements and 50% in pseudo-measurements.

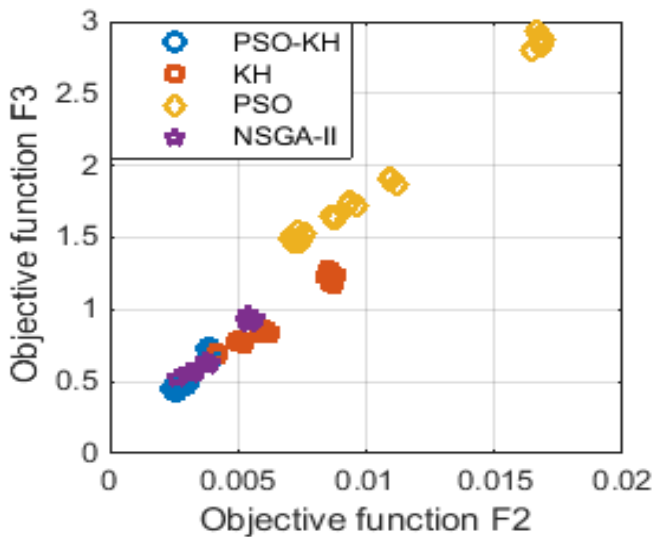


Figure 3.2(c): Optimal Pareto-front between objectives F_2 and F_3 for 1% error in real measurements and 50% in pseudo-measurements.

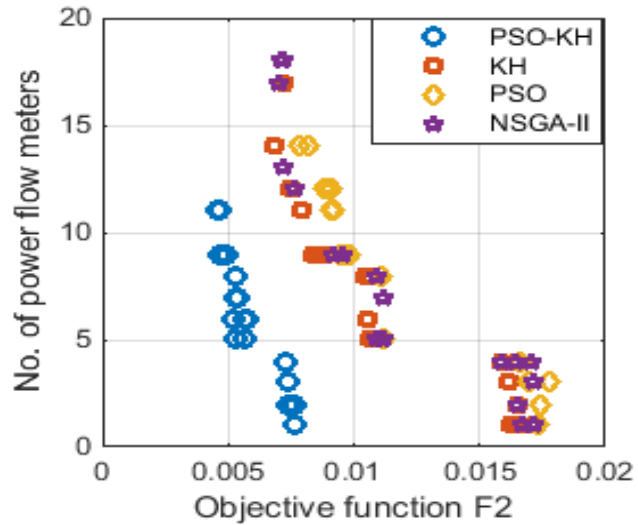


Figure 3.3(a): Optimal Pareto-front between no. of flow meters and F_2 for 3% error in real measurements and 50% in pseudo-measurements.

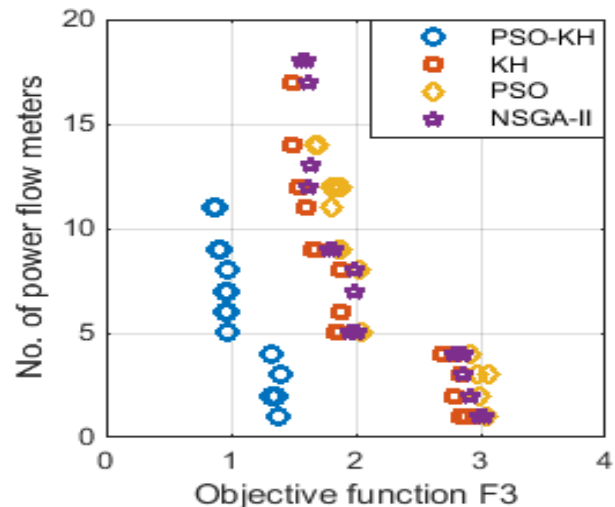


Figure 3.3(b): Optimal Pareto-front between no. of flow meters and F_3 for 3% error in real measurements and 50% in pseudo-measurements.

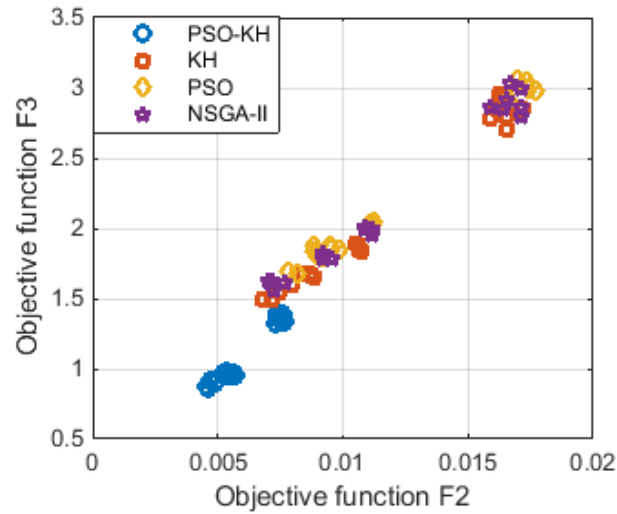


Figure 3.3(c): Optimal Pareto-front between objectives F_2 and F_3 for 3% error in real measurements and 50% in pseudo-measurements.

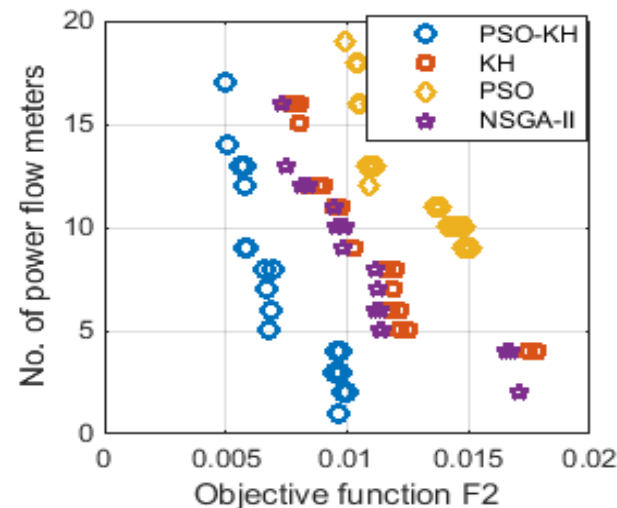


Figure 3.4(a): Optimal Pareto-front between no. of flow meters and F_2 for 5% error in real measurements and 50% in pseudo-measurements.

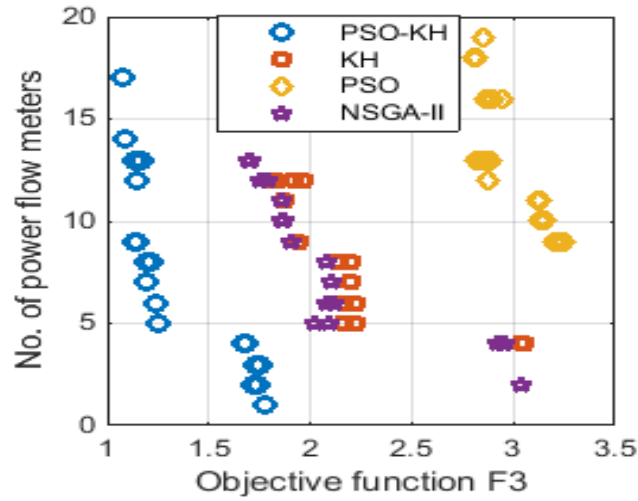


Figure 3.4(b): Optimal Pareto-front between no. of flow meters and F_3 for 5% error in real measurements and 50% in pseudo-measurements.

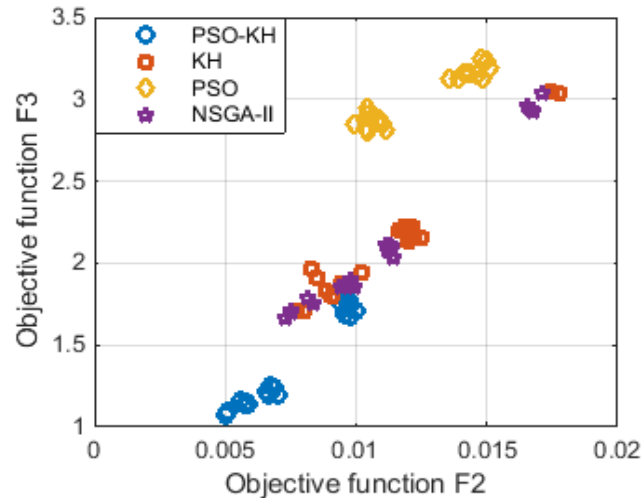


Figure 3.4(c): Optimal Pareto-front between objectives F_2 and F_3 for 5% error in real measurements and 50% in pseudo-measurements.

For meter accuracy of 3% and 5%, the optimal Pareto-front between different objectives has been shown in Figure 3.3 and 3.4. It can be observed from the figures that the number of meters requirement is increased compare to previous case i.e. when 1% accuracy of the meter was considered. Moreover, the objectives F_2 and F_3 values are also increased due to large error

incorporated into real measurements i.e. in power flow measurements. From this, it can be concluded that if the error in power flow measurements is more then it influences the estimation accuracy of the state estimator and also on number of meter requirements. It is important to note that both metrological errors and the location of the measurement devices significantly affecting the accuracy of the state estimator. From the figures, it is observed that even though the number of meters are same but SE accuracies are different because the location of meters also influencing the estimation accuracy. The obtained results are reported in Table 3.3 and the optimal Pareto-front between objectives 2 and 3 is shown in Figure 3.2. It is noticed that the two objectives are not conflicting with each other rather these are correlated. Therefore, the Pareto front curve is not possible between the objectives F_2 and F_3 .

The result provided in Table 3.3 refers to a passive distribution network i.e. when there is no DG installed in the network. There are two observation can be made by analyzing the results provided in Table 3.3. The first one is, as the accuracy of the measurements decreases the number of power flow meters have to be increased for better state estimation. The second one is the performance of the proposed PSO-KH algorithm is found to be better due to its efficient searching capability. The hybridization of PSO and KH algorithm brings a higher degree of balance between the intensification and diversification during the search process. Therefore, a new hybrid PSO-KH algorithm has been proposed for the distribution state estimation in multi-objective environment to solve the meter placement problem. The obtained results are also compared with PSO, KH and NSGA-II algorithms to check superiority of the proposed algorithm.

Furthermore, the proposed methodology has also been applied in active distribution network. Two DGs of 0.270 MW and 0.180 MW are installed at nodes 50 and 61 and it is assumed that both are injecting only real power to the network. Moreover, the results reported considering DG refer only to a particular case because the location of DGs is based on to achieve minimum power loss and voltage deviations [97]. The results obtained in presence of DGs are reported in Table 3.4. It is worth noticing that, the number of power flow meters requirement is reduced as compared to the passive case and moreover, the objective function F_3 value is reduced as compared to without DG case. The reason behind is that the DG supplying power to the local load connected to that bus. Therefore, the power drawn by that load from the feeder section is reduced i.e. the current in the lines get reduce. As a consequence, the magnitude of error

associated with the flow measurements will reduce. Furthermore, the presence of DG provides more real-time measurements and increases the redundancy level of the system which helps in getting more accurate results.

From the location of the power flow meters shown in Table 3.4, it can be stated that, if the flow meters are placed nearer to the sources and in the main feeder, then much better results can be expected than the meters at the laterals or far away from sources. Therefore, in the optimization process, some real meters like power flow meters and voltage meters are kept at the substation and DG location for further improvement in state estimation accuracy.

Table 3.3: IEEE-69 bus system: optimal location of the power flow meters under different loadings including metrological errors of the flow meters

Metrological Errors	Algorithm	Default Measurements (node/line number)	location of flow meters(Line number)	No. of flow meters	Objective functions value			Max. error in bus voltage magnitude (V) (%)	Max. error in bus voltage angle (δ) (%)
					F ₁	F ₂	F ₃		
1%	Proposed PSO-KH	1/1	1,7,24,54,66	5	6	0.0028	0.4947	0.0381	5.7922
	KH	1/1	1,9,17,23,32,47, 56,61,63	9	10	0.0052	0.7837	0.0399	6.9994
	PSO	1/1	1,18,28,37,56, 65,42, 49	8	9	0.0112	1.8731	0.0475	7.9249
	NSGA-II	1/1	1,5,19,27,54	5	6	0.0037	0.6273	0.0772	9.3022
3%	Proposed PSO-KH	1/1	1,11,18,43,52	5	6	0.0053	0.9782	0.0417	5.9154
	KH	1/1	1,2,4,12,21,24, 30,59,67	9	10	0.0084	1.6767	0.0479	7.8239
	PSO	1/1	1,13,17,25,31,39, 45,51,59,64,65	11	12	0.0091	1.7990	0.0638	11.6239
	NSGA-II	1/1	1,3,10,19,27,30, 32,4,45,49,54,65	12	13	0.0077	1.6130	0.0488	10.3332
5%	Proposed PSO-KH	1/1	1,7,14,21,28, 33,49,53,61	9	10	0.0058	1.1491	0.0523	6.3172
	KH	1/1	1,5,11,30,35, 41,47,52,61	9	10	0.0102	1.9423	0.0927	9.6717
	PSO	1/1	1,5,18,30,34,35, 44,47,50,56,63,67	12	13	0.0109	2.8704	0.0838	12.7865
	NSGA-II	1/1	1,4,9,14,20,32,38, 40,43,45,51,57,65	13	14	0.0075	1.7001	0.0776	12.4533

Table 3.4 IEEE 69 bus system: optimal location of the power flow meters under different loadings including metrological errors of the flow meters (with two DGs at bus no. 50 and 61)

Metrological Errors	Algorithm	Default Measurements (node/line number)	location of flow meters(Line number)	No. of flow meters	Objective functions value			Max. error in bus voltage magnitude (V) (%)	Max. error in bus voltage angle (δ) (%)
					F ₁	F ₂	F ₃		
1%	Proposed PSO-KH	1,50,61/1	1,49,52,59,67	5	8	0.0011	0.2653	0.0289	5.3122
	KH	1,50,61/1	1,27,34,37,51,62,67	7	10	0.0037	0.6123	0.0371	8.7895
	PSO	1,50,61/1	1,13,24,30,34,49,67	7	10	0.0093	1.6224	0.0421	8.0123
	NSGA-II	1,50,61/1	1,9,18,29,51	5	8	0.0034	0.5827	0.0569	9.4322
3%	Proposed PSO-KH	1,50,61/1	1,29,41,53,66	5	8	0.0025	0.5386	0.0411	5.8923
	KH	1,50,61/1	1,29,32,33,41,61,66	7	10	0.0072	1.1604	0.0567	8.2213
	PSO	1,50,61/1	1,14,41,43,44,51, 56,62,67	9	12	0.0060	1.0535	0.0422	9.1325
	NSGA-II	1,50,61/1	1,9,21,23,37,38,42, 44,66	9	12	0.0060	1.0211	0.0612	9.1009
5%	Proposed PSO-KH	1,50,61/1	1,3,17,25,34,42,50,63	8	11	0.0063	1.0587	0.0499	6.5122
	KH	1,50,61/1	1,4,22,36,47,54,61,64	8	11	0.0064	1.0667	0.0733	10.6567
	PSO	1,50,61/1	1,2,5,24,29,33,34,41 ,43,63	10	13	0.0060	1.9560	0.0645	12.2564
	NSGA-II	1,50,61/1	1,10,21,24,28,33, 34,36,46,49	11	14	0.0061	1.7509	0.0614	11.0011

3.7.3 Practical Indian 85-bus system

To demonstrate the effectiveness of the proposed algorithm, in a large scale practical distribution system, Indian 85-bus, 11kV radial distribution network has been considered in this study. The system comprises of 85 nodes and 84 branches with two DG sources. The total load of the system is 2.574MW and 2.622MVar respectively. Furthermore, the total number of zero injection buses it includes is 26. The network and load data for Indian 85 bus system are taken from [100]. The parameters of the algorithms mentioned in Table 3.1 are also applicable for this test system.

The results obtained using the proposed algorithm has been shown in Table 3.5. When 1% error in power flow meter and 50% error in pseudo-measurements are considered, the total number of power flow meters required is 7 using the proposed PSO-KH algorithm whereas in case of PSO, KH and NSGA-II, the total number of flow meters required is 8, 8 and 8 respectively. The respective objective functions value is also provided in Table 3.5. Furthermore, the optimal Pareto fronts between objective functions have been shown in Figure 3.5, 3.6 and 3.7 respectively, for different metrological errors of the power flow meters. From the results it is observed that as the accuracy of the meter is decreased, more number of real meters have to be

placed to get better estimation performance because the quality of the estimates decreases with the increase in the error in measurements and this decrease in quality is significant with the increase in error in the real measurements as compared to the pseudo-measurements. Therefore, more meters are needed to bring down the relative errors in voltage and phase angle estimates below the pre-specified thresholds which is reported in Table 3.5. It is proven that the solution obtained using hybrid PSO-KH is a near global optimal solution.

The results obtained in presence of DGs at bus number 45 and 61 are also shown in Table 3.6. It can also be visualized that the presence of DGs impacts on accuracy of the estimated quantities. It reduces the phase angle error because DG supplies power to the local loads connected to that bus therefore, the power drawn by the load from the main feeder section is reduced. In Table 3.6, the results obtained using the proposed hybrid PSO-KH algorithm has been reported. From the Table 3.5 and 3.6, it is observed that both the location and metrological error of the measurement devices significantly affecting the state estimation accuracy. Therefore, it is necessary to consider these items into account to assure that the state variables comply within predefined thresholds. A best compromised solution between relative percentage error in voltage magnitude and angle with the cost of meter is established which is the main advantage of using this Pareto based multi-objective optimization technique.

Table 3.5 Indian 85-bus system: Optimal location of the power flow meters under different loadings including metrological errors of the flow meters

Metrological Errors	Algorithm	Default Measurements (node/line number)	location of flow meters(Line number)	No. of flow meters	Objective functions value			Max. error in bus voltage magnitude (V) (%)	Max. error in bus voltage angle (δ) (%)
					F ₁	F ₂	F ₃		
1%	Proposed PSO-KH	1/1	1,13,18,26, 75 79,84	7	8	0.0385	1.1077	0.1853	5.1722
	KH	1/1	1,28,32,35,42,43 .60,68	8	9	0.0390	1.2449	0.2891	6.3321
	PSO	1/1	1,8,15,32,48,56, 70,71	8	9	0.0387	1.2911	0.2786	6.6143
	NSGA-II	1/1	1,18,28,31,40,52 .64,70	8	9	0.0390	1.2641	0.2399	7.8259
3%	Proposed PSO-KH	1/1	1,17,22,30,36,73 .81	7	8	0.0438	1.3355	0.2347	5.5217
	KH	1/1	1,28,42,52,58, 73,78,81,84	9	10	0.0430	1.3255	0.4011	6.7162
	PSO	1/1	1,20,34,40,54,58 .71,81	8	9	0.0452	1.4298	0.3217	7.3192
	NSGA-II	1/1	1,13,14,21,26,50 .58,60,65,77	10	11	0.0431	1.1851	0.3019	9.8822
5%	Proposed PSO-KH	1/1	1,16,21,24,33,69 .77,79	8	9	0.0439	1.2855	0.2896	5.9407
	KH	1/1	1,9,19,24,37,53, 63,67,74	9	10	0.0467	1.5213	0.3342	7.6721
	PSO	1/1	1,6,23,32,68,70, 72,76,79,81,84	11	12	0.0468	1.5478	0.3211	8.6434
	NSGA-II	1/1	1,20,28,38,40,41 .43,68,73,76	10	11	0.0459	1.3836	0.2898	8.6315

Table 3.6 Indian 85-bus system: Optimal location of the power flow meters under different loadings including metrological errors of the flow meters (with DGs at bus no. 45 and 61)

Metrological Errors	Default Measurements (node/line number)	Location of flow meters(Line number)	No. of flow meters	Objective functions value			Max. error in bus voltage magnitude (V) (%)	Max. error in bus voltage angle (δ) (%)
				F ₁	F ₂	F ₃		
1%	1,45,61/1	1,9,27,33,44	5	8	0.0347	1.0013	0.1622	5.1137
3%	1,45,61/1	1,9,34,51,79,81	6	9	0.0411	1.1220	0.2181	5.377
5%	1,45,61/1	1,9,19,28,46,62,79	7	10	0.0419	1.2124	0.2214	5.5231

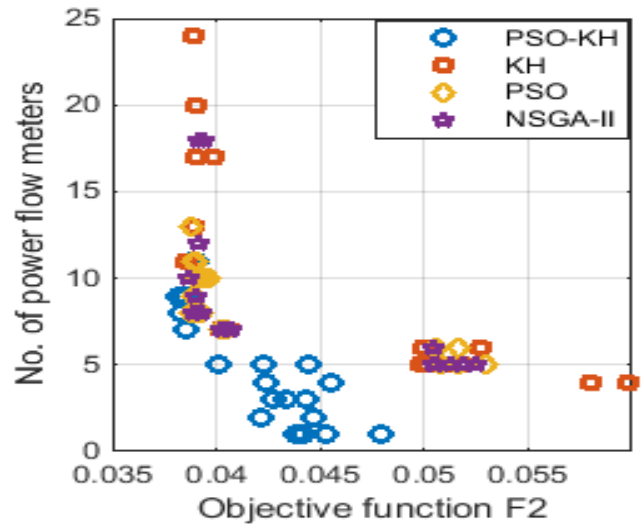


Figure 3.5(a): Optimal Pareto-front between no. of flow meters and F_2 for 1% error in real measurements and 50% in pseudo-measurements.

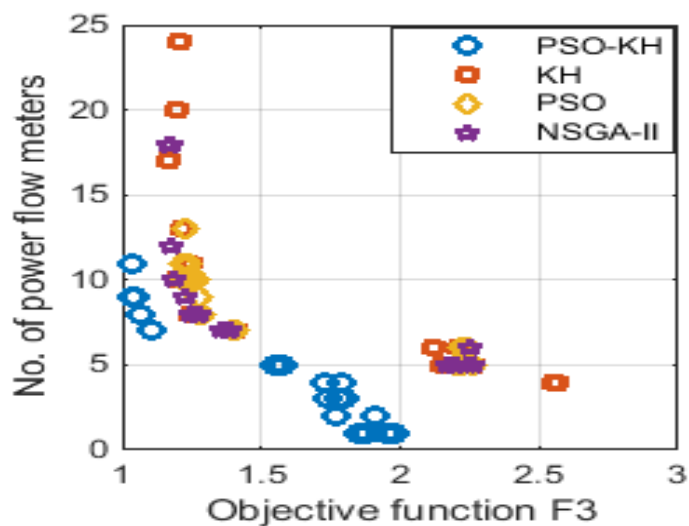


Figure 3.5(b): Optimal Pareto-front between no. of flow meters and F_3 for 1% error in real measurements and 50% in pseudo-measurements.

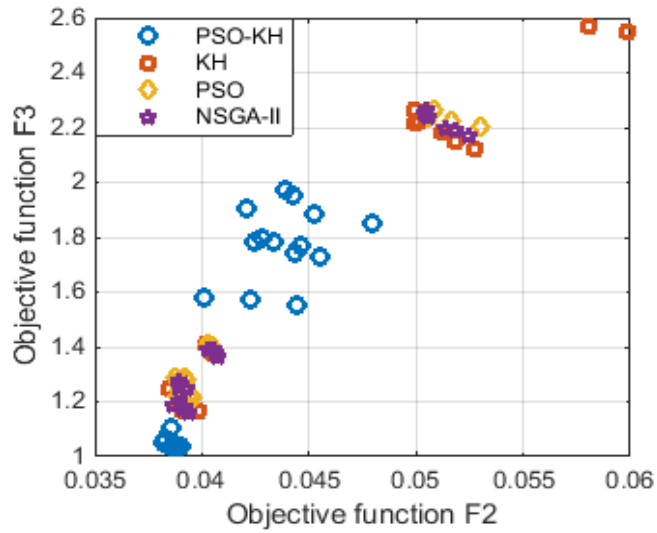


Figure 3.5(c): Optimal Pareto-front between objectives F_2 and F_3 for 1% error in real measurements and 50% in pseudo-measurements.

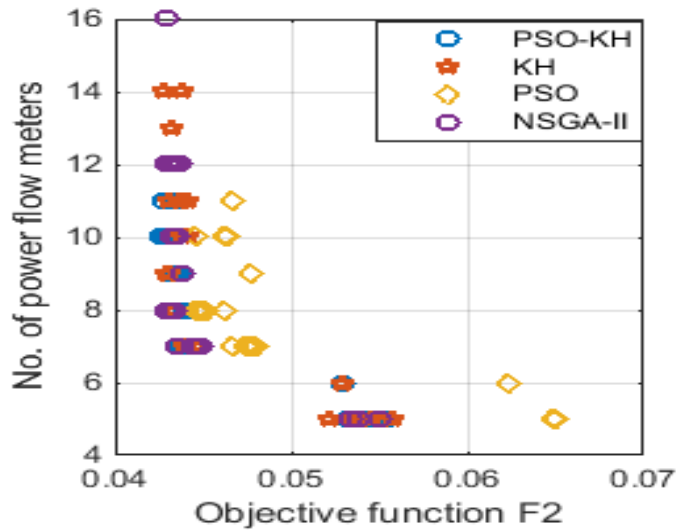


Figure 3.6(a): Optimal Pareto-front between no. of flow meters and F_2 for 3% error in real measurements and 50% in pseudo-measurements.

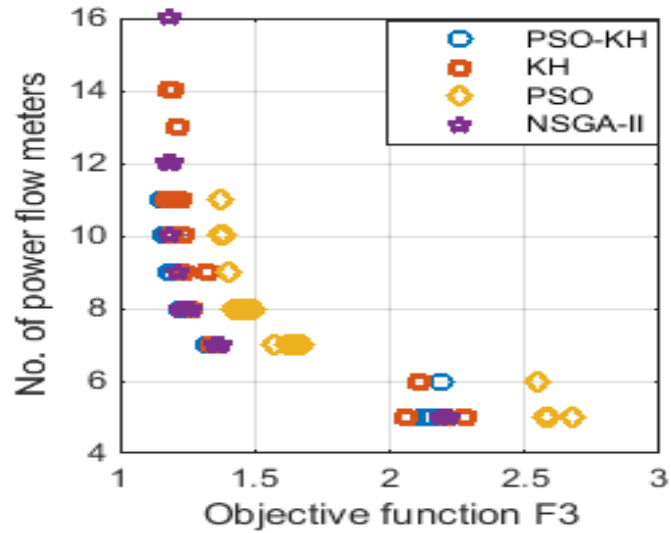


Figure 3.6(b): Optimal Pareto-front between no. of flow meters and F_3 for 3% error in real measurements and 50% in pseudo-measurements.

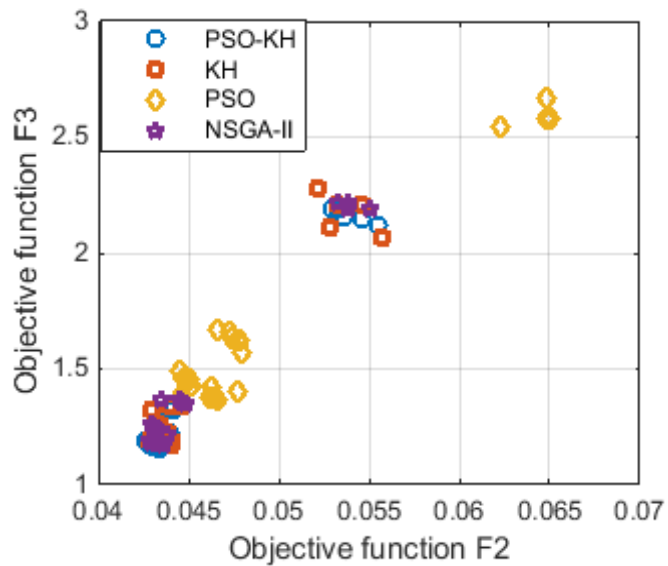


Figure 3.6(c): Optimal Pareto-front between objectives F_2 and F_3 for 3% error in real measurements and 50% in pseudo-measurements.

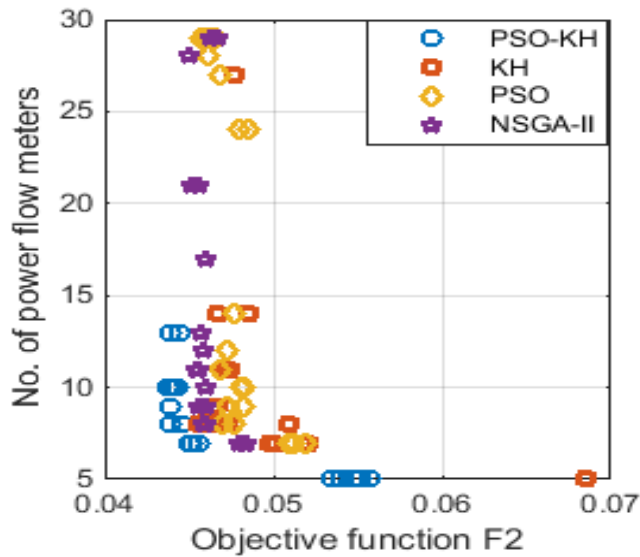


Figure 3.7(a): Optimal Pareto-front between no. of flow meters and F_2 for 5% error in real measurements and 50% in pseudo-measurements.

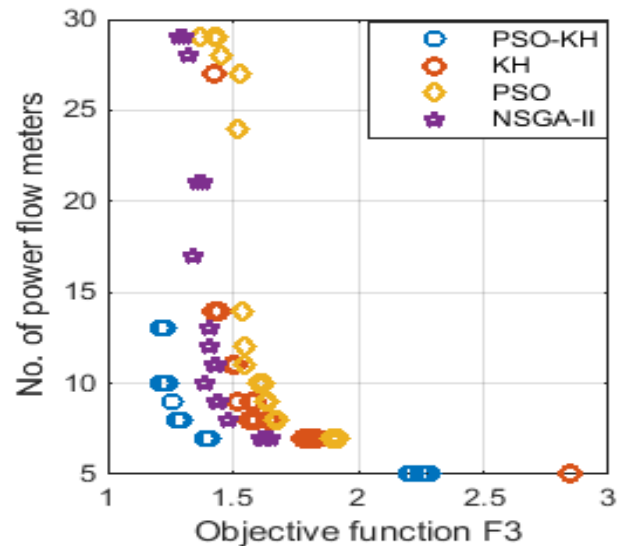


Figure 3.7(b): Optimal Pareto-front between no. of flow meters and F_3 for 5% error in real measurements and 50% in pseudo-measurements.

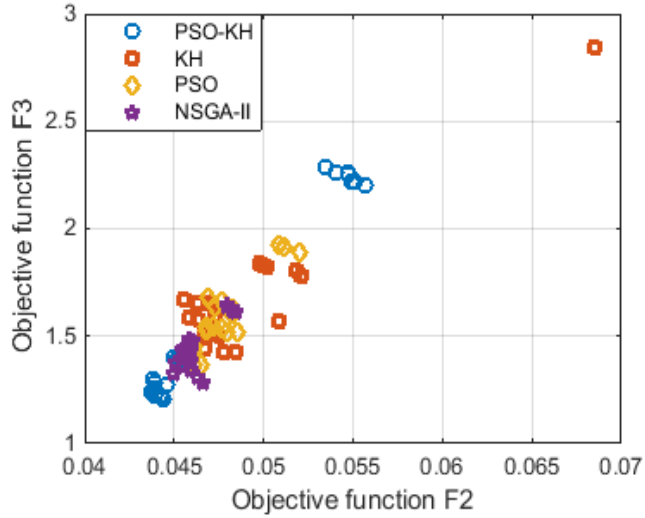


Figure 3.7(c): Optimal Pareto-front between objectives F_2 and F_3 for 5% error in real measurements and 50% in pseudo-measurements.

3.8 Summary

This chapter proposed a multi-objective optimization methodology that optimizes the number and location of measurement devices for state estimation in distribution networks. A new hybrid PSO-KH optimization algorithm has been proposed which considers variation in load power demand as well as the uncertainty of the measurement devices using Monte Carlo algorithm. A trade-off solution between the relative errors in voltage and phase angle estimates is established with the total cost of meters in a multi-objective framework to achieve best compromised solution between the cost and state estimation errors. Furthermore, the impacts of DG on state estimation accuracy have also been discussed.

The proposed hybrid PSO-KH algorithm is tested on IEEE 69-bus system and Indian 85-bus distribution network. The competitive results obtained using the proposed algorithm is compared with the existing algorithm such as PSO, KH and NSGA-II algorithm under various operating scenarios of the distribution networks. It is verified that the proposed algorithm is reliable and robust with respect to different metrological characteristics of the devices and load variation. Moreover, it can guarantee in getting global optimal solution. Therefore, the proposed approach of meter placement technique can be used for the planning study of the Smart distribution networks.

Chapter 4

A Multi-Objective Hybrid Estimation of Distribution Algorithm-Interior Point Method based Meter Placement for Distribution System State Estimation

Chapter 4

A Multi-Objective Hybrid Estimation of Distribution Algorithm-Interior Point Method based Meter Placement for Distribution System State Estimation

4.1 Introduction

This chapter proposed a new multi-objective hybrid Estimation of distribution algorithm (EDA)-interior point method (IPM) algorithm to obtain the optimal location of power flow meters for state estimation in distribution networks. The objective functions to be minimized are, (i) the total configuration cost of the distribution network, (ii) the average relative percentage error (APE) of bus voltage magnitude and (iii) APE of bus voltage angle. As the objectives are conflicting in nature, a multi-objective hybrid Pareto-based non-dominated sorting EDA-IPM algorithm has been proposed. Moreover, due to poor exploitation capability of the EDA, it is hybridized with IPM to improve its local searching ability in the search space. The hybridization of EDA and IPM brings a higher degree of balance between the exploration and exploitation capability of the algorithm during the search process. Furthermore, the loads and generators output are treated as stochastic variable and the impact of different type of DGs on state estimation performance has also been investigated. The efficiency of the proposed algorithm is tested on IEEE 69-bus system and Practical Indian 85-bus radial distribution network. The obtained results are compared with conventional EDA, PSO and NSGA-II.

4.2 Problem Formulation

The proposed multi-objective based meter placement optimization problem considered three objective functions to minimize: (1) the total cost of meters (2) the average relative percentage error (APE) of bus voltage magnitude and (3) APE of voltage angle. From the observation it is found that the above three objectives are conflicting in nature because if more number of meter are placed then estimation errors will get reduce and vice-versa. Therefore, the concept of optimal Pareto front and fast non-dominated sorting approach have been incorporated in this multi-objective optimization problem to find the best compromised solution [88]-[89].

The objectives to be minimized are described as follows:

$$F_1 = \sum_{i=1}^{nl} C_{pf,i} P_{pf,i} + \sum_{i=1}^n C_{VMM,i} P_{VMM,i} \quad (4.1)$$

$$F_2 = \frac{1}{m} \sum_m \frac{1}{n} \left(\sum_{i=1}^n \left| \frac{V_i^a - V_i^{est}}{V_i^a} \right| \right) \times 100 \quad (4.2)$$

$$F_3 = \frac{1}{m} \sum_m \frac{1}{n} \left(\sum_{i=1}^n \left| \frac{\delta_i^a - \delta_i^{est}}{\delta_i^a} \right| \right) \times 100 \quad (4.3)$$

Subjected to constraints: The constraints imposed describe in Eq. (4.4)-(4.5) considers for 95 % of the simulated cases [54]-[56] and is expressed as:

$$\left| \frac{V_i^a - V_i^{est}}{V_i^a} \right| \times 100 \leq 1 \quad (4.4)$$

$$\left| \frac{\delta_i^a - \delta_i^{est}}{\delta_i^a} \right| \times 100 \leq 5 \quad (4.5)$$

where F_1 , F_2 and F_3 represents three objective functions, n and nl are the number of nodes and lines in a distribution network, m is the number of operating scenarios, C_{pf} and C_{VMM} indicates the relative cost of power flow and voltage magnitude meter respectively. The cost of these meters is normalized to unity.

In the optimization process, the cost value assigned to both power flow meter and VMM are supposed to be equal because VMM are considered to be as default measurements. In this chapter, the location and number of VMM are taken as same for all optimization algorithm considered. Different cost values can be assumed for both the meters. But in actual practice, the cost of a measuring instrument depends on specific application scenarios. In the above equation, P_{pf} and P_{VMM} represents the binary decision variables i.e. if a meter is situated in a bus or lines then its value becomes one, else its value will be treated as zero, V_i^a and δ_i^a indicates the actual voltage magnitude and phase angle of i^{th} bus. Similarly, V_i^{est} and δ_i^{est} are denoted as estimated voltage magnitude and angle of i^{th} bus respectively.

The performance of state estimator deteriorates due to the presence of more number of pseudo-measurements with high variances. But, the performance can be improved by deploying additional real meters at suitable locations. In this chapter, the optimal number of VMM and power flow meters has been considered for the design of measurement infrastructure of an active distribution system. For state estimation, branch current based

distribution system state estimation (BC-DSSE) algorithm is used for estimating the states of the system such as branch current magnitudes and their angles [40]. The next section of this chapter describes the solution methodology for the above proposed multi-objective optimization problem.

4.3 Solution Methodology

For the solution of the multi-objective optimization problem, a new hybrid EDA-IPM algorithm has been proposed in this chapter. Therefore, in this section, a brief introduction to traditional EDA and Interior point method (IPM) has been presented as follows.

4.3.1 Estimation of Distribution Algorithm (EDA)

The EDA is a population based evolutionary optimization algorithm which employs a probabilistic model to generate new individuals for the next generation [90]-[91]. It has efficient diversification capability to explore the search space to achieve prominent solutions for the optimization problem. In EDA, new solutions are generated without using crossover and mutation operators like in genetic algorithm (GA). A probabilistic model is estimated in order to sample the new individuals from the database containing previous generation data and some selected population. The movement of each individual in the population is predicted by the probability model used in EDA. The pseudo-code of EDA is described as follows:

Begin

1. *Initialization: Generate R initial population randomly within limits.*

While termination criteria not met Do

2. *Evaluation: Calculate the fitness value of R individuals.*

3. *Selection: By using any selection method select N<R individuals.*

4. *Probabilistic model: Estimate the probability $p_s(x)$ that an individual being among the selected population.*

5. *Sampling: Sample R individuals from $p_s(x)$ using sampling technique.*

End while

End

4.3.2 Interior Point Method (IPM)

The primal dual IPM is basically used to solve non-linear constraint optimization problem [92]-[93]. The Lagrange multipliers are employed to deal with the equality and inequality constraints of the optimization problem. In order to avoid the negativity conditions of the slack variables the logarithmic barrier functions are added to the objective function. In

this method, the decision variables are considered to be continuous. The non-linear constraint optimization problem can be transformed to unconstraint optimization problem of the following Lagrange function:

$$L(z, y, l, u, v, w) = f(x) - v^T (x - l - x_{\max}) - y^T g(x) + w(x + u - x_{\max}) - \mu \sum_i (\ln l_i + \ln u_i) \quad (4.6)$$

where u and l are the slack variables; y , v and w are the Lagrange multipliers; and the barrier parameter is represented by μ .

In order to satisfy the Karush-Kuhn-Tucker (KKT) conditions, first order derivatives of a set of non-linear algebraic equations have been formed and then Newton-Raphson method is employed to solve the above first order differential equations [92]. During the iterative procedure of the IPM, if the KKT conditions shown below are satisfied then the algorithm will stop. The KKT conditions are described as follows:

$$\|L_x\| = \|\nabla f(x) - \nabla g^T(x)y - v + w\| < \epsilon \quad (4.7)$$

$$\|L_y\| = \|g(x)\| < \epsilon \quad (4.8)$$

$$\|L_w\| = \|x + u - x_{\max}\| \leq \epsilon \quad (4.9)$$

$$\|L_v\| = \|x - l - x_{\min}\| \leq \epsilon \quad (4.10)$$

According to primal-dual theory, x is the primal variable, l and u is the slack variable y , v and w are the dual variables respectively. The equations (4.8)-(4.10) are called the primal feasible conditions and eq. (4.7) is known as dual feasible conditions. If the solution satisfies the above conditions then it is an optimal solution for the optimization problem.

4.3.3 Proposed Multi-objective Hybrid EDA-IPM algorithm

In this work, the meter placement problem is formulated as multi-objective optimization problem. The main advantage of using this approach is, a best compromised solution can be established between the various objectives described in section 2. Simultaneously, the impacts of meter location on state estimation accuracy can be investigated. Therefore, a trade-off solution is essential between the objectives to reduce the cost and state estimation error. In order to achieve best compromised solution among the objectives, hybrid EDA-IPM algorithm has been proposed. The reason for this hybridization of two algorithms is described as follows.

EDA has been used widely in variety of engineering applications because of its efficient exploration capability in the search space. Although, EDA has good exploration ability but it suffers from poor exploitation capability to get global optimal solution. However,

the local searching capability of IPM algorithm is more effective. Therefore, the conventional EDA is hybridized with IPM to enhance the exploitation capability of the algorithm to get near global optimal solutions. The solution obtained from EDA is taken as inputs to IPM.

In multi-objective optimization case if objective functions are conflicting in nature, then no solution can be improved itself in one objective without worsening the other objectives. Since the objectives are conflicting, non-dominated sorting principle has been incorporated to get the best optimal Pareto front [88]. All solutions in a non-dominated Pareto front are treated as best optimal solution. Thus, in this approach, the solution is not a single optimal solution like single objective optimization case rather it is a set of optimal solution. In this chapter, non-dominated sorting approach has been employed with hybrid EDA-IPM algorithm to achieve best trade-off solution between different objectives such as cost, ARPE in voltage magnitude and phase angle.

In the proposed algorithm, initially solutions are generated randomly using seeding approach within the search space. Each solution represents number of power flow meters as well as their locations. Based on their locations the objective functions [Eq. (1)-(3)] are evaluated using BC-DSSE algorithm [40]. Then, the selection mechanism has been used to select some of the best solutions obtained so far. These selected solutions are updated using IPM algorithm to obtain best neighborhood solution. After updating the selected solutions, probabilistic Bayesian model has been incorporated to predict the new solutions for future generation based on the selected solution. After evaluating the fitness, constraints violation checking has been carried out. To satisfy the constraints, Monte Carlo simulation is used and relative deviations in voltage magnitude and angle is determined at each bus for all Monte Carlo trials. In 95% of cases, if the relative errors are within the pre-specified limits, then that solution is stored for the next generation. On the other hand, if it is not, then a higher objective value is to be assigned to that solution so that this solution can be eliminated from the next generation. After that sampling technique is utilized. Then, this procedure is repeated till the convergence criterion is met. To get the best solution in optimal Pareto front, fuzzy theory [95] has been used.

In the optimization process different population size like 20, 30 and 50 have been tried. But, it has been found that there is no such significant variation in result for taking different population sizes for both the test system. Therefore, population size of 20 has been fixed for evaluating the performance of the proposed optimization algorithm. The flowchart of the proposed method has been shown in Figure 4.1. Furthermore, the pseudo code of the

proposed multi-objective hybrid EDA-IPM algorithm has been presented as follows:

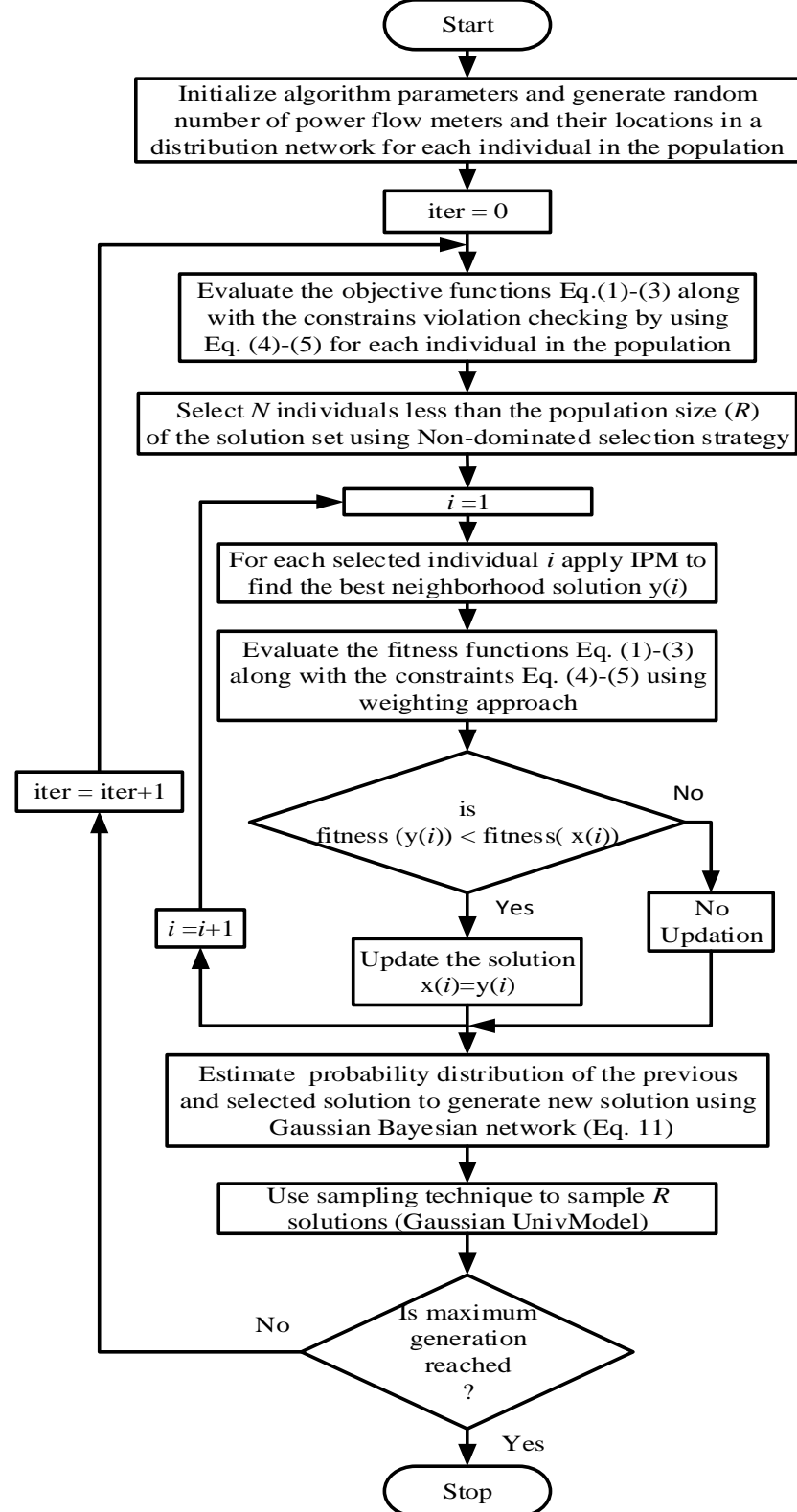


Figure 4.1: Flowchart of the proposed multi-objective hybrid EDA-IPM algorithm

The steps of the proposed algorithm are as follows:

Step1. Initialization: Generate random number of power flow meters and their locations for each individual in the population (*Pop*).

Do while (“Stopping criterion is not satisfied”)

Step 2. Fitness evaluation: Evaluate the fitness functions for each individual in the *Pop*.

Step 3. Selection: Select $N < R$ solutions from *Pop* using Non-dominated sorting selection strategy. *R* is the size of the population and *N* is a number less than *R*.

Begin

Do while (“Stopping criterion is not satisfied”)

For $i = 1$: S_{soln} (Number of selected solutions.)

1. Use each solution i as initial point in IPM to find the best optimal solution for each i .

2. Evaluation: Calculate fitness value of $y(i)$ using weighting approach.

3. Update solution:

if Fitness ($y(i)$) < Fitness ($x(i)$)

&& *if solution y dominates x*

then $x(i) = y(i)$

End for i

End Do

End

Step 4. Probabilistic graphical model: Estimate the probability distribution of the previous solutions and selected solution to predict new population for the next generation using Gaussian Bayesian network. Mathematically, it can be expressed as:

$$p(x_i | pa(X_i)) = N(\mu_i + \sum_{X_j \in Pa(X_i)} w_{ij} (x_j - \mu_j), v_i^2) \quad (4.11)$$

where μ_i represents the mean of the variable X_i , v_i is the standard deviation of the distribution and w_{ij} is the weight associated with each of the parents. x_j is the value of the variable X_j in $pa(X_i)$.

Step 5. Sampling technique: Sample *R* number of solutions from the Gaussian Bayesian network using sample Gaussian UnivModel.

End Do

End

4.4 Test and Simulation Conditions

To analyze the efficiency of the proposed state estimation formulation and algorithm, several test conditions and network operating scenarios have been considered in MATLAB 2014b environment. For state estimation in radial network, BC-DSSE algorithm has been employed. In BC-DSSE, the magnitude of branch currents and their angles are treated as state variables [40]. In order to generate the measurement data for state estimation, first backward forward sweep method has been used to obtain the load flow solution of a distribution network. This load flow solution is treated as the reference or actual values of the measured quantities. Then, the measurement data is generated by adding random noise following the Gaussian distribution to the actual values of the quantities obtained from the load flow solution. Mainly, there are four types of measurement data are considered for state estimation such as: substation measurements, real measurements, pseudo-measurements and virtual measurements [75]. The error associated with each type of measurement data is based on the maximum percentage of error assumed for that measurement. The following conditions are considered for the measurement uncertainties:

- 1) Substation Measurements: In this work, it is assumed that the maximum percentage of error associated with substation measurement is 1%. This measurement is called as default measurement.
- 2) Real measurements: Generally, the real measurements are more accurate. Therefore, the maximum error assumed for this is 1%, 3% and 5%. The power flow meters are assumed as real meters and it measures both real and reactive power flows in a line.
- 3) Pseudo-measurements: Basically, the pseudo-measurements are obtained from the historical customer load data. Therefore, these measurements are less accurate than other types of measurements. The maximum percentage of error assumed for pseudo-measurements is 50% [75].
- 4) Virtual-measurements: The virtual measurements are obtained from the zero-injection buses and these measurements are highly accurate than other measurements with a variance value of 10^{-7} [94].

Furthermore, the load and generators are considered as stochastic variable to analyze the performance of the proposed meter placement scheme. Different measurement uncertainties for better analysis of the proposed technique have been considered. In simulation study, it is considered that the load and generator outputs are stochastic in nature and it is assumed to be distributed normally around the mean value with fixed standard deviation.

Moreover, the Monte Carlo trials have been utilized to study the effects of measurement uncertainties on state estimation performance. There are 100 number of different network operating conditions are generated. From each network operating condition, 600 number of different network states are generated by using Monte Carlo simulation. Thus, in this simulation study, the total number of network scenarios considered is 100×600 . A standard deviation of $\pm 10\%$ around the base value has been assumed for each operating condition. Different measurement uncertainties considered for real meters are 1%, 3% and 5% respectively.

The number of meters required and their locations in presence of different type of DG has also been investigated in this chapter. Moreover, it is assumed that the locations of DGs are fixed [97], [98] and their output is a stochastic in nature. Various types of network scenarios such as meter placement impacts on passive as well as active distribution networks have been considered. Further, the active network consists of DG only producing real power to the networks, DG producing real power as well as absorbing reactive power, and DG producing both real power as well as reactive power to the network. Since, the DG outputs are not controlled in this case so these belong to non-dispatchable type. In presence of these kinds of DGs, the meter placement impact on state estimation accuracy in a multi-objective environment has been discussed in this work. The types of DG and their capacity are provided in Table 4.2.

The parameters used for PSO, NSGA-II and EDA are provided in Table 4.1. In PSO, the parameters used are inertia weight (W_{\max}, W_{\min}) and the learning factors $C1$ and $C2$. The value of inertia weight decides the balance between exploration and exploitation capability of the PSO algorithm. It is found that the best performance is obtained by setting w initially to some relatively high value (e.g. 0.9) to perform extensive exploration in the search space. When w is reduced gradually to a lower value (e.g. 0.4), the system becomes more dissipative and exploitative. This will improve the local searching capability of the algorithm. Therefore, the appropriate values of W_{\max} and W_{\min} chosen is 0.9 and 0.4 respectively [86]-[87]. Furthermore, the parameter $C1$ and $C2$ represents the speed of flying of particles to the most optimize position of the swarm in the search space and its own best position. It regulates the length and time taken by particle to reach most optimum position. So that, the particle land in an appropriate position. For example if too big a value of acceleration constants is selected, then the particle may fly past the appropriate position and for too small value, the particle will not be able to reach the target position. Generally, each of these constants are set to 2 to

make the times taken to move towards the particle's personal best and swarm's global best as equal.

Table 4.1 Parameter values of PSO, NSGA-II and EDA algorithm

PSO	Population size=20, C1=2,C2=2 $W_{\max} = 0.9, W_{\min} = 0.4$ Maximum number of generations=50,
NSGA-II	Population size=20 Crossover rate (P_c)=0.8, Mutation rate (M_c) =0.02, Maximum number of generations=50
EDA	Population size: 20 Learning method : Learn Gaussian Bayesian Model, Sampling method: Sample Gaussian Universal Model Replacement method: Pareto Rank ordering Selection method : Non-Dominated selection Repairing method: Set In Bounds repairing

Table 4.2 Distribution generation (DG) installation bus and capacity

Test System	Bus Number	DG type and capacity(in MW) Base Value		
		Type-1 (P)	Type-2 (P+jQ)	Type-3 (P+jQ)
IEEE 69-bus System	50	0.180	0.180-j0.087	0.180+j0.087
	61	0.270	0.270-j0.130	0.270+j0.130
Indian 85- Bus System	45	0.277	0.235-j0.145	0.235+j0.145
	61	0.290	0.246-j0.152	0.246+j0.152

4.4.1 IEEE 69 Bus System

The performance of the proposed algorithm has been investigated on standard IEEE 69-bus, 12.66kV radial distribution network. This network consists of 69 buses, 68 lines along with 48 loads and DGs at bus number 50 and 61. The system line and load data are taken from [99].The total load of the system is 3.802MW and 2.692Mvar respectively. In this system, there are 21 number of zero injection buses. The virtual measurements are obtained from these zero injection buses. One VMM and a power flow meter are kept at the substation which is treated as default meters.

From the simulation result it is observed that when the meter accuracy is 1%, the number of flow meter needed is 5 using the proposed hybrid EDA-IPM algorithm. On the other hand the number of power flow meters required is 7, 9 and 7 using EDA, PSO and NSGA-II respectively. In Table 4.3, the APE of voltage magnitude and phase angle are specified. It is observed that APE of voltage magnitude and angle using proposed hybrid

EDA-IPM algorithm is 0.0025% and 0.4821%. In case of EDA and PSO these are 0.0081%, 1.3421% and 0.0053%, 0.8985% and using NSGA-II it is 0.0060% and 0.9352% respectively. The optimal Pareto front of all the algorithms is shown in Figure 4.2 when the meter accuracy is 1%. Among all the solution in the Pareto front, the best optimal solution is selected by using fuzzy theory [95]. Moreover, the maximum relative percentage error using different methods in voltage and angle estimates are also presented in Table 4.3. It is worth noticing that the maximum deviations in state variables using the proposed algorithm are significantly lower than using PSO, EDA and NSGA-II.

The optimal Pareto-front for meter accuracy of 3% and 5% between different objectives has also been shown in Figure 4.3 and 4.4. In this case the objectives F_2 and F_3 values are little higher than 1% case because meter error considered is higher than 1%. It is observed that if the errors are more in direct measurements then its impacts on the state estimation accuracy is significant and also meters requirement is more. Moreover, it is worth noticing that the impact of measurement uncertainties and meter locations on state estimator performance is more significant. In Table 4.3, it is seen that, for EDA, the total number of power flow meters required is 7. Figure 4.2 shows the optimal Pareto-front between F_2 and F_3 . It is observed that F_2 and F_3 are correlated to each other. Thus, the optimal Pareto is not established between the two objectives.

The results shown in Table 4.3 refer to a passive distribution network. From these two observations can be made, first as the accuracy of the meters decreases the number of power flow meters needed is more for better state estimation performance. Secondly, the efficiency of the proposed hybrid EDA-IPM algorithm is found to be better due to its higher degree of balance between the exploration and exploitation capability. This results in efficient searching ability of the proposed algorithm in the search space. Thus, a new hybrid EDA-IPM algorithm has been employed for the distribution state estimation in multi-objective framework to resolve the meter placement issues. The results obtained using PSO, EDA and NSGA-II are compared with the proposed algorithm to test it's the efficiency.

Furthermore, the proposed methodology has also been tested in presence of DG. There are different kinds of DG considered are provided in Table 4.2. Two DGs of type 1 are installed at bus number 50 and 61. To get minimum power loss and voltage deviation, the two DGs are placed at these buses. The obtained results are provided in Table 4.4. It is observed that, there is a reduction in number of power flow meter requirement as compared to passive case. The phase angle error is also reduced. The reason is, DG provides power to the

local bus. Therefore, the real power drawn by that load from the feeder section is reduced i.e. the magnitude of current in the lines will go down. As a result, the magnitude of error associated with power flow measurements will get reduce. Moreover, due to the presence of DGs, the redundancy level of measurement is increased which helps to improve the accuracy of the estimator to a further extent. The presence of type 2 and 3 DG has been studied and the results obtained are provided in Table 4.5. It is observed that, in all the cases, the proposed algorithm outperforms all other algorithms used. In case of type 2 and 3 DGs, it is assumed that the DGs are generating both real and reactive power to the network. In one case DG supplying reactive power and in other case it is absorbing reactive power from the network.

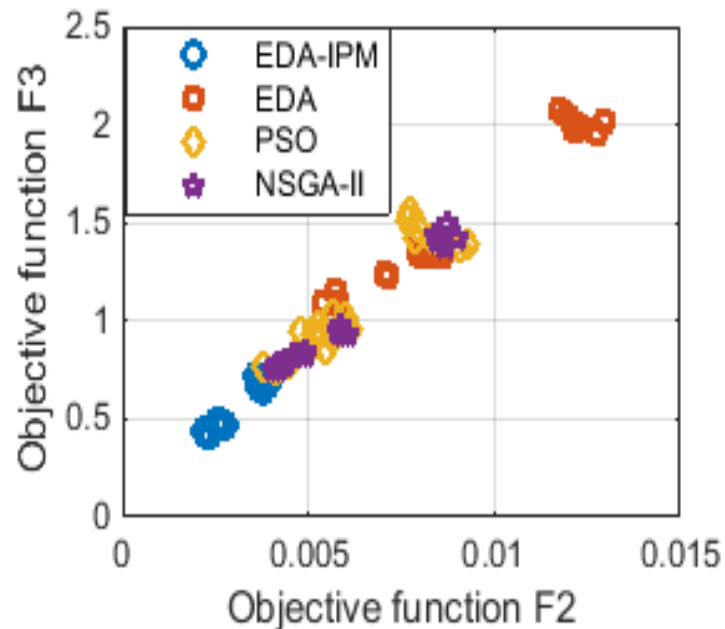


Figure 4.2(a) Optimal Pareto front between objectives F_3 and F_2 (1% error in real and 50% in pseudo-measurements)

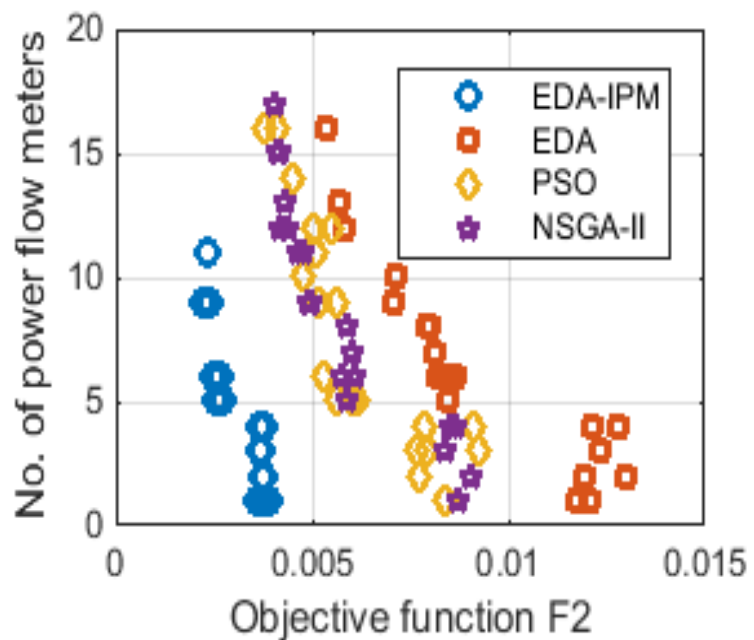


Figure 4.2(b) Optimal Pareto front between number of flow meters and F_2 (1% error in real and 50% in pseudo-measurements)

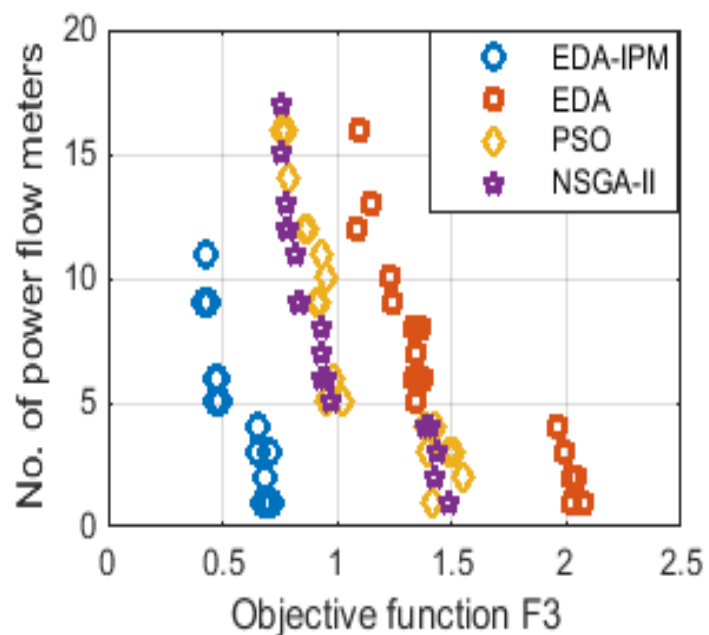


Figure 4.2(c) Optimal Pareto front between number of flow meters and F_3 (1% error in real and 50% in pseudo-measurements)

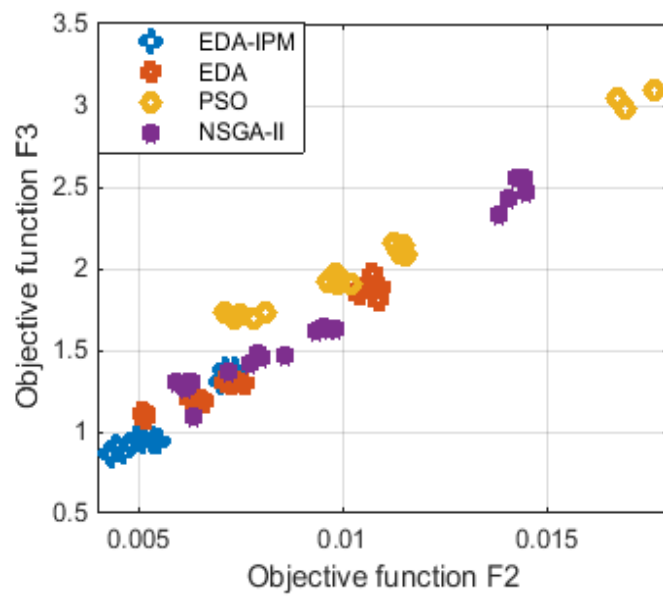


Figure 4.3(a) Optimal Pareto front between the objectives F_2 and F_3 (3% error in real and 50% in pseudo-measurements)

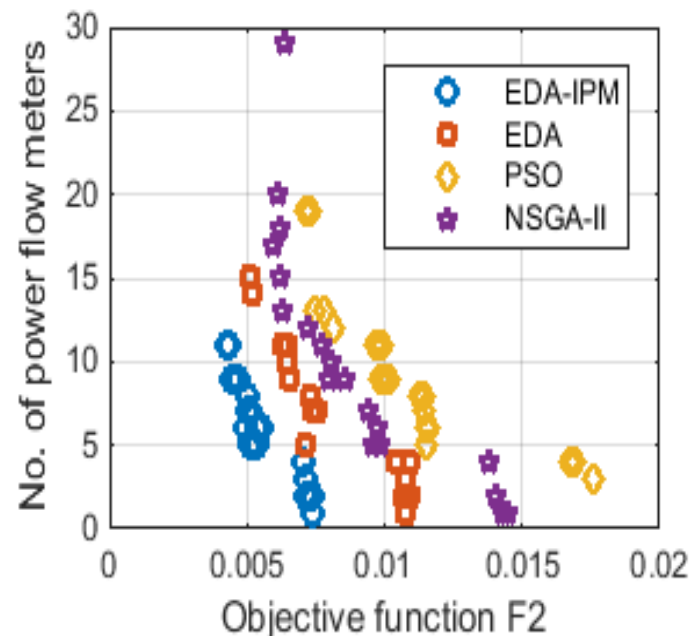


Figure 4.3(b) Optimal Pareto front between number of flow meters and F_2 (3% error in real and 50% in pseudo-measurements)

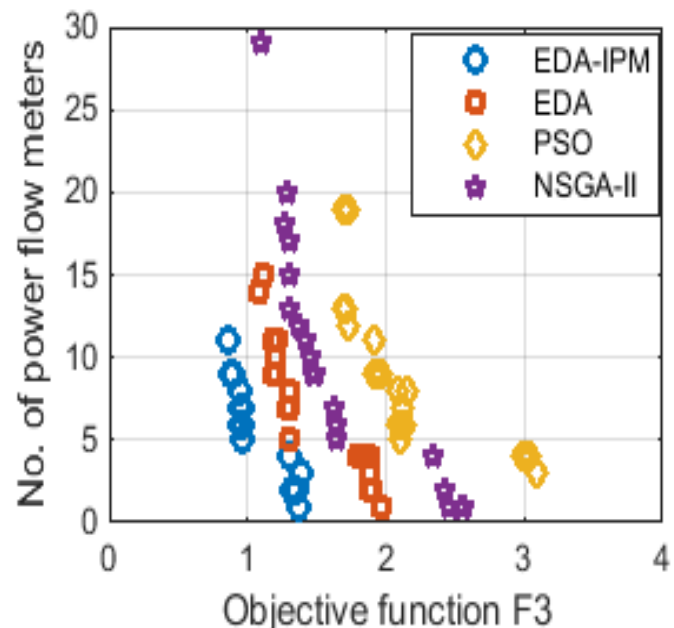


Figure 4.3(c) Optimal Pareto front between number of flow meters and F_3 (3% error in real and 50% in pseudo-measurements)

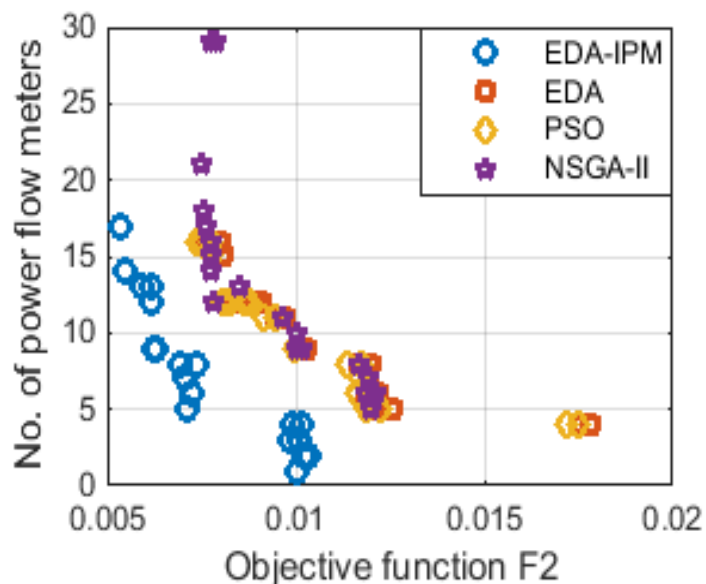


Figure 4.4(a) Optimal Pareto front between number of flow meters and F_2 (5% error in real and 50% in pseudo-measurements)

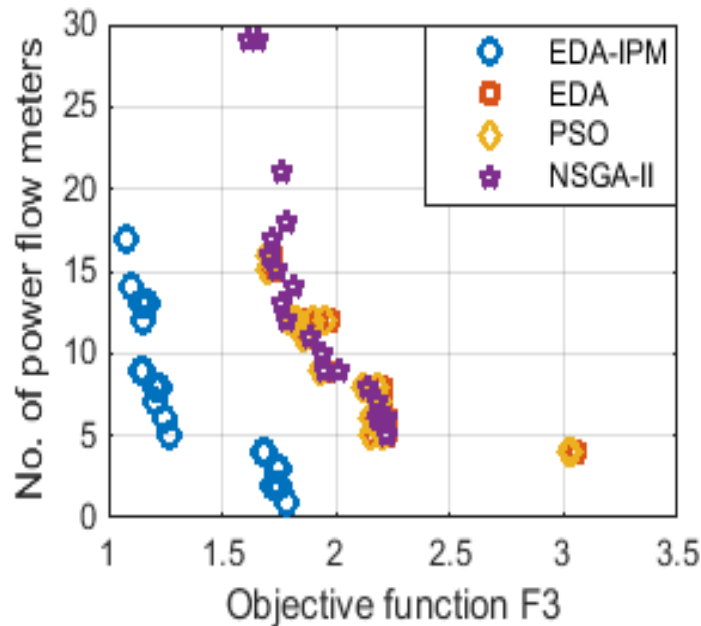


Figure 4.4(b) Optimal Pareto front between number of flow meters and F_3 (5% error in real and 50% in pseudo-measurements)

Table 4.3 IEEE 69-bus system: The number and location of the power flow meters of different meter accuracy (without DG)

Metrological Errors	Algorithm	location of flow meters(Line number)	Number of flow meters	Objective functions value			Maximum error in bus voltage magnitude (V) (%)	Maximum error in bus voltage angle (δ) (%)
				F_1	F_2	F_3		
1%	Proposed EDA-IPM	1,7,24,3,51	5	6	0.0025	0.4821	0.0201	5.2137
	EDA	1,11,17,23,41,47,56	7	8	0.0081	1.3421	0.0318	6.9784
	PSO	1,10,21,27,30,32,33,49,67	9	10	0.0053	0.8985	0.0375	8.4249
	NSGA-II	1,5,17,20,25,56,67	7	8	0.0060	0.9352	0.0272	9.2313
3%	Proposed EDA-IPM	1,11,19,43,52	5	6	0.0051	0.9657	0.0317	5.7321
	EDA	1,9,17,23,29,36,44,57	8	9	0.0072	1.2950	0.0475	7.9238
	PSO	1,4,37,39,44,49,54,58,68	9	10	0.0102	1.9119	0.0338	10.7899
	NSGA-II	1,3,4,14,17,21,43,47,48,53,57,61,63	13	14	0.0063	1.3083	0.0434	9.9812
5%	Proposed EDA-IPM	1,7,14,19,28,33,47,53,61	9	10	0.0056	1.1273	0.0513	6.2379
	EDA	1,11,19,26,33,39,44,47,53,57,61,65	12	13	0.0055	1.1289	0.07543	9.3417
	PSO	1,2,11,17,18,28,32,40,45,47,51,57,66,67	14	15	0.0074	1.7642	0.0538	13.2314
	NSGA-II	1,4,13,14,16,25,30,3,45,56,63,66	12	13	0.0078	1.7876	0.0673	12.2324

Table 4.4 IEEE 69-bus system: The number and location of the power flow meters of different meter accuracy (Type 1 DG at bus 50 and 61)

Metrological Errors	Algorithm	location of flow meters(line number)	Number of flow meters	Objective functions value			Maximum error in bus voltage magnitude (V) (%)	Maximum error in bus voltage angle (δ) (%)
				F_1	F_2	F_3		
1%	Proposed EDA-IPM	1,49,52,60,68	5	8	0.0018	0.3125	0.0130	5.2983
	EDA	1,28,33,37,51,62	6	9	0.0063	1.1021	0.0200	9.1936
	PSO	1,13,24,27,30,33,49,67	8	11	0.0047	0.7985	0.0347	7.9243
	NSGA-II	1,7,19,29,34,59,67	7	10	0.0062	0.8152	0.0278	9.2713
3%	Proposed EDA-IPM	1,19,23,29,53	5	8	0.0043	0.8357	0.0204	6.0125
	EDA	1,5,11,19,24,33,41, 44,49,51,65,67	7	10	0.0068	1.1027	0.0321	10.2773
	PSO	1,7,17,39,41, 49,57,59,63	9	12	0.0110	1.3411	0.0438	10.1324
	NSGA-II	1,5,9,15,19,28, 49,57,59,61,63	11	14	0.0049	1.0830	0.0374	9.1119
5%	Proposed EDA-IPM	1,3,17,24,33, 41,50,63	9	12	0.0051	1.1122	0.0230	6.9124
	EDA	1,4,24,36,47, 54,63,64,67	11	14	0.0049	1.1113	0.0319	10.0087
	PSO	1,7,15,17,26,37,43,45, 49,51,58,62,65	14	17	0.0072	1.0642	0.0317	13.9342
	NSGA-II	1,6,9,11,15,20,22, 41,54,63,65	11	14	0.0120	1.1834	0.0713	11.9807

Table 4.5 IEEE 69-bus system: The number and location of the power flow meters in presence of type 2 and 3 DGs at bus 50 and 61

DG Type	Measurement error	Algorithm	Location of flow meters(Line number)	Number of power flow meters	Objective functions value			Maximum error in bus voltage magnitude (V) (%)	Maximum error in bus voltage angle (δ) (%)
					F_1	F_2	F_3		
Type 2 (P-jQ)	1%	Proposed EDA-IPM	1,5,24,37,42	5	8	0.0069	1.1807	0.0291	5.8912
		EDA	1,4,14,61,65,66	6	9	0.0086	1.6091	0.0314	6.3732
		PSO	1,2,4,14,28,43,51,68	8	11	0.0098	1.8356	0.0377	6.8123
		NSGA-II	1,5,30,39,44,58	6	9	0.0097	1.8651	0.0299	5.9927
		Proposed EDA-IPM	1,11,32,45,51	5	8	0.0067	0.9864	0.0326	5.6734
		EDA	1,13,34,49,51,52,60	7	10	0.0096	1.5240	0.0541	6.3422
Type 3 (P+jQ)	3%	PSO	1,8,25,35,45,49,55	8	11	0.0098	1.4713	0.0491	6.4532
		NSGA-II	1,11,32,50,51,54,60	7	10	0.0106	1.6617	0.0613	6.2459
		Proposed EDA-IPM	1,3,5,18,19,21,25,26,51	9	10	0.00643	1.3490	0.0328	5.9978
		EDA	1,6,20,28,32,35,40,45,48, 63,65,68	12	13	0.0071	1.5294	0.0537	6.8970
		PSO	1,4,15,21,24,31,33,36,44, 47,51,66	12	13	0.0073	1.5966	0.0768	6.9846
		NSGA-II	1,3,15,20,22,27,28,29,32, 38,42,43,62,65	14	15	0.0073	1.8386	0.0712	6.8878
Type 3 (P+jQ)	5%	Proposed EDA-IPM	1,12,33,42,50	5	6	0.0067	1.1509	0.0311	6.0125
		EDA	1,8,14,32,36,41,60,68	8	11	0.0063	1.2030	0.0527	7.1112
		PSO	1,7,11,17,22,28,30,33, 49,51,61,65,67	13	16	0.0075	1.4489	0.0492	6.9864
		NSGA-II	1,3,22,23,41,47,65,67, 68	9	12	0.0077	1.3544	0.0512	6.8823
		Proposed EDA-IPM	1,2,4,11,14,33,43,44, 46,51,65,66,68	13	16	0.0065	1.6044	0.04351	6.3724
		EDA	1,6,9,16,18,26,28,40,43, 49,50,60,61,65,68	15	18	0.0063	1.4943	0.0543	7.0103
Type 2 (P-jQ)	5%	PSO	1,17,25,31,33,34,35,37, 42,44,49,55,62,66	14	17	0.0081	1.8438	0.0612	7.8712
		NSGA-II	1,5,7,17,18,23,26,29,36,37, 38,40,41,45,67	15	18	0.0071	1.7005	0.0666	8.0128
		Proposed EDA-IPM	1,12,13,23,25,26,39,50, 56,64	10	13	0.0071	1.3298	0.0626	6.8934
		EDA	1,13,14,22,23,26,30,36,40, 41,62,65	12	15	0.0066	1.3549	0.0666	9.0127
		PSO	1,5,8,19,21,22,23,25,29,34, 40,43,54,63,68	15	18	0.0083	1.6628	0.0686	8.9997
		NSGA-II	1,6,11,14,21,37,47,50,67	9	12	0.0100	1.8346	0.0712	9.0128

4.4.2 Practical Indian 85-bus System

To investigate the performance of the proposed algorithm, in practical distribution network, Indian 85-bus, 11kV radial distribution system has been taken into consideration. This system consists of 85 nodes and 84 numbers of lines. The total load of the system is

2.574MW and 2.622MVar respectively. This system consists of 21 zero injection buses. The network line and load data are obtained from [100]. Furthermore, the parameters of the algorithms specified in Table 4.1, can also be applicable for this test system.

The results obtained for this system have been reported in Table 4.6. It is seen that when meter error is 1% and pseudo-measurement error is 50%, the number of meters required is 7 by using proposed hybrid EDA-IPM algorithm whereas in case of PSO, EDA and NSGA-II, the number of meters required is 8, 8 and 9 respectively. The corresponding objective functions value is also provided in Table 4.6. The optimal Pareto front curve between the objectives has been shown in Figure 4.5, 4.6 and 4.7 respectively, for different measurement uncertainties of the power flow meters. It is noticed that if meter accuracy is decreased from 1% to 3 or 5%, then the network needs more number of meters to improve the quality of state estimation. Therefore, more real meters are employed to bring down the relative errors in voltage and angle estimates below the pre-specified thresholds.

The performance of the proposed algorithm in presence of different kind of DGs at bus number 45 and 61 has also been tested. The results obtained using type 1, 2 and 3 DGs are provided in Table 4.6, 4.7 and 4.8 respectively. From the results shown in Table 4.6, 4.7 and 4.8, the impact of different types of DGs on state estimation accuracy is clearly visualised. In case of type 1 DG, the phase angle error is reduced to a great extent because of DG supplies only real power to the local loads where it is connected. Therefore, the magnitude of power flow in the main feeder section is getting reduced. Table 4.7 represents the results obtained using the proposed hybrid EDA-IPM algorithm. From the results reported in Table 4.6, 4.7 and 4.8, it is observed that both the location and measurement uncertainties significantly affecting the state estimation accuracy. The results obtained using DG type 2 and 3 are also reported in Table 4.7 and 4.8 respectively. The main motive of using this Pareto based multi-objective optimization technique is to obtain a best compromised solution between the objectives such as relative percentage error in voltage magnitude and angle with respect to the total cost of meter.

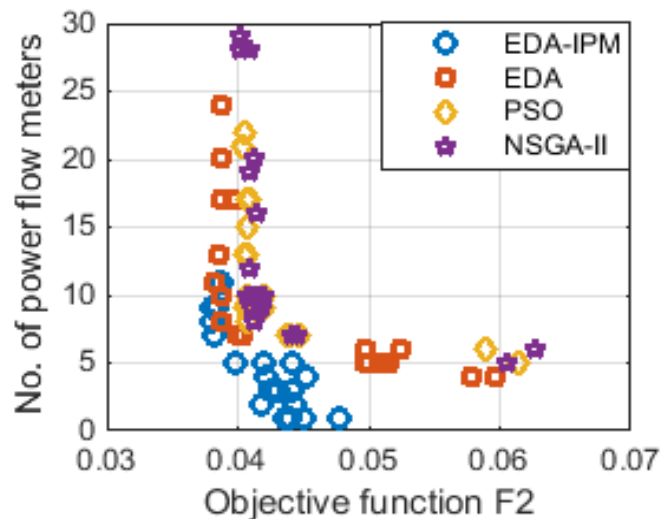


Figure 4.5(a) Optimal Pareto front between number of flow meters and F_2 (1% error in real and 50% in pseudo-measurements)

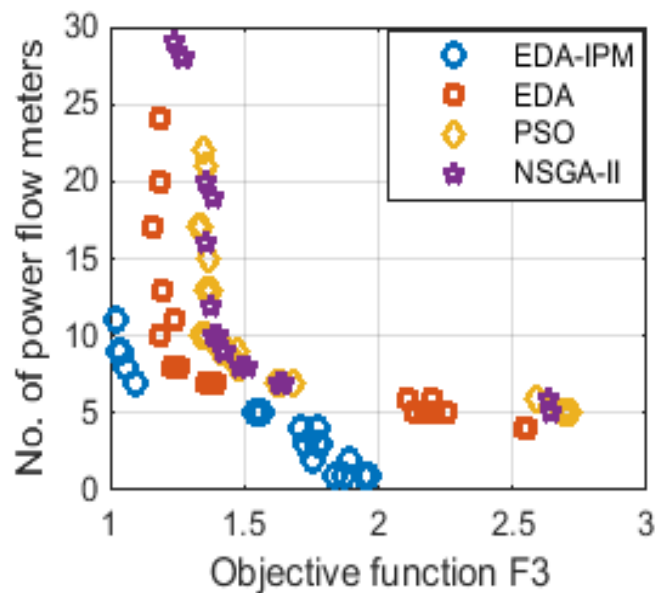


Figure 4.5(b) Optimal Pareto front between number of flow meters and F_3 (1% error in real and 50% in pseudo-measurements)

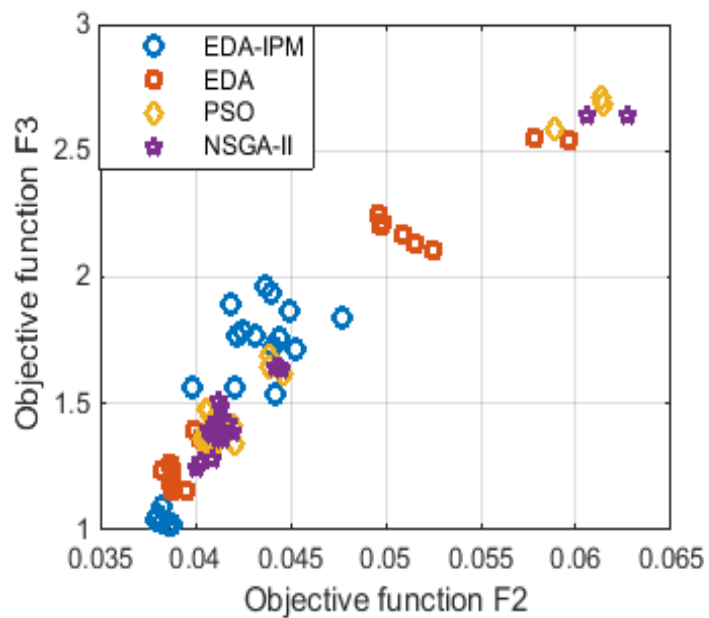


Figure 4.5(c) Optimal Pareto front between objective F_2 and F_3 (1% error in real and 50% in pseudo-measurements)

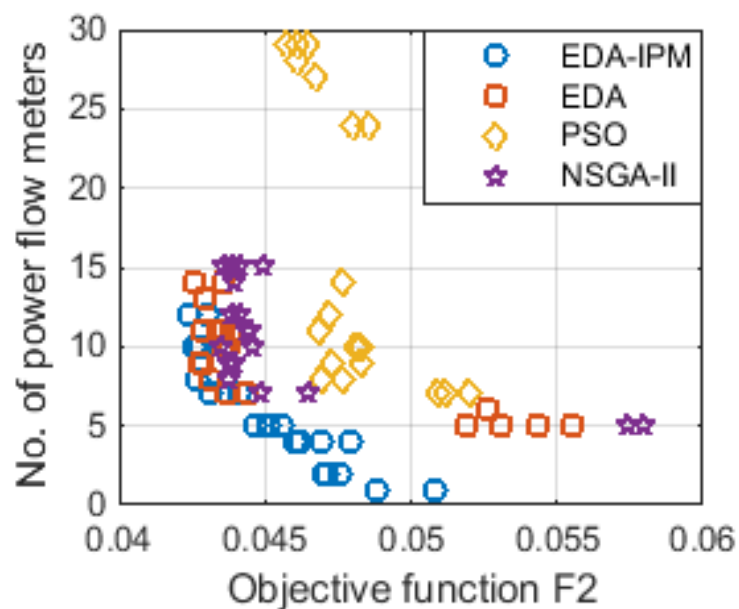


Figure 4.6(a) Optimal Pareto front between number of flow meters and F_2 (3% error in real and 50% in pseudo-measurements)

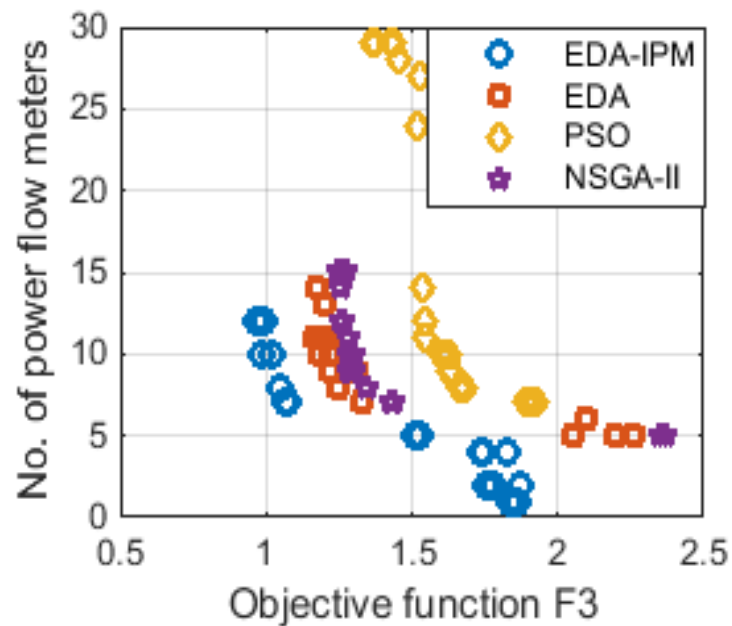


Figure 4.6(b) Optimal Pareto front between number of flow meters and F_3 (3% error in real and 50% in pseudo-measurements)

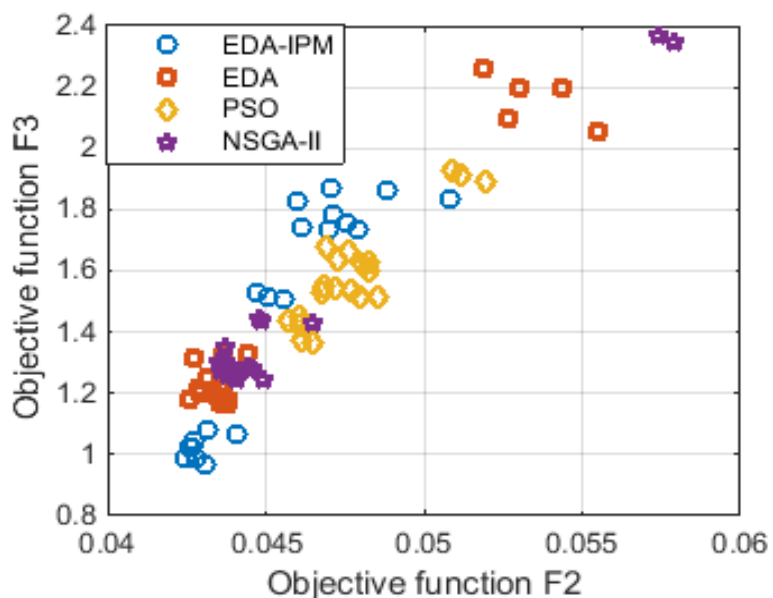


Figure 4.6(c) Optimal Pareto front between objective F_2 and F_3 (3% error in real and 50% in pseudo-measurements)

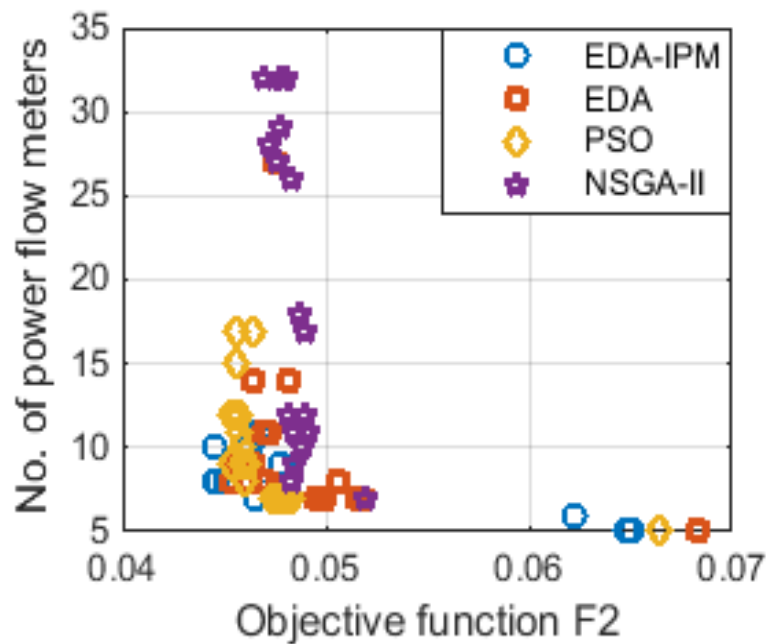


Figure 4.7(a) Optimal Pareto front between number of flow meters and F_2 (5% error in real and 50% in pseudo-measurements)

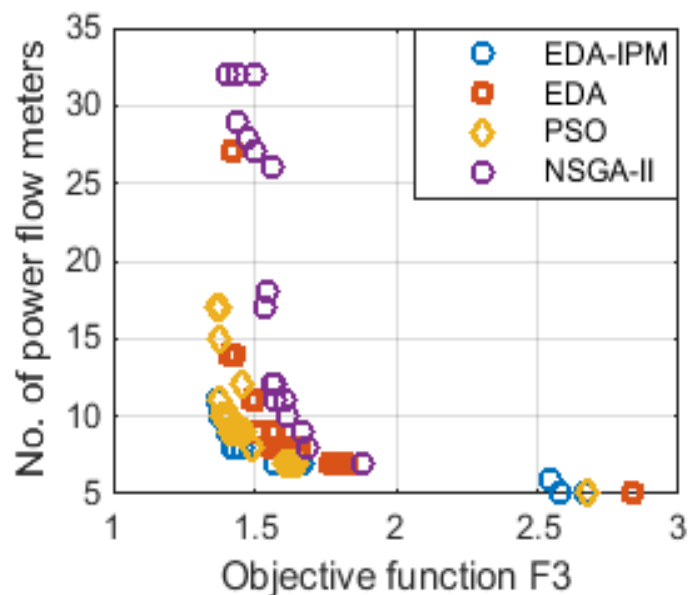


Figure 4.7(b) Optimal Pareto front between number of flow meters and F_3 (5% error in real and 50% in pseudo-measurements)

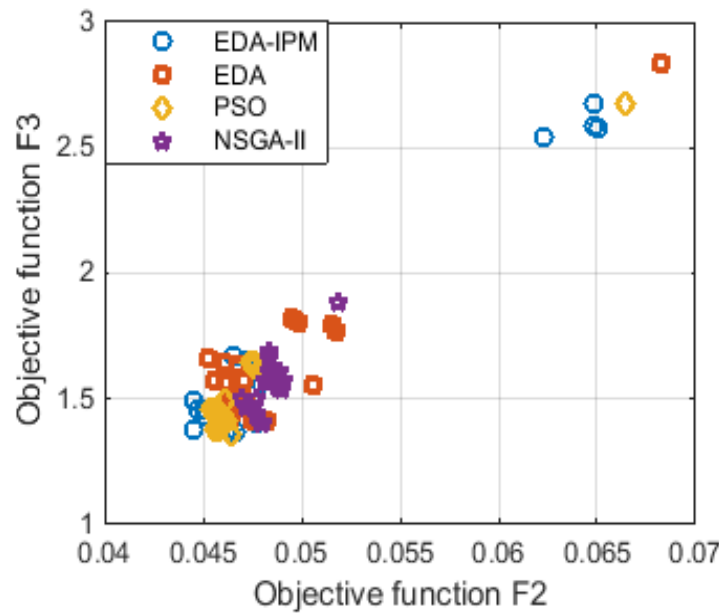


Figure 4.7(c) Optimal Pareto front between objective F_2 and F_3 (5% error in real and 50% in pseudo-measurements)

Table 4.6 Indian 85-bus system: The number and location of the power flow meters of different meter accuracy (without DG)

Metrological Errors	Algorithm	location of flow meters(Line number)	Number of flow meters	Objective functions value			Maximum error in bus voltage magnitude (V) (%)	Maximum error in bus voltage angle (δ) (%)
				F_1	F_2	F_3		
1%	Proposed EDA-IPM	1,13,19,25,75,78,84	7	8	0.0383	1.0952	0.1692	5.0660
	EDA	1,30,32,35,36,42, 43,60,68	8	9	0.0387	1.2323	0.2797	6.4132
	PSO	1,30,32,35,36,42, 43,60,68	8	9	0.0407	1.4739	0.2593	6.6143
	NSGA-II	1,16,34,37,40,42, 43,50,55	9	10	0.0411	1.4289	0.2897	7.7394
3%	Proposed EDA-IPM	1, 34, 40,46,52, 53,67,69	8	9	0.0427	1.0433	0.2117	5.2305
	EDA	1,28,42,52,53,58,71,74	8	9	0.0431	1.2486	0.3984	6.0022
	PSO	1,15,18,20,23, 39,45,50,77	11	12	0.0468	1.5478	0.3041	7.1198
	NSGA-II	1,10,15,17,26,42,58, 70,71,74,26,84	8	9	0.0438	1.3478	0.2999	9.9812
5%	Proposed EDA-IPM	1,12, 20, 43,50, 68,75,83	8	9	0.0452	1.4298	0.2896	5.4821
	EDA	1,9,17,23,37,53, 61,67,73	9	10	0.0464	1.5088	0.3342	6.7623
	PSO	1,17,19,20,30,40, 43,49,58,66,71	8	9	0.0461	1.4893	0.3211	8.3421
	NSGA-II	1,6,21,32,68,69, 70,76	12	13	0.0482	1.5740	0.2898	8.4359

Chapter 4 Optimal Allocation of Measurement Devices using Hybrid EDA-IPM Algorithm

Table 4.7 Indian 85-bus system: The number and location of the power flow meters of different meter accuracy (Type 1 DG at bus 45 and 61)

Metrological errors	Algorithm	Location of flow meters(Line number)	Number of power flow meters	Objective functions value			Maximum error in bus voltage magnitude (V) (%)	Maximum error in bus voltage angle (δ) (%)
				F_1	F_2	F_3		
1%	Proposed EDA-IPM	1,9,23,28,44	5	8	0.0367	1.0473	0.1423	5.0237
	EDA	1,8,21,32,68,69,76	7	10	0.0574	1.0585	0.2427	5.9823
	PSO	1,25,39,55,65,73	6	9	0.0583	1.3910	0.2137	5.1242
	NSGA-II	1,16,30,33,44,51,68,73	8	11	0.0575	1.1165	0.1998	6.1123
3%	Proposed EDA-IPM	1,11,37,51,79,84	6	9	0.0333	1.0372	0.2073	5.3241
	EDA	1,26,32,57,64,71,79	7	10	0.0636	1.0223	0.3231	6.1226
	PSO	1,23,26,36,43,55,83	7	10	0.0644	1.2166	0.2981	6.8799
	NSGA-II	1,23,26,36,43,83	7	10	0.0646	1.2105	0.2861	7.1981
5%	Proposed EDA-IPM	1,9,17,28,42,62,79	7	10	0.0400	1.1001	0.2441	5.5134
	EDA	1,14,33,37,41,65,83,84	8	11	0.0696	1.4032	0.3244	6.5312
	PSO	1,11,19,28,42,51,57,71,79	9	12	0.0589	1.3891	0.4523	7.2213
	NSGA-II	1,13,14,17,20,42,44,54,56,57	10	13	0.0661	1.3588	0.4129	7.4512

Chapter 4 Optimal Allocation of Measurement Devices using Hybrid EDA-IPM Algorithm

Table 4.8 Indian 85-bus system: The number and location of the power flow meters in presence of type 2 and 3 DGs at bus 45 and 61

DG Type	Measurement error	Algorithm	Location of flow meters(Line number)	Number of power flow meters	Objective functions value			Maximum error in bus voltage magnitude (V) (%)	Maximum error in bus voltage angle (δ) (%)
					F_1	F_2	F_3		
Type 2 (P+jQ)	1%	Proposed EDA-IPM	1,17,25,29,34,58,80	7	10	0.0386	1.1584	0.2741	5.4671
		EDA	1,14,21,26,56,65,75,84	8	11	0.0388	1.3619	0.4714	5.7417
		PSO	1,11,12,17,20,27,41,71,74	9	12	0.0396	1.2677	0.3939	5.9923
		NSGA-II	1,17,20,24,27,37,68,69	8	11	0.0395	1.3121	0.3428	6.1798
	Type 3 (P+jQ)	Proposed EDA-IPM	1,23,31,49,58,59,61	7	10	0.0500	1.1191	0.2998	5.7326
		EDA	1,28,31,50,68,79	6	9	0.0686	1.1611	0.3887	5.9679
Type 2 (P+jQ)	3%	PSO	1,14,33,37,41,65,83,84	8	11	0.0525	1.3306	0.3924	6.8324
		NSGA-II	1,10,13,26,48,60,73,74,80,82	10	13	0.0506	1.1375	0.4713	6.9813
		Proposed EDA-IPM	1,9,25,28,30,31,40,49	9	12	0.0574	1.1773	0.2998	5.7324
		EDA	1,2,8,14,37,59,60,64,74	9	12	0.0597	1.2696	3.4761	6.0147
	Type 3 (P+jQ)	PSO	1,7,19,21,36,65,75,77,79,80	10	13	0.0605	1.2929	4.7782	6.2231
		NSGA-II	1,14,30,36,44,58,61,69,73,74,76,80	12	15	0.0598	1.2695	3.9874	6.7923
Type 2 (P+jQ)	5%	Proposed EDA-IPM	1,24,33,38,43,73,76,81	8	11	0.0559	1.1878	0.3427	6.0125
		EDA	1,12,24,29,32,53,54,64,71,73	10	13	0.0607	1.1306	0.4129	6.7790
		PSO	1,16,18,39,41,46,50,75,81	9	12	0.0578	1.3732	0.4389	6.8931
		NSGA-II	1,26,28,31,40,45,49,55,61,80,83	11	14	0.05925	1.2789	0.5513	7.0127
	Type 3 (P+jQ)	Proposed EDA-IPM	1,12,50,52,59,67,70,73,76	9	12	0.0589	1.2057	0.4317	6.6823
		EDA	1,19,27,37,38,45,48,53,62,68,81	11	14	0.0608	1.2685	0.4738	8.0134

4.5 Comparison Results Analysis

In this section, a comparison study has been carried out between all the algorithms used in this thesis such as proposed hybrid PSO-KH and hybrid EDA-IPM algorithm, PSO, KH, EDA and NSGA-II. The performance of all the algorithms is tested on IEEE 69-bus system and practical Indian 85-bus distribution systems. Total number of operating condition considered is

100×1000. The optimal Pareto-fronts for three objectives F_1 , F_2 and F_3 is provided in Figure 4.8-4.13 respectively. The obtained results are also shown in Table 4.9 and 4.10. It is seen that in most of the cases the proposed algorithms are more superior than the conventional algorithms considered in this thesis for comparison purpose. In some of the cases it is also seen that proposed EDA-IPM algorithm is dominating hybrid PSO-KH algorithm. Therefore, the proposed algorithms can be used for the planning study of the distribution networks.

4.5.1 Comparison results analysis of IEEE 69-bus system

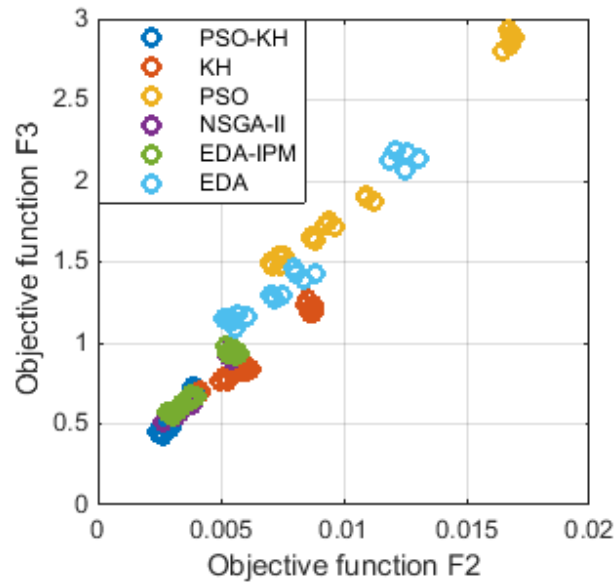


Figure 4.8(a): Optimal Pareto fronts between the objectives F_2 and F_3 for 1% error in real meters and 50% in pseudo-measurements

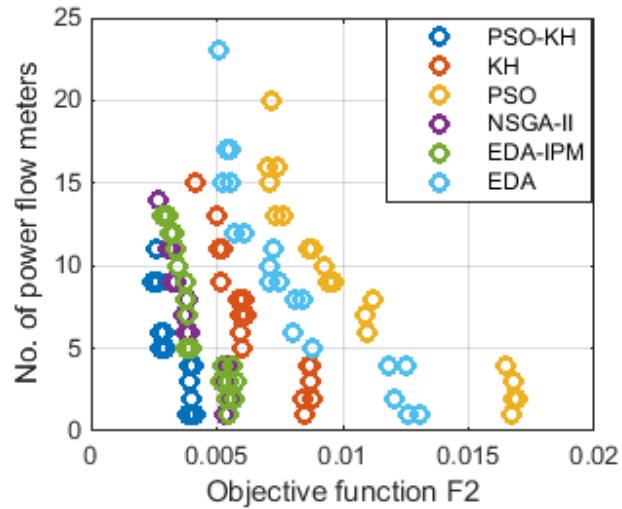


Figure 4.8(b): Optimal Pareto fronts between no. of power flow meters and the objective F_2 for 1% error in real meters and 50% in pseudo-measurements

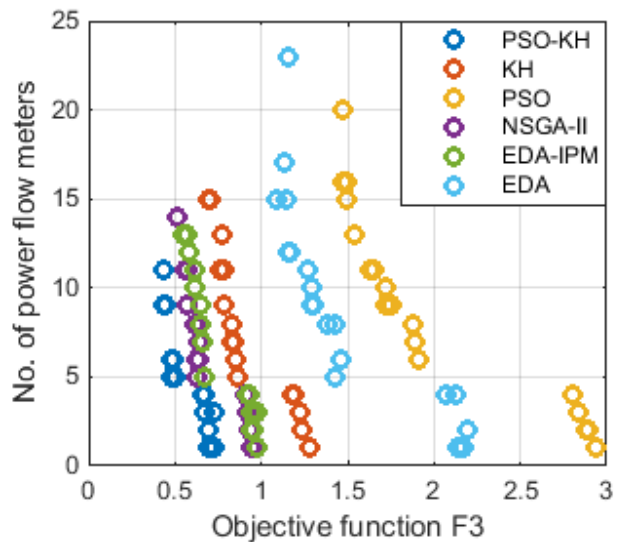


Figure 4.8(c): Optimal Pareto fronts between no. of power flow meters and the objective F_3 for 1% error in real meters and 50% in pseudo-measurements

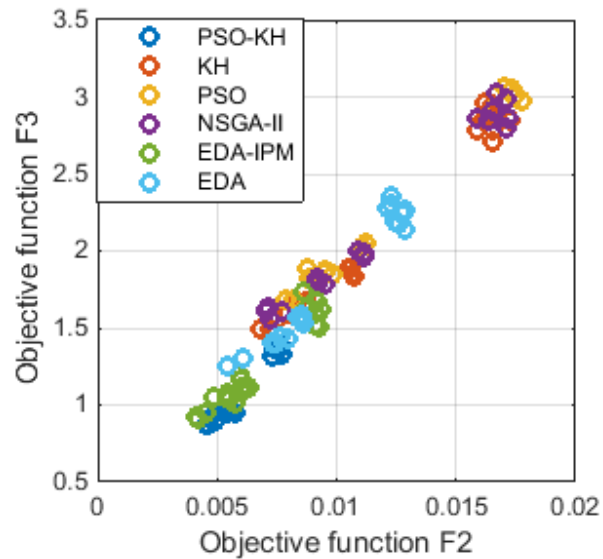


Figure 4.9(a): Optimal Pareto fronts between the objectives F_2 and F_3 for 3% error in real meters and 50% in pseudo-measurements

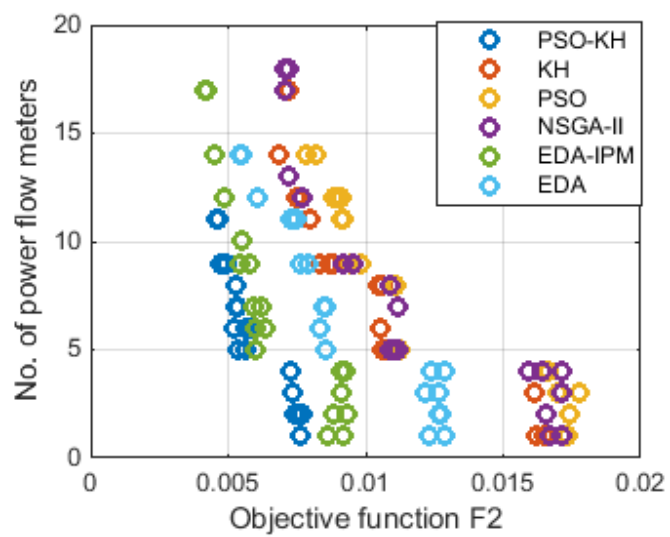


Figure 4.9(b): Optimal Pareto fronts between no. of power flow meters and the objective F_2 for 3% error in real meters and 50% in pseudo-measurements

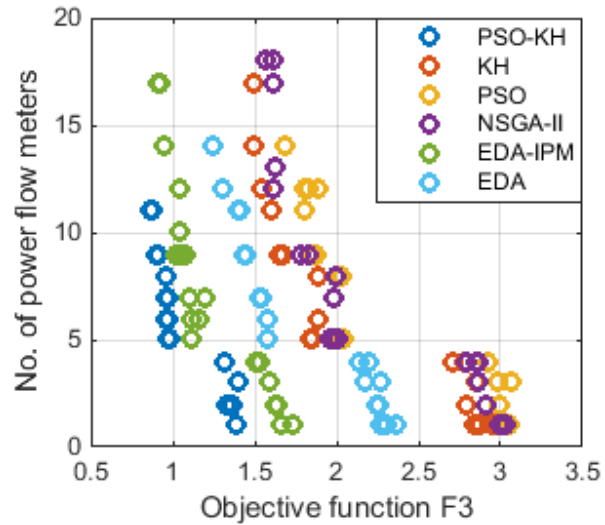


Figure 4.9(c): Optimal Pareto fronts between no. of power flow meters and the objective F_3 for 3% error in real meters and 50% in pseudo-measurements

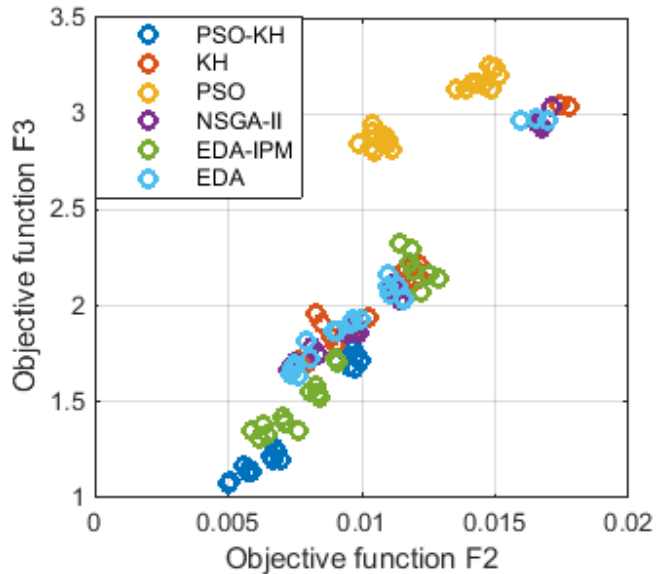


Figure 4.10(a): Optimal Pareto fronts between the objectives F_2 and F_3 for 5% error in real meters and 50% in pseudo-measurements

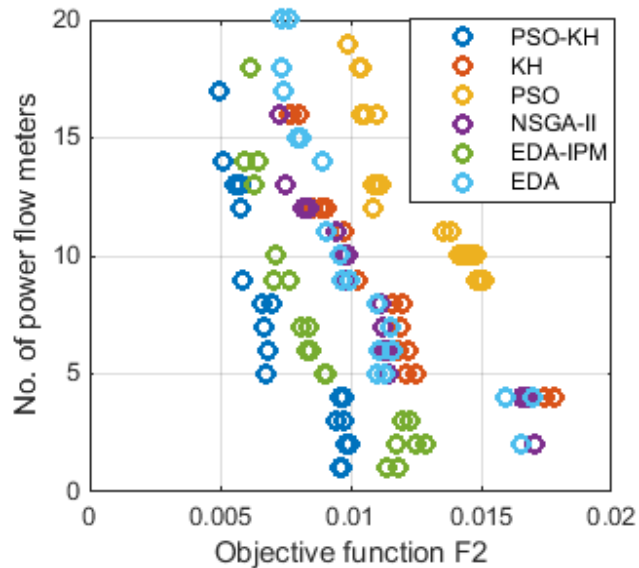


Figure 4.10(b): Optimal Pareto fronts between no. of power flow meters and the objective F_2 for 5% error in real meters and 50% in pseudo-measurements

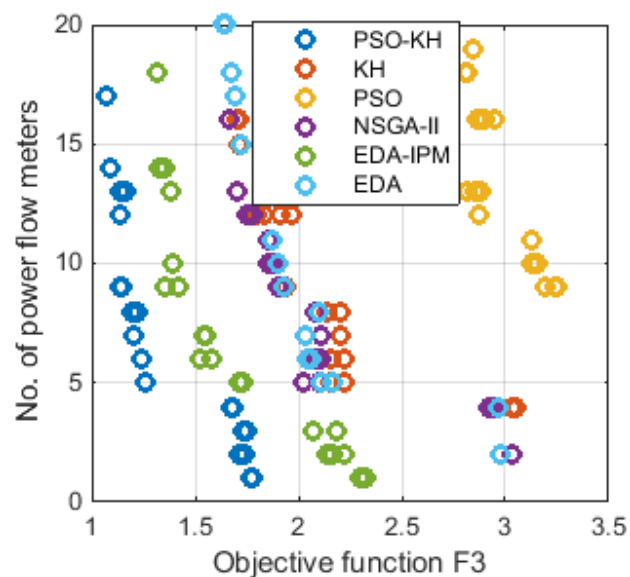


Figure 4.10(c): Optimal Pareto fronts between no. of power flow meters and the objective F_3 for 5% error in real meters and 50% in pseudo-measurements

Chapter 4 Optimal Allocation of Measurement Devices using Hybrid EDA-IPM Algorithm

Table 4.9 IEEE 69-bus system: The number and location of the power flow meters of different meter accuracy (without DG)

Metrological Errors	Algorithm	Default Measurements (node/line number)	location of flow meters(Line number)	No. of flow meters	Objective functions value			Max. error in bus voltage magnitude (V) (%)	Max. error in bus voltage angle (δ) (%)
					F ₁	F ₂	F ₃		
1%	Proposed PSO-KH	1/1	1,7,24,54,66	5	6	0.0028	0.4947	0.0381	5.7922
	KH	1/1	1,9,17,23,32,47, 56,61,63	9	10	0.0052	0.7837	0.0399	6.9994
	PSO	1/1	1,18,28,37,56, 65,42, 49	8	9	0.0112	1.8731	0.0475	7.9249
	NSGA-II	1/1	1,5,19,27,54	5	6	0.0037	0.6273	0.0772	9.3022
	Proposed EDA-IPM	1/1	1,2,20,26,27	5	6	0.0039	0.6678	0.0413	5.8215
	EDA	1/1	1,2,10,20,21,23,36 .41	8	9	0.0083	1.3871	0.0739	6.0127
3%	Proposed PSO-KH	1/1	1,11,18,43,52	5	6	0.0053	0.9782	0.0417	5.9154
	KH	1/1	1,2,4,12,21,24, 30,59,67	9	10	0.0084	1.6767	0.0479	7.8239
	PSO	1/1	1,13,17,25,31,39, 45,51,59,64,65	11	12	0.0091	1.7990	0.0638	11.6239
	NSGA-II	1/1	1,3,10,19,27,30, 32,4,45,49,54,65	12	13	0.0077	1.6130	0.0488	10.3332
	Proposed EDA-IPM	1/1	1,14,23,26,67	5	6	0.0060	1.1098	0.0523	6.2198
	EDA	1/1	1,7,12,24,32,34,48 .58,61,65,66,67	12	13	0.0060	1.3036	0.0412	6.3214
5%	Proposed PSO-KH	1/1	1,7,14,21,28, 33,49,53,61	9	10	0.0058	1.1491	0.0523	6.3172
	KH	1/1	1,5,11,30,35, 41,47,52,61	9	10	0.0102	1.9423	0.0927	9.6717
	PSO	1/1	1,5,18,30,34,35, 44,47,50,56,63,67	12	13	0.0109	2.8704	0.0838	12.7865
	NSGA-II	1/1	1,4,9,14,20,32,38, 40,43,45,51,57,65	13	14	0.0075	1.7001	0.0776	12.4533
	Proposed EDA-IPM	1/1	1,7,18,23,33,60,63 .65,66	9	10	0.0070	1.4178	0.06781	6.9993
	EDA	1/1	1,7,28,33,34,42,44 .45,59,67,68	11	12	0.0090	1.8684	0.0823	8.3927

4.5.2 Comparison result analysis of Practical Indian 85-bus system

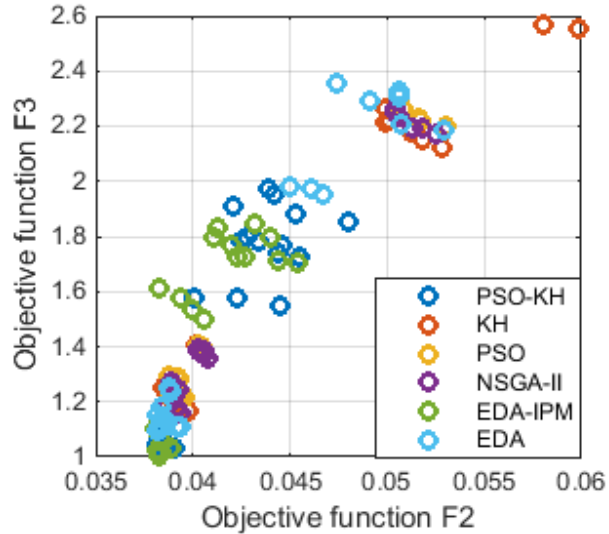


Figure 4.11(a): Optimal Pareto fronts between the objectives F_2 and F_3 for 1% error in real meters and 50% in pseudo-measurements

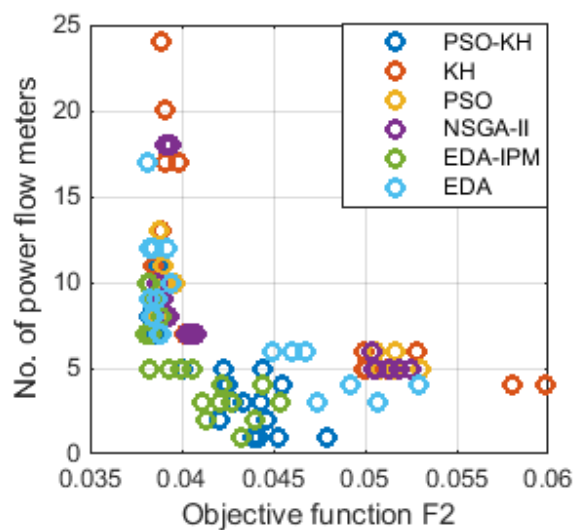


Figure 4.11(b): Optimal Pareto fronts between no. of power flow meters and the objective F_2 for 1% error in real meters and 50% in pseudo-measurements

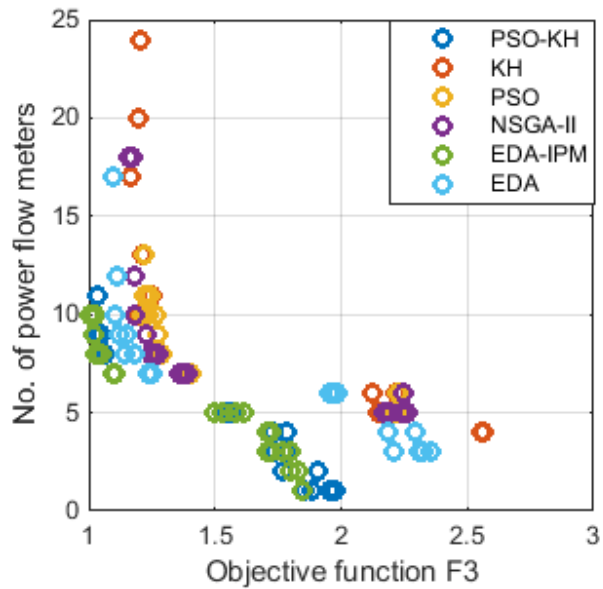


Figure 4.11(c): Optimal Pareto fronts between no. of power flow meters and the objective F_3 for 1% error in real meters and 50% in pseudo-measurements

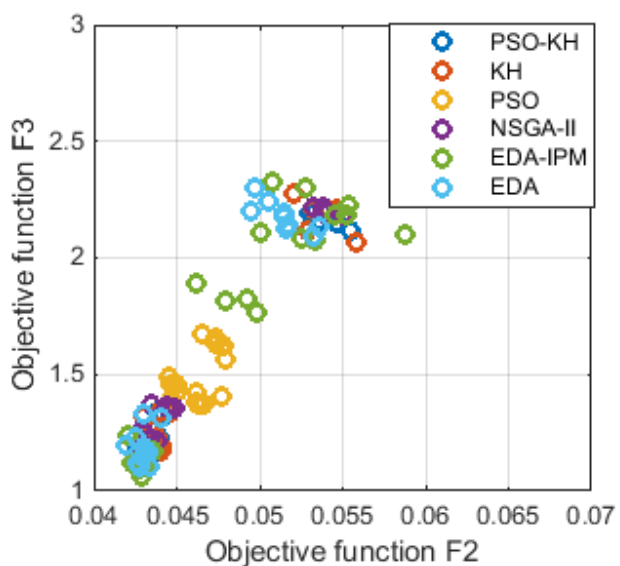


Figure 4.12(a): Optimal Pareto fronts between the objectives F_2 and F_3 for 3% error in real meters and 50% in pseudo-measurements

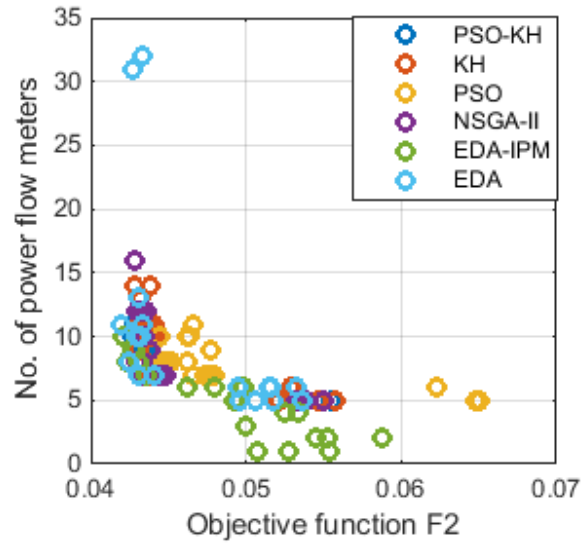


Figure 4.12(b): Optimal Pareto fronts between no. of power flow meters and the objective F_2 for 3% error in real meters and 50% in pseudo-measurements

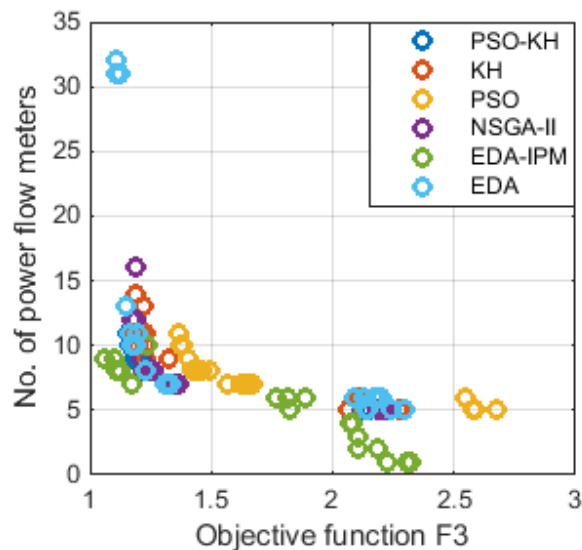


Figure 4.12(c): Optimal Pareto fronts between no. of power flow meters and the objective F_3 for 3% error in real meters and 50% in pseudo-measurements

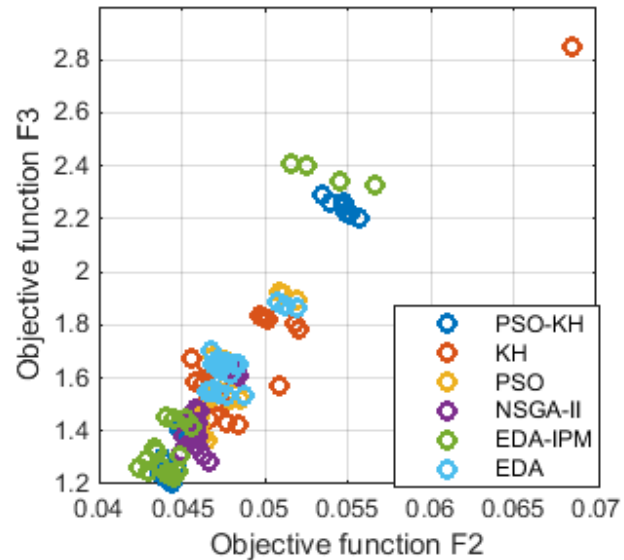


Figure 4.13(a): Optimal Pareto fronts between the objectives F_2 and F_3 for 5% error in real meters and 50% in pseudo-measurements

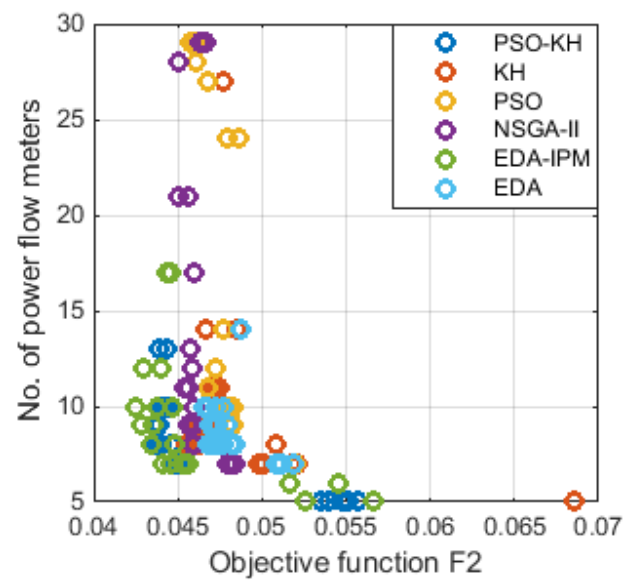


Figure 4.13(b): Optimal Pareto fronts between no. of power flow meters and the objective F_2 for 5% error in real meters and 50% in pseudo-measurements

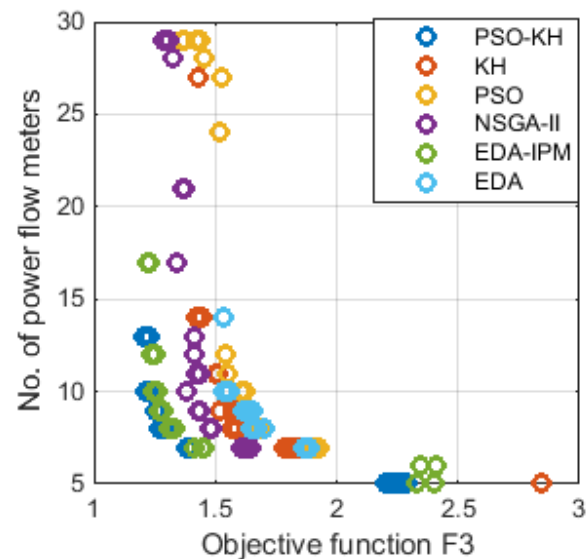


Figure 4.13(c): Optimal Pareto fronts between no. of power flow meters and the objective F_3 for 5% error in real meters and 50% in pseudo-measurements

Chapter 4 Optimal Allocation of Measurement Devices using Hybrid EDA-IPM Algorithm

Table 4.10 Indian 85-bus system: The number and location of the power flow meters of different meter accuracy (without DG)

Metrological Errors	Algorithm	Default Measurements (node/line number)	location of flow meters(Line number)	No. of flow meters	Objective functions value			Max. error in bus voltage magnitude (V) (%)	Max. error in bus voltage angle (δ) (%)
					F_1	F_2	F_3		
1%	Proposed PSO-KH	1/1	1,13,18,26, 75 79,84	7	8	0.0385	1.1077	0.1853	5.1722
	KH	1/1	1,28,32,35,42,43 .60,68	8	9	0.0390	1.2449	0.2891	6.3321
	PSO	1/1	1,8,15,32,48,56, 70,71	8	9	0.0387	1.2911	0.2786	6.6143
	NSGA-II	1/1	1,18,28,31,40,52 .64,70	8	9	0.0390	1.2641	0.2399	7.8259
	Proposed EDA-IPM	1/1	1,8,21,32,68,69, 76	7	8	0.0380	1.1033	0.2104	5.3573
	EDA	1/1	1,31,43,54,60,69 .75,80	8	9	0.0384	1.1452	0.2978	6.1327
3%	Proposed PSO-KH	1/1	1,17,22,30,36,73 .81	7	8	0.0438	1.3355	0.2347	5.5217
	KH	1/1	1,28,42,52,58, 73,78,81,84	9	10	0.0430	1.3255	0.4011	6.7162
	PSO	1/1	1,20,34,40,54,58 .71,81	8	9	0.0452	1.4298	0.3217	7.3192
	NSGA-II	1/1	1,13,14,21,26,50 .58,60,65,77	10	11	0.0431	1.1851	0.3019	9.8822
	Proposed EDA-IPM	1/1	1,12,13,20,44,55 .75,79	8	9	0.0423	1.1219	0.2814	6.2865
	EDA	1/1	1,11,13,28,33,36 .37,69	8	9	0.0425	1.2280	0.3427	6.9832
5%	Proposed PSO-KH	1/1	1,16,21,24,33,69 .77,79	8	9	0.0439	1.2855	0.2896	5.9407
	KH	1/1	1,9,19,24,37,53, 63,67,74	9	10	0.0467	1.5213	0.3342	7.6721
	PSO	1/1	1,6,23,32,68,70, 72,76,79,81,84	11	12	0.0468	1.5478	0.3211	8.6434
	NSGA-II	1/1	1,20,28,38,40,41 .43,68,73,76	10	11	0.0459	1.3836	0.2898	8.6315
	Proposed EDA-IPM	1/1	1,18,19,23,42,44 .64,82,84	8	9	0.0434	1.3240	0.3124	6.3415
	EDA	1/1	1,9,26,27,31,47, 48,52,53,54	10	11	0.0465	1.5498	0.4128	7.9865

4.6 Summary

This chapter proposed a Pareto based multi-objective optimization technique that optimizes the number and location of measuring devices for state estimation in smart distribution network. To find the optimal placement of meters a new hybrid EDA-IPM algorithm has been proposed. The hybridization of traditional EDA with IPM is done to improve the local searching capability of the EDA. In state estimation metrological characteristics of meters as well as the load

Chapter 4 Optimal Allocation of Measurement Devices using Hybrid EDA-IPM Algorithm

variations have also taken into consideration to test the efficiency of the proposed meter placement technique. The best optimal trade-off solution between the objective functions such as cost and state estimation error is established. Moreover, the impact of different kind of DGs on state estimation accuracy has also been presented in an active distribution network.

The proposed hybrid EDA-IPM algorithm based meter placement technique is tested on IEEE 69-bus system and practical Indian 85-bus distribution network. The obtained result using the proposed hybrid EDA-IPM algorithm has been compared with some existing algorithm in literature such as PSO, EDA and NSGA-II under various operating conditions of the distribution systems. It is reported that the proposed algorithm is robust, reliable and more superior than existing algorithms considered in this chapter.

Chapter 5

Trade-offs in PMU and IED Deployment for Active Distribution System State Estimation Using Multi-Objective Hybrid EDA-IPM Algorithm

Chapter 5

Trade-offs in PMU and IED Deployment for Active Distribution System State Estimation Using Multi-Objective Hybrid EDA-IPM Algorithm

5.1 Introduction

In distribution grids, due to the presence of different kinds of actors such as distributed generation (DG), energy storage devices, system becomes more complex, dynamic and uncertain in nature. Because of this changing behavior of actors, real-time monitoring and control becomes more challenging task for the power system engineers. Thus, PMUs are of great interest because it provides synchronized measurements of voltage and current phasors. The application of PMU for state estimation in transmission system has been widely used to improve the performance of the state estimator. Therefore it would be more advantageous to use PMUs in DSSE. In transmission systems, PMUs have been used widely to improve the state estimator performance using different approaches. Therefore, utilization of the phasor measurements in distribution network for state estimation is of great interest. The PMU provides synchronized measurements e.g. voltage, current phasors and frequency along with some indirect measurements [71]. The measurements obtained from the PMUs are synchronized with the coordinated Universal Time. In transmission systems, the synchronized measurements obtained from PMUs along with the non-synchronized measurements from Supervisory Control and Data Acquisition (SCADA) system have been used by many researchers for improvising the performance of state estimator.

However, due to lack of sufficient direct measurements in distribution networks, locating PMUs is economically unreasonable. Therefore, the techniques used for locating PMUs in transmission grids cannot be directly transformed at the distribution level. In order to compensate this, a large number of pseudo-measurements derived from historical customer load data are being used for the state estimation in distribution systems. But, as a result, it deteriorates the accuracy of state estimation to a very large extent. Many researchers have been proposed different techniques to deploy PMUs in distribution grids [77],[79], [82].

In chapter 3 and 4, meter placement problem has been formulated as a multi-objective optimization problem to find optimal number and location of power flow meters. A trade-off

solution is established between total configuration cost, voltage magnitude and phase angle errors. Only power flow meters have been considered to find the best optimal solution. This chapter proposes a new multi-objective optimization problem to find trade-offs in deployment of phasor measurement units (PMUs) and intelligent electronic devices (IEDs) for state estimation in active distribution networks. A new hybrid estimation of distribution algorithm (EDA) has been used to find the optimal number and location of measurement devices such as PMU and IED for accurate state estimation. The objective functions to be minimized in this optimization problem are the total cost of PMUs and IEDs, and the RMS value of state estimation error. Since, the objectives are conflicting nature, a multi-objective Pareto-based non-dominated sorting EDA algorithm is proposed. Moreover, to improve the local searching capability of the traditional EDA algorithm, the Interior point method (IPM) is hybridized with EDA to get near global optimal solution. The hybridization of EDA with IPM brings a higher degree of balance between the exploration and exploitation capability of the traditional EDA during the search process. Furthermore, the random variation in loads and generators is also considered to check the reliability of proposed meter placement technique. The viability of the proposed algorithm has been tested on IEEE 69-bus system and Practical Indian 85-bus system to validate the results. The obtained results have been compared with the conventional EDA algorithm, non-dominated sorting genetic algorithm (NSGA-II) and also with hybrid EDA-simulated annealing algorithm existing in the literature.

5.2 Distribution system state estimation in presence of PMUs and IEDs

The state estimation is a mathematical relation between the system state variables and available measurements that can estimate the system states accurately from the noisy measurement data. The well established weighted Least Square (WLS) algorithm has been employed to minimize the following objective function:

$$J = [z - h(x)]^T W^{-1} [z - h(x)] \quad (5.1)$$

$$\text{Subjected to: } z = h(x) + r \quad (5.2)$$

where z is the measurement vector, x is the system state vector, consisting of magnitude and phase angle of all branch current, $h(x)$ is a nonlinear measurement function of system state variables and r represents a small noise following the Gaussian distribution and w is the covariance matrix of the measurement errors.

To improve the state estimation accuracy, PMUs have been employed along with the existing IEDs, for online monitoring of the distribution networks [82]-[83]. Therefore, in this chapter a mixed approach has been considered which includes measurements from PMUs and traditional measurements from IEDs to estimate the states of an active distribution network. A mathematical model for state estimation based on PMU and IED data is described below.

There are different types of measurement such as substation measurement, pseudo-measurement, virtual measurement, smart meter measurement and phasor measurement obtained from PMU have been utilized for state estimation in distribution network. Additionally, it is assumed that, PMU installed at a particular bus provides voltage phasor measurements of that bus.

For state estimation, BC-DSSE algorithm has been used where branch current magnitude and their phase angle are considered as state of the distribution system [40]. The initial values for the state variables are assumed as discussed in [41] and the WLS based iterative process has been conducted to estimate the state variables.

The estimated value of the state variable x at $(k+1)^{th}$ iteration can be expressed as follows:

$$x_{k+1} = x_k + G(x_k)^{-1} [H(x_k)^T W^{-1}] [z - h(x_k)] \quad (5.3)$$

where H represents the Jacobian matrix and it is calculated by taking the partial derivative of each non-linear measurement function $h(x)$ with respect to state variable x and G represents the gain matrix given by

$$G(x_k) = H(x_k)^T W^{-1} H(x_k) \quad (5.4)$$

The inverse of the covariance matrix W can be defined as

$$W^{-1} = \begin{bmatrix} W_S^{-1} & 0 & 0 & 0 & 0 & 0 \\ 0 & W_{IED}^{-1} & 0 & 0 & 0 & 0 \\ 0 & 0 & W_{PMU,real}^{-1} & 0 & 0 & 0 \\ 0 & 0 & 0 & W_{PMU,imag}^{-1} & 0 & 0 \\ 0 & 0 & 0 & 0 & W_P^{-1} & 0 \\ 0 & 0 & 0 & 0 & 0 & W_V^{-1} \end{bmatrix} \quad (5.5)$$

The subscripts in equation (5.5) S , IED , P and V represent substation measurement, IED measurement, pseudo-measurement and virtual measurement respectively. In equation (5) W_{IED} and W_{PMU} represents the covariance matrix of the uncertainty of the IED measurement and phasor measurements obtained from PMU. The error vector r can be expressed as:

$$r = \begin{bmatrix} z_s - h_s(x) \\ z_{IED} - h_{IED}(x) \\ z_{PMU,real} - h_{PMU,real}(x) \\ z_{PMU,imag} - h_{PMU,imag}(x) \\ z_p - h_p(x) \\ z_v - h_v(x) \end{bmatrix} \quad (5.6)$$

In state estimation, it is assumed that IEDs are used to measure real and reactive power flows in a line and PMUs are incorporated to measure voltage phasors at a bus. According to state estimation theory, the diagonal elements of the error covariance matrix represent the estimation variances of the states and this can be expressed as follows:

$$E_{xx} = G(x)^{-1} \quad (5.7)$$

Furthermore, the above equation can be expressed as $E_{xx} = E_x(x \cdot x^T) = E_x(x - \hat{x})^2$.

where E_x is the operator of statistical expectation. It includes both state estimation error variance of bus voltage magnitude and phase angle. The error vector is represented as $x = \hat{x} - x$.

5.3 Mathematical Model of the Proposed Multi-objective Optimization Problem (MOOP)

The proposed meter placement technique is designed as a three objective optimization problem. The main objective is to determine the optimal deployment of PMU and IED in a distribution network to achieve minimum cost as well as it ensures that state variables are estimated within the predefined accuracy limit. The objective functions considered to be minimized are: (1) the total cost of PMUs (2) the total cost of IEDs and (3) RMS value of state estimation error. Since, the objectives considered here are conflicting in nature, the meter placement problem can be designed as multi-objective Pareto based optimization problem [88]-[89]. Furthermore, to find the optimal trade-off solution, a hybrid EDA-IPM algorithm has been utilized to find the optimal position of PMU and IED ensuring the relative deviations in voltage and angle estimates to be within the pre-specified thresholds for 95% of the test cases.

Mathematically, the proposed MOOP can be expressed as:

Minimize

$$J_1 = \sum_{i=1}^{nl} C_{IED,i} \cdot P_{IED,i} \quad (5.8)$$

$$J_2 = \sum_{i=1}^n C_{PMU,i} \cdot P_{PMU,i} \quad (5.9)$$

$$J_3 = \frac{1}{m} \sum_{j=1}^m \sqrt{\frac{1}{n_v} \sum_{i=1}^{n_v} E_x \left(\hat{x}_i - x_i \right)^2} \quad (5.10)$$

Subjected to constraints: In 95% of the operating scenarios the maximum relative deviations in voltage and angle estimates are to be within the specified limits given as follows:

$$\left| \frac{V_i^a - V_i^{est}}{V_i^a} \right| \times 100 \leq 1 \quad (5.11)$$

$$\left| \frac{\delta_i^a - \delta_i^{est}}{\delta_i^a} \right| \times 100 \leq 5 \quad (5.12)$$

where the three objective functions are represented as J_1 , J_2 and J_3 , n_v and nl represents number of state variables and lines in a distribution network, x is the state variable and \hat{x} is the estimated value of the state variable x , C_{IED} and C_{PMU} are respectively, the relative cost of a IED and PMU and m denotes total number of operating scenarios. P_{IED} and P_{PMU} are treated as binary decision vectors i.e. the presence and absence of a meter in a line or at a bus is indicated by 1 or 0, V_i^a and δ_i^a are the actual or true value of the voltage magnitude and angle of i^{th} bus and V_i^{est} and δ_i^{est} represents the estimated bus voltage magnitude and angle at i^{th} bus respectively.

5.4. Solution Methodology

To find the optimal solution of the proposed MOOP, a hybrid EDA-IPM algorithm has been used which has been discussed in Chapter 4. Therefore, a brief introduction to the traditional EDA and IPM algorithm has been discussed as follows.

5.4.1 Estimation of Distribution Algorithm (EDA)

In conventional genetic algorithm (GA), crossover and mutation operators are being used for generating new solutions as well as to explore the search space for finding near global

optimal solutions. However, these operators may disrupt the good solutions during the evolution process and also obstructing to get the optimal solutions. This situation is more likely to occur when the problem variables are correlated. Therefore, estimation of distribution algorithm (EDA) has been using widely in various field of engineering applications to overcome these shortcomings of traditional GA [90]-[91]. It is a population based evolutionary optimization algorithm which employs a probabilistic model to generate new solutions for the immediate generation. Moreover, the sampling of new individuals is based on the probabilistic model estimated from the database consisting of some selected individuals from the previous generation. Therefore, the EDA algorithm is good at exploring the search space to find prominent solutions.

The basic steps of a traditional EDA algorithm have been provided below. First, the initial solutions are generated randomly within the specified limits. Then, the fitness function is evaluated for each individual solution. Out of the total population P , $N < P$ solutions are selected as best solutions using any selection mechanism. Based upon the selected individuals, a probabilistic model is estimated to lead the searching process toward the regions contains better fitness values. However, the choice of probabilistic model influences the performance and efficiency of the EDA algorithms. Then, the offspring is created using different sampling techniques. The above steps are repeated until it meets the stopping criteria. The pseudo-code of the above procedure is provided as follows:

```

Begin
  Initialization: Generate  $P$  initial population randomly within the search space.

  Do While (termination criteria is not met)
    Evaluation: Calculate the fitness value of  $P$  individuals.
    Selection: By using any selection method, select  $N < P$  individuals.
    Probabilistic model: Estimate the probability  $p_s(x)$  that an individual being
      among the selected population.
    Sampling: Sample  $P$  individuals from  $p_s(x)$  using sampling technique.

  End Do
End

```

5.4.2 Interior Point Method (IPM)

The interior point method is basically used to solve linear and non-linear convex optimization problems [92]. In this, the Lagrange multipliers are employed to deal with the

equality and inequality constraints of the optimization problem. In order to avoid the negativity conditions of the slack variables the logarithmic barrier functions has been added to the objective function [93]. The decision variables are considered to be continuous. The proposed non-linear constraint optimization problem can be transformed to unconstraint optimization problem as follows:

$$\begin{aligned} L(z, y, l, u, v, w) = & f(x) - v^T(x - l - x_{\min}) - y^T g(x) \\ & + w^T(x + u - x_{\max}) - \mu \sum_i (\ln l_i + \ln u_i) \end{aligned} \quad (5.13)$$

where u and l are the slack variables; y , v and w are the Lagrange multipliers; and the barrier parameter is represented by μ .

In order to satisfy the Karush-Kuhn-Tucker (KKT) conditions, first order derivatives of a set of non-linear algebraic equations have to be formed and then Newton-Raphson method is employed to solve the above first order differential equations. During the iterative procedure of the IPM, if the KKT conditions shown below are satisfied then the algorithm will stop. The KKT conditions are described as follows:

$$\|L_x\| = \|\nabla f(x) - \nabla g^T(x)y - v + w\| < \epsilon \quad (5.14)$$

$$\|L_y\| = \|g(x)\| < \epsilon \quad (5.15)$$

$$\|L_w\| = \|x + u - x_{\max}\| \leq \epsilon \quad (5.16)$$

$$\|L_v\| = \|x - l - x_{\min}\| \leq \epsilon \quad (5.17)$$

According to primal-dual theory, x is the primal variable, l and u are the slack variables, y , v and w are the dual variables respectively and ϵ is a very small number. The equations (15)-(17) are called the primal feasible conditions and eq. (14) is known as dual feasible conditions. If the solution satisfies the above conditions then it is an optimal solution for the optimization problem.

5.4.3 Proposed multi-objective hybrid EDA-IPM algorithm

The EDA algorithm has been used widely in variety of engineering applications because it is efficient in exploring search space more efficiently. Although, EDA has good exploration ability but it suffers from poor exploitation capability [90]. Therefore, the optimal solutions obtained using EDA may not be a global optimal solution. On the other hand, local searching capability of IPM algorithm is more effective [93]. Hence, the traditional EDA algorithm has been hybridized with IPM to enhance the balance between exploration and exploitation capability

of the traditional EDA algorithm to obtain near global optimal solutions.

First of all the objective functions considered are modeled as a MOOP. Moreover, since the objectives are conflicting nature, the simultaneous optimization needs a compromised solution because each objective in the model is conflicting to one another. Therefore, to achieve better compromised solution between the objectives, Pareto based non-dominated sorting approach has been implemented [88], [89]. It states that, in a non-dominated Pareto front all solutions are equally important because no solution is dominating the other in the population. In MOOP, solution relies on a set of solutions unlike single objective optimization problem. Therefore, Pareto based non-dominated sorting technique have been employed with hybrid EDA-IPM to achieve best trade-offs solution between the multiple objectives. A trade-off solution between the total cost of PMU and IED needed for the accurate estimation of system states is determined using multi-objective hybrid EDA-IPM algorithm. The pseudo code of the proposed Bayesian network based probabilistic hybrid EDA-IPM algorithm is presented below.

The Pseudo-code of the proposed multi-objective hybrid EDA-IPM algorithm

Step1. Initialization: Generate random number and location of IEDs and PMUs for each individual solution in the population (Pop) within the limits. Where Pop represents size of the population

Do while (“Stopping criterion is not met”)

Step 2. Fitness evaluation: Evaluate the objective functions J_1, J_2 and J_3 for each solution based on the position of PMUs and IEDs.

Step 3. Selection: Select $N < Pop$ solutions from Pop using Non-dominated sorting selection strategy. Pop is the size of the population and N is a number less than Pop .

Begin

Do while (“Stopping criterion is not met”)

For $i = 1:N$ (number of selected solutions)

1. Use each selected solution $s(i)$ as initial point in IPM algorithm to find a best solution $y(i)$ (location of PMU and IED) for that solution i .

2. Evaluation: Calculate the objective functions J_1, J_2 and J_3 and evaluate the fitness value for each i using weighting approach.

3. Update solution:

```

if Fitness  $y(i) <$  Fitness  $s(i)$ 
&& if solution  $y(i)$  dominates  $s(i)$ 
then  $s(i) = y(i)$ 

```

End for i

End Do

End

Step 4. Probabilistic graphical model: Estimate the probability distribution of the previous solutions and selected solution to predict new population for the next generation using Gaussian Bayesian network. Mathematically, it can be expressed as:

$$p(x_i | pa(X_i)) = N(\mu_i + \sum_{X_j \in Pa(X_i)} w_{ij} (x_j - \mu_j), v_i^2)$$

where μ_i represents the mean of the variable X_i , v_i is the standard deviation of the distribution and w_{ij} is the weight associated with each of the parents and x_j is the value of the variable X_j in $pa(X_i)$.

Step 5. Sampling technique: Sample Pop number of solutions from the Gaussian Bayesian network using sample Gaussian UnivModel.

End Do

Post-procession of the results

In most of EDAs, it is a common practice to estimate the probabilistic model of the selected solution obtained from the previous generation and there after sampling algorithm is expected to use for the generation of new solutions based upon the statistics obtained from the selected solutions. In this work, Gaussian Bayesian network has been used as a probabilistic model to estimate the new solution for the next generation during the optimization process. The proposed hybrid EDA-IPM algorithm uses this probabilistic model to study the characteristics of the selected solutions to generate new individuals for the optimization problem in searching for the optimal Pareto front. In case of MOOP, one of the most commonly used ranking methods is

non-dominated sorting (NDS) technique to rank each individual for the selection purpose [88]. In NDS, the solutions are sorted into non-dominated Pareto fronts and then each solution in the same Pareto front is sorted based upon their crowding distances in the objective space. The new solutions are sampled from the probability distribution employed in the Bayesian network. Basically, sample Gaussian UnivModel has been used to sample the solutions.

In the beginning of the optimization process, the initial solutions are generated randomly using seeding approach within the search space. Each solution represents the combinations of number of PMUs and IEDs as well as their locations. Based on each combination of PMUs and IEDs, the objective functions are evaluated using BCDSSE algorithm. Then, the selection mechanism is used to select some of the best solutions so far. In order to achieve better performance, the selected solutions are updated using IPM algorithm. After the update, the probabilistic Bayesian model has been used to predict the new solutions for the future generation by using the selected solution. During fitness calculation, the constraints violation checking has to be carried out. In each Monte Carlo trial, the error in bus voltage magnitude and angle estimate is determined. For each combination of PMUs and IEDs in a solution, if in 95% of the simulated cases, the estimated errors are below the threshold limits, then for that solution the objective functions are evaluated and stored. On the contrary, if it is not within the threshold limit, then for that particular solution, a higher value of objective is been assign. Hence, this particular solution can be eliminated during next immediate generation. Then, the above steps are repeated until all the solutions in a given population size are in first front. The convergence criterion for the algorithm to stop is, when all the solutions are reached in optimal Pareto-front curve. To get the best solution in the optimal Pareto front fuzzy theory has been used. In the optimization process population size of different values like 20, 30 and 50 have been tried. But, it has been found that there is no such significant variation in result for taking different population sizes for the IEEE 69-bus system and Indian 85-bus system reported. Finally, population size of 20 has been fixed for evaluating the performance of the proposed optimization algorithm.

5.5 Test and Simulation Conditions

The following test and simulation conditions have been considered for analyzing the performance of the proposed state estimation formulation and algorithm in MATLAB 2014b environment. To estimate the system state (branch current magnitude and angle) BC-DSSE algorithm has been utilized. The measurement data are generated by adding small Gaussian noise

of 1%, 3% and 5% to the actual or reference value of the quantity of interest to be measured. There are different kinds of measurements have been considered for state estimation such as: substation measurement, pseudo-measurement, real measurement and virtual measurement [75]. It is assumed that, the former two types of measurements give the information about real and reactive power injections at the buses. The real measurements are obtained from IEDs and PMUs, and it is assumed that IED gives the information about real and reactive power flows in a line and PMU provides the information about bus voltage phasors. Furthermore, the measurement uncertainties are considered based upon the maximum percentage of error associated with each type of measurement [75]. The information about the measurement data are provided below:

- 1) Substation Measurements: The measurements that are collected from the substation are called as default measurements. Generally, the substation measurements are considered to have high accuracy and therefore, in this test 1% error has been chosen for substation measurements.
- 2) Real measurements: The measurements obtained from IEDs and PMUs are assumed as real measurements. In this test, different accuracy values have been chosen for IEDs measurements. For IEDs, the maximum allowable error considered is 1%, 3% and 5%. In case of PMU (synchronized measurements), the maximum allowable error of 0.7% have been considered [75].
- 3) Pseudo-measurements: Basically, the pseudo-measurements are obtained from the historical customer load data and the error associated with the pseudo-measurements is relatively very high. Thus, the maximum percentage of error assumed for this is 50%.
- 4) Virtual-measurements: The measurements at the zero injection buses are treated as virtual measurements with a low variance of 10^{-7} [94].

Furthermore, in this study, for better visualization, random variations in load and generator have been considered. Different operating scenarios are simulated by considering the load demands and generator output as stochastic variable following the Gaussian distribution around the mean value with prefixed standard deviation. Moreover, the impacts of measurement uncertainties on state estimation performance have been studied using Monte-Carlo simulation. There are 1000 number of different network states are generated from each network condition to study the impacts of measurement uncertainties on state estimation performance. The total number of operating condition considered is 100. Hence, the total number of operating scenarios

considered in this study is 100×1000 . A standard deviation of $\pm 10\%$ of the base value is assumed for each operating condition.

The number of IEDs and PMUs required and their locations in an active distribution network is presented. It is assumed that the DG output is stochastic in nature and following normal distribution. Furthermore, it is specified that all DGs are injecting only real power to the buses where it is integrated. The base values of DG power output and their locations are provided in Table 5.2 [97], [98]. All the parameters used in EDA and NSGA-II algorithm have been shown in Table 5.1. Different parameters used in EDA algorithm for probabilistic learning, sampling, selection and repairing process are provided in Table 5.1.

For the simulation study, the relative cost of each PMU is assumed as 1pu and for an IED, the cost is 0.6pu. Actually, in practice, the cost of the measurement devices depends on the application scenarios. Generally, the cost of a PMU is more than the IED, therefore, in this study, the relative cost of PMU and IED are considered as 1pu and 0.6pu respectively. To obtain the optimal trade-off solution, fuzzy theory has been used and is discussed in [95].

Table 5.1 Parameters used in EDA, NSGA-II and SA algorithm

EDA	NSGA-II	Simulated Annealing (SA)
Population size = 20, Learning method -Learn Gaussian Bayesian Model	Population size=20	Initial Temperature (T_e) = 100
Sampling method- Sample Gaussian Universal Model	Cross over rate = 0.8	Scheduling factor (α) =0.99
Replacement method- Pareto Rank ordering	Mutation rate = 0.02	
Selection method - Non-Dominated selection	Maximum generations = 20	
Repairing method-Set In Bounds repairing		
Maximum generations=20		

Table 5.2 Distribution generation (DG) installation bus and capacity

Test System	Bus Number	DG capacity(in MW) Base Value
IEEE 69-bus System	50	0.180
	61	0.270
Practical Indian 85-bus System	45	0.277
	61	0.290

5.5.1 IEEE 69-bus system

A standard IEEE 69-bus, 12.66kV radial distribution network has been considered to test the effectiveness of the proposed algorithm. This test system includes 69 buses, 68 lines along with 48 loads and two DGs integrated at bus 50 and 61. The load and line parameters of the test system are obtained from [99]. The total load of the system is 3.802MW and 2.692MVar respectively. In this system there are 21 buses where there is no source or load is connected. Therefore, these are treated as zero injection buses [94]. The real and reactive power injections at the zero injection buses are assumed as virtual measurements with higher degree of accuracy level.

The obtained results using the proposed algorithm under different measurement uncertainties have been shown in Table 5.3. The total number of PMU and IED require to obtain quality state estimation results are also provided in Table 5.3. It is seen that when 1% error is considered for IED measurements and 50% for pseudo-measurement, the total configuration cost is 2.8 using hybrid EDA-IPM algorithms and the RMS value of state estimation error is 0.0103pu. Similarly, in case of EDA-SA, EDA and NSGA-II, the total cost obtained is 5, 4.8 and 4. The RMS values of state estimation error obtained using EDA-SA, EDA and NSGA-II are 0.0144, 0.0183 and 0.0144pu respectively. Furthermore, the optimal Pareto fronts between the objectives J_1 , J_2 and J_3 have been shown in Figure 5.1. The optimal number and location of PMUs and IEDs are obtained from the optimal Pareto fronts for their respective algorithms using fuzzy theory discussed in [95]. From the figures, it is worth noticing that the global optimal Pareto fronts have been achieved using the proposed algorithm due to its higher degree of balance between the exploration and exploitation during the search process. In most of the cases it is seen that, IEDs are placed at main feeders to reduce the state estimation error and the combination of IEDs and PMUs provide better solution to improve the state estimation accuracy in the modern active distribution networks. Additionally, the maximum relative percentage error in voltage magnitude and phase angle under all the measurement uncertainty cases is also provided in Table 5.3 to check the reliability of the respective algorithm.

Furthermore, the test has been carried out by considering 3% and 5% error in IEDs along with 50% error in pseudo-measurements and the optimal Pareto-fronts are shown in Figure 5.2 and 5.3 respectively. The obtained results have been reported in Table 5.3. It is seen that, the total cost of the configuration is slightly increased because of more noise has been added to IEDs. In

these cases also, the performance of the proposed hybrid EDA-IPM algorithm is found to be better than all other algorithm used in this chapter. The main advantage of using this multi-objective meter placement technique is that the operator can obtain a best compromised or a trade-off solution between the objectives to minimize the cost as well as the state estimation error. Basically, the selection of optimal solution depends on the decision maker. However, fuzzy theory has been used to find the best compromised solution between the objectives. Generally, meter placement techniques are used for planning study of the distribution systems. Therefore, computational cost and complexity of the proposed technique does not have significant impact on planning study of the distribution system. The computational cost can be reduced if less number of Monte-Carlo trials is considered in simulation study. However, if MC value is high then more accurate results can be expected.

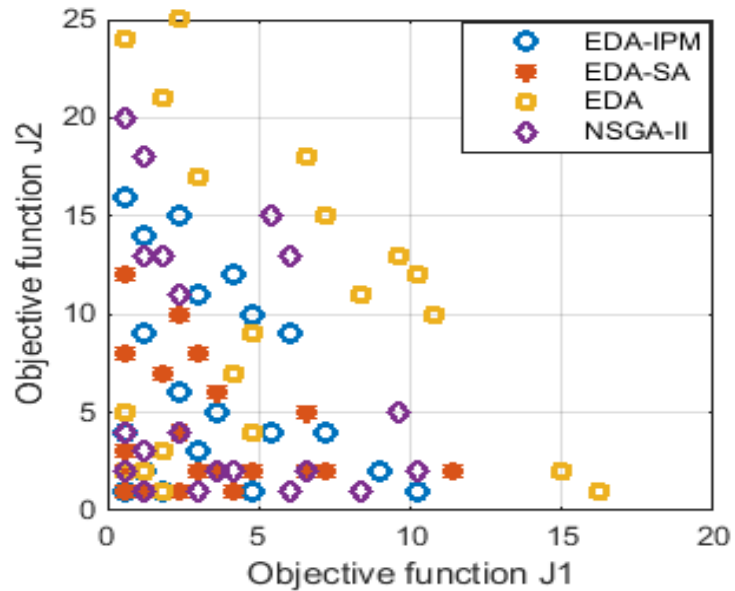


Figure 5.1(a) Optimal Pareto front between objective J1 and J2 (1% error in IEDs and 50% for Pseudo-measurements).

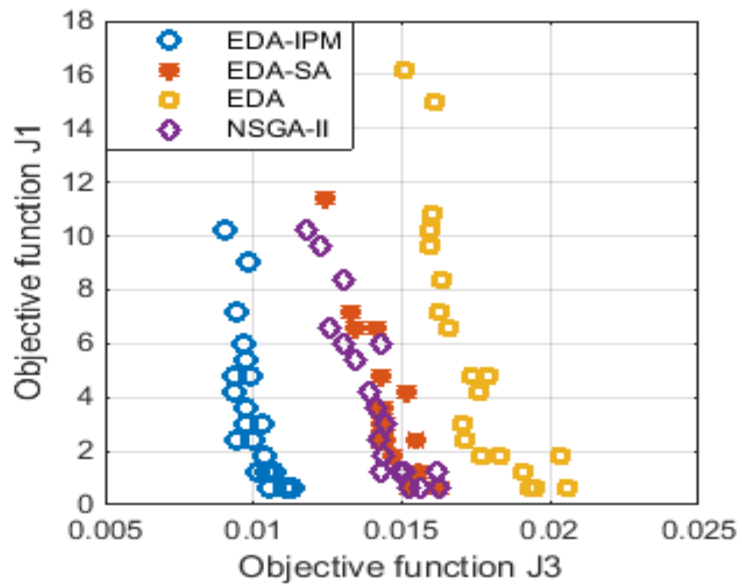


Figure 5.1(b) Optimal Pareto front between objective J1 and J3 (1% error in IEDs and 50% for Pseudo-measurements).

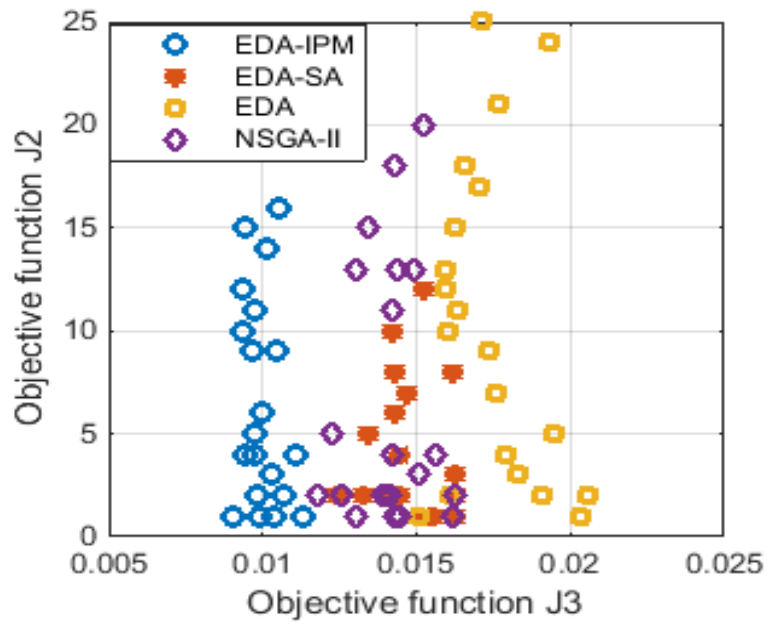


Figure 5.1(c) Optimal Pareto front between objective J2 and J3 (1% error in IEDs and 50% for Pseudo-measurements).

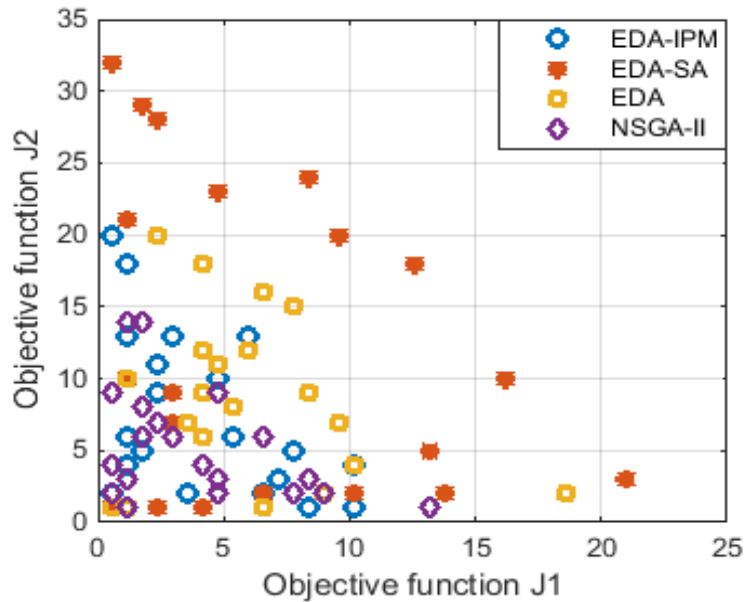


Figure 5.2(a) Optimal Pareto front between objective J1 and J2 (3% error in IEDs and 50% for Pseudo-measurements).

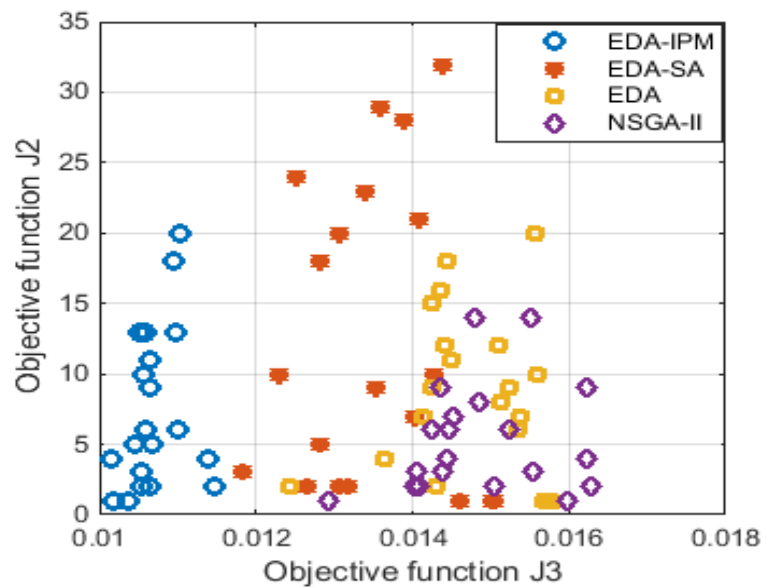


Figure 5.2(b) Optimal Pareto front between objective J2 and J3 (3% error in IEDs and 50% for Pseudo-measurements).

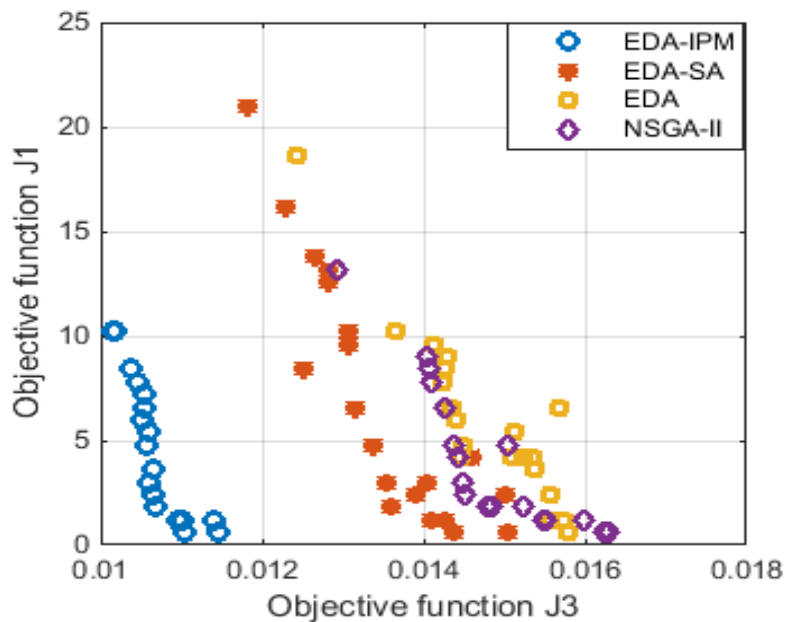


Figure 5.2(c) Optimal Pareto front between objective J1 and J3 (3% error in IEDs and 50% for Pseudo-measurements)

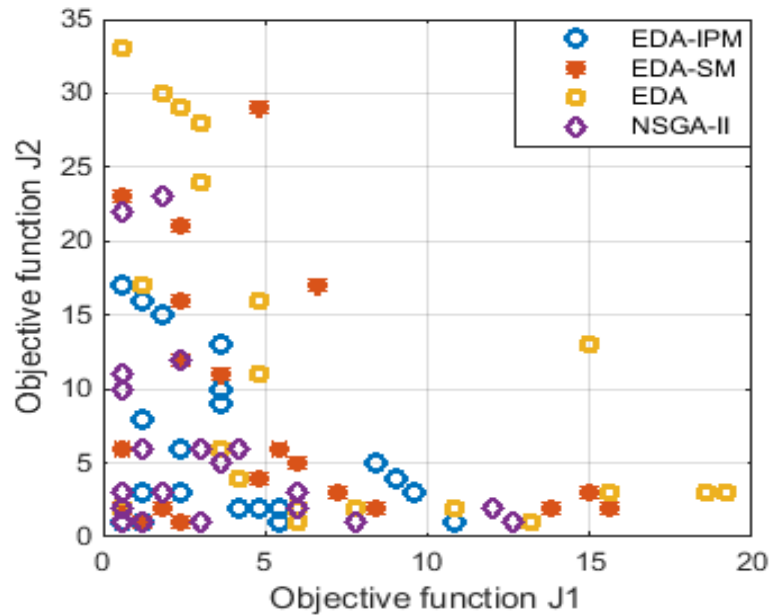


Figure 5.3(a) Optimal Pareto front between objective J1 and J2 (5% error in IEDs and 50% for Pseudo-measurements)

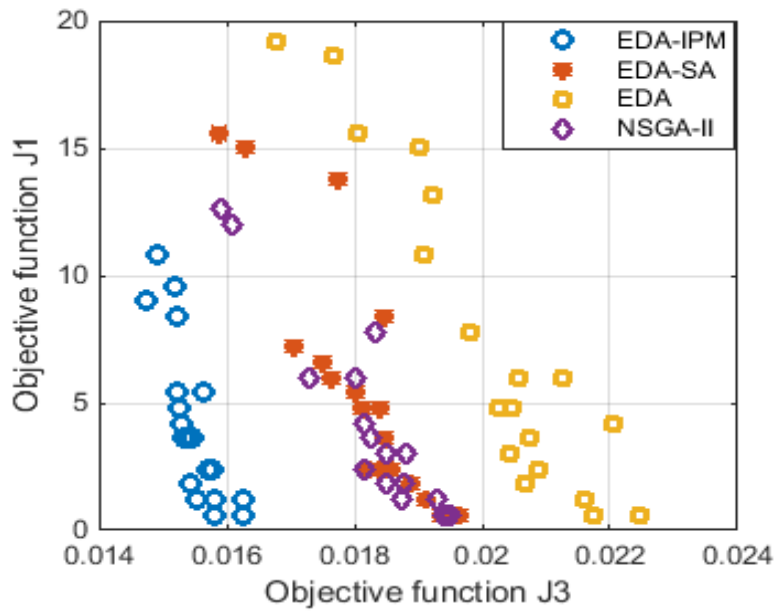


Figure 5.3(b) Optimal Pareto front between objective J1 and J3 (5% error in IEDs and 50% for Pseudo-measurements)

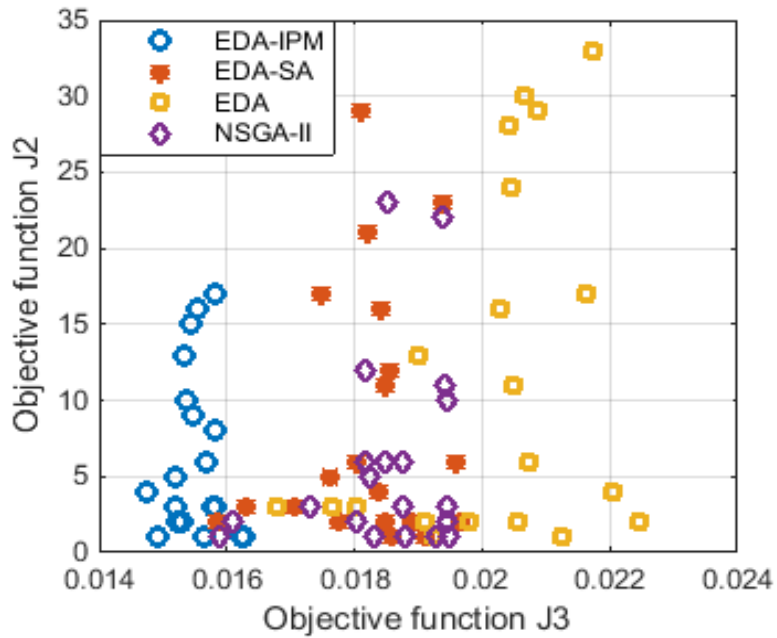


Figure 5.3(c) Optimal Pareto front between objective J1 and J3 (5% error in IEDs and 50% for Pseudo-measurements)

Table 5.3 Optimal location of PMU and IED in IEEE 69 bus active distribution system

Metrological Error of IEDs	Algorithm	PMUs location	IEDs location	Objective functions value			Maximum relative percentage error in voltage magnitude (%)	Maximum relative percentage error in voltage angle (%)
				J_1	J_2	J_3		
1%	Proposed EDA-IPM	27	1,2,10	1.8	1	0.0103	0.2777	6.1936
	EDA-SA	27,67	1,4,8,10,18,20	3	2	0.0144	0.4962	8.3211
	EDA	45,48,59	1,3,54	1.8	3	0.0183	0.3211	10.8978
	NSGA-II	68	1,2,48,56,61	3	1	0.0144	0.3786	9.4631
3%	Proposed EDA-IPM	15,27,36,50,58	1,4,8	1.8	5	0.0106	0.3645	7.3719
	EDA-SA	50,64	1,3,4,13,16,19,23, 30,34,50,56	6.6	2	0.0132	0.4216	8.7546
	EDA	20,23,50,53, 59,64	1,2,5,10,11,13,54	4.2	6	0.0153	0.4056	11.9871
	NSGA-II	43,48,68	1,3,4,8,11,15,27,62	4.8	3	0.0143	0.3927	9.7632
5%	Proposed EDA-IPM	45,67	1,3,23,25,29,57,65	4.2	2	0.0152	0.3625	8.1910
	EDA-SA	43,65,67	1,3,6,7,16,20,38, 49,56,58,60,63	7.2	3	0.0170	0.5089	9.0935
	EDA	52,64	1,3,4,6,13,14,17, 19,21,23,29,41,56	7.8	2	0.0198	0.5897	11.0124
	NSGA-II	60,62,65	1,3,6,10,38,50,52, 54,56,57	6	3	0.0173	0.6083	10.5739

5.5.2 Practical Indian 85-bus system

The effectiveness of the proposed algorithm, has also been tested on a large scale practical Indian 85-bus, 11kV radial distribution network. The system includes of 85 buses, 84 lines along with two DG at bus number 45 and 61 respectively. This system carries a total load of 2.574 MW and 2.622 MVAr. Furthermore, it includes 26 number of zero injection buses. The single line diagram of this test system has been shown in Figure 5.2. The network load and line data are taken from [100].

The simulation results for Indian 85 bus system using the proposed algorithm under different operating conditions have been shown in Table 5.4. When the IEDs accuracy is considered as 1%, the total configuration cost is 3.2 using proposed EDA-IPM algorithm. The RMS value of state estimation error is 0.0096pu. In case of EDA-SA, EDA and NSGA-II, the total cost is 2.8, 4.8 and 5 and the average RMS value of estimation errors obtained are 0.0143, 0.0129 and 0.0160pu respectively. Furthermore, the optimal Pareto fronts between the objectives J_1 , J_2 and J_3 have been shown in Figure 5.4. From the figures, it is seen that the global optimal Pareto fronts has been achieved using the proposed algorithm due its higher degree of balance between the exploration and exploitation during the search process. Moreover, to test the

efficiency of the proposed algorithm, different metrological error of the IEDs have been considered such as 3% and 5% along with 50% error in pseudo-measurements and the obtained results have been reported in Table 5.4. Furthermore, the optimal Pareto-fronts are shown in Figure 5.5 and 5.6 respectively. It is observed that the total configuration cost is increased because of more noise has been added in IED measurements. It is worth noticing that the performance of the proposed hybrid EDA-IPM algorithm is found to be more superior than all other algorithms used in this chapter due to its higher degree of balance between the intensification and diversification capability. This is possible due to the hybridization of IPM algorithm of higher exploitation level with traditional EDA of having better exploration ability.

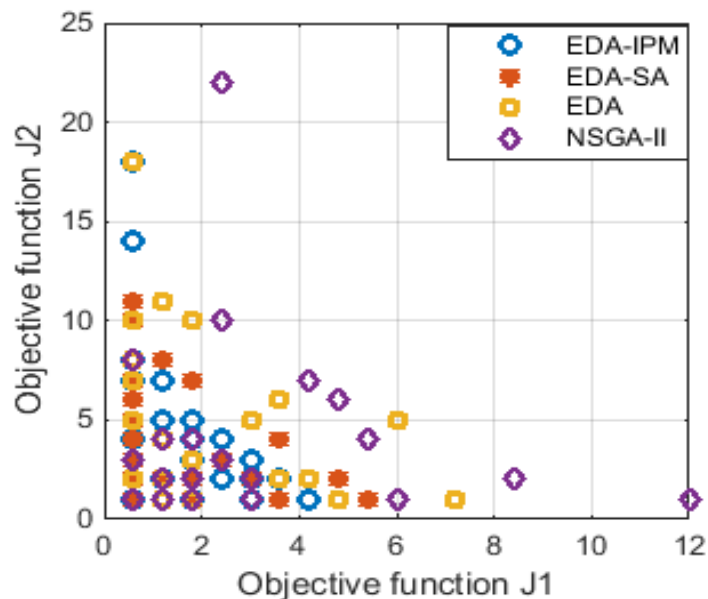


Figure 5.4(a) Optimal Pareto front between objective J1 and J2 (1% error in IEDs and 50% for Pseudo-measurements).

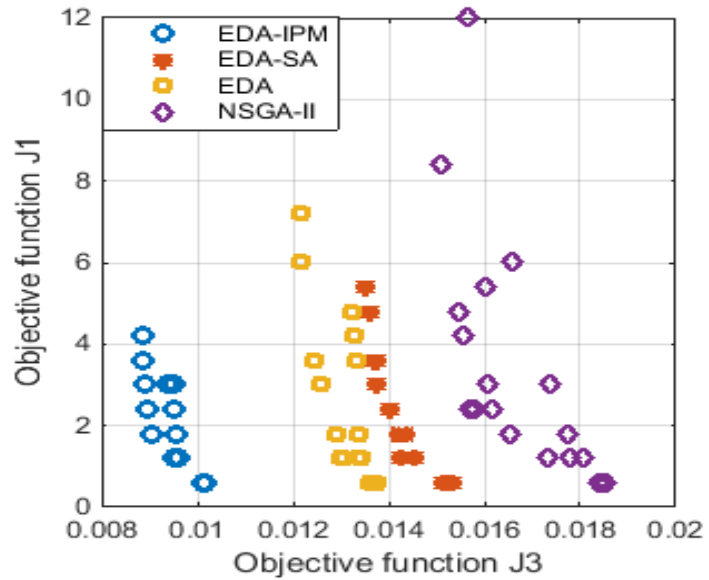


Figure 5.4(b) Optimal Pareto front between objective J1 and J3 (1% error in IEDs and 50% for Pseudo-measurements).

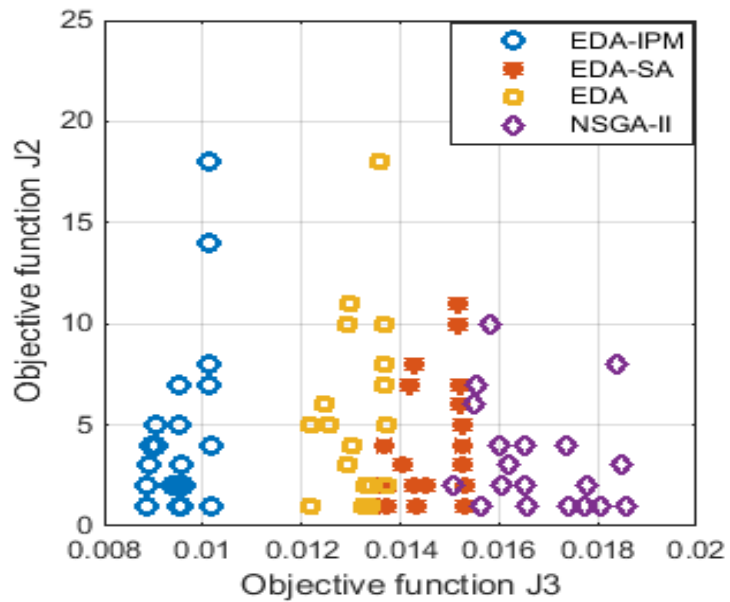


Figure 5.4(c) Optimal Pareto front between objective J2 and J3 (1% error in IEDs and 50% for Pseudo-measurements).

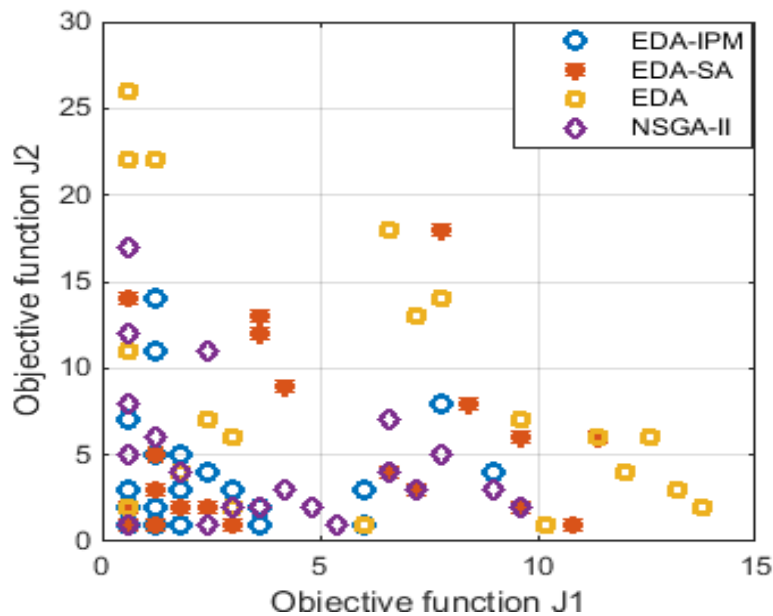


Figure 5.5(a) Optimal Pareto front between objective J1 and J2 (3% error in IEDs and 50% for Pseudo-measurements).

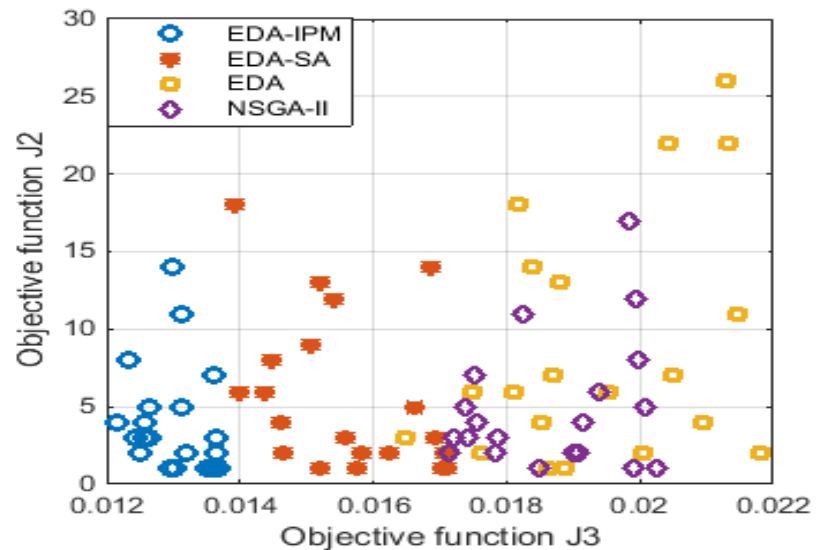


Figure 5.5(b) Optimal Pareto front between objective J2 and J3 (3% error in IEDs and 50% for Pseudo-measurements).

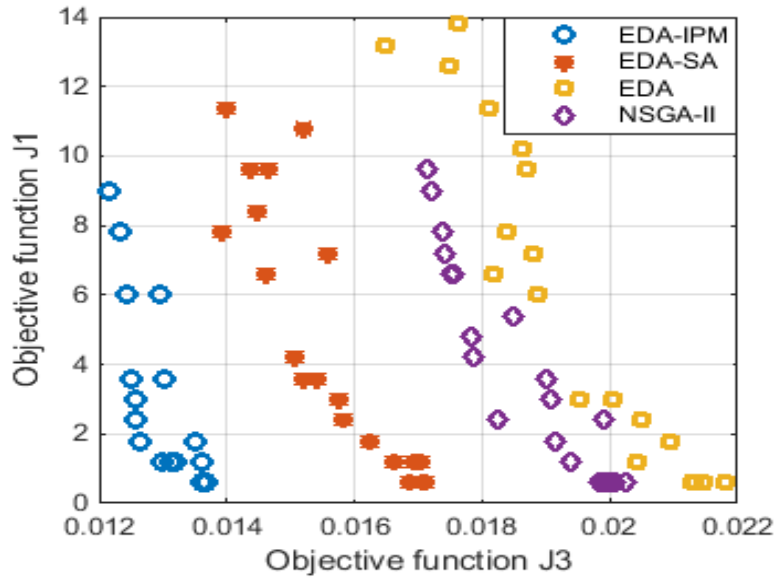


Figure 5.5(c) Optimal Pareto front between objective J1 and J3 (3% error in IEDs and 50% for Pseudo-measurements).

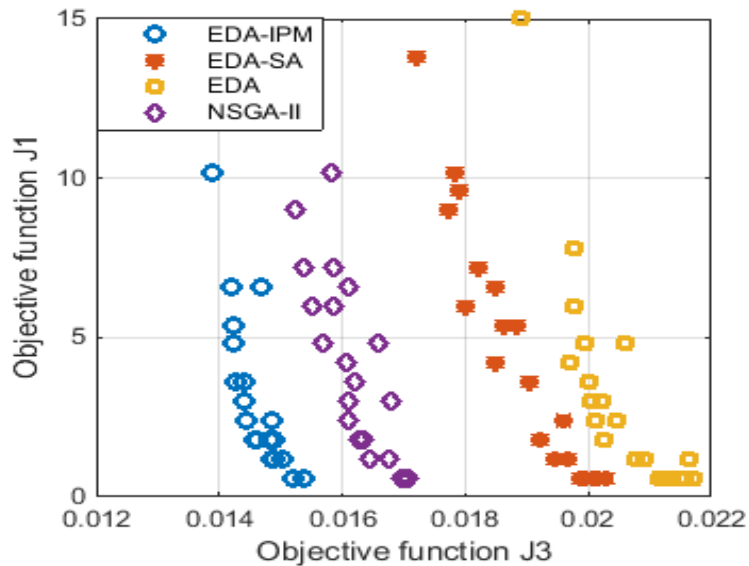


Figure 5.6(a) Optimal Pareto front between objective J1 and J3 (5% error in IEDs and 50% for Pseudo-measurements).

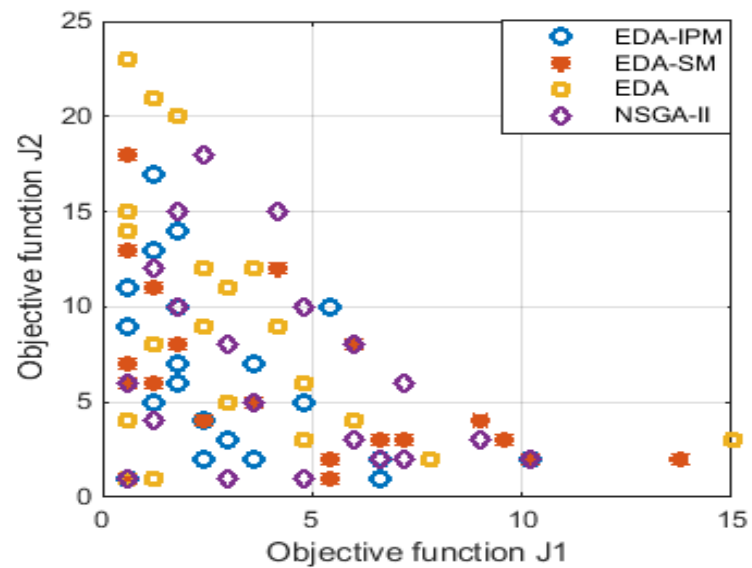


Figure 5.6(b) Optimal Pareto front between objective J1 and J2 (5% error in IEDs and 50% for Pseudo-measurements).

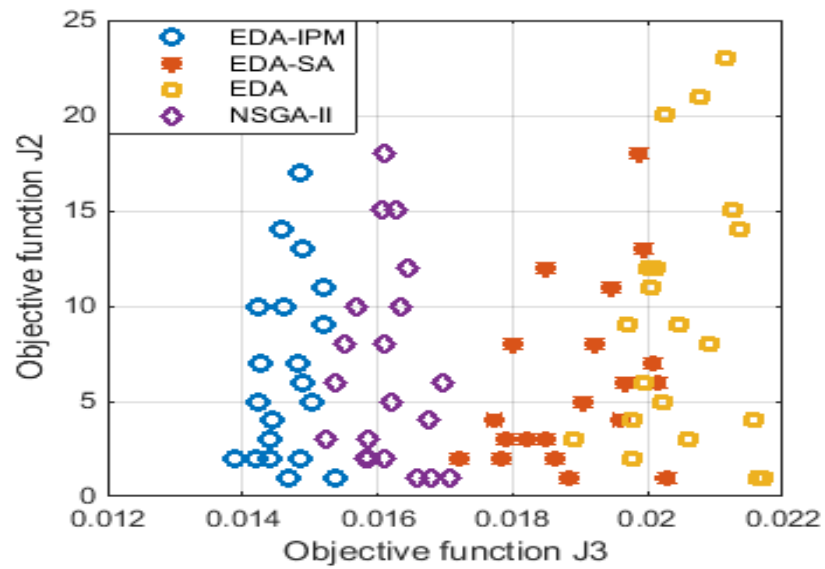


Figure 5.6(c) Optimal Pareto front between objective J2 and J3 (5% error in IEDs and 50% for Pseudo-measurements).

Table 5.4 Optimal location of PMU and IED in Indian 85 bus active distribution system

Metrological Error of IEDs	Algorithm	PMUs location (Bus number)	IEDs location (Line number)	Objective functions value			Maximum relative percentage error in voltage magnitude (%)	Maximum relative percentage error in voltage angle (%)
				J_1	J_2	J_3		
1%	Proposed EDA-IPM	50,54	1,7	1.2	2	0.0096	0.3179	7.5437
	EDA-SA	81	1,5,27	1.8	1	0.0143	0.3672	8.9821
	EDA	40,57,62	1,6,32	1.8	3	0.0129	0.3781	10.8239
	NSGA-II	72,76	1,4,5,26,34	3	2	0.0160	0.3364	8.4772
3%	Proposed EDA-IPM	36,67,71	1,4,5,25,67	1.8	3	0.0126	0.3649	6.9723
	EDA-SA	42,68,70	1,7,8,10,12,29,32, 34,36,46,60,65	7.2	3	0.0155	0.3438	8.2674
	EDA	77	1,3,6,7,15,30, 38,41,48,72	6	1	0.0188	0.4126	11.3037
	NSGA-II	49,76	1,4,5,16,28,42, 57,68	4.8	2	0.0178	0.3986	9.9721
5%	Proposed EDA-IPM	42,74	1,3,5,8,31,60	3.6	2	0.0144	0.4023	8.0593
	EDA-SA	78,83	1,4,5,13,20, 22,26,66,75	5.4	2	0.0186	0.4821	7.7331
	EDA	67,73,78,83	1,2,3,7,12,15, 21,32,48,49	6	4	0.0197	0.4872	11.0241
	NSGA-II	76,81,84	1,3,4,5,6,9,11,12,23, 25,33,51,67,71,74	9	3	0.0152	0.5673	12.7671

5.6 Summary

This chapter formulated a new multi-objective optimization problem to find an optimal trade-offs in PMUs and IEDs deployment for state estimation in active distribution networks. A new hybrid estimation of distribution algorithm is proposed to find the optimal number and location of PMUs and IEDs for accurate state estimation. The local searching capability of the classical EDA algorithm is improved by hybridizing with the Interior point method (IPM). The hybridization of EDA and IPM brings a balance between exploration and exploitation capability of the algorithm during the search process. Furthermore, different uncertainties level of measurement devices and load variations are also taken into consideration for testing the reliability of the state estimator. The performance of the hybrid EDA-IPM algorithm is tested on a standard IEEE 69-bus as well as Indian 85-bus system. The obtained results using hybrid EDA-IPM algorithm are compared with the conventional EDA, NSGA-II and also with EDA-simulated annealing algorithm existing in the literature. It is found that the proposed algorithm is more efficient, reliable and robust under various operating conditions and metrological characteristics

of the measurement devices. Moreover, the performance of the proposed algorithm is found to be more superior than all other algorithms used in this chapter. Hence, the proposed multi-objective based meter placement technique can be used for the planning study and monitoring of the smart distribution networks.

Chapter 6

Robust Meter Placement for Distribution System State Estimation in presence of Wind Generators Using new Multi-Objective Hybrid PSO-KH Algorithm

Chapter 6

Robust Meter Placement for Distribution System State Estimation in presence of Wind Generators Using New Multi-Objective Hybrid PSO-KH Algorithm

6.1 Introduction

In this chapter, trade-offs in deployment of phasor measurement units (PMUs) and intelligent electronic devices (IEDs) for state estimation in distribution networks in presence of wind generators are presented. Due to the stochastic nature, the output of each wind generator is modeled using Weibull distribution function. In the optimization problem the objective functions considered to be minimized are the total cost of PMUs and IEDs as well as the root mean square (RMS) value of state estimation error. Since the objectives are in conflict, a multi-objective Pareto-based non-dominated sorting algorithm has been employed to get a compromise solution. To get the best optimal solution, multi-objective hybrid PSO-Krill Herd algorithm has been used. Furthermore, the random variation in loads and generators is also considered to check the reliability of the proposed meter placement technique. The viability of the proposed algorithm has been tested on IEEE 69-bus system and Practical Indian 85-bus system to validate the results. The results obtained have been compared with Particle Swarm Optimization (PSO), Krill Herd (KH) algorithm and also with well known Non-dominated sorting genetic algorithm (NSGA-II).

6.2 Distribution system state estimation in presence of PMUs and IEDs

Basically, distribution networks are monitored partially due to insufficient real time measurement data. Therefore, the knowledge about the system is obtained from a priori information along with some limited real time measurements. The a priori information is nothing but historical customer load data and known as pseudo-measurement. The real measurements are obtained from PMUs and IEDs. For state estimation, the well established Weighted Least Square (WLS) algorithm has been employed to minimize the following objective function:

$$J = [z - h(x)]^T W^{-1} [z - h(x)] \quad (6.1)$$

$$\text{Subject to: } z = h(x) + r \quad (6.2)$$

where z is the measurement vector, x represents system state vector consisting of branch

current magnitudes and phase angles, $h(x)$ is a nonlinear measurement function of system state variables and r represents a small Gaussian noise and W is the covariance matrix.

For better estimation accuracy, PMUs have been employed along with IEDs for online monitoring of the distribution networks. Therefore, a mixed approach has been considered which includes measurements from PMUs and IEDs to enhance the state estimation accuracy of an active distribution network. A mathematical model for state estimation based on PMUs and IEDs data is described below.

There are different types of measurements such as substation measurement, pseudo-measurement; virtual measurement, smart meter measurement and phasor measurement obtained from PMU which have been utilized for state estimation in distribution networks. Additionally, it is assumed that, PMU installed at a particular bus provides voltage phasor measurements of that bus.

For state estimation, branch current based state estimation (BC-DSSE) algorithm has been used where branch current magnitudes and their phase angles are considered as states of the distribution system [40]. The initial values for the state variables are assumed as discussed in [41] and the WLS based iterative process has been conducted to estimate the state variables.

The estimated value of the state variable x at $(k+1)^{th}$ iteration can be expressed as follows:

$$x_{k+1} = x_k + G(x_k)^{-1} [H(x_k)^T W^{-1}] [z - h(x_k)] \quad (6.3)$$

where H represents the Jacobian matrix, which is calculated by taking the partial derivative of each non-linear measurement function $h(x)$ with respect to each state variable x and G represents the gain matrix given by

$$G(x_k) = H(x_k)^T W^{-1} H(x_k) \quad (6.4)$$

The inverse of the covariance matrix W can be defined as

$$W^{-1} = \begin{bmatrix} W_S^{-1} & 0 & 0 & 0 & 0 & 0 \\ 0 & W_{IED}^{-1} & 0 & 0 & 0 & 0 \\ 0 & 0 & W_{PMU,real}^{-1} & 0 & 0 & 0 \\ 0 & 0 & 0 & W_{PMU,imag}^{-1} & 0 & 0 \\ 0 & 0 & 0 & 0 & W_P^{-1} & 0 \\ 0 & 0 & 0 & 0 & 0 & W_V^{-1} \end{bmatrix} \quad (6.5)$$

The subscripts in eq. (6.5) S , IED , P and V represent substation measurement, IED

measurement, pseudo-measurement and virtual measurement respectively. In eq. (6.5), W_{IED} and W_{PMU} represent the covariance matrix of the IED measurements and phasor measurements. W represents the covariance matrix. The error vector r can be expressed as:

$$r = \begin{bmatrix} z_S - h_S(x) \\ z_{IED} - h_{IED}(x) \\ z_{PMU,real} - h_{PMU,real}(x) \\ z_{PMU,imag} - h_{PMU,imag}(x) \\ z_P - h_P(x) \\ z_V - h_V(x) \end{bmatrix} \quad (6.6)$$

In this work, it is assumed that IEDs are used to measure real and reactive power flows in a line and PMUs are incorporated to measure voltage phasors at a bus. According to state estimation theory [23], the diagonal elements of the error covariance matrix represent the estimation variances of the states and mathematically this can be expressed as follows:

$$E_{xx} = G(x)^{-1} \quad (6.7)$$

Furthermore, this can be expressed as $E_{xx} = E_x(x \cdot x^T) = E_x(x^T - \hat{x})^2$. Where E_{xx} is the error covariance matrix, E_x is the operator of statistical expectation, G is the gain matrix and $\hat{x} = x - \hat{x}$.

6.3 Mathematical model of the proposed meter placement technique

The proposed meter placement problem is designed as a MOOP. The objective is to determine the optimal number and location of PMU and IED in a distribution network to achieve minimum cost as well as ensure error within the predefined threshold limit. The objective functions considered are: (i) the total cost of PMUs and (ii) IEDs, and (iii) the RMS value of state estimation error. Since, the objectives considered are conflicting in nature, the meter placement problem can be designed as multi-objective Pareto based optimization problem [88]-[89]. Mathematically, it can be expressed as:

Minimize

$$J_1 = \sum_{i=1}^{nl} C_{IED,i} \cdot P_{IED,i} \quad (6.8)$$

$$J_2 = \sum_{i=1}^n C_{PMU,i} \cdot P_{PMU,i} \quad (6.9)$$

$$J_3 = \frac{1}{m} \sum_{j=1}^m \sqrt{\frac{1}{n_v} \sum_{i=1}^{n_v} E_x \left(\hat{x}_i - x_i \right)^2} \quad (6.10)$$

The constraints considered for this optimization problem is the maximum relative deviations in voltage and the angle estimates are to be within the specified limits in 95% of the operating scenarios as follows:

$$\left| \frac{V_i^a - V_i^{est}}{V_i^a} \right| \times 100 \leq 1 \quad (6.11)$$

$$\left| \frac{\delta_i^a - \delta_i^{est}}{\delta_i^a} \right| \times 100 \leq 5 \quad (6.12)$$

where J_1 , J_2 and J_3 are the three objectives, n_v represents number of state variables and n_l indicates the total number of lines in a distribution network, x is the state variable and \hat{x} is the estimated value of the state variable x . In eq. (6.8) and (6.9), C_{IED} and C_{PMU} are respectively, the relative cost of an IED and PMU, P_{IED} and P_{PMU} are treated as binary decision vectors i.e. the presence and absence of a meter in a line or at a bus is indicated by 1 or 0, V_i^a and δ_i^a is the actual or true value of i^{th} bus voltage magnitude and angle, V_i^{est} and δ_i^{est} represents the estimated value at i^{th} bus respectively and in eq. (6.11) and (6.12), m denotes total number of operating scenarios.

In practice, the cost of the measurement devices depends on the application scenarios. Generally, the cost of a PMU is more than that of the IED; therefore, in this study, the relative cost of PMU and IED are considered as 1.0pu and 0.6pu respectively.

6.4 Solution methodology

To find the optimal solution of the proposed MOOP described in Section 6.3, a hybrid PSO-KH algorithm has been used and is described as follows.

6.4.1 Krill Herd Algorithm (KHA)

The Krill Herd algorithm is a population based bio-inspired algorithm. It is based on the herding behavior of the Krill swarms searching for food. The fitness of each Krill particle depends on the distance of it from food location and density of the swarms in the search space [84]. According to the theory, the Krill swarms always try to build high density in the search space and move their positions due to mutual effects. Three effects are produced which are local effect due to local Krill density, a target effect and finally a repulsive effect during their movement towards the optimal solution. The movement of each Krill particle in the search

space is based on three actions:

- a) Induced motion
- b) Foraging motion and
- c) Random diffusion of the Krill individuals

The Lagrangian model of the Krill herd algorithm in an n dimensional decision space can be described as:

$$\frac{dL_i}{dt} = M_i + F_i + D_i$$

where L_i is the position of i^{th} particle, M_i is the induced motion, F_i represents foraging motion and D_i is the random diffusion of the i^{th} particle. The details about the Krill herd algorithm have been discussed in chapter 3.

6.4.2 PSO

The PSO algorithm is a population based swarm intelligence algorithm. It mimics the behavior of birds flocking in search of food in a particular area. Initially no bird has information about the exact location of the food in the search area [50]-[51]. The flock of birds follows the bird nearest to the food location which is called the best solution among all birds looking for food. Each solution in PSO represents a bird which is called as a particle in the search space. In each generation of the optimization algorithm the fitness value of each individual is evaluated using a fitness function. The velocity of each particle is updated based on the current best position of the particle in the search space. Each individual particle knows its best position so far called p_{best} and each individual knows also the information about the best value so far in the group called g_{best} . Each particle tries to update its position using the information provided below:

- The distance between p_{best} and current position of the particle
- The distance between g_{best} and current position of the same particle

Based on this the modification in the velocity of each particle is expressed as follows:

$$v_i^{k+1} = wv_i^k + C_1 \text{rand}_1 \times (p_{best} - p_i^k) + C_2 \text{rand}_2 \times (g_{best} - p_i^k) \quad (6.13)$$

$$p_i^{k+1} = p_i^k + v_i^k \quad (6.14)$$

where

v_i^k Velocity of i^{th} particle at k^{th} iteration

w Weighting function

C_1, C_2 Learning factors

<i>rand</i>	Random number between 0 and 1
p_i^k	Position of i^{th} particle at k^{th} iteration
$pbest_i$	Personal best of i^{th} particle at k^{th} iteration
$gbest$	Best position of the group

6.4.3 Optimal placement of PMU and IED using multi-objective hybrid PSO-KH algorithm

Since the objectives are conflicting in nature; the simultaneous optimization needs a compromised solution because each objective in the model is conflicting with one another. Therefore, to achieve a better compromise solution between the objectives, Pareto based non-dominated sorting approach has been implemented. It states that, in a non-dominated Pareto front all solutions are equally important because no solution is dominating the other in the population. In MOOP, the solution relies on a set of other solutions. Therefore, Pareto based non-dominated sorting technique has been employed with hybrid PSO-KH algorithm to achieve best trade-offs solution between the objectives. Furthermore, a trade-off solution between the total cost of PMU and IED needed for the accurate state estimation is to be determined using multi-objective hybrid PSO-KH algorithm. The pseudo code of the hybrid PSO-KH algorithm is presented as follows.

Step 1. Initialization: Initialize the parameters of the PSO and KH algorithm such as:

D^{\max}	Maximum diffusion speed
M^{\max}	Maximum induced speed
W_f	Inertia of the foraging motion
V_f	Foraging speed
C_1, C_2	Learning factors

Step 2. Initialize random solutions:

- 1) Randomly generate number and location of PMU and IED for each solution in the population.

Step 3. Objective functions evaluation:

- 1) Evaluate the objectives J_1, J_2 and J_3 for each solution based on the position of PMUs and IEDs
- 2) Calculate the fitness value of each solution using weighting approach.

3) Use non-dominated sorting (NDS) and crowding distance (CD) method to sort the solution in ascending order.

4) Calculate the best and worst particles in the population.

Step 4. Generate new Krill individuals using PSO.

Step 5. Calculate the following motions for each Krill individual such as:

- 1) Induced motions
- 2) Foraging motions
- 3) Physical diffusions

Step 6. Update position of the Krill individuals.

Step 7. Genetic operator: For further improvement in the solution apply crossover and mutation operator to update the solutions.

Step 8. Repeat steps 3-7 for maximum number of iterations.

Step 9. Use fuzzy theory to obtain best compromised solution between the objectives [95].

Post-processing of the results

In the beginning of the optimization process, the initial solutions i.e. the number and locations of PMUs and IEDs are generated randomly within the search space. Each solution represents the combinations of a number of PMUs and IEDs as well as their locations. Based on each combination of PMUs and IEDs, the objective functions J_1 , J_2 are evaluated and J_3 is calculated using BC-DSSE algorithm. Then, among the population the best and worst Krill is obtained using weighting approach. Basically, if the weights represent the trade-offs between the objective functions, then the original units of the objective functions are retained. It is not required to transfer them between 0 and 1. In this case all weights are assumed to be equal to 1. All objective values are retained with their original units without transferring them between 0 and 1. Furthermore, the sum of all the objectives is determined to know the best and worst solutions. In order to achieve better performance, the solutions are updated using PSO algorithm. In PSO, the PMU and IED's positions are updated using equations (13)-(14). After the positions are updated using PSO, three motions such as induced motion, foraging and diffusion motion are calculated for each Krill particle using Krill herd algorithm. Furthermore, during fitness evaluation, the constraints violation checking needs to be carried out. For each combination of PMU and IED, the relative percentage error in bus voltage magnitude and angle estimate is determined using Monte Carlo trial. For each combination of PMUs and IEDs in a solution, if in 95% of the simulated cases, the estimated relative errors

are below the threshold limits, then for that solution the objective functions are evaluated and stored. On the contrary, if it is not within the threshold limit, then for that particular solution, a higher value of objective is to be assigned. This particular solution can be eliminated during the next immediate generation. Then, genetic operators are used to update the solutions. After updating the solutions, the above steps are repeated until all the solutions in a given population size are in first front. The convergence criterion for the algorithm to stop is, when all the solutions are reached in optimal Pareto-front curve. To get the best solution in the optimal Pareto front fuzzy theory has been used [95]. In the optimization process population sizes of different values like 20, 30 and 50 have been tried. But, it has been found that there is no such significant variation in the result when taking different population sizes for IEEE 69-bus system and Indian 85-bus system. Finally, a population size of 20 has been fixed for to reduce the computational time of the algorithm.

6.5 Test and Simulation Conditions

The following test and simulation conditions have been considered for analyzing the performance of the proposed state estimation formulation and algorithm in MATLAB 2014b environment. To estimate the system state (branch current magnitude and angle) BCDSSE algorithm has been employed. The measurement data are generated by adding small Gaussian noise of 1%, 3% and 5% to the actual or reference value of the quantity of interest to be measured. There are different kinds of measurements considered for state estimation such as: substation measurement, pseudo-measurement, real measurement and virtual measurement [75]. It is assumed that, the former two types of measurements give information about real and reactive power injections at the buses. The real measurements are obtained from IEDs and PMUs, and it is assumed that IED gives information about real and reactive power flows in a line and PMU provides the information about bus voltage phasors. Furthermore, the measurement uncertainties are considered based upon the maximum percentage of error associated with each type of measurement [75]. The information about the measurement data are provided below:

- 1) Substation Measurements: The measurements that are collected from the substation are called as default measurements. Generally, the substation measurements are considered to have high accuracy and therefore, in this test 1% error has been chosen for substation measurements.
- 2) Real measurements: The measurements obtained from IEDs and PMUs are taken as real measurements. In this test, different accuracy values have been chosen for IEDs

measurements. For IEDs, the maximum allowable error considered is 1%, 3% and 5% respectively. In case of PMU (synchronized measurements), the maximum allowable error of 0.7% have been considered.

- 3) Pseudo-measurements: Basically, the pseudo-measurements are obtained from the historical customer load data and the errors associated with the pseudo-measurements are relatively very high. Thus, the maximum percentage of error assumed for this is 50% [75].
- 4) Virtual-measurements: The measurements at the zero injection buses are treated as virtual measurements with a low variance of 10^{-7} [94].

In this study, for better visualization, random variations in loads and generators have been considered. Different operating scenarios are simulated by considering the load demands and generators output as stochastic variable following the Gaussian distribution around the mean value with prefixed standard deviation. Moreover, the impact of measurement uncertainties on state estimation performance has been studied using Monte-Carlo simulation. There are 1000 different network states generated using Monte-Carlo simulation from each network condition to study the impact of measurement uncertainties on state estimation performance. The total number of operating condition considered is 100. A standard deviation of $\pm 10\%$ of the base value is assumed for each operating condition. All parameter values used for specific algorithms are provided in Table 6.1 and also the DG capacities are shown in Table 6.2 respectively [97]-[98]. The parameters value used for model the wind generators are provided in Table 6.3. The Weibull distribution function has been used for predicting the wind speed based on the data collected from the National Renewable Energy laboratory (NREL) site [101].

Table 6.1 Parameter values of KH, PSO and NSGA-II algorithm

KHA	PSO	NSGA-II
Population size=20	Population size=20	Population size=20
D^{\max} (maximum diffusion speed) $\in [0.002 \ 0.01]$	$C_1=2, C_2=2$	Crossover rate (P_c)=0.8
$C_t \in [0, 2]$	$W_{\max}=0.9, W_{\min}=0.4$	Mutation rate (M_c)=0.02
V_f (foraging speed)= 0.02ms^{-1}	Maximum generations=20	Maximum generations=20
W_f (inertia of the foraging motion)=0.9	-	-
M^{\max} (maximum induced speed)= 0.025ms^{-1}	-	-

Table 6.2 Wind generators base case value and their locations

Test system	Bus Number	DG capacity in MW (Base value)
IEEE 69-bus system	50	0.180
	61	0.270
Practical Indian 85-bus system	45	0.277
	61	0.290

Table 6.3 Parameters value for wind generators

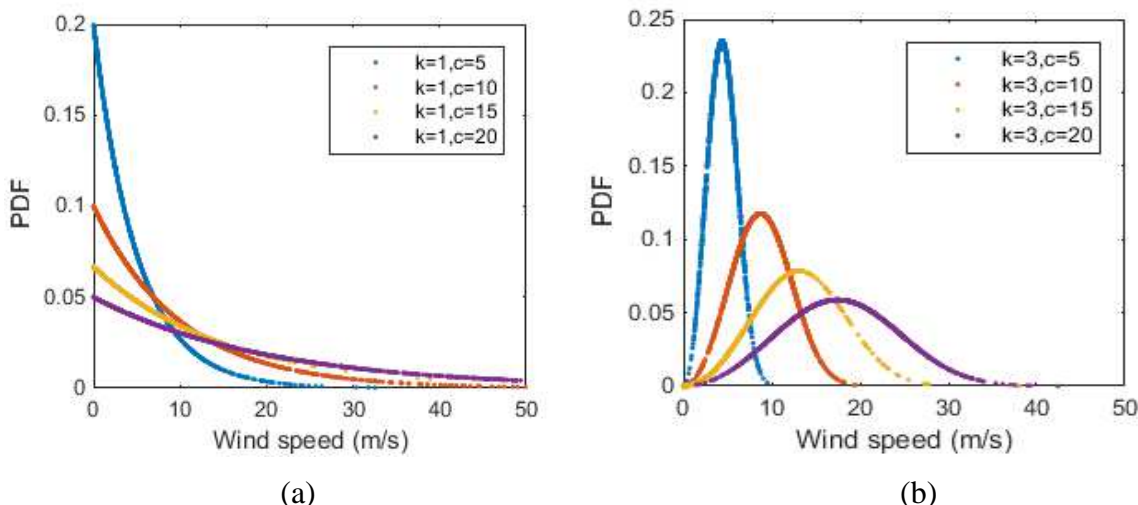
Parameters
Cut-in speed(v_{in}) = 3m/sec
Cut out speed (v_o)= 25m/sec
Rated speed (v_r)= 10.28m/sec

6.5.1 Modelling of wind generator output using Weibull distribution

In this work, all DGs are considered as wind generator and output of each DG is modeled using Weibull distribution function, since wind speed is stochastic in nature [96]. Furthermore, it is assumed that DGs are producing only real power to the network. The Weibull probability density function over a period of time is expressed as follows:

$$f(v) = \left(\frac{k}{c}\right)\left(\frac{v}{c}\right)^{(k-1)} \exp^{-\left(\frac{v}{c}\right)^k}, \quad 0 < v < \infty \quad (6.15)$$

where k and c are indicated as shape and scale factor of the wind speed respectively. The wind speed is represented as v . For different value of k and c the PDF of the Weibull distribution function is shown in Figure 6.1.

Figure 6.1 Variations of wind speed for (a) $k=1$ and (b) $k=3$

The value of the shape and scale factor of a wind generator depends on the location and geographical condition where it is situated. These parameters are determined using mean and variance of the wind speed over a period of time. Once the characteristic of wind speed is known, the output of wind generator can be determined using the following transformation discussed below:

$$P = \begin{cases} 0; & 0 < v < v_{in} \\ P_r \left(\frac{v - v_{in}}{v_r - v_{in}} \right); & v_{in} \leq v \leq v_r \\ P_r; & v_r \leq v \leq v_o \\ 0; & v > v_o \end{cases} \quad (6.16)$$

In the above equation, v_{in} , v_o and v_r are indicated as cut-in speed, cut-out speed and rated speed of the wind respectively and their value for a specific data has been provided in Table 6.3. The rated output power of the wind generator is represented as P_r . Several methods are available to determine the value of k and c . One of the widely used approximations is mean wind speed and standard deviation approach. By using this approach the value of k and c is determined as follows:

$$\begin{aligned} k &= \left(\frac{\sigma}{u} \right)^{-1.086} \\ c &= 1.12u \end{aligned} \quad (6.18)$$

where σ represents standard deviation and u is the mean wind speed respectively.

6.5.2 Simulation result and discussions

The optimal location of PMU and IED is determined in a standard IEEE 69 bus system and also in a practical distribution network such as Indian 85 bus radial distribution network discussed below.

6.5.2.1 IEEE 69 bus system

A standard IEEE 69-bus, 12.66kV radial distribution network has been considered to test the effectiveness of the proposed algorithm. It includes 69 buses, 68 lines along with 48 loads and two DGs injected at bus number 50 and 61. The DGs locations are selected based on to achieve minimum power loss in the network. The network data are obtained from [99]. The total load of the system is 3.802MW and 2.692MVar respectively. In this system there are 21 buses where there is no source or load is connected. Therefore, these are treated as zero injection buses. The real and reactive power injections at the zero injection buses are assumed as virtual measurements with higher degree of accuracy level.

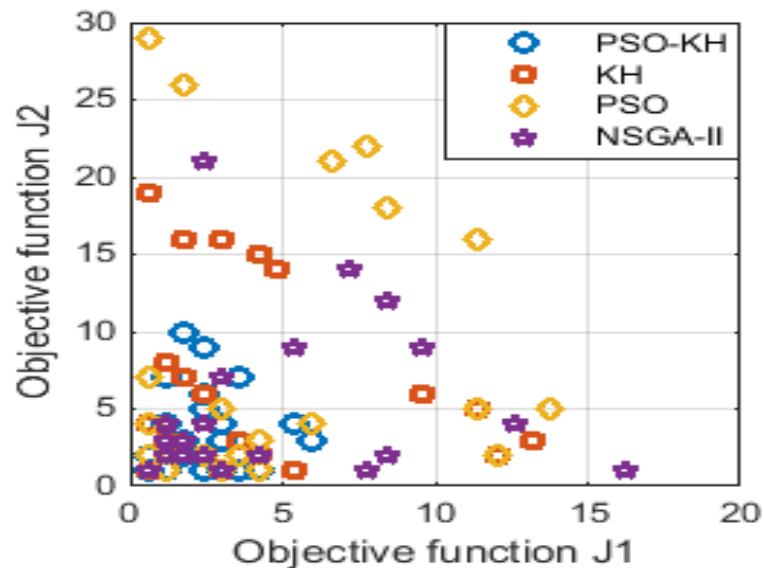


Figure 6.2(a) Optimal Pareto fronts between the objectives J_1 and J_2 for 1% error IED measurements and 50% in pseudo-measurements

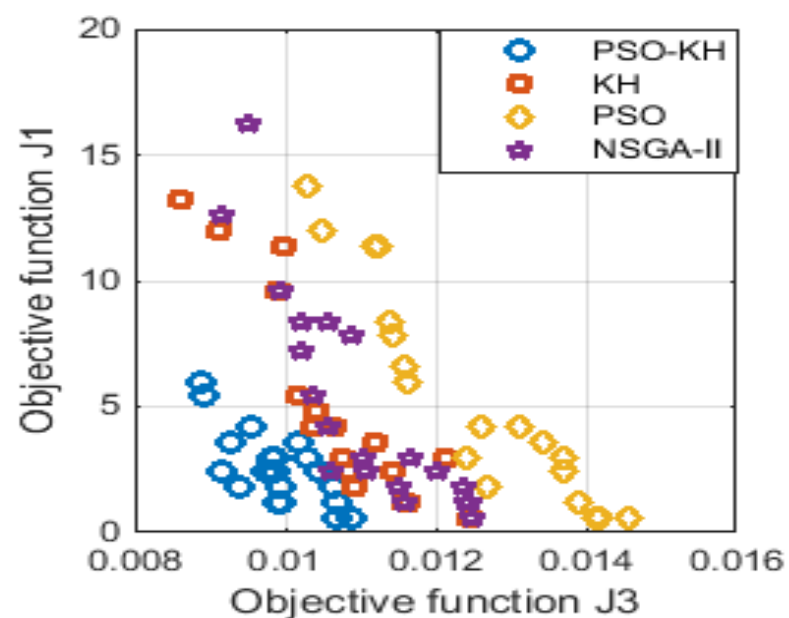


Figure 6.2(b) Optimal Pareto fronts between the objectives J_1 and J_3 for 1% error IED measurements and 50% in pseudo-measurements

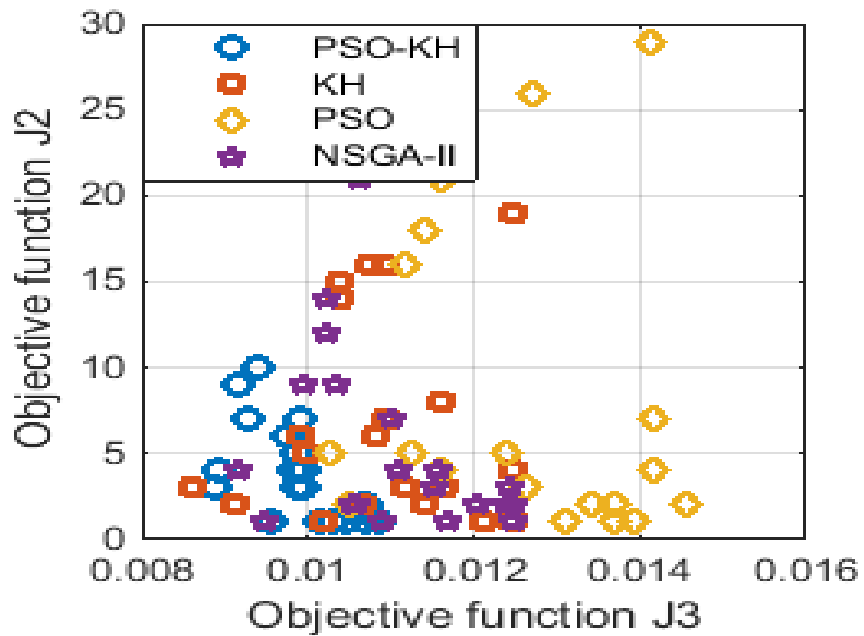


Figure 6.2(c) Optimal Pareto fronts between the objectives J_2 and J_3 for 1% error IED measurements and 50% in pseudo-measurements

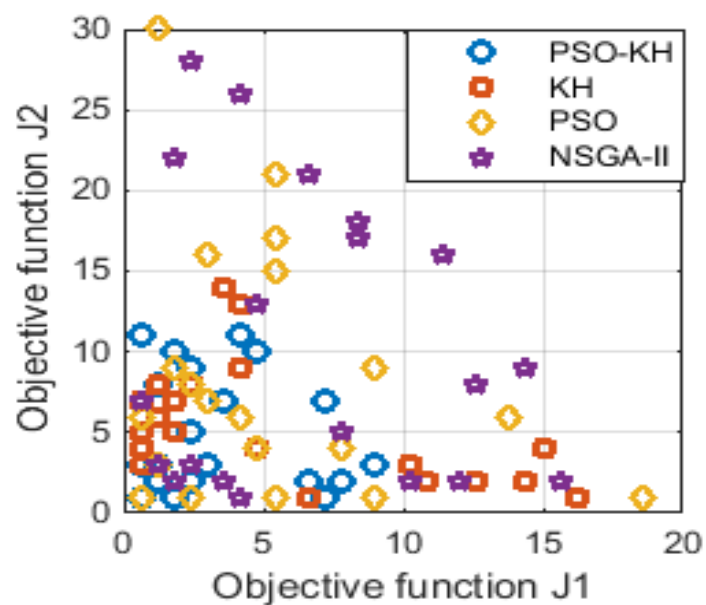


Figure 6.3(a) Optimal Pareto fronts between the objectives J_1 and J_2 for 3% error IED measurements and 50% in pseudo-measurements.

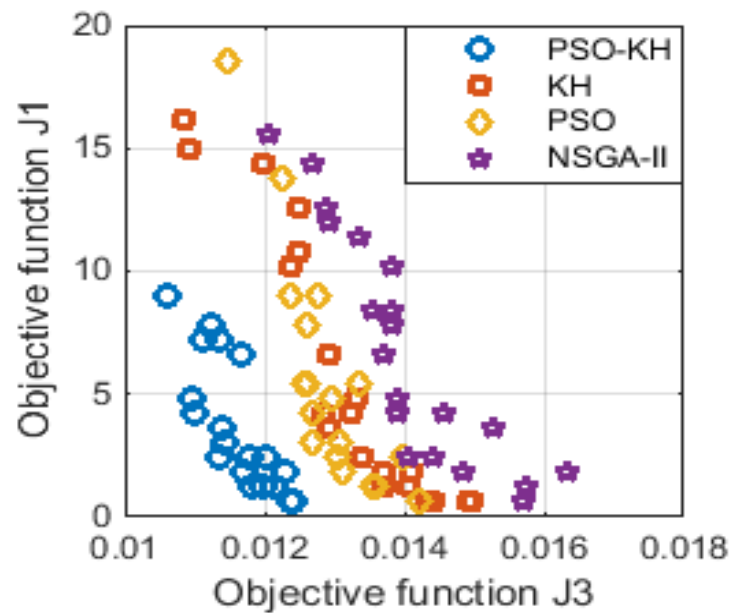


Figure 6.3(b) Optimal Pareto fronts between the objectives J_1 and J_3 for 3% error IED measurements and 50% in pseudo-measurements.

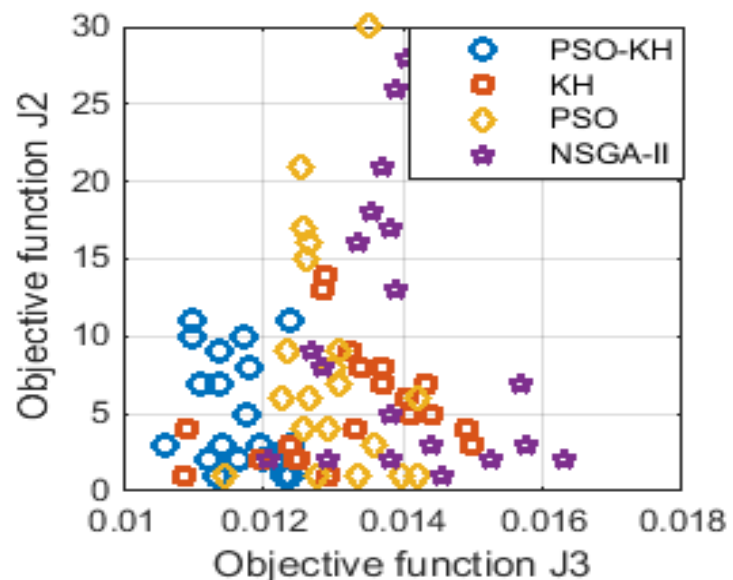


Figure 6.3(c) Optimal Pareto fronts between the objectives J_2 and J_3 for 3% error IED measurements and 50% in pseudo-measurements.

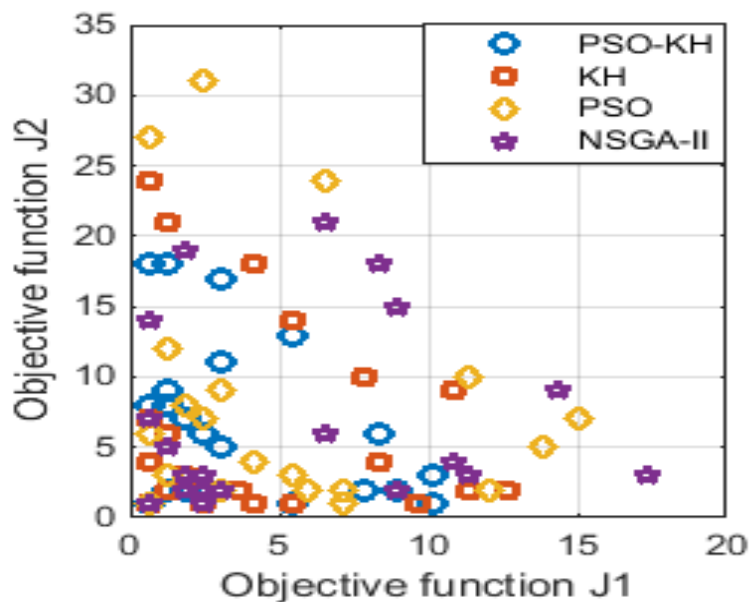


Figure 6.4(a) Optimal Pareto fronts between the objectives J_1 and J_2 for 5% error IED measurements and 50% in pseudo-measurements

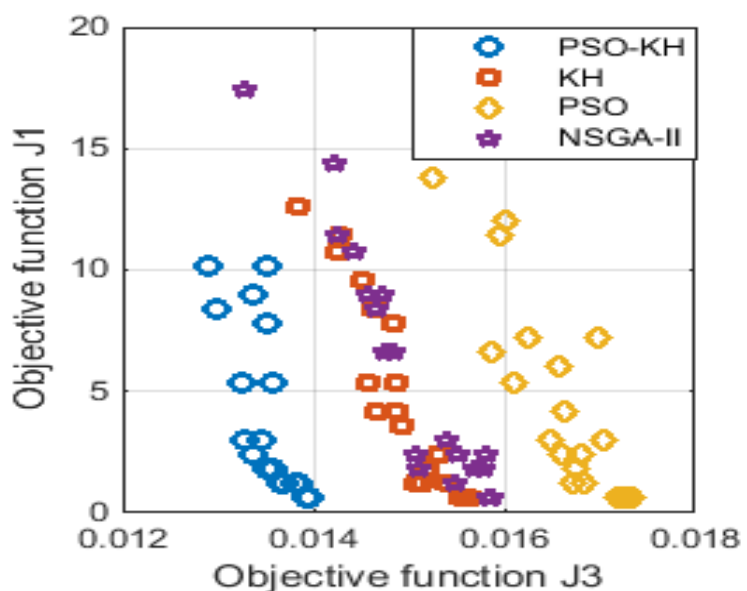


Figure 6.4(b) Optimal Pareto fronts between the objectives J_1 and J_3 for 5% error IED measurements and 50% in pseudo-measurements

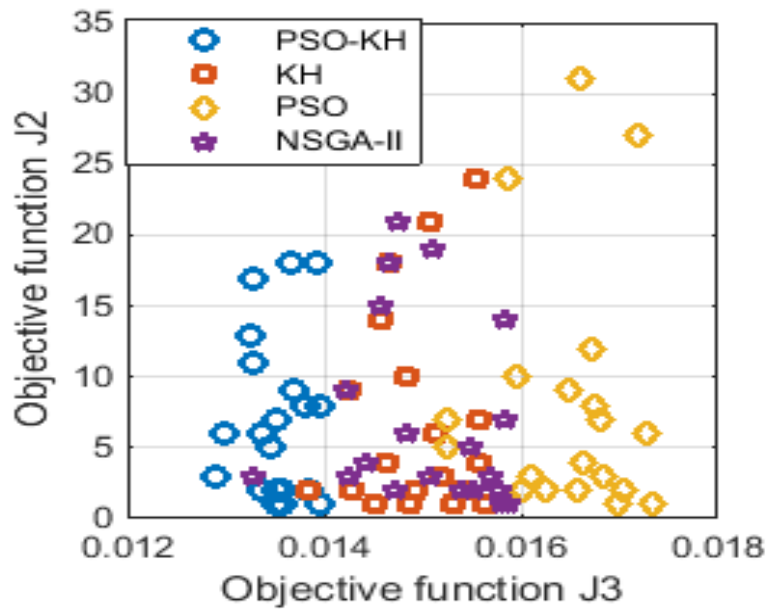


Figure 6.4(c) Optimal Pareto fronts between the objectives J_2 and J_3 for 5% error IED measurements and 50% in pseudo-measurements

Table 6.4 Optimal location of PMU and IED in IEEE 69 bus active distribution system.

Metrological Error of IEDs	Algorithm	PMUs location (Bus number)	IEDs location (Line number)	Objective functions value			Maximum relative percentage error in voltage magnitude (%)	Maximum relative percentage error in voltage angle (%)
				J_1	J_2	J_3		
1%	Proposed PSO_KH	4,14,21,36	1, 13	1.2	4	0.0099	0.3037	6.0436
	KH	68	1,4,9,12,21,43,51,53,65	5.4	1	0.0101	0.4435	7.8210
	PSO	29,30,34,48, 67	1,2,4,17,23	3	5	0.0124	0.3911	9.0118
	NSGA-II	31,64	1,3,4,5,9,21,26	4.2	2	0.0105	0.4679	9.6661
3%	Proposed PSO_KH	43,61,68	1,2,4,15,40	3	3	0.0114	0.3645	7.1719
	KH	40	1,2,4,6,13,16,20,22, 27,33,62	6.6	1	0.0129	0.4911	8.7581
	PSO	22,28,35,45,63, 65	1,2,4,6,1012,18	4.2	6	0.0126	0.4111	10.9431
	NSGA-II	12,14,43	1,2,4,9	2.4	3	0.0144	0.4723	9.23142
5%	Proposed PSO_KH	9,35	1,3,5	1.8	2	0.0135	0.3956	7.3410
	KH	63	1,3,26,35,38,53,62	4.2	1	0.0146	0.5567	8.9465
	PSO	54,63,64	1,2,21,25,30,46,51,56	5.4	3	0.0161	0.5312	10.0124
	NSGA-II	12,14,43	1,2,4,9	2.4	3	0.0150	0.6077	9.5469

The obtained results using the PSO-KH algorithm under different measurement uncertainties have been shown in Table 6.4. The total number of PMU and IED required for quality state estimation results are also provided in Table 6.4. It is seen that when 1% error is considered for IED measurements and 50% for pseudo-measurement, the total configuration cost is 5.2pu using hybrid PSO-KH and the RMS value of state estimation error is 0.0099pu.

Similarly, in case of KH, PSO and NSGA-II, the total cost obtained is 6.4pu, 8pu and 6.2pu. The RMS values of state estimation error obtained using KH, PSO and NSGA-II are 0.0101pu, 0.0124pu and 0.0105pu respectively. Furthermore, the optimal Pareto fronts between the objectives J_1 , J_2 and J_3 have been shown in Figure 6.2. The optimal number and location of PMUs and IEDs are obtained from the optimal Pareto fronts for their respective algorithms using fuzzy theory [36]. From the figures, it is worth noticing that the global optimal Pareto fronts has been achieved using hybrid PSO-KH algorithm due to its higher degree of balance between the exploration and exploitation during the search process. In most of the cases it is seen that, IEDs are placed at main feeders to reduce the state estimation error and the combination of IEDs and PMUs provide better solution to improve the state estimation accuracy in the modern active distribution networks. Additionally, the maximum relative percentage error in voltage magnitude and phase angle under all the measurement uncertainty cases is also provided in Table 6.4 to check the reliability of the respective algorithm.

The test has been carried out by considering 3% and 5% error in IEDs along with 50% error in pseudo-measurements. The obtained results have been reported in Table 6.4 and also the optimal Pareto front plots are shown in Figure 6.3 and 6.4 respectively. It is seen that, the total cost of the configuration is slightly increased because of more noise has been added to IEDs. In 3% error case, the total number of PMU and IED required is 3 and 5 respectively. The RMS value of state estimation error obtained is 0.0114pu using hybrid PSO-KH. Though, the total meter cost using NSGA-II is slightly less than hybrid PSO-KH, but the RMS value of state estimation error is 0.0144pu which is more than hybrid PSO-KH. This is due to the fact that the locations of meters also have an impact on state estimation accuracy. Similarly, in case of 5% error also the total cost of meters using hybrid PSO-KH algorithm is less than other algorithms considered in this chapter. Furthermore the state estimation error is less as compared to other algorithms. In these cases also, the performance of hybrid PSO-KH algorithm is found to be better than all other algorithm used in this work. The main advantage of using this multi-objective meter placement technique is that the operator can obtain a best compromised or a trade-off solution between the objectives to minimize the cost as well as the state estimation error. Basically, the selection of optimal solution depends on the decision maker. Fuzzy theory has been used to find the best compromised solution between the objectives. Generally, meter placement techniques are used for planning study of the distribution systems. Therefore, computational cost and complexity of the proposed technique

does not have significant impact on planning study of the distribution system. The computational cost can be reduced if less number of Monte-Carlo (MC) trials is considered in simulation study. However, if MC value is high then more accurate results can be expected.

6.5.2.2 Practical Indian 85 Bus System

The effectiveness of the proposed algorithm, has also been tested on a large scale practical Indian 85-bus, 11kV radial distribution network. The system includes of 85 nodes, 84 lines along with two wind generators at bus number 45 and 61 respectively. The DGs locations are selected based on to achieve minimum power loss in the network. This system carries a total load of 2.574 MW and 2.622 MVar. Furthermore, it includes 26 zero injection buses. The line and load data of the system are obtained from [100].

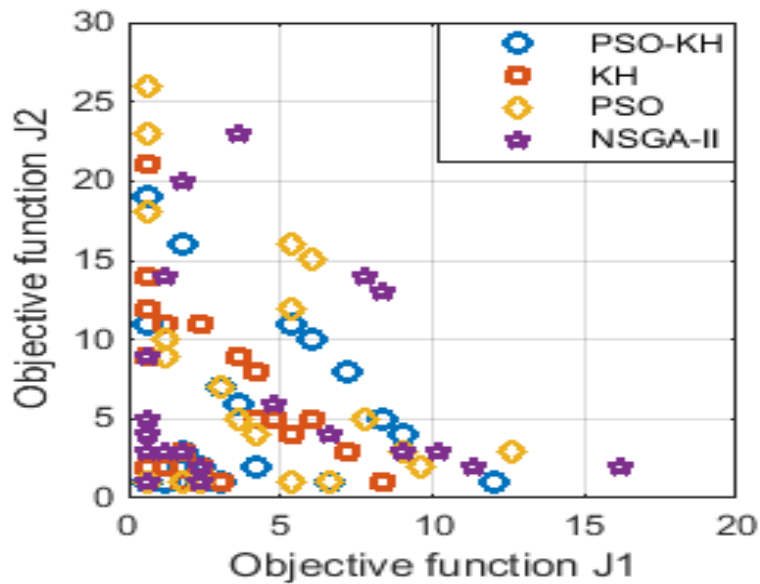


Figure 6.5(a) Optimal Pareto fronts between the objectives J_1 and J_2 for 1% error IED measurements and 50% in pseudo-measurements

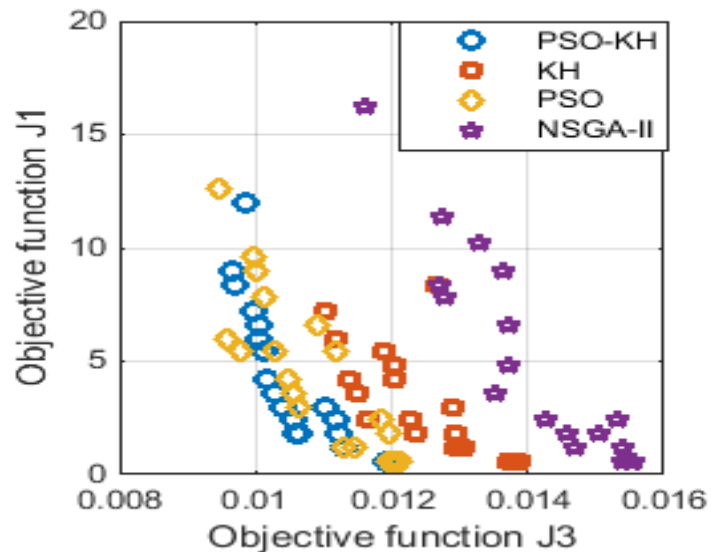


Figure 6.5(b) Optimal Pareto fronts between the objectives J_1 and J_3 for 1% error IED measurements and 50% in pseudo-measurements

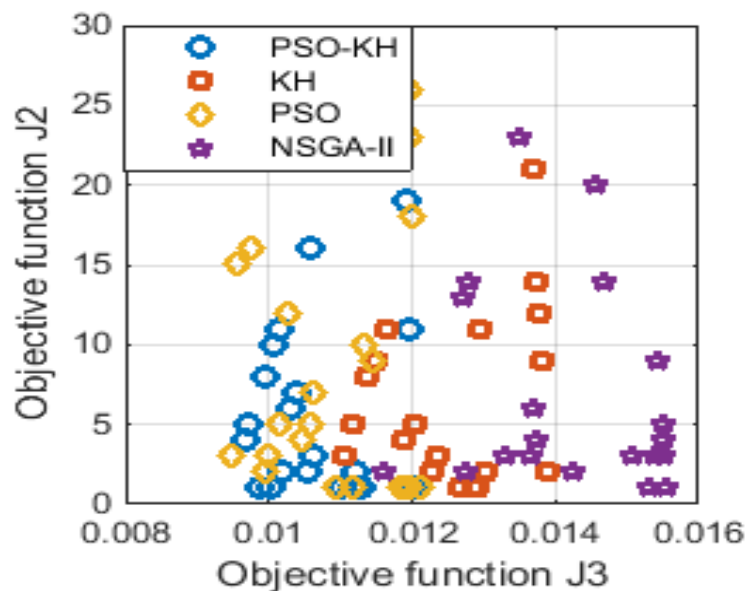


Figure 6.5(c) Optimal Pareto fronts between the objectives J_2 and J_3 for 1% error IED measurements and 50% in pseudo-measurements

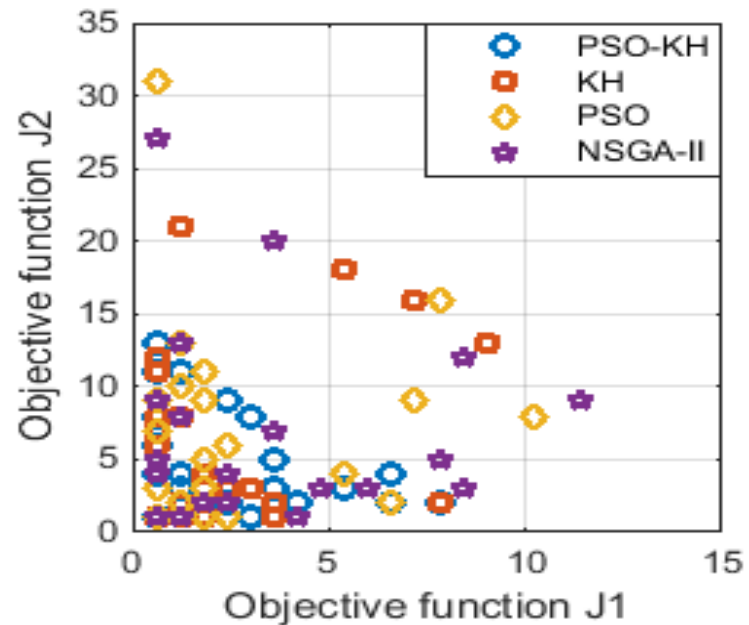


Figure 6.6(a) Optimal Pareto fronts between the objectives J_1 and J_2 for 3% error IED measurements and 50% in pseudo-measurements

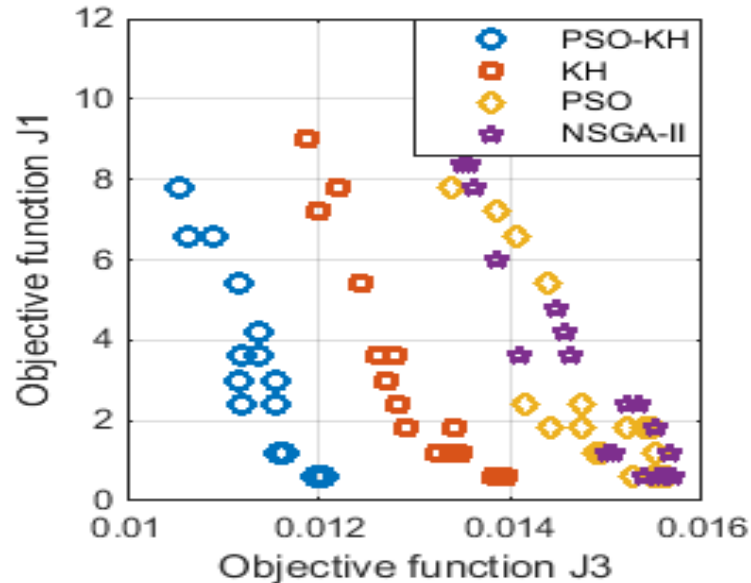


Figure 6.6(b) Optimal Pareto fronts between the objectives J_1 and J_3 for 3% error IED measurements and 50% in pseudo-measurements

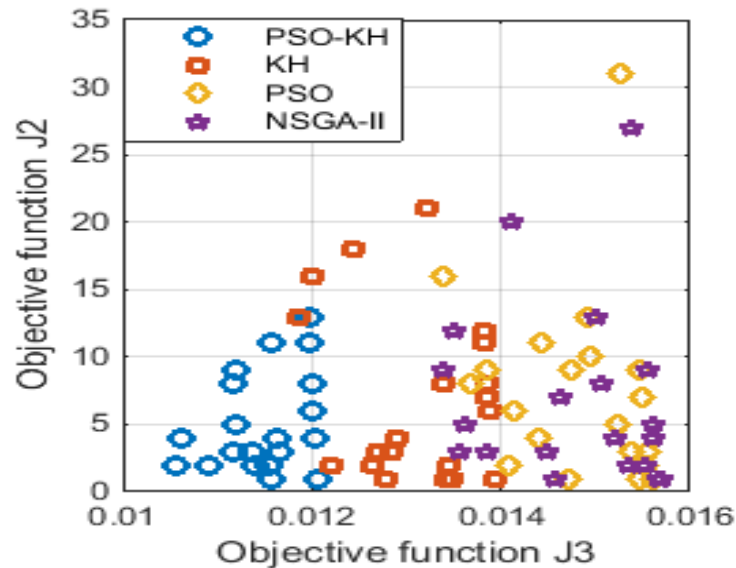


Figure 6.6(c) Optimal Pareto fronts between the objectives J_2 and J_3 for 3% error IED measurements and 50% in pseudo-measurements

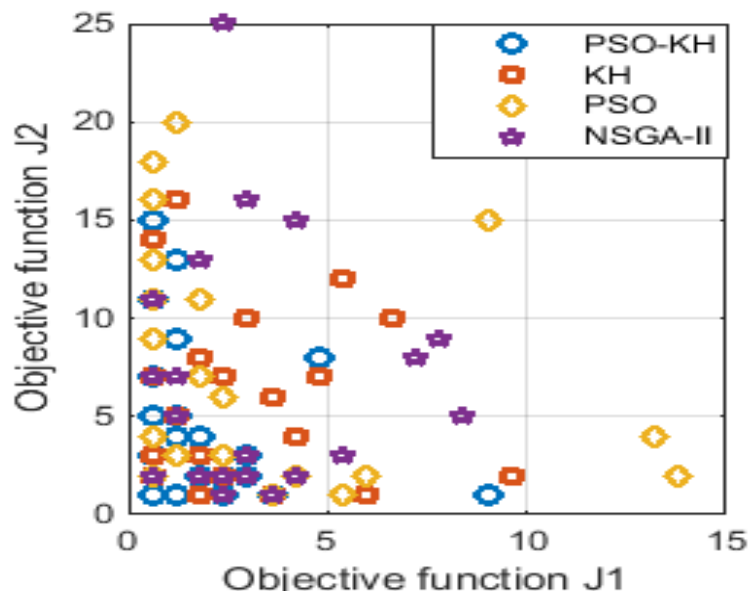


Figure 6.7(a) Optimal Pareto fronts between the objectives J_1 and J_2 for 5% error IED measurements and 50% in pseudo-measurements

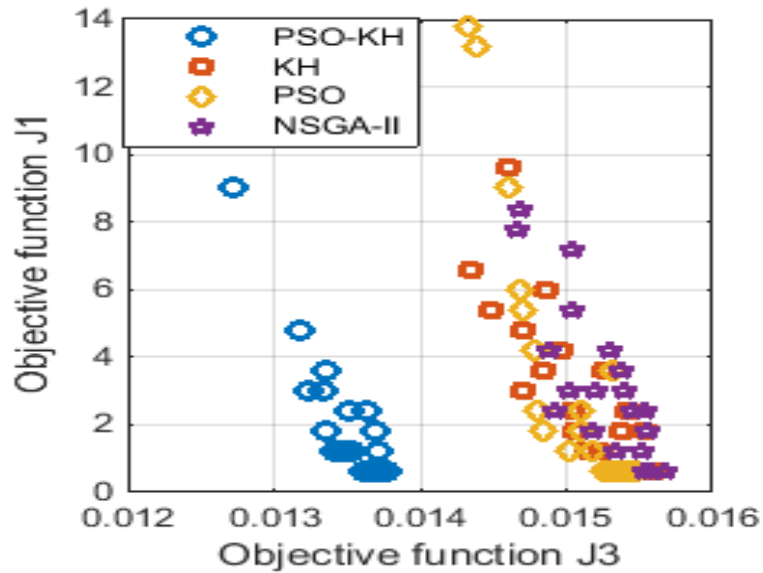


Figure 6.7(b) Optimal Pareto fronts between the objectives J_1 and J_3 for 5% error IED measurements and 50% in pseudo-measurements

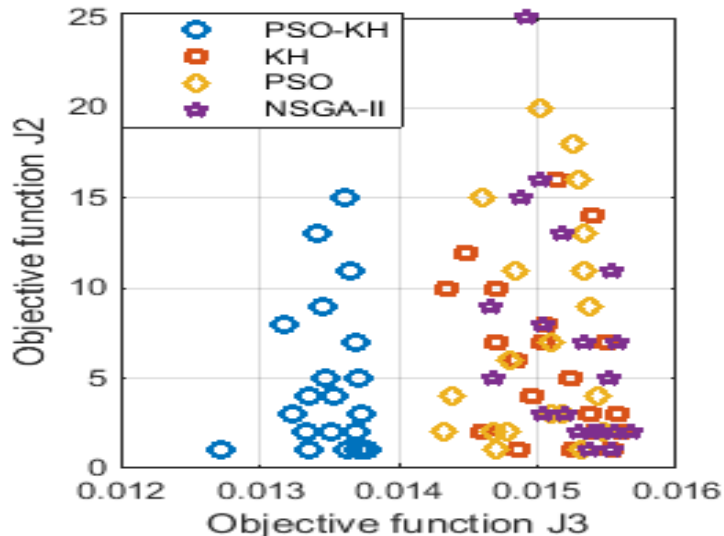


Figure 6.7(c) Optimal Pareto fronts between the objectives J_2 and J_3 for 5% error IED measurements and 50% in pseudo-measurements

The simulation results for Indian 85 bus system using the hybrid PSO-KH algorithm under different operating conditions have been shown in Table 6.5. When the IEDs accuracy is considered as 1%, the total configuration cost is 4.4pu using hybrid PSO-KH. The RMS value of state estimation error is 0.0105pu. In case of KH, PSO and NSGA-II, the total cost is 4.8pu, 8.2pu and 4.4pu and the average RMS value of estimation errors obtained are 0.0123pu,

0.0105pu and 0.0142pu respectively. Furthermore, the optimal Pareto fronts between the objectives J_1 , J_2 and J_3 have been shown in Figure 6.5. From the figures, it is seen that the global optimal Pareto fronts has been achieved using the proposed algorithm due its higher degree of balance between the exploration and exploitation during the search process.

Moreover, to test the efficiency of the proposed algorithm, different metrological error of the IEDs have been considered such as 3% and 5% along with 50% error in pseudo-measurements and the obtained results have been reported in Table 6.5 and Figure 6.6 to 6.7 shows the optimal Pareto fronts between the objectives. It is observed that the total configuration cost is increased because of more noise has been added in IED measurements. It is worth noticing that the performance of the proposed hybrid PSO-KH algorithm is found to be more superior than all other algorithms used in this work due to its higher degree of balance between the intensification and diversification capability. In 3% error case, the total number of PMU and IED required is 3 and 6 respectively. The RMS value of state estimation error obtained is 0.0113pu using hybrid PSO-KH. Though, the total meter cost using KH is slightly less than hybrid PSO-KH, but the RMS value of state estimation error is 0.0126pu which is more than hybrid PSO-KH. This is due to the fact that the locations of meters also have an impact on state estimation accuracy. Similarly, in case of 5% error also the total cost of meter using hybrid PSO-KH algorithm is less than other algorithms considered as well as the state estimation error is less compared to other algorithms used. The main advantage of this meter placement model is trade-offs between the PMU and IED can be determined to reduce the total configuration cost of the distribution network.

Table 6.5 Optimal location of PMUs and IEDs in Indian 85-bus active distribution system

Metrological Error of IEDs	Algorithm	PMUs location (Bus number)	IEDs location (Line number)	Objective functions value			Maximum relative percentage error in voltage magnitude (%)	Maximum relative percentage error in voltage angle (%)
				J_1	J_2	J_3		
1%	Proposed PSO_KH	34,84	1,3,5,33	2.4	2	0.0105	0.2731	5.7831
	KH	22,77,81	1,3,36	1.8	3	0.0123	0.4743	9.1354
	PSO	33,61,79,82	1,2,6,9,19,27,39	4.2	4	0.0104	0.3877	9.3199
	NSGA-II	42,54	1,4,11,24	2.4	2	0.0142	0.2981	9.4891
3%	Proposed PSO_KH	69,70,76	1,6,8,21,32,68	3.6	3	0.0113	0.3213	6.9834
	KH	33,68	1,4,6,9,25,30	3.6	2	0.0126	0.3987	9.6646
	PSO	9,42,54,71,76,82	1,2,6,8	2.4	6	0.0141	0.4011	11.0341
	NSGA-II	66,72,79	1,2,4,18,24,28,30,37, 41,44	6	3	0.0138	0.3887	8.3455
5%	Proposed PSO_KH	31,50,56	1,2,6,10,26	3	3	0.0132	0.3665	8.0103
	KH	1,6,8,18,21,32,68, 69,70,75	76	6	1	0.0148	0.5121	9.0245
	PSO	81	1,5,17,29,31,49,68,78	5.4	1	0.0147	0.5769	11.3421
	NSGA-II	8,26,29,36,47,69,79	1,3	1.2	7	0.0153	0.6613	10.8759

6.6 Comparison Results analysis

In this section, a comparison study has been carried out between all the algorithms used in this thesis such as proposed hybrid PSO-KH and hybrid EDA-IPM, PSO, KH, EDA and NSGA-II algorithms. The performance of all the algorithms is tested on IEEE 69-bus system and practical Indian 85-bus system. It is assumed that all DGs are generating real power to the network and two DGs are injected at bus 50 and 61 for IEEE 69-bus system and at bus 45 and 61 for Indian 85-bus system. Furthermore a trade-off solution is obtained between PMU and IED deployment in both the test cases. The optimal Pareto-fronts for three objectives J_1 , J_2 and J_3 is provided in Figure 6.8, 6.9 and 6.10 respectively. The obtained results are also shown in Table 6.6 and 6.7 respectively. It is seen that in most of the cases the proposed algorithms are more superior than the conventional algorithms considered in this thesis for comparison purpose. In some the cases it is also seen that proposed EDA-IPM algorithm is dominating PSO-KH algorithm in objectives J_1 and J_2 . Therefore, the proposed algorithms can be used for the planning study of the distribution networks.

6.6.1 Comparison results analysis of IEEE 69-bus system

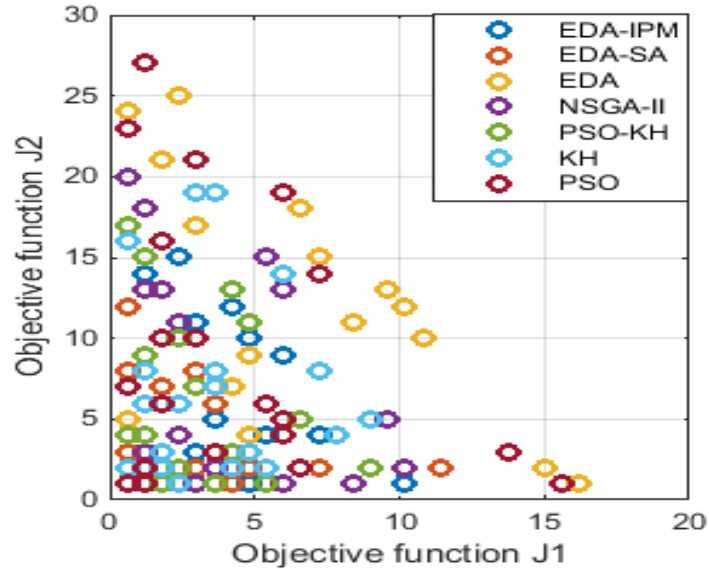


Figure 6.8(a): Optimal Pareto fronts between the objectives J_1 and J_2 for 1% error in IED and 50% in pseudo-measurements

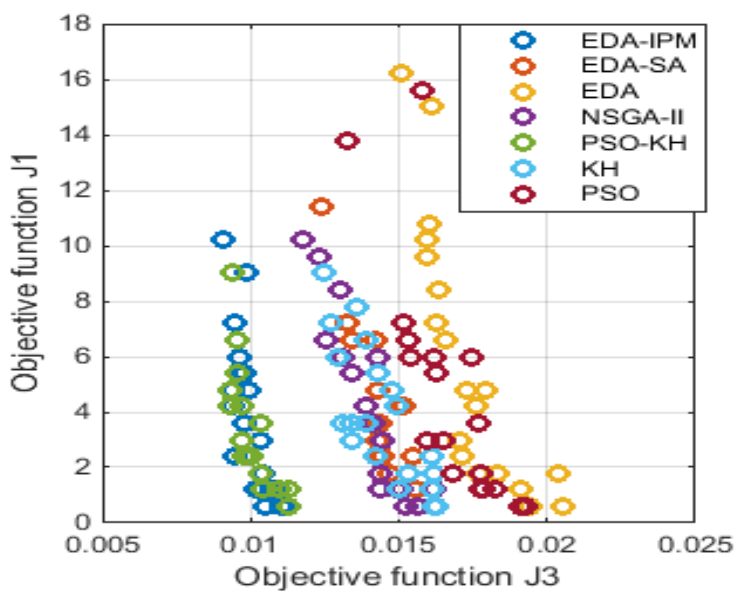


Figure 6.8(b): Optimal Pareto fronts between the objectives J_1 and J_3 for 1% error in IED and 50% in pseudo-measurements

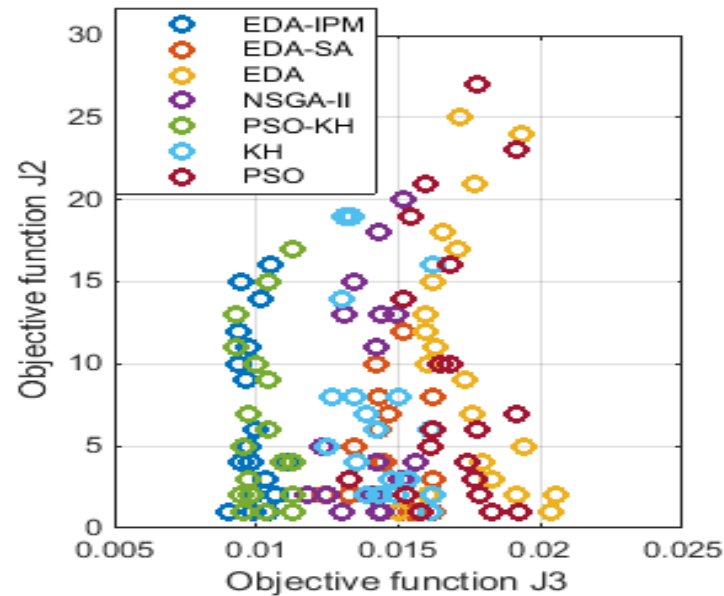


Figure 6.8(c): Optimal Pareto fronts between the objectives J_2 and J_3 for 1% error in IED and 50% in pseudo-measurements

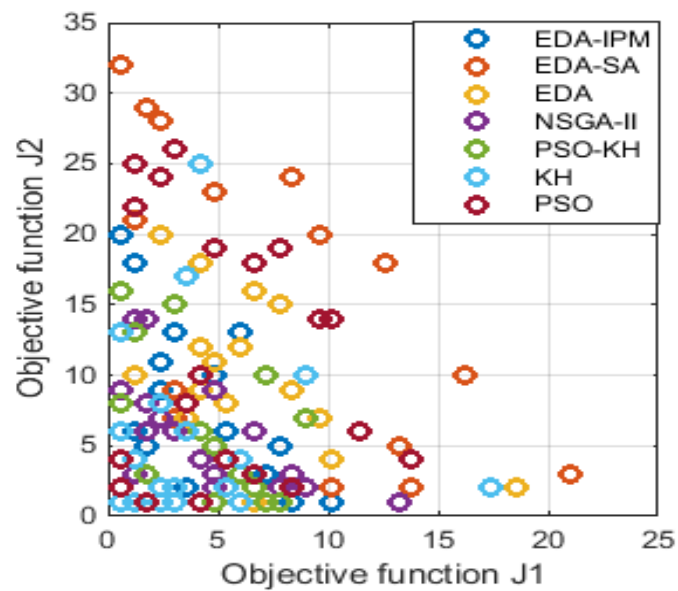


Figure 6.9(a): Optimal Pareto fronts between the objectives J_1 and J_2 for 3% error in IED and 50% in pseudo-measurements

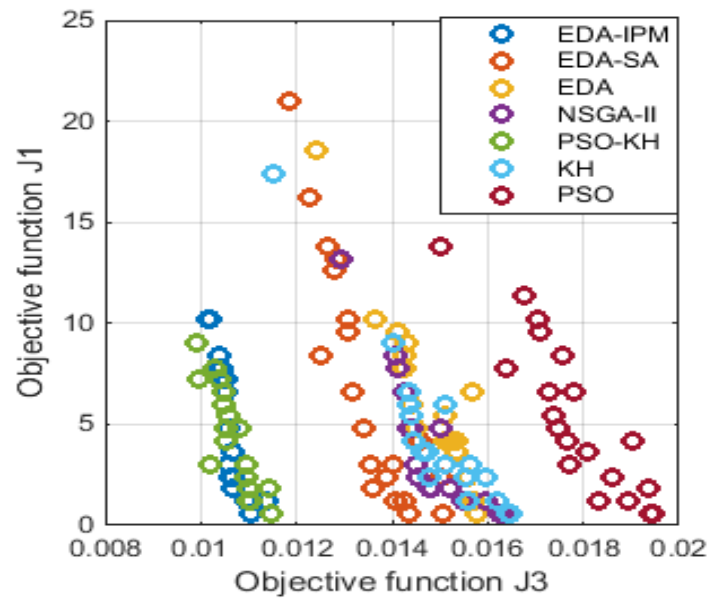


Figure 6.9(b): Optimal Pareto fronts between the objectives J_1 and J_3 for 3% error in IED and 50% in pseudo-measurements

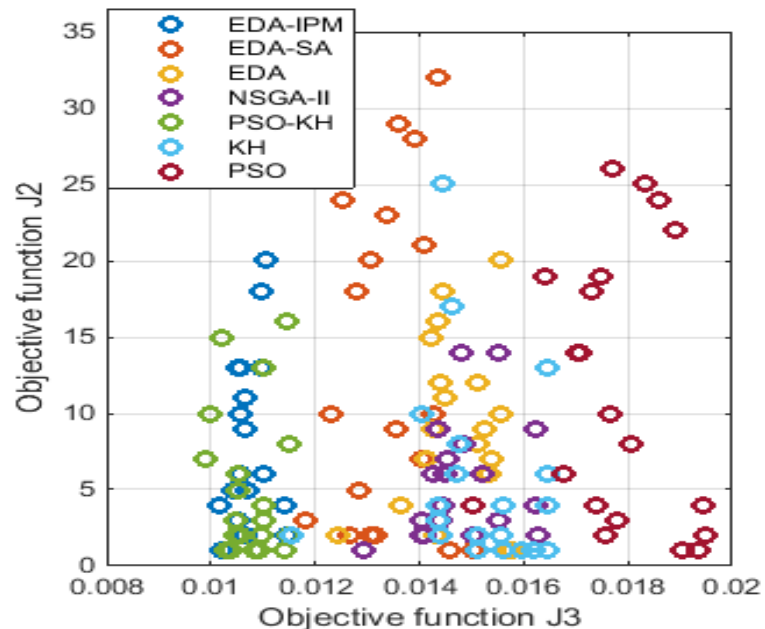


Figure 6.9(c): Optimal Pareto fronts between the objectives J_2 and J_3 for 3% error in IED and 50% in pseudo-measurements

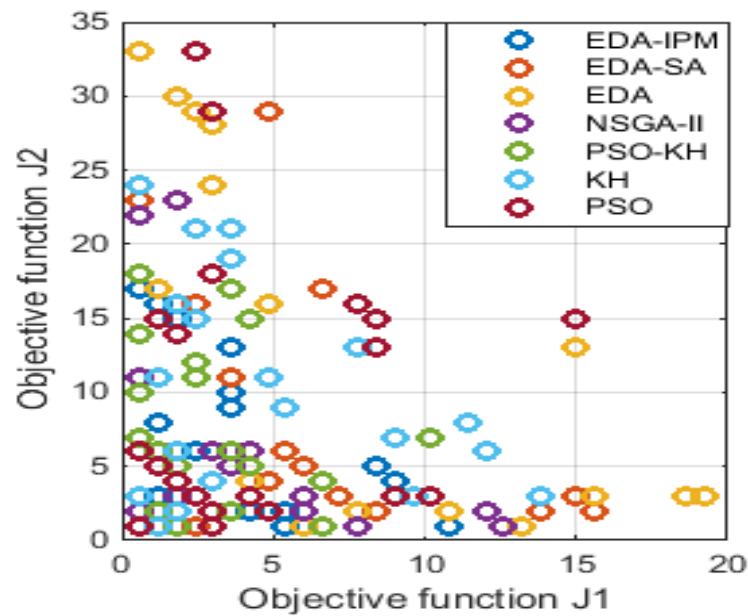


Figure 6.10(a): Optimal Pareto fronts between the objectives J_1 and J_2 for 5% error in IED and 50% in pseudo-measurements

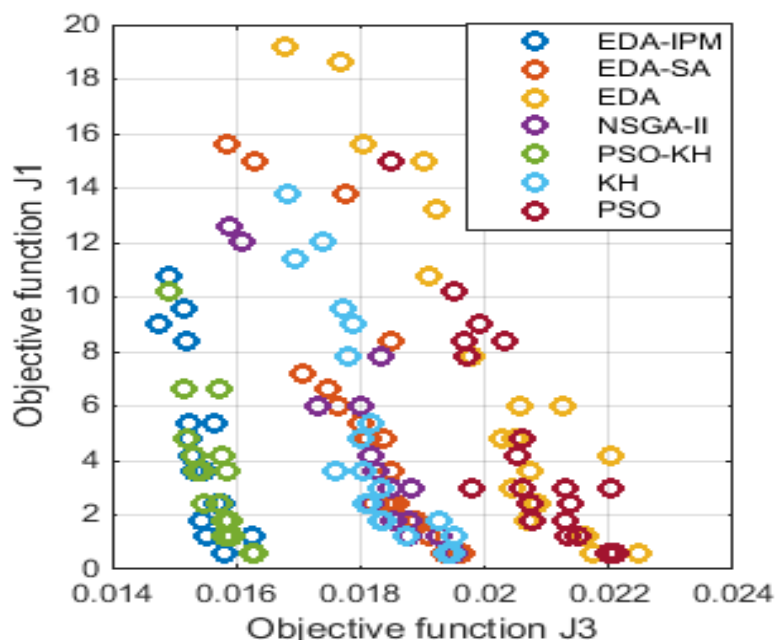


Figure 6.10(b): Optimal Pareto fronts between the objectives J_1 and J_3 for 5% error in IED and 50% in pseudo-measurements

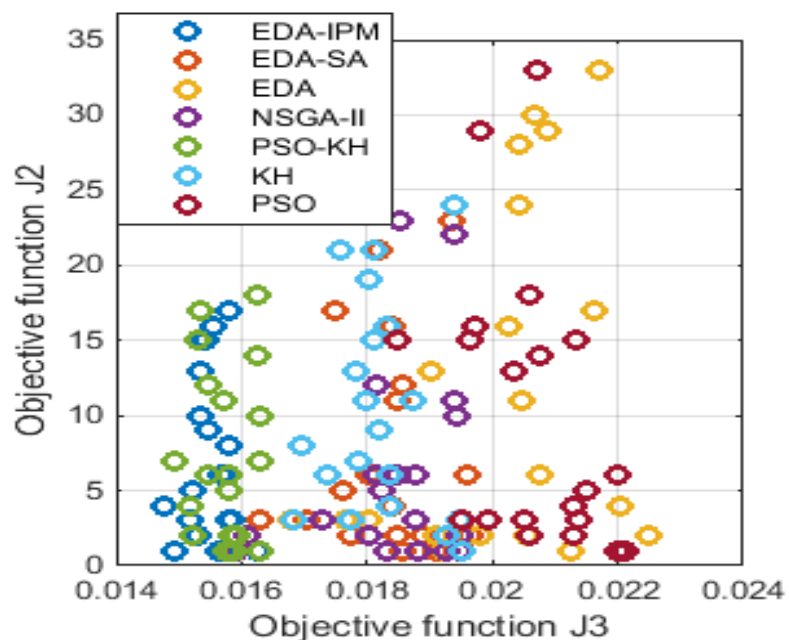


Figure 6.10(c): Optimal Pareto fronts between the objectives J_2 and J_3 for 5% error in IED and 50% in pseudo-measurements

Table 6.6 Optimal location of PMUs and IEDs in IEEE 69- bus active distribution system

Metrological errors	Algorithm	PMUs location (Bus number)	IEDs location (Line number)	Objective function(s) value			Maximum relative percentage error in voltage magnitude (%)	Maximum relative percentage error in voltage angle (%)
				J ₁	J ₂	J ₃		
1%	EDA-IPM	27	1,2,10	1.8	1	0.0103	0.2777	6.1936
	EDA-SA	27,67	1,4,8,10,18,20	3	2	0.0144	0.4962	8.3211
	EDA	45,48,59	1,3,54	1.8	3	0.0183	0.3211	10.8978
	NSGA-II	68	1,2,48,56,61	3	1	0.0144	0.3786	9.4631
	PSO-KH	41,43	1,2,4,29	2.4	2	0.0097	0.2947	5.9761
	KH	37,38,50,54,57,59	1,3,4,26	2.4	6	0.0142	0.3762	6.8746
	PSO	3,14,20,32,35,38,4 7,49,59,60,66	1,6	6.6	2	0.0152	0.4827	7.3241
3%	EDA-IPM	15,27,36,50,58	1,4,8	1.8	5	0.0106	0.3645	7.3719
	EDA-SA	50,64	1,3,4,13,16,19, 23,30,34,50,56	6.6	2	0.0132	0.4216	8.7546
	EDA	20,23,50,53,59,64	1,2,5,10,11,13, 54	4.2	6	0.0153	0.4056	11.9871
	NSGA-II	43,48,68	1,3,4,8,11,15,27, 62	4.8	3	0.0143	0.3927	9.7632
	PSO-KH	56	1,3,39,48,49	3	1	0.0109	0.3216	7.1243
	KH	58,62	1,3,18,32,56	3	2	0.0151	0.4312	7.4379
	PSO	49,56,59,64	1,3,5,8,11,15,17, 39,41	5.4	4	0.0173	0.4139	8.4612
5%	EDA-IPM	45,67	1,3,23,25,29,57,65	4.2	2	0.0152	0.3625	8.1910
	EDA-SA	43,65,67	1,3,6,7,16,20, 38,49,56,58,60, 63	7.2	3	0.0170	0.5089	9.0935
	EDA	52,64	1,3,4,6,13,14,17, 19,21,23,29,41, 56	7.8	2	0.0198	0.5897	11.0124
	NSGA-II	60,62,65	1,3,6,10,38,50, 52,54,56,57	6	3	0.0173	0.6083	10.5739
	PSO-KH	61,68	1,2,3,7,10,18,33, 54	4.8	2	0.0152	0.4437	7.9537
	KH	30,37,62,65	1,2,3,15,27,	3	4	0.0183	0.5139	8.4923
	PSO	27,29,35	1,3,5,7,9,11,25	4.2	3	0.0205	0.5823	8.0482

6.6.2 Comparison results analysis of Practical Indian 85-bus system

Table 6.7 Optimal location of PMU and IED in Indian 85-bus active distribution system

Metrological Error of IEDs	Algorithm	PMUs location (Bus number)	IEDs location (Line number)	Objective functions value			Maximum relative percentage error in voltage magnitude (%)	Maximum relative percentage error in voltage angle (%)
				J_1	J_2	J_3		
1%	Proposed EDA-IPM	50,54	1,7	1.2	2	0.0096	0.3179	7.5437
	EDA-SA	81	1,5,27	1.8	1	0.0143	0.3672	8.9821
	EDA	40,57,62	1,6,32	1.8	3	0.0129	0.3781	10.8239
	NSGA-II	72,76	1,4,5,26,34	3	2	0.0160	0.3364	8.4772
	PSO-KH	76	1,2,53,56	2.4	1	0.0094	0.3341	6.9823
	KH	11,53,66	1,3	1.2	3	0.0143	0.4127	8.1124
3%	Proposed EDA-IPM	36,67,71	1,4,5,25,67	1.8	3	0.0126	0.3649	6.9723
	EDA-SA	42,68,70	1,7,8,10,12,29,32, 34,36,46,60,65	7.2	3	0.0155	0.3438	8.2674
	EDA	77	1,3,6,7,15,30, 38,41,48,72	6	1	0.0188	0.4126	11.3037
	NSGA-II	49,76	1,4,5,16,28,42, 57,68	4.8	2	0.0178	0.3986	9.9721
	PSO-KH	53,56,73,77	1,2	1.2	4	0.0130	0.3708	7.0122
	KH	27,31,58,60	1,4,7,12	2.4	4	0.0158	0.4498	8.889
5%	Proposed EDA-IPM	42,74	1,3,5,8,31,60	3.6	2	0.0144	0.4023	8.0593
	EDA-SA	78,83	1,4,5,13,20, 22,26,66,75	5.4	2	0.0186	0.4821	7.7331
	EDA	67,73,78,83	1,2,3,7,12,15, 21,32,48,49	6	4	0.0197	0.4872	11.0241
	NSGA-II	76,81,84	1,3,4,5,6,9,11,12,23, 25,33,51,67,71,74	9	3	0.0152	0.5673	12.7671
	PSO-KH	23,25,71	1,4,5,9	2.4	3	0.0144	0.4629	7.8924
	KH	34,56,60,67,69,71	1,2,5,6,24	3	6	0.0160	0.5371	9.4534

6.7 Summary

This chapter formulated a new MOOP to find an optimal trade-offs in PMUs and IEDs deployment for state estimation in active distribution networks. A hybrid PSO-KH algorithm has been used to find the optimal number and location of PMUs and IEDs for accurate state estimation. Furthermore, different uncertainties level of measurement devices, load variations as well as presence of wind generators are taken into consideration for testing the robustness and reliability of the state estimator. The performance of the hybrid PSO-KH algorithm is tested on a standard IEEE 69-bus system as well as Indian 85-bus system. The obtained results using hybrid

PSO-KH algorithm are compared with the conventional KH algorithm, NSGA-II and also with PSO algorithm. It is found that the PSO-KH algorithm is more efficient, reliable and robust under various operating conditions and metrological characteristics of the measurement devices. Moreover, the performance of the proposed algorithm is found to be more superior than all other algorithms used in this work in most of the cases. Hence, the proposed multi-objective based meter placement technique can be used for the planning and monitoring of the smart distribution networks.

Chapter 7

Conclusions

Chapter 7

Conclusions

7.1 General

In this thesis, an optimal allocation of measurement devices such as power flow meters, Phasor measurement units (PMUs) and intelligent electronic devices (IEDs) for distribution system state estimation has been investigated using new multi-objective hybrid evolutionary algorithms. Furthermore, the optimal locations of the measurement devices are obtained both in passive as well as active distribution network under various operating scenarios. This chapter presents in brief the important findings proposed in this thesis while also discussing future extension of the proposed research work.

7.2 Summary of important findings

This chapter presents the overall conclusion of the research work presented in this thesis and future scope of the research work. The following conclusions have been arrived at from the research carried out and reported in previous chapters in this thesis.

(i) The overall objective of the research is to find the optimal number and location of the power flow meters to improve the estimation accuracy of the state estimator in distribution networks.

- First of all, a multi-objective optimization model is designed to find optimal number and location of power flow meters to improve the accuracy of the state estimator in passive as well as active distribution networks.
- A new hybrid PSO-KH optimization algorithm has been proposed to find the optimal number and location of the power flow meters in distribution networks.
- Various operating scenarios are considered in this optimization problem, such as variations in load power demand, generator output and metrological characteristics of the measurement devices.
- A trade-off solution between the relative errors in voltage and phase angle estimates is established with the total cost of meters in a multi-objective framework to achieve best compromise solution between the cost and state estimation errors.

- Furthermore, the impacts of DG on state estimation accuracy has also been discussed.
- The effectiveness of the proposed hybrid PSO-KH algorithm is tested on IEEE 69-bus system and Indian 85-bus distribution system. The competitive results obtained using the proposed algorithm is compared with the existing algorithm such as PSO, KH and NSGA-II under various operating scenarios of the distribution networks.
- It has been verified that the proposed algorithm is reliable and robust with respect to different metrological characteristics of the devices and load variations. Moreover, it can guarantee getting a near global optimal solution. Therefore, the proposed approach of meter placement technique can be used for planning the study of smart distribution networks.

(ii) A new hybrid EDA-IPM algorithm has been proposed to find optimal number and locations of power flow meters in presence of various kinds of DGs in distribution networks.

- The hybridization of traditional EDA with IPM is done to improve the local searching capability of the EDA.
- The best optimal trade-off solution between the objective functions such as cost and state estimation error is established. Moreover, the impact of different kinds of DGs on state estimation accuracy has also been presented under various operating scenarios such as variations in load power demand, generator output and metrological characteristics of the measurement devices.
- The proposed multi-objective hybrid EDA-IPM algorithm based meter placement technique is tested on IEEE 69-bus system and practical Indian 85-bus distribution network. The results obtained using the proposed hybrid EDA-IPM algorithm have been compared with some existing algorithm in literature such as PSO, EDA and NSGA-II under various operating conditions of the distribution systems.
- It is reported that the proposed algorithm is robust, reliable and much superior to existing algorithms considered in this research.

(iii) To further improve the estimation accuracy of the state estimator, advance measuring devices such as PMU and IED have been considered in this thesis.

- A new multi-objective optimization model has been developed to find an optimal trade-offs in PMUs and IEDs deployment for state estimation in active distribution networks.

- A new hybrid EDA-IPM algorithm is proposed to find the optimal number and location of PMUs and IEDs required for accurate state estimation. The local searching capability of the classical EDA algorithm is improved by hybridizing the Interior point method (IPM). The hybridization of EDA and IPM brings a balance between exploration and exploitation capability of the algorithm during the search process.
- Various operating scenarios are considered, such as variations in load power demand, generator output and metrological characteristics of the measurement devices.
- The performance of the proposed hybrid EDA-IPM algorithm has been tested on IEEE 69-bus system as well as on Indian 85-bus system. The results obtained using hybrid EDA-IPM algorithm are compared with the conventional EDA, NSGA-II and also with EDA-simulated annealing algorithm available in the literature.

(iv) The robustness of the proposed meter placement technique in presence of wind generators in distribution networks has also been investigated in this thesis.

- The optimal trade-offs in PMUs and IEDs deployment for accurate state estimation in distribution networks is proposed.
- A hybrid PSO-KH algorithm has been used to find the optimal number and location of PMUs and IEDs for accurate state estimation.
- Furthermore, different levels of uncertainty of measurement devices, load variations as well as presence of wind generators have been taken into consideration for testing the robustness and reliability of the state estimator. The output of wind generators is modeled using Weibull probability distribution function.
- The performance of the hybrid PSO-KH algorithm is tested on IEEE 69-bus system as well as on Indian 85-bus system. The results obtained using the proposed hybrid PSO-KH algorithm are compared with the conventional KH algorithm, NSGA-II and also with PSO. It is found that the PSO-KH algorithm is more efficient, reliable and robust under various operating conditions and metrological characteristics of the measurement devices.

7.3 Scope for future work

In this thesis, the optimal allocation of measurement devices such as power flow meters, PMU and IED for distribution system state estimation has been investigated using multi-objective hybrid evolutionary algorithms. My research in future can be extended on the following aspects:

- Accurate, adaptive and efficient feeder modeling and DSSE methodologies for wide area monitoring and coping with the active nature of the distribution network can be investigated in future.
- Data synergy and fusion techniques for exploiting a large amount of heterogeneous data in DMS environment can be incorporated in DSSE study.
- Communication infrastructures, big data and edge computing techniques to tackle the problem of efficiently collecting and coordinating the measurement results in state estimation can be contemplated for future research.
- A global and multi-level state estimation concept can be utilized for better interaction between distribution and transmission system operators.

References

- [1] F. C. Schweppe and J. Wildes, "Power system static -state estimation, part I: Exact model," *IEEE Trans. on Power Apparatus and Systems*, vol. PAS-89, no. 1, pp. 120-125, Jan. 1970.
- [2] F. C. Schweppe and D. B. Rom, "Power system static-state estimation, part-II: Approximate model," *IEEE Trans. on Power Apparatus and Systems*, vol. PAS-89, no. 1, pp. 125-130, Jan. 1970.
- [3] F. C. Schweppe, "Power system static -state estimation, part-III: Implementation", *IEEE Trans. on Power Apparatus and Systems*, vol. PAS-89, no. 1, pp. 130-135, Jan. 1970.
- [4] A. Abur and A. Gomez-Exposito, *Power System State Estimation. Theory and Implementation*. Mar el Dekker, New York, 2004.
- [5] A. Montielli, "Electric power system state estimation," *Proceedings of the IEEE*, vol. 88, no. 2, pp. 262-282, Feb. 2000.
- [6] G. T. Heydt, "The next generation of power distribution systems", *IEEE Trans. on Smart Grid*, vol. 1, no. 3, pp. 225-235, Dec. 2010.
- [7] L. Pieltain Fernandez, T. G. S. Roman, R. Cossent, C. M. Domingo, and P. Frias, "Assessment of the impact of plug-in electric vehicles on distribution networks, *IEEE Trans. on Power Systems*, vol. 26, no. 1, pp. 206-213, Feb. 2011.
- [8] D. A. Haughton and G. T. Heydt, 'A linear state estimation formulation for smart distribution systems,' *IEEE Trans. on Power Systems*, vol. 28, no. 2, pp. 1187-1195, 2013.
- [9] A.T. Saric, R.M. Ceric, 'Integrated fuzzy state estimation and load flow analysis in distribution networks', *IEEE Trans. on Power Systems*, 2003, **18**, (2), pp. 571-578.
- [10] M. Pau, P.A. Pegoraro, S. Sulis, 'Efficient branch-current –based distribution system state estimation including synchronized measurement', *IEEE Trans. on Instrumentation and Measurement*, 2013, vol. 62, no. 9, pp. 2419-2429.
- [11] M. Baran, J. Zhu, A. Kelly, 'Meter placement for real time monitoring of distribution feeders', *IEEE Trans. on Power Systems*, 1996, vol. 11, no. 1, pp. 332-337.
- [12] J. De, L. Ree, V. Centeno, J. S. Thorp, and A. G. Phadke, "Synchronized phasor measurement applications in power systems," *IEEE Trans. on Smart Grid*, vol. 1, no. 1, pp. 20–27, June 2010.

- [13] J. Thorp, A. Abur, M. Begovic, J. Giri, and R. Avila-Rosales, "Gaining a wider perspective," *IEEE Power and Energy Magazine*, vol. 6, no. 5, pp. 43–51, Sept. 2008.
- [14] A. G. Phadke and J. S. Thorp, *Synchronized Phasor Measurements and Their Applications*. : Springer Science, 2008.
- [15] M. Pau, A. Pegoraro and S. Sulis, " Efficient branch current based distribution system state estimation including synchronized measurements," *IEEE Transactions on Instrumentation and Measurement*, vol. 62, no. 9, pp. 2419-2429, June 2009.
- [16] M. Albu, G. T. Heydt, and S. C. Cosmescu, "Versatile platforms for wide area synchronous measurements in power distribution systems," in *North American Power Symposium (NAPS)*, Sept. 2010.
- [17] M. Paolone, A. Borghetti, and C. A. Nucci, "Development of an RTU for synchrophasors estimation in active distribution networks," *IEEE Bucharest in Power Tech*, 2009, July 2, 2009, pp. 1–6.
- [18] D. Della Giustina, M. Pau, P. A. Pegoraro, F. Ponci, and S. Sulis, "Electrical distribution system state estimation: measurement issues and challenges", *IEEE Instrumentation Measurement Magazine*, vol. 17, no. 6, pp. 36-42, Dec. 2014.
- [19] W. H. Kersting, *Distribution System Modeling and Analysis*. Bo a Raton, Florida, 2001.
- [20] W. H. Kersting and R. K. Green, "The application of Carson's equation to the steady-state analysis of distribution feeders, *IEEE International Conference on Power Systems Conference and Exposition (PSCE)*, 2011 IEEE/PES, Mar. 2011, pp. 1-6.
- [21] E. Manitsas, R. Sing, B.C.Pal, and G. Strbas, "Distribution system state estimation using an artificial neural network approach for pseudo measurement modeling," *IEEE Trans. On Power Systems*, vol. 27, no. 4, pp. 1888-1896, November 2012.
- [22] R. Singh, B. C. Pal, and R. A. Jabr, "Distribution system state estimation through Gaussian mixture model of the load as pseudo-measurement", *IET Generation, Transmission Distribution*, vol. 4, no. 1, pp. 50-59, Jan. 2010.
- [23] T. Schlosser, A. Angioni, F. Ponci, and A. Monti, "Impact of pseudo-measurements from new load profiles on state estimation in distribution grids, *IEEE International in Instrumentation and Measurement Technology Conference (I2MTC) Proceedings*, 2014, May 2014, pp. 625-630.

- [24] M. R. Irving, R. C. Owen, and M. J. H. Sterling, "Power-system state estimation using linear programming", *Electrical Engineers, Proceedings of the Institution of*, vol. 125, no. 9, pp. 879-885, Sep. 1978.
- [25] A. Garcia, A. Monti elli, and P. Abreu, "Fast decoupled state estimation and bad data processing", *IEEE Trans. on Power Apparatus and Systems*, vol. PAS-98, no. 5, pp. 1645-1652, Sep. 1979.
- [26] M. K. Celik and A. Abur, "A robust WLAV state estimator using transformations", *IEEE Trans on Power Systems*, vol. 7, no. 1, pp. 106-113, Feb. 1992.
- [27] A. Abur and M. K. Celik, "Least absolute value state estimation with equality and inequality constraints", *IEEE Trans. on Power Systems*, vol. 8, no. 2, pp. 680-686, May 1993.
- [28] H. Singh and F. L. Alvarado, "Weighted least absolute value state estimation using interior point methods", *IEEE Trans. on Power Systems*, vol. 9, no. 3, pp. 1478-1484, Aug. 1994.
- [29] R. Baldi k, K. A. Clements, Z. Pinjo-Dzgal, and P. W. Davis, "Implementing non-quadratic objective functions for state estimation and bad data rejection", *IEEE Trans. on Power System*, vol. 12, no. 1, pp. 376-382, Feb. 1997.
- [30] J. Roytelman and S. Shahidehpour, 'State estimation for electric power distribution systems in quasi real-time conditions', *IEEE Trans. on Power Deliv.*, vol. 8, no. 4, pp. 2009-2015, 1993.
- [31] M. E. Baran and A. W. Kelly, " State estimation for real time monitoring of distribution systems," *IEEE Trans. on Power systems*, vol. 9, no. 3, pp. 1601-1609, Aug. 1994.
- [32] M. E. Baran and A. W. Kelly, " A branch-current based state estimation method for distribution systems," *IEEE Trans. on Power Systems*, vol. 10, no. 1, pp. 483-491, Feb. 1995.
- [33] C. N. Lu, J. H. Teng and W.H.E. Liu, " Distribution system state estimation," *IEEE Trans. on Power Syst.*, vol. 10, no. 1, pp. 229-240, Feb. 1995.
- [34] K. Li, " State estimation for power distribution system and measurement impacts," *IEEE Trans. on Power Systems*, vol. 11, no. 2, pp. 911-916, May 1996.
- [35] W. M. Lin, and J. H. Teng, "State estimation for distribution systems with zero-injection constraints," *IEEE Trans. on Power Systems*, vol. 11, no. 1, pp. 518-524, Feb. 1996.

- [36] A. K. Ghosh, D. L. Lubkeman, M.J. Downey, and R.H. Jones, “ Distribution circuit state estimation using a probabilistic approach,” *IEEE Trans. on Power systems*, vol. 12, no. 1,pp. 45-51, Feb.1997.
- [37] D. Thukaram, J. Jerome, and C. Surapong, “A robust three-phase state estimation algorithm for distribution networks,” *Electric Power systems Research*, vol. 55, no. 3, pp. 191-200, Sept. 2000.
- [38] W.M. Lin, J.H. Teng, and S.J. Chen, “ A highly efficient algorithm in treating current measurements for branch-current-based distribution state estimation,” *IEEE Trans. on Power Delivery*, vol. 16, no. 3, pp. 433-439, July 2001.
- [39] Y. Deng, Y. He, and B. Zhang, “A branch estimation based state estimation method for radial distribution systems,” *IEEE Trans. on Power Delivery*, vol. 17, no. 4, pp. 1057-1062, Oct. 2002.
- [40] H. Wang, and N. Schulz, “ A revised branch current based distribution system state estimation algorithm and meter placement impact,” *IEEE Trans. Power Syst.*, vol. 19,no. 1,pp. 207-213, Feb. 2004.
- [41] M. Pau, P.A. Pegoraro, and S. Sulis, “ Efficient branch-current-based distribution system state estimation including synchronized measurements,” *IEEE Trans. on Instrumentation and Measurements*, vol. 62, no. 9, pp. 2419-2429, Sept. 2013.
- [42] M. F. Medeiros Junior, M.A.D. Almeida, M.C.S. Cruz, R.V.F. Monteiro, and A.B. Oliveira, “ A three-phase algorithm for state estimation in power distribution feeders based on the powers summation load flow method,” *Electric Power systems Research*, vol.123, pp.76-84, Jun. 2015.
- [43] A. K. Ghosh, D. L. Lubkeman and R. H. Jones, “Load modeling for distribution circuit state estimation,” *IEEE Trans. on Power systems*, vol. 12, no. 2, pp. 999-1005, Apr. 1997.
- [44] V. Miranda, J. Pereira and J.T. Saraiva, “Load allocation in DMS with a fuzzy state estimator,” *IEEE Trans. on Power systems*, vol. 15, no. 2, pp.529-534, May 2000.
- [45] H. Wang and N. N. Schulz, “A load modeling algorithm for distribution system state estimation,” in *Proc. 2001 IEEE/Power Eng. Society Transmission and Distribution Conference and Exposition*, pp. 102-106.

- [46] E. Puthooran, and Biswarup Das, “Load estimation in balanced radial distribution system with reduced measurements,” *Electric Power Components and Systems*, vol. 37, no. 5, pp 547-559, April 2009.
- [47] J. Wan and K.N. Miu, “ A WLS method for load estimation in unbalanced distribution networks,” in *Proc. 2002 IEEE Power Eng. Soc. Winter Meeting*, New York, Jan. 2002.
- [48] Jie Wan and K. N. Miu, “ Weighted least square methods for load estimation in distribution networks,” *IEEE Trans. on Power Systems*, vol. 18, no. 4, pp. 1338-1345, Nov. 2003.
- [49] M. E. Baran, L.A.A. Freeman, F. Hanson and V. Ayers, “ Load estimation for load monitoring at distribution substations,” *IEEE Trans. on Power Systems*, vol. 20, no. 1, pp. 164-170, 2005.
- [50] S. Naka, T. Genji, T. Yura, and Y. Fukuyama, “ A hybrid particle swarm optimization for distribution state estimation,” *IEEE Trans. on Power Systems*, vol. 18, no. 1, pp. 60-68, Feb. 2003.
- [51] S. Nanchian, A. Mazumdar and B.C. Pal, “Three-phase state estimation using hybrid particle swarm optimization,” *IEEE Trans. on Smart Grid*, vol. 8, no. 3, May 2017.
- [52] S. Nanchian, A. Mazumdar and B.C. Pal, “Ordinal optimization technique for three-phase distribution network state estimation including discrete variables,” *IEEE Trans. on Sustainable Energy*, vol. 8, no. 4, pp. 1528-1535, May 2017.
- [53] M. Baran, J. Zhu and A. Kelly, “ Meter placement for real time monitoring of distribution feeders,” *IEEE Trans. on Power Systems*, vol. 11, no. 1, pp. 332-337, Feb. 1996.
- [54] C. Muscas, F. Pilo, G. Pisano and S. Sulis, “ Optimal allocation of multichannel measurement devices for distribution state estimation,” *IEEE Trans. on Instrumentation and Measurement*, vol. 58, no. 6, pp. 1929-1937, June 2009.
- [55] J. Liu, J. Tang, F. Ponci, A. Monti, C. Muscas and P.A. Pegoraro, “ Trade-offs in PMU deployment for state estimation in active distribution grids, “ *IEEE Trans. on Smart Grid*, vol. 3, no. 2, pp. 915-924, June 2012.
- [56] P.A. Pegoraro and S. Sulis, “Robustness-oriented meter placement for distribution system state estimation in presence of network parameter uncertainty,” *IEEE Trans. on Instrumentation and Measurement*, vol. 62, no. 5, pp. 954-962, May 2013.

- [57] R. Sing, B. C. Pal, R. A. Jabr and R. B. Vinter, " Meter placement for distribution system state estimation: An ordinal optimization approach," *IEEE Trans. on Power Systems*, vol. 26, no. 4, pp. 2328-2335, Nov. 2011.
- [58] A. Shafiu, N. Jenkins and G. Strbac, "Measurement location for state estimation of distribution networks with generation," *IEE Proc. Gener. Transm. Distrib.*, vol. 152, no. 2, pp. 240-246, March 2005.
- [59] R. Sing, B. C. Pal and R. B. Vinter, "Measurement placement in distribution system state estimation," *IEEE Trans. on Power Systems*, vol. 24, no. 2, pp. 668-675, May 2009.
- [60] X. Chen, J. Lin, C. Wan and Y. Song, " Optimal Meter Placement for Distribution Network State Estimation: A Circuit Representation Based MILP Approach" *IEEE Trans. on Power Systems*, vol. 31,no. 6, pp. 4357-4370, 2016.
- [61] P. A. Pegoraro, J. Tang, J. Liu, F. Ponci, A. Monti, and C. Muscas, "PMU and smart metering deployment for state estimation in active distribution grids, in Energy Conference and Exhibition (ENERGYCON), 2012 IEEE International, Sep. 2012, pp. 873-878.
- [62] M.G. Damavandi, V. Krishnamurthy and J.R. Marti, "Robust meter placement for state estimation in active distribution systems", *IEEE Trans on Smart Grids*, vol. 6, no. 4, pp. 1972-1982, 2015.
- [63] P. Janssen, T. Sezi, and J. C. Maun, "Meter placement impact on distribution system state estimation," in Electricity Distribution (CIRED 2013), 22nd International Conference and Exhibition on, Jun. 2013, pp. 1-4.
- [64] C. Muscas, S. Sulis, A. Angioni, F. Ponci, and A. Monti, "Impact of different uncertainty sources on a three-phase state estimator for distribution networks," *IEEE Transactions on Instrumentation and Measurement*, vol. 63, no. 9, pp. 2200-2209, Sep. 2014.
- [65] M. Pau, P. A. Pegoraro, S. Sulis, and C. Muscas, "Uncertainty sources affecting voltage profile in distribution system state estimation, in Instrumentation and Measurement Technology Conference (I2MTC), 2015 IEEE International, pp. 1-6.
- [66] A. K. Ghosh, D. L. Lubkeman, M. J. Downey, and R. H. Jones, Distribution circuit state estimation using a probabilistic approach, "Power Systems, IEEE Trans. on, vol. 12, no. 1, pp. 45-51, Feb. 1997.

- [67] J. M. Morales, L. Baringo, A. J. Conejo, and R. Minguez, "Probabilistic power flow with correlated wind sources," *Generation, Transmission Distribution, IET*, vol. 4, no. 5, pp. 641-651, May 2010.
- [68] G. Valverde, A. T. Sari , and V. Terzija, Stochastic monitoring of distribution networks including correlated input variables," *Power Systems, IEEE Trans. on*, vol. 28, no. 1, pp. 246-255, Feb. 2013.
- [69] E. Caro, A. J. Conejo, and R. Minguez, "Power system state estimation considering measurement dependencies," *IEEE Trans. on Power Systems*, vol. 24, no. 4, pp. 18751885, Nov. 2009.
- [70] E. Caro and G. Valverde, Impact of transformer correlations in state estimation using the unscented transformation," *IEEE Trans. on Power Systems*, vol. 29, no. 1, pp. 368-376, Jan. 2014.
- [71] Y. Chakhchoukh, V. Vittal, and G. T. Heydt, PMU based state estimation by integrating correlation," *IEEE Trans. on Power Systems*, vol. 29, no. 2, pp. 617-626, Mar. 2014.
- [72] C. Muscas, M. Pau, P. A. Pegoraro, and S. Sulis, Effects of measurements and pseudo-measurements correlation in distribution system state estimation, " *IEEE Trans. on Instrumentation and Measurement*, vol. 63, no. 12, pp. 2813-2823, Dec. 2014.
- [73] Evaluation of data - Guide to the expression of uncertainty in measurement, JCGM 100:2008, Sep. 2008.
- [74] M. E. Baran, "Challenges in state estimation on distribution systems," *IEEE Conference on Power Engineering Society Summer Meeting*, vol. 1, pp. 429-433, 2001.
- [75] R. Singh, B. C. Pal, and R. A. Jabr, "Choice of estimator for distribution system state estimation," *IET Generation, Transmission & Distribution*, vol. 3, no. 7, pp. 666–678, 2009.
- [76] R. Madlener, J. Liu, A. Monti, C. Muscas, and C. Rosen, Measurement and Metering Facilities as Enabling Technologies for Smart Electricity Grids in Europe Oct. 2009, Special Study No. 1/2009, Sectoral e-Business Watch.
- [77] J. De, L. Ree, V. Centeno, J. S. Thorp, and A. G. Phadke, "Synchronized phasor measurement applications in power systems," *IEEE Trans. on Smart Grid*, vol. 1, no. 1, pp. 20–27, 2010.

[78] F.G. Duque, L.W. de Oliveira, E.J. de Oliveira and A. A. Augusto, “ State estimation for electrical distribution systems based on an optimization model,” *Electric Power System Research, Elsevier*, vol. 152, pp. 122-129, 2017.

[79] A. G. Phadke and J. S. Thorp, *Synchronized Phasor Measurements and Their Applications*. : Springer Science, 2008.

[80] M. Pau, A. Pegoraro and S. Sulis, “Efficient branch current based distribution system state estimation including synchronized measurements,” *IEEE Trans. on Instrumentation and Measurement*, vol. 62, no. 9, pp. 2419-2429, 2013.

[81] G. T. Heydt, “The next generation of power distribution systems,” *IEEE Trans. on Smart Grid*, vol. 1, no. 3, pp. 225-235, 2010.

[82] M. Rashidi and E. Farjah, “Lyapunov exponent-based optimal PMU placement approach with application to transient stability assessment,” *IET Science, Measurement and Technology*, vol. 10, no. 5, pp. 492-497, 2016.

[83] M. Paolone, A. Borghetti, and C. A. Nucci, “Development of an RTU for synchrophasors estimation in active distribution networks,” in *PowerTech, 2009 IEEE Bucharest*, July 2, 2009, pp. 1–6.

[84] A. H. Gandomi and A. H. Alavi, “Krill herd: A new bio-inspired optimization algorithm,” *Commun Nonlinear Sci Numer Simulat, Elsevier*, vol. 17, pp. 4831-4845, 2012.

[85] P. Angelov, K.T. Atanassow, L. Doukovska, M. Hadjiski, V. Jotsov, J. Kacprzyk, E. Szmidz and S. Zadrozny, “ Advances in intelligent systems and computing,” *Springer International Publishing Switzerland*, 2015.

[86] S. Naka, T. Genji, T. Yura and Y. Fukuyama, “A Hybrid particle swarm optimization for distribution state estimation,” *IEEE Trans. on Power Systems*, vol. 18, no. 1, pp.60-68, 2003.

[87] J. Kennedy and R. Eberhart, “Particle swarm optimization,” in *Proc. IEEE Int. Conf. Neural Networks*, vol. 4, Perth, Australia, pp. 1942-1948, 1995.

[88] K. Deb, “Multi-objective optimization using evolutionary algorithms,” *Wiley India Pvt. Ltd*, New Delhi, India, 2001.

[89] K. Deb, A. Pratap, S. Agarwal and T. Meyarivan, “A fast and elitist multi-objective genetic algorithm: NSGA-II,” *IEEE Trans. on Evolutionary Computation*, vol. 6, no. 2, pp. 182-197, April 2002.

- [90] V.A. Shim, K.C. Tan and C.Y. Cheong, “A hybrid estimation of distribution algorithm with decomposition for solving the multi-objective multiple traveling salesman problems,” *IEEE Trans. on systems Man and Cybernetics-Part C: Applications and Reviews*, vol. 42, No. 5, pp. 682-691, Sept. 2012.
- [91] H. Karshenas, R. Santana and P. Larranaga, “Multi-objective estimation of distribution algorithm based on joint modeling of objectives and variables,” *IEEE Trans. on Evolutionary computation*, vol. 18, no.4, pp. 519-542, Aug. 2014.
- [92] W. Yan, F. Liu, C.Y. Chung, and K. P. Wong, “A hybrid genetic algorithm-Interior point method for optimal reactive power flow, *IEEE Trans. on Power Systems*, vol. 21, no. 3, pp. 1163-1169, Aug. 2006.
- [93] Y. Wang and Q. Jiang, “Reactive power optimization of distribution network based on primal dual interior point method and simplified branch and bound method,” *IEEE PES T&D conference and Exposition*, pp. 1-4, 2004.
- [94] W. M. Lin and J. H. Teng, “State estimation for distribution systems with zero-injection constraints,” *IEEE Trans. on Power Systems*, vol. 11, no. 1, pp. 518-524, 1996.
- [95] S. Kayalvizhi and D. M. Vinod Kumar, “Dispatchable DG planning in distribution networks considering costs,” *IEEE international conference on Recent Development in Control, Automation and Power Engineering (RDCAPE)*, 2015.
- [96] Kiran Teeparthi and D.M.Vinod Kumar, “Security-constrained optimal power flow with wind and thermal power generators using fuzzy adaptive artificial physics optimization algorithm,” *Neural Computing and Application*, July 2016.
- [97] B. Avandin, R. Hooshmand and E. Gholipour, “Decreasing activity cost of a distribution system company, by reconfiguration and power generation control of DGs based on shuffled frog leaping algorithm,” *International Journal of Electrical Power and Energy Systems*, vol. 61, pp. 48-55, 2014.
- [98] G. V. N. Lakshmi, A. Jaya Laxmi and S. V. Reddy, “Optimal allocation and sizing of distributed generation in distribution network using ant colony search algorithm,” *Proc. Of Int. Conf. on Advances in Communication, Network, and Computing, CNC, Elsevier*, 2014.
- [99] J. S. Savier and D. Das, “Impact of network reconfiguration on loss allocation of radial distribution systems,” *IEEE Trans. on Power Delivery*, vol. 22, no. 4, pp. 2473-2480, 2007.

[100]D. Das, D.P. Kothari and A. Kalam, “Simple and efficient method for load flow solution of radial distribution network,” *International Journal of Electrical Power and Energy Systems*, vol. 17, no. 5, pp. 335-346, Oct. 1995.

Appendix

IEEE 69-bus Distribution System Data

Number of buses: 69

Number of lines: 68

Bus voltage: 12.66kV

Total active power load: 3.80MW

Total reactive power load: 2.69 MW

System active power loss: 0.226MW

System reactive power loss: 0.098MVAR

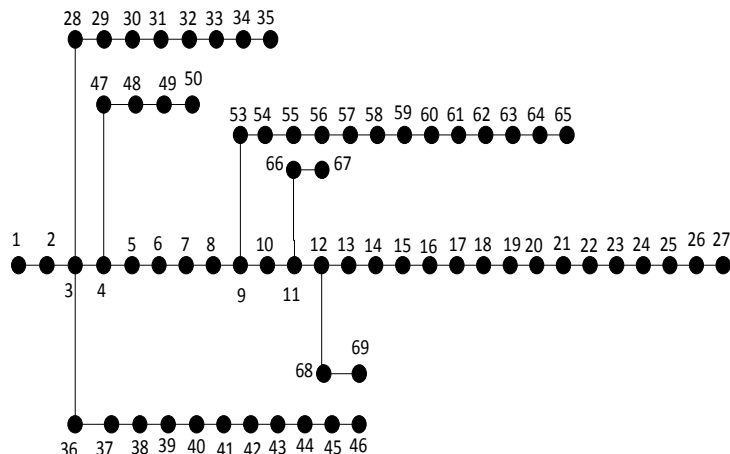


Figure A.1 Single-line diagram of IEEE 69-bus system

Table A.1 Line data of IEEE 69-bus distribution system

Line No.	From	To	R (in pu)	X (in pu)
1	1	2	3.12E-06	7.49E-06
2	2	3	3.12E-06	7.49E-06
3	3	4	9.36E-06	2.25E-05
4	4	5	0.00016	0.00018
5	5	6	0.00228	0.00116

6	6	7	0.00238	0.00121
7	7	8	0.00058	0.00029
8	8	9	0.00031	0.00016
9	9	10	0.00511	0.00169
10	10	11	0.00117	0.00039
11	11	12	0.00444	0.00147
12	12	13	0.00643	0.00212
13	13	14	0.00651	0.00215
14	14	15	0.0066	0.00218
15	15	16	0.00123	0.00041
16	16	17	0.00234	0.00077
17	17	18	2.93E-05	9.98E-06
18	18	19	0.00204	0.00068
19	19	20	0.00131	0.00043
20	20	21	0.00213	0.0007
21	21	22	8.73E-05	2.87E-05
22	22	23	0.00099	0.00033
23	23	24	0.00216	0.00071
24	24	25	0.00467	0.00154
25	25	26	0.00193	0.00064
26	26	27	0.00108	0.00036
27	3	28	2.75E-05	6.74E-05
28	28	29	0.0004	0.00098
29	29	30	0.00248	0.00082
30	30	31	0.00044	0.00015
31	31	32	0.00219	0.00072
32	32	33	0.00524	0.00176
33	33	34	0.01066	0.00352
34	34	35	0.0092	0.00304
35	3	36	2.75E-05	6.74E-05
36	36	37	0.0004	0.00098
37	37	38	0.00066	0.00077
38	38	39	0.00019	0.00022
39	39	40	1.12E-05	1.31E-05
40	40	41	0.00454	0.00531
41	41	42	0.00193	0.00226
42	42	43	0.00026	0.0003
43	43	44	5.74E-05	7.24E-05
44	44	45	0.00068	0.00086

45	45	46	5.62E-06	7.49E-06
46	4	47	2.12E-05	5.24E-05
47	47	48	0.00053	0.0013
48	48	49	0.00181	0.00442
49	49	50	0.00051	0.00126
50	8	51	0.00058	0.0003
51	51	52	0.00207	0.0007
52	9	53	0.00109	0.00055
53	53	54	0.00127	0.00065
54	54	55	0.00177	0.0009
55	55	56	0.00176	0.00089
56	56	57	0.00992	0.00333
57	57	58	0.00489	0.00164
58	58	59	0.0019	0.00063
59	59	60	0.00241	0.00073
60	60	61	0.00317	0.00161
61	61	62	0.00061	0.00031
62	62	63	0.00091	0.00046
63	63	64	0.00443	0.00226
64	64	65	0.0065	0.00331
65	11	66	0.00126	0.00038
66	66	67	2.93E-05	8.73E-06
67	12	68	0.00461	0.00153
68	68	69	2.93E-05	9.98E-06

Table A.2 Load data of IEEE 69-bus distribution system

Bus No.	P (in pu)	Q (in pu)
1	0	0
2	0	0
3	0	0
4	0	0
5	0	0
6	0.0026	0.0022
7	0.0404	0.03
8	0.075	0.054
9	0.03	0.022
10	0.028	0.019

11	0.145	0.104
12	0.145	0.104
13	0.008	0.0055
14	0.008	0.0055
15	0	0
16	0.0455	0.03
17	0.06	0.035
18	0.06	0.035
19	0	0
20	0.001	0.0006
21	0.114	0.081
22	0.0053	0.0035
23	0	0
24	0.028	0.02
25	0	0
26	0.014	0.01
27	0.014	0.01
28	0.026	0.0186
29	0.026	0.0186
30	0	0
31	0	0
32	0	0
33	0.014	0.01
34	0.0195	0.014
35	0.006	0.004
36	0.026	0.0186
37	0.026	0.0186
38	0	0
39	0.024	0.017
40	0.024	0.017
41	0.0012	0.001
42	0	0
43	0.006	0.0043
44	0	0
45	0.0392	0.0263
46	0.0392	0.0263
47	0	0
48	0.079	0.0564
49	0.3847	0.2745

50	0.3847	0.2745
51	0.0405	0.0283
52	0.0036	0.0027
53	0.0043	0.0035
54	0.0264	0.019
55	0.024	0.0172
56	0	0
57	0	0
58	0	0
59	0.1	0.072
60	0	0
61	1.244	0.888
62	0.032	0.023
63	0	0
64	0.227	0.162
65	0.059	0.042
66	0.018	0.013
67	0.018	0.013
68	0.028	0.02
69	0.028	0.02

Practical Indian 85-bus Distribution System Data

Number of buses: 85

Number of lines: 84

Bus voltage: 11kV

Total active power load: 2.5708MW

Total reactive power load: 2.6218 MW

System active power loss: 0.3136MW

System reactive power loss: 0.134MVAR

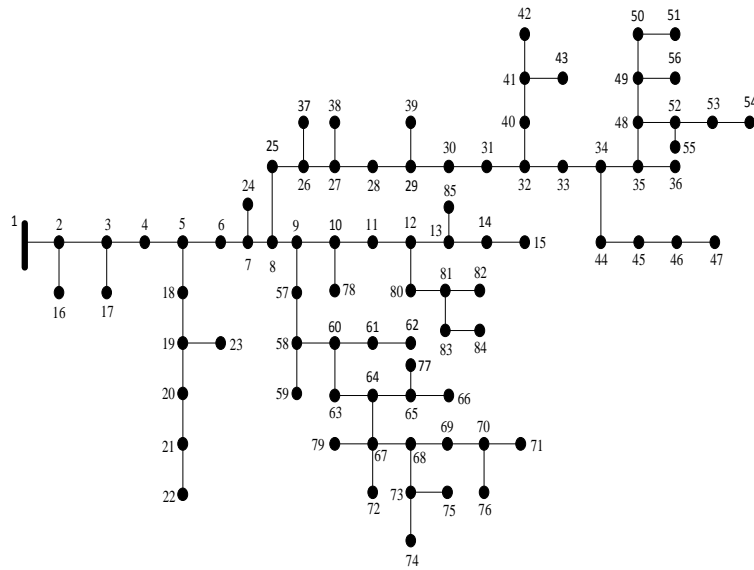


Figure A.2 Single-line diagram of Indian 85-bus system

Table A.3 Line data of Indian 85-bus distribution system

Line No.	From	To	R (in pu)	X (in pu)
1	1	2	0.0009	0.0006
2	2	3	0.0013	0.0009
3	3	4	0.0018	0.0012
4	4	5	0.0009	0.0006
5	5	6	0.0036	0.0025
6	6	7	0.0022	0.0015
7	7	8	0.0099	0.0068
8	8	9	0.0009	0.0006
9	9	10	0.0049	0.0034
10	10	11	0.0045	0.0031
11	11	12	0.0045	0.0031
12	12	13	0.0049	0.0034
13	13	14	0.0022	0.0015
14	14	15	0.0027	0.0018
15	2	16	0.006	0.0025
16	3	17	0.0038	0.0016
17	5	18	0.0068	0.0028
18	18	19	0.0053	0.0022
19	19	20	0.0038	0.0016
20	20	21	0.0068	0.0028

21	21	22	0.0128	0.0053
22	19	23	0.0015	0.0006
23	7	24	0.0075	0.0031
24	8	25	0.0038	0.0016
25	25	26	0.003	0.0012
26	26	27	0.0045	0.0019
27	27	28	0.0023	0.0009
28	28	29	0.0045	0.0019
29	29	30	0.0045	0.0019
30	30	31	0.0023	0.0009
31	31	32	0.0015	0.0006
32	32	33	0.0015	0.0006
33	33	34	0.0068	0.0028
34	34	35	0.0053	0.0022
35	35	36	0.0015	0.0006
36	26	37	0.003	0.0012
37	27	38	0.0083	0.0034
38	29	39	0.0045	0.0019
39	32	40	0.0038	0.0016
40	40	41	0.0083	0.0034
41	41	42	0.0023	0.0009
42	41	43	0.0038	0.0016
43	34	44	0.0083	0.0034
44	44	45	0.0075	0.0031
45	45	46	0.0075	0.0031
46	46	47	0.0045	0.0019
47	35	48	0.0053	0.0022
48	48	49	0.0015	0.0006
49	49	50	0.003	0.0012
50	50	51	0.0038	0.0016
51	48	52	0.0113	0.0047
52	52	53	0.0038	0.0016
53	53	54	0.0045	0.0019
54	52	55	0.0045	0.0019
55	49	56	0.0045	0.0019
56	9	57	0.0023	0.0009
57	57	58	0.0068	0.0028
58	58	59	0.0015	0.0006
59	58	60	0.0045	0.0019

60	60	61	0.006	0.0025
61	61	62	0.0083	0.0034
62	60	63	0.0015	0.0006
63	63	64	0.006	0.0025
64	64	65	0.0015	0.0006
65	65	66	0.0015	0.0006
66	64	67	0.0038	0.0016
67	67	68	0.0075	0.0031
68	68	69	0.009	0.0037
69	69	70	0.0038	0.0016
70	70	71	0.0045	0.0019
71	67	72	0.0015	0.0006
72	68	73	0.0098	0.0041
73	73	74	0.0023	0.0009
74	73	75	0.0083	0.0034
75	70	76	0.0045	0.0019
76	65	77	0.0008	0.0003
77	10	78	0.0053	0.0022
78	67	79	0.0045	0.0019
79	12	80	0.006	0.0025
80	80	81	0.003	0.0012
81	81	82	0.0008	0.0003
82	81	83	0.009	0.0037
83	83	84	0.0083	0.0034
84	13	85	0.0068	0.0028

Table A.3 Load data of Indian 85-bus distribution system

Bus No.	P (in pu)	Q (in pu)
1	0	0
2	0	0
3	0	0
4	0.056	0.0571
5	0	0
6	0.0353	0.036
7	0	0
8	0.0353	0.036
9	0	0

10	0	0
11	0.056	0.0571
12	0	0
13	0	0
14	0.0353	0.036
15	0.0353	0.036
16	0.0353	0.036
17	0.112	0.1143
18	0.056	0.0571
19	0.056	0.0571
20	0.0353	0.036
21	0.0353	0.036
22	0.0353	0.036
23	0.056	0.0571
24	0.0353	0.036
25	0.0353	0.036
26	0.056	0.0571
27	0	0
28	0.056	0.0571
29	0	0
30	0.0353	0.036
31	0.0353	0.036
32	0	0
33	0.014	0.0143
34	0	0
35	0	0
36	0.0353	0.036
37	0.056	0.0571
38	0.056	0.0571
39	0.056	0.0571
40	0.0353	0.036
41	0	0
42	0.0353	0.036
43	0.0353	0.036
44	0.0353	0.036
45	0.0353	0.036
46	0.0353	0.036
47	0.014	0.0143
48	0	0

49	0	0
50	0.0363	0.037
51	0.056	0.0571
52	0	0
53	0.0353	0.036
54	0.056	0.0571
55	0.056	0.0571
56	0.014	0.0143
57	0.056	0.0571
58	0	0
59	0.056	0.0571
60	0	0
61	0.112	0.1143
62	0.056	0.0571
63	0.014	0.0143
64	0	0
65	0	0
66	0.056	0.0571
67	0	0
68	0	0
69	0.056	0.0571
70	0	0
71	0.0353	0.036
72	0.056	0.0571
73	0	0
74	0.056	0.0571
75	0.0353	0.036
76	0.056	0.0571
77	0.014	0.0143
78	0.056	0.0571
79	0.0353	0.036
80	0.056	0.0571
81	0	0
82	0.056	0.0571
83	0.0353	0.036
84	0.014	0.0143
85	0.0353	0.036

Publications

Refereed International Journals:

1. **Sachidananda Prasad** and D. M. Vinod Kumar, “ Optimal allocation of measurement devices for distribution state estimation using multi-objective hybrid PSO-Krill herd algorithm”, *IEEE Transactions on Instrumentation and Measurement*, vol. 66, no. 8, pp. 2022-2035, August 2017.
2. **Sachidananda Prasad** and D. M. Vinod Kumar, “A multi-objective hybrid estimation of distribution algorithm- Interior point method based meter placement for active distribution state estimation”, *IET Generation, Transmission and Distribution*, vol. 12, no. 3, pp. 767-779, 2018.
3. **Sachidananda Prasad** and D.M. Vinod Kumar “Trade-offs in PMU and IED Deployment for Active Distribution State Estimation Using Multi-objective Evolutionary Algorithm” *IEEE Transactions on Instrumentation and Measurement*, 2018. **(Available Online)**
4. **Sachidananda Prasad** and D.M. Vinod Kumar “Robust meter placement for Active Distribution State Estimation Using new multi-objective optimization model” *IET Science, Measurement and Technology*. **(Provisionally Accepted for Publication)**
5. **Sachidananda Prasad** and D. M. Vinod Kumar, “Hybrid fuzzy charged system search algorithm based state estimation in distribution networks”, *Engineering Science and Technology, an International Journal, Elsevier*, vol. 20, no. 3, pp. 922-933, 2017.

International/ National Conferences:

1. **Sachidananda Prasad** and D.M. Vinod Kumar, “Distribution system state estimation-A bibliographical survey”, *14th IEEE India Council International Conference (INDICON 2017), IIT Roorkee*, 15-17th Dec 2018.
2. **Sachidananda Prasad** and D.M. Vinod Kumar, “Fuzzy charged system search algorithm based state estimation in distribution networks”, *40th National Science Conference (NSC 2016)*, National Institute of Technology Warangal, pp. 1-6, 2016.

Curriculum-Vitae

Name : Sachidananda Prasad
Date of Birth : 20th May 1986
Gender : Male
Contact Number : +91-8897816084
Email Id : Sachidananda_prasad@yahoo.in

Academic Qualifications:

Program	Institution	%/CGPA	Year of completion
M. Tech (Power Systems Engineering)	Veer Surendar Sai University of Technology, Burla	8.83	2013
B. Tech (Electrical Engineering)	GHITM, Puri	7.22	2007